UiT The Arctic University of Norway

Department of Geosciences
Faculty of Science and Technology
UiT The Arctic University of Norway

Assessing the relationship between living benthic foraminifera and methane emission in the Arctic Ocean

Katarzyna Melaniuk

A dissertation for the degree of Philosophiae Doctor August 2021

Preface

This thesis is the result of a four-year PhD study undertaken at the Centre for Arctic Gas Hydrate, Environment and Climate (CAGE), Department of Geosciences, at the University of Tromsø (UiT the Arctic University of Norway), between October 2015 and August 2021. The project was financed by the Research Council of Norway through its Centre of Excellence funding scheme grant no. 223259, the NORCUST project, The Loeblich and Tappan Student Research Award, and a Travel grant from The Norwegian Research School in Climate Dynamics (ResClim). The candidate wishes to thank the supervisors of the first part of the PhD study and who supervised the study for the first paper: J. Bernhard, G. Panieri and M. Hald. The candidate also thanks supervisors J. Bernhard and M. Hald, who supervised the study for the second paper that included samples provided by G. Panieri. The candidate also thanks the supervisors for the second part of the PhD study: T.L. Rasmussen, T. Treude and M. Zajączkowski, and K. Sztybor, who supplied the samples and supervised the project part for the last two papers.

The PhD program at UiT required that 25% (one-year equivalent) of the four-year period be dedicated to undertaking duty work which was fulfilled through the preparation and teaching classes in *Micropaleontology (*GEO-3122) and *Reconstructing Quaternary Marine Climate and Environments* (GEO-3111), as well as assistance in The Stable Isotope Laboratory (SIL) at the Department of Geosciences, UiT. Samples for this project were obtained during a 5-month laboratory experimental period at the Bernhard Lab: Benthic Foraminifera Ecology and Paleoecology, Woods Hole Oceanographic Institution, along with collecting surface sediment samples during several CAGE research expeditions to the Svalbard margin on board the R.V. *Helmer Hanssen* (2015 to 2017). Samples were also made available for the second part of the PhD study from a cruise with R.V. *Poseidon* to Vestnesa Ridge, NV Svalbard margin in 2011.

The doctoral thesis resulted in four first-authored scientific articles, which contribute new knowledge on benthic foraminifera and their geochemistry associated with methane cold seeps. These articles are listed below:

1. **Melaniuk, K., Bernhard, J.M., Hald, M., Panieri, G.** Impact of hypoxia and high pCO_2 and diet on benthic foraminiferal growth: experiment with propagules. Manuscript in revision.
2. **Melaniuk, K.** Effectiveness of Fluorescent Viability Assays in Studies of Arctic Cold Seep Foraminifera. *Frontiers in Marine Science* **8**, doi:10.3389/fmars.2021.587748 (2021).
3. **Melaniuk, K., Sztybor, K., Treude, T., Sommer, S., Rasmussen, T.L**. Evidence for influence of methane seepage on isotopic signatures in living deep-sea foraminifera, 79 °N. Manuscript in revision in Scientific Reports.
4. **Melaniuk, K., Sztybor, K., Treude, T., Sommer, S., Zajączkowski, M., Rasmussen, T.L.** Response of benthic foraminifera to ecological succession in cold seeps from Vestnesa Ridge; implications for interpretations of paleo-seepage environments. Manuscript in preparation.

Acknowledgements

I would like to thank my former supervisor Giuliana Panieri for the opportunity to start the PhD program at CAGE, study seep- environments, and the opportunity to attend several cruises to the Arctic Ocean. I would like to express my sincere gratitude to my former supervisor Joan M. Bernhard for the time I spent in her lab at Woods Hole Oceanographic Institution, for her insightful comments and suggestions to my work. I also thank co-supervisor Morten Hald for his input to the first manuscript.

As Franklin D. Roosevelt said, “a smooth sea never made a skilled sailor”. Undertaking this PhD has been a truly life-changing experience for me and it would not have been possible to do without the support and guidance that I received from many people, but mostly from my main supervisor Tine L. Rasmussen. I could not have completed this dissertation without her support. I want to thank you for the support, encouragement, and all of the opportunities I was given to further my research. I would like to show my appreciation for my current co-supervisors Tina Treude and Marek Zajączkowski, for their strong support and scientific input which greatly improved my work.

I’d like to acknowledge the assistance from the lab staff Trine Dahl, Karina Monsen, Ingvild Hald, Matteus Lindgren, and A.G. Hestnes, as well as assistance from the crew and cruise participants during cruises with R/V *Helmer Hanssen*, in particular during the CAGE 17-2 cruise.

I would like to thank the following friends who have helped me (significantly) over the last few years. First, for my very close friend and partly PhD advisor Kamila Sztybor for providing me with the samples I used in the two last manuscripts and overall support and understanding during the PhD journey. To Anna Osiecka for proofreading my thesis and manuscripts and for her mental support during the last months of my PhD. To Sunil Vadakkepuliyambatta for making every single map in this thesis and for being such a great friend.

I would like to thank my colleagues at the Department of Geosciences, who have supported me and had to put up with my stresses and moans for the past three years of study. Especially I would like to mention: Marina, Siri, Lina, Naima, Kasia, Przemek, Arunima, and Haoyi.

Finally, I also appreciate all the unconditional support I received from my parents, my brother, and friends back in Poland.

Table of Contents

1 MOTIVATION AND OBJECTIVES

Methane is a powerful greenhouse gas, produced in marine sediments either by exposing deep complex organic molecules to high temperatures or by microbial transformation of organic and inorganic carbon at more shallow depths (Reeburgh, 2007; Strąpoć et al., 2020). At temperatures lower than 25°C and a moderate pressure greater than 3–5 MPa, corresponding to a combined water and sediment depth of 300–400 m, methane forms ice-like structures called methane hydrates (Reeburgh et al., 2007; Ruppel and Kessler, 2017). Deposits of methane hydrates are widespread in marine sediments on continental margins and are known to be sensitive to environmental changes, such as for example temperature increases and/or changes in pressure or sediment movements (e.g., Archer et al., 2009; Maslin et al., 2010). Past massive methane releases from sub-seabed reservoirs have been linked to changes in climatic conditions, with an increase in temperature recorded during Quaternary and the Paleocene (Wefer et al., 1994; Smith et al., 2001), Late Paleocene (Kennett and Stott, 1991; Dickens et al., 1997; Katz et al., 1999), and Cretaceous (Jahren et al., 2001). As large amounts of methane are stored on Arctic continental margins in the form of gas hydrates, concern has increased that ongoing ocean warming will trigger destabilization of the gas hydrate reservoirs and cause further release of methane in the future (IPCC, 2007; Phrampus and Hornbach, 2012).

Several studies have proposed that the negative carbon isotope signature ($\delta^{13}C$ up to -40‰) measured in carbonate tests of fossil foraminifera might reflect past methane seepages, and that fossil foraminifera have a high potential as a tool in tracking past methane releases (Millo et al., 2005; Martin et al., 2010; Consolaro et al., 2015; Sztybor and Rasmussen, 2017; Schneider et al., 2017). The $\delta^{13}C$ levels in calcium carbonate of some fossil foraminifera can be lower than -10‰ (Hill et al., 2003; Schneider et al., 2017) and $\delta^{13}C$ measured in calcite of 'live' (Rose Bengal stained) foraminifera generally do not exceed -7.5‰ (Mackensen et al., 2006; Wollenburg et al., 2015). Thus, it still remains unclear whether (and to what extent) living foraminifera incorporate methane-derived carbon during their biomineralization, and/or if the isotopic signatures in their shells are mostly a result of authigenic overgrowth from precipitation of carbonates by diagenetic processes. It has also been suggested that the ^{13}C-depleted carbon from methane might be incorporated by the benthic foraminifera from the dissolved inorganic carbon (DIC) pool from the ambient seawater and porewater. Alternatively, foraminifera might feed on (Panieri, 2006), or live in symbiosis with, methane-oxidizing bacteria, which carry a ^{13}C-depleted carbon signal as suggested by Hill et al. (2004). Remarkably negative $\delta^{13}C$ values (up to -40‰) in foraminiferal tests have been shown to derive mainly from overgrowth by methane-derived authigenic carbonates (MDAC; Torres et al., 2003; Consolaro et al., 2015; Sztybor and Rasmussen, 2017; Schneider et al., 2017).

At cold seeps, the biogeochemical processes involving methane, such as aerobic and anaerobic methane oxidation, affect the properties of pore water in which the benthic foraminifera live. The venting of methane from sub-seabed deposits supports growth of methane-oxidizing bacteria that may serve as food for foraminifera, but simultaneously, microbial activity causes a decrease in the surrounding oxygen concentration, leading to hypoxia or even anoxia, release of hydrogen sulfide H_2S, and an increase in the partial pressure of carbon dioxide (pCO_2). For many foraminiferal species, oxygen is crucial for an efficient generation of cellular energy (Heinz and Geslin, 2012) and changes in water chemistry, such as increase in pCO_2, might affect the process of calcification (Allison et al., 2010). For these reasons, some studies assert that despite the abundance of food (e.g., methanotrophic bacteria) due to the local environmental conditions, cold seeps are hostile environments for foraminifera, and that foraminifera do not calcify during active methane seepage (Torres et al., 2003; Herguera et al., 2014), and the foraminifera which inhabit cold seeps should be adapted to organic-rich and reducing environments (Rathburn et al., 2000, 2003; Bernhard et al., 2001; Torres et al., 2003; Fontanier et al., 2014). Modern cold seeps provide a good analogue for past methane-rich environments and offer an opportunity to investigate possible effects of methane seepage on isotopic signatures and distribution patterns of living benthic foraminifera, which can be further used as an analogue in interpretation of palaeoceanography and intensity of paleo-methane seepage.

The main objectives of this doctoral thesis are to:

- study the ability of foraminifera to survive under low oxygen (hypoxia) conditions, elevated pCO_2, and a combined effect of both in conjunction with diet (methanotroph vs algal) by experiments with juvenile benthic foraminifera in Biospherix C-Chambers; Article 1
- testing the effectiveness of fluorescent viability assays in studies of living cold seep foraminifera; Article 2
- compare the carbon isotopic signature ($\delta^{13}C$ and $\delta^{18}O$) in tests of metabolically active (CellTracker™ Green CMFDA and CellHunt Green labelled) foraminifera (Article 2) and Rose Bengal stained (Article 3) to determine whether methane seepage has any effect on the isotopic signatures of the calcite of living benthic foraminifera.
- investigate modern foraminiferal assemblages from the Arctic cold seeps; Articles 3 and 4
- investigate the impact of methane-related biological processes (MOx and AOM) on the benthic foraminiferal communities; Article 4

2 BACKGROUND

2.1 Methane cold seeps

Cold seeps are chemosynthetic ecosystems, in which hydrocarbon-rich fluids seep from the sub-seabed gas hydrate deposits or from other petroleum reservoirs providing a carbon and/or energy source (e.g., Sloan 1990; Barry et al., 1997; Olu et al., 1997; Coleman and Ballard 2001; Sahling et al., 2003; Levin, 2005). These ecosystems are commonly found in continental margin environments, both tectonically active and passive, and in terrestrial lake areas (Fig. 1).

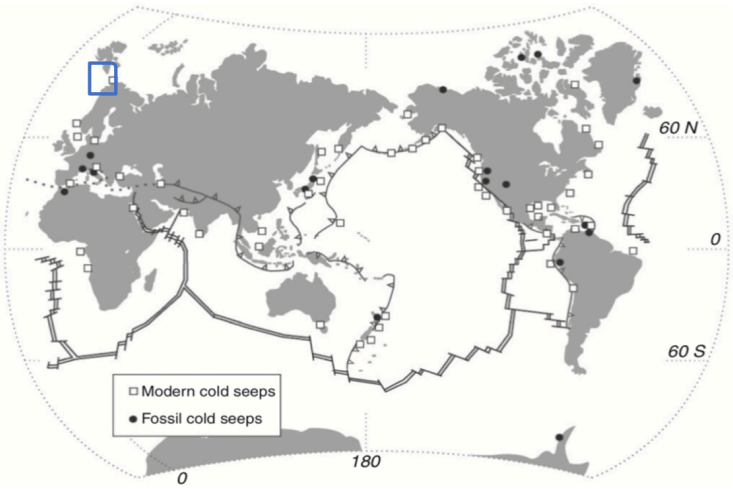

Figure 1. Distribution of modern and fossil cold seeps, blue square indicate the study area (Figure from Levin, 2005, modified from Campbell et al. 2002).

The hydrocarbon-rich fluids originate from decaying organic matter (e.g., sapropel), from thermogenic degradation of organic matter of marine or terrestrial origin, or biogenic processes (Strąpoć, 2020). Gas seepage can manifest itself in form of gas bubbles escaping from the seabed observable by eye, or evident as acoustical plumes recorded through echo sounding. Other signs are pockmarks (i.e. shallow seabed depressions) or other topographic and geomorphological structures, such as pingos or mud volcanoes. Concentration and strength of flow of methane varies between seeps, and within the same seep site creating different microhabitats. The supply of methane can fluctuate over time, so that the methane flux determines the ephemeral nature of cold seep environments. Heterogeneity in permeability and methane flux results in a spatial heterogeneity in the flux rates and environments. This in turn results in a patchy distribution of biological communities (Tryon and Brown 2001; Levin, 2005). For example, vesicomyid clams hosting endosymbiotic chemoautotrophic bacteria are commonly associated with downward directed flows (inflow) and oscillatory flows (Tryon and Brown

2001; Levin, 2005). Bacterial mats are dominated by large, filamentous, sulphide-oxidizing bacteria: *Beggiatoa*, *Thioploca*, *Arcobacter*, and *Thiothrix* that indicate a more consistent and high methane flux (Tryon and Brown 2001; Tryon et al., 2002). Cold-seep biota largely relies on oxidation of sulphur and methane reduced by microorganisms for nutrition, and possibly even on nitrogen fixation (Levin, 2005). Within a cold seep, gas emission from the sub-seabed reservoirs are controlled by aerobic methane oxidation (MOx) or, in a lack of oxygen, by anaerobic methane oxidation (AOM) coupled with sulphate reduction (Knittel and Boetius, 2009; Treude et al., 2007; Orphan et al., 2001). The process of AOM is conducted by anaerobic methanotrophic archaea (ANME; Milucka et al. 2012) or by microbial consortia of ANME and sulphate-reducing bacteria found within the sulphate-methane transition zone (SMTZ; Boetius et al., 2000; Knittel et al., 2005). The carbon isotopic signature ($\delta^{13}C$) of methane depends on the origin of the methane, with the result that the $\delta^{13}C$ from microbial methane have much lighter ^{13}C signatures (from -110‰ to -60‰) than the thermogenic methane (from -50‰ to -20‰; Whiticar, 1999; Valentine, 2002). As a product of microbial activity, the light ^{13}C carbon isotope is released in the form of carbon dioxide gas (CO_2) or bicarbonate ions (HCO_3^2) into the sediment and/or ambient water, leading to changes in the water chemistry and isotopic signature of the ambient seawater and pore water (Whiticar, 1999; Treude et al., 2007). Bicarbonate produced during AOM enables carbonate precipitation, which provides a secondary hard-bottom for tubeworms to grow on. Additionally, in anoxic conditions hydrogen sulphide (H_2S) is produced. The compound is highly toxic for marine organisms; it inhibits ATP (Adenozyno-5'-trifosforan) production by binding to cytochrome c oxidase (CytOx; Somero et al., 1989).

2.2 Modern cold-seep benthic foraminifera

Studies on 'live' benthic foraminifera (Rose Bengal-stained) inhabiting hydrocarbon seeps were previously conducted at several locations worldwide, including Oregon Hydrate Ridge (Torres et al., 2003; Hill et al., 2004), Monterey Bay (Rathburn et al., 2003), northern Adriatic Sea (Panieri, 2006), Gulf of Guinea (Fontanier et al., 2014), Blake Ridge (Panieri and Sen Gupta, 2008), Barents Sea (Mackensen et al., 2006; Wollenburg and Mackensen, 2009; Dessandier et al., 2019), and New Zealand (Martin et al., 2010). Several studies have shown that the abundance of foraminifera increases near active fluid discharge spots, indicating that benthic foraminifera may potentially be attracted by the availability of food, for example microbial mats (see e.g., Rathburn et al., 2000; Torres et al., 2003; Heinz et al., 2005; Panieri, 2006; Panieri and Sen Gupta, 2008). However, this may not hold true for all seeps. In Monterey Bay, for example, the abundance of foraminifera is lower at seep sites than at non-seep sites (Bernhard et al., 2001). The distribution of foraminifera might be uneven within one seep,

and is most likely conditioned by variation in microhabitats e.g., presence of bacterial mats or clam beds (e.g., Rathburn et al., 2000; Torres et al., 2003; Panieri and Sen Gupta, 2008, Wollenburg and Mackensen, 2009; Dessandier et al., 2019).

So far, the results of different studies of species compositions of benthic foraminiferal faunas have been consistent and show that there are no endemic species associated with cold seep ecosystems (e.g., Sztybor and Rasmussen, 2017 and references therein). Species which are usually present within seep sites have been documented in non-seep marine environments (e.g., Rathburn et al., 2000; Bernhard et al., 2001; Hill et al., 2003; Panieri, 2006; Etiope et al., 2014; Herguera et al., 2014). With a majority of foraminiferal species being aerobic, individuals present at cold seep sites should be able to survive the local geochemical constraints, such as for example low oxygen levels (including temporary anoxia) or presence of toxic hydrogen sulfide (H_2S; Herguera et al., 2014). The most common species observed at cold seeps belong to several genera, such as *Bolivina*, *Bulimina*, *Nonionella* and *Uvigerina*, which are adapted to organic-rich and reducing environments (e.g., Akimoto et al., 1994, Rathburn et al., 2000, 2003, Bernhard et al., 2001, Torres et al., 2003, Fontanier et al., 2014). Studies from the Gulf of Mexico show that some species, such as *Bolivina albatrossi*, *Cassidulina neocarinata* and *Trifarina bradyi,* are facultative anaerobes able to survive temporary anoxic conditions below bacterial mats (*Beggiatoa* sp.) and show some H_2S tolerance (Sen Gupta et al., 1997). Epifaunal species, for example *Cibicidoides wuellerstorfi* or *Cibicides lobatulus*, show very specific adaptations, where individuals tend to colonize the outer surface of *Siboglinidae* tubeworms in order to escape H_2S and/or anoxic conditions (Sen Gupta et al., 2007; Wollenburg et al., 2009).

2.3 Stable isotope signatures in modern benthic foraminifera from cold seeps

Opinions are divided on whether the carbon isotopic signatures ($\delta^{13}C$) of living calcareous foraminiferal tests from methane seeps reflect any sort of incorporation of methane-derived carbon. Some studies show that the $\delta^{13}C$ measured in tests of living foraminifera collected from active seeps are not markedly lower than those from non-seep sites, indicating that living foraminifera might not be able to record the episodes of methane release (e.g., Torres et al., 2003, Rathburn et al., 2003, Etiope et al., 2014; Melaniuk, 2021). A shift of approximately 0–4‰ towards a more negative $\delta^{13}C$ was shown to have an origin from a local organic matter degradation (e.g., Torres et al., 2003, Martin et al., 2004). Hostile conditions, such as low oxygen or anoxia combined with high carbon dioxide concentration (pCO_2), most likely inhibit calcification during methane seepage (Herguera et al., 2014). Thus, it has been proposed that foraminifera do not calcify during active methane discharges, but

instead build tests during no or reduced methane flux (Torres at al., 2003). Alternatively, in case of lack of oxygen the foraminifera might migrate to other more oxygenated locations (Bernhard et al., 2010).

Several studies indicate that methane has an effect on isotopic signatures of 'live' benthic foraminifera (i.e. Rose Bengal-stained). For example, the $\delta^{13}C$ of tests of *Uvigerina peregrina* was found to be as low as -5.64‰ at cold seeps, while at the control site the value was not lower than -0.81‰ (Hill et al., 2004), and the isotopic signature of *Cassidulina neoteretis* was as low as -7.5‰ (Mackensen et al., 2006), thus indicating that both species were potencially affected by methane. Similarly, the negative $\delta^{13}C$ value in tests of epifaunal species, such as *Cibicioides* sp., can be explained by the incorporation of light carbon isotope from the ambient seawater (i.e. pore water or bottom water in which the foraminifera calcified) which was transported from deeper sediments by tubeworms inhabiting the methane seeps (Mackensen et al., 2006; Wollenburg et al., 2009). In most cases, the $\delta^{13}C$ measured on foraminiferal tests from cold seeps has shown larger degrees of variations when compared to non-seep sites (e.g., Rathburn et al., 2003; Bernhard et al., 2010). Addtionally, individuals collected from sites covered with bacterial mats show more negative $\delta^{13}C$ both in tests and cytoplasm when compared to individuals from non-seep sites (e.g., Hill et al., 2005; Panieri, 2006). This implies that isotopically lighter food, such as for example methanotrophic bacteria, and/or presence of symbionts contribute to the isotopic signatures of foraminifera from cold seeps (Hill et al., 2004; Bernhard et al., 2010).

2.4 Fossil foraminifera from cold seeps

Both planktic and benthic foraminifera preserved in the methane influenced sediments can be affected by precipitation of Methane-Derived Authigenic Carbonates (MDAC) (Torres et al., 2003; Uchida et al., 2004; Martin et al., 2010). Bicarbonate ions (HCO_3^2) are products of anaerobic oxidation of methane (AOM) and enable MDAC formation (see above; chapter 2.1). As a result, the tests of fossil foraminifera from cold seeps are characterized by strongly depleted $\delta^{13}C$ values and high Mg content from overgrowth of their shells by MDAC. Eventual primary signals in foraminiferal tests can thus be overprinted by the diagenetic alterations from coatings of both the outsite and/or inside of the tests (Schneider et al., 2017) and consist of up to 60% of the total volume of the tests (Torres et al., 2003). Overprinting results in shift in the $\delta^{13}C$ of the primary signal of about 15–29‰ and results in $\delta^{13}C$ values lower that -10‰ as it was suggested by Schneider et al. (2017) and up to -34.1‰ (Panieri et al., 2017). It is believed that those highly negative values recorded in tests are evidence of increase in methane flux, particulary the past migrations of the sulphate-methane transition zone (SMTZ; Consolaro et al., 2015; Sztybor and Rasmussen., 2017; Schneider et al., 2017). Methane seepage events are recorded

in the isotopic signature of foraminiferal tests, but because of the coating of MDAC the foraminifera may date (based on AMS^{14}C dating) significantly older than the foraminiferal tests itself. Distinction between the primary and the sedondary isotopic signals in fossil foraminifera is a large challenge, thus signals cannot be used to determine a precise stratigraphic history and timing of the seepage (Torres et al., 2003; Martin et al., 2004). Abnormal depletions in δ^{13}C can only provide qualitative information about presence of cold seeps (Martin et al., 2004).

3 BACKGROUND

3.1 Laboratory experiment

Propagule Method

The Propagule Method is an experimental tool for testing the ecology of benthic foraminifera, and the response of multi-species assemblages to selected environmental parameters (Alve and Goldstein, 2014; Article 1). Propagules are small juvenile foraminifera approximately 10 µm in size, stored in the sediment in form of a "propagule bank". Propagules are able to delay growth (from months to years) until the environmental conditions become favorable (Alve and Goldstein, 2010). Propagules are isolated from adult foraminifera by sieving the sediment on mesh-size <53 µm.

Advantages using the Propagule Method: (from Alve and Goldstein 2014).

- both live and dead individuals harvested at the end of the experiments have responded positively to the treatment,
- focuses on the critical, juvenile developmental stages,
- simple experimental set-up, design to test the effects of changing environmental conditions at assemblage level under controlled conditions (i.e., different assemblages grown from the same propagule bank),
- both small and large foraminiferal species can be studied,
- use the original sediments, which helps to optimally mimic their natural conditions,

Experimental set-up

For the purpose of the experiment (Article 1), foraminifera-bearing sediments were collected from the Barents Sea and the Norwegian Sea using a box corer (Fig. 2). Samples were processed according to the propagule method (Goldstein and Alve, 2011). The <53 µm-sediment fraction was divided between four experimental treatments I, II, III, IV, and incubated inside Biospherix C-Chambers

(Parish, New York, USA) for 5 months. Four experimental treatments were designed to simulate different environmental conditions, including oxygen-saturated to hypoxic conditions, modern-day pCO_2 to elevated pCO_2, and dual-stress conditions (hypoxia and elevated pCO_2; Fig. 5; Table 2). To investigate whether diet can affect the growth of foraminifera, once a week the foraminifera were fed by either a mix of algae (*Dunaliella tertiolecta*, Butcher, and *Isochrysis galbana*, Parke) or by a methanotrophic bacterium (*Methyloprofundus sedimenti* PKF-14).

Table. 2. Experimental treatments (I, II, III, IV), O_2 (ml/L) and CO_2 (ppm) concentration, gas sources (400-ppm CO_2, 1% CO_2 /99% N_2, and N_2), gas sensors and controllers used for the experiment.

Treatment	O_2 (ml/L)	pCO_2 (ppm)	Gas source	Gas sensors and controllers	Imitated environmental conditions
I	saturated	400	400-ppm CO_2	No controllers	Modern atmospheric conditions
II	0.7	400	1% CO_2 in N_2; N_2	ProCO$_2$, ProOx	Hypoxia, modern pCO_2 concentration
III	saturated	2000	1% CO_2 in N_2	ProCO$_2$	Oxygenated, elevated-pCO_2 concentration
IV	0.7	2000	1% CO_2 in N_2; N_2	ProCO$_2$, ProOx	Dual-stress

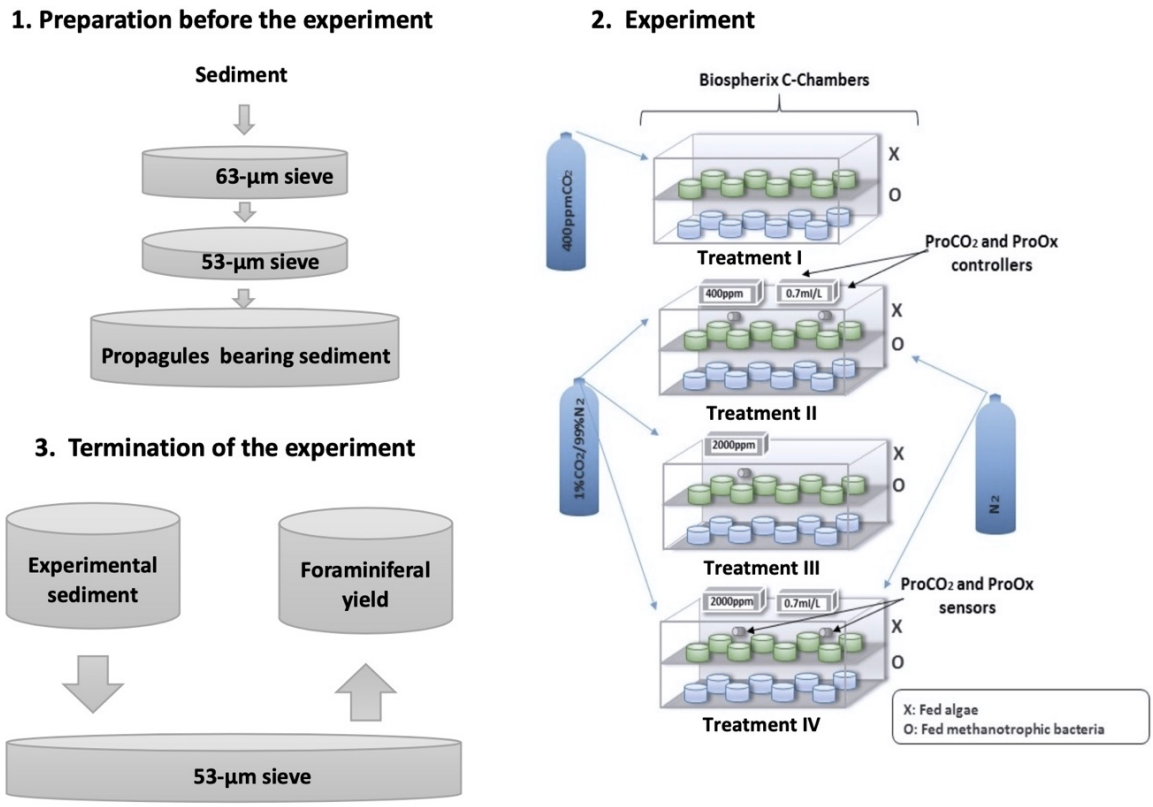

Figure. 5. Schematic of experiment.

3.2 Benthic foraminiferal faunas and isotopic signatures

3.2.1 Study areas

Vestnesa Ridge:

Vestnesa Ridge is a deep-sea cold seep area (>1000 m), located in the Fram Strait (~ 1200 m depth), northwest of Svalbard in the Arctic Ocean (79°N, 5–7°E; Fig. 2). The ridge is characterized by a series of perforations called pockmarks (i.e., shallow seabed depressions) where methane-rich fluids are found seeping from gas hydrates and other free-gas reservoirs (Bünz et al., 2012; Plaza Faverola et al., 2015). Of these, the two most active pockmarks have been informally called 'Lomvi' and 'Lunde' (Bünz et al., 2012). The presence of methane (mostly of thermogenic origin) has been documented both in the sediment and water column and by the recovery of methane hydrates in sediment cores. Sediment core analyses have shown presence of fossil seep-related macrofaunal communities at Vestnesa Ridge (Ambrose et al., 2015; Sztybor and Rasmussen, 2017; Hansen et al., 2017; Thomsen et al., 2019) and diagenetic alterations in isotopic signatures ($\delta^{13}C$) of fossil foraminiferal tests caused by MDAC precipitation (Schneider et al., 2017; Sztybor and Rasmussen, 2017). Several seafloor observations revealed presence of megafaunas (Åström et al., 2016, 2017) and carbonate outcrops (Sztybor and Rasmussen, 2017; Himmler et al., 2018) associated with methane emission.

Storfjordrenna pingos:

Storfjordrenna is located at the SW Svalbard continental shelf, in the north-western Barents Sea (76°N, 16°E), at an approximate water depth of 400 m (Fig. 2). The area is characterized by five gas hydrate mounds (pingo-like features) spread within a 2 km^2 area. Gas hydrates pingos (GHP) are known to be 8–12 m high, with diameters ranging from 280–450 m. Georeferenced seabed imagery indicates the presence of chemosynthetic macrofaunas associated with cold seeps (Åström et al., 2016; Sen et al., 2018). Four out of five GHPs show active methane seepage in the form of gas flares around summits, where one is mostly in a "post-active stage" (no visible flare on echo sounder recordings) (Serov et al., 2017; Sen et al., 2018; Hong et al., 2018). Elevated concentrations of methane mostly of thermogenic origin have been detected in both sediments and bottom water and gas hydrates were also discovered from several sediment cores (Hong et al., 2018).

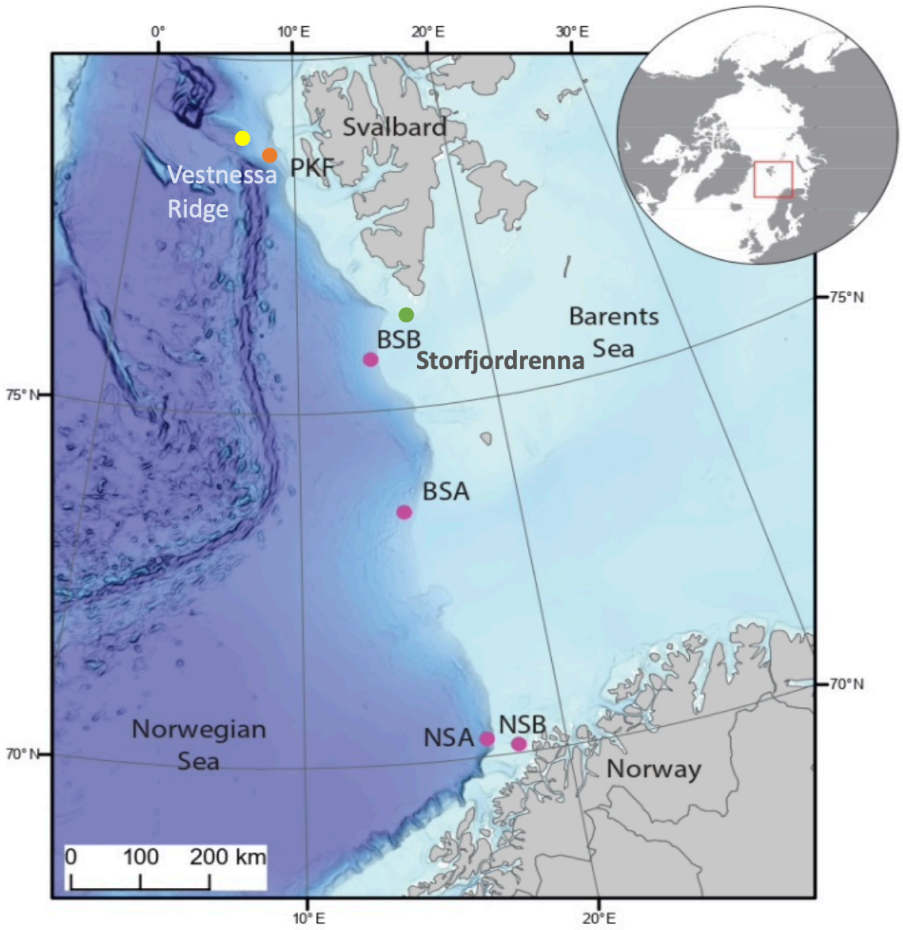

Figure 2. Map showing sampling locations for Article 1 indicated by pink dots: BSA-Barents Sea A, BSB- Barents Sea B, NSA- Norwegian Sea A, NSB- Norwegian Sea B. Sampling locations for Articles 2, 3, and 4 are indicated by dots: yellow - Vestnesa Ridge (2, 3, 4); orange - control site (2); green - Storfjordrenna pingo site (2).

3.2.2 Sampling and samples treatments

The sediment samples used in Article 2 were collected from Lomvi and Lunde pockmarks at the Vestnesa Ridge during the CAGE 15-2 cruise and from the Storfjordrenna pingos during the CAGE 17-2 cruise (Fig. 2; Table 1), both onboard R.V *Helmer Hanssen* using combined Towed Digital Camera and Multicoring System (TowCam) developed at the Woods Hole Oceanographic Institution's (WHOI) Multidisciplinary Instrumentation in Support of Oceanographic (MISO) Facility. The live-stream feed from TowCam system were used to describe the seafloor conditions and locate active methane vents, authigenic carbonates and bacterial mats, which then enabled an accurate guide of different sampling locations. Cores collected from the Vestnesa Ridge were subsampled onboard into 1-cm thick (10 cm in diameter) horizontal intervals (0–1cm, 1–2 cm, 2–3 cm) using a flat spatula and transferred into plastic containers (HDPE bottles). The sediment was divided on the basis of different treatments:

CellTracker™ Green CMFDA (*Thermo Fisher Scientific) w*ith final concentration of CellTracker™ Green CMFDA 1µM in a sample (Bernhard et al., 2006), and Rose Bengal (2g/L; Schönfeld et al., 2007), preserved with formalin and stored at 4°C until further laboratory processing. Cores collected from Storfjordrenna were processed following a similar protocol, except that the whole sediment was labelled with CellHunt Green and preserved in 96% ethanol.

The sediment used for Article 3 and 4 was collected during the POS419 expedition of the R.V *Poseidon* from the Lunde pockmark (Table 1). Selected multicores were processed on board, and subsampled into 1-cm thick horizontal slices down to 5 cm core depth. The samples were transferred into plastic containers, and stained with Rose Bengal-ethanol solution following the FOBIMO protocol (2 g\L; Schönfeld et al., 2007). Samples were kept onboard in a dark, cool room at +4 °C until further processing. Additional subcores were sampled for sediment pore water analyses, sediment methane analyses and for the determination of methane concentration, methane oxidation, and sulfate reduction. All sediment sampling procedures were conducted at +4 °C inside a cooled laboratory.

Table 1. Sampling sites locations, coordinates, water depth, date of sampling, and environmental characteristics at site of multicores used in from Article 2, 3, and 4.

Core number	Location	Coordinates	Water depth (m)	Date	Environmental characteristics
Article 2					
MC 893A MC 893B	Vestnesa Ridge (Lomvi pockmark)	79.18N, 00.44E	1200	20 May 2015	bacterial mats
MC 886	Vestnesa Ridge (Lunde pockmark)	79.38N, 00.04E	1200	20 May 2015	black mud, *Siboglinidae* tubeworms
MC 880A MC 880B	Site 7808 (Control site)	78.44N, 00.50E	889	19 May 2015	grey homogeneous mud
MC 884	Site 7808 (Control site)	78.30N, 00.82E	900	19 May 2015	grey homogeneous mud
MC 902	Storfjordrenna Pingo (GHP1)	76.91N, 16.08E	377	22 June 2017	strong flares, anemones, *Siboglinidae* tube worms
MC 917	Storfjordrenna Pingo (GHP1)	76.93N, 16.02E	377	23 June 2017	trawl marks, muddy sediment, anemones, *Siboglinidae* tubeworms, sea spider, patches of bacterial mats
MC 919	Storfjordrenna Pingo (GHP1)	76.96N, 15.98E	378	23 June 2017	trawl mark, *Siboglinidae* tubeworms, bacterial mats, anemones, carbonates
MC 920	Storfjordrenna Pingo (GHP5)	76.70N, 16.00E	379	23 June 2017	trawl marks, anemones, hard substrate (carbonates)
MC 921	Storfjordrenna Pingo (GHP5)	76.72N, 16.40E	380	23 June 2017	trawl marks, anemones, hard substrate (carbonates)

MC 922	Storfjordrenna Pingo (GHP5)	76.74N, 16.37E	386	23 June 2017	trawl marks, muddy sediment, Siboglinidae tube worms, anemones, seastars, shrimps
Article 3 and 4					
MUC 10	Vestnesa Ridge (Lunde pockmark)	79.46N 06.27E	1241	25.08.2011	*Siboglinidae* tubeworms
MUC 8	Vestnesa Ridge (Lunde pockmark)	79. 60N 06.09E	1204	25.08.2011	*Siboglinidae* tubeworms
MUC 12	Vestnesa Ridge (Lunde pockmark)	79.41N 06.13E	1235	29.08.2011	bacterial mats
MUC 11	Control site	78,77N 06,06E	1191	28.08. 2011	grey homogeneous mud

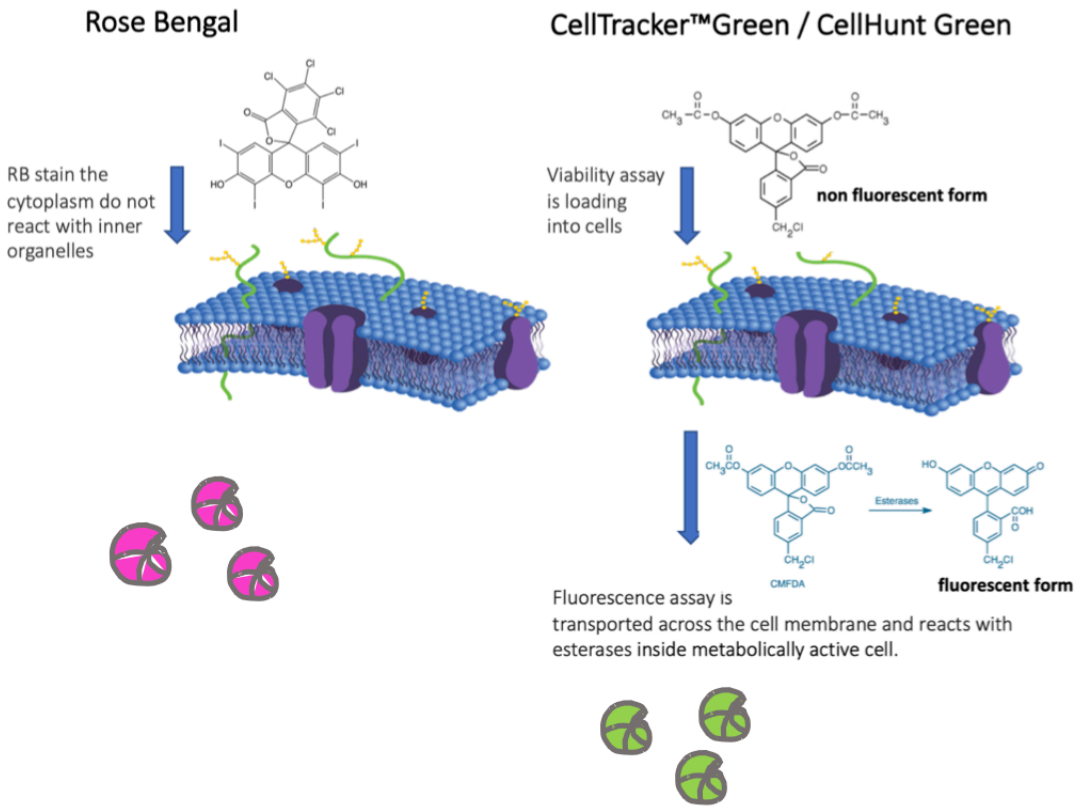

Figure 3. Comparison between Rose Bengal staining method and CellTracker™ Green/ CellHunt Green labelling. Rose Bengal reacts with cytoplasm of foraminiferal tests giving the pink colorization (panel on the left). Fluorescent assays enter a cell and non-fluorescent form is converted into the fluorescent form which further can react with thiols on proteins and peptides, giving green colours in fluorescent light (right panel).

Rose Bengal was designed to detect the presence of cytoplasm; thus, this staining method is known to colour both live and recently dead foraminiferal cytoplasm. The stain can also adhere to the organic lining of foraminiferal tests as well as to the bacteria that can be found attached or located inside these tests (Bernhard et al., 2001, 2006). Rose Bengal staining of recently dead specimens may

occur from several weeks to months after an individual's death, especially in colder, low oxygenated waters as decomposition of cytoplasm is relatively slower (Jorissen et al., 1995; Bernhard et al., 2001). Consequently, already dead, or recently dead foraminifera appear as live individuals (Bernhard et al., 2006). In contrast, CellTracker™ Green CMFDA (5-chloromethyl fluorescein diacetate; *Thermo Fisher Scientific*) and CellHunt Green (SETAREH biotech, LLC) are vital non-toxic fluorescent dyes (the same compounds) which react with internal cell components, resulting in green-fluorescent adducts (Fig. 3). Probes react with metabolically active cells only.

3.2.3 Benthic foraminiferal faunas

In Article 2, the live benthic foraminifera were identified and quantified in wet samples of material >63µm. Both CellTracker™ Green and CellHunt Green labelled organisms were examined using an epifluorescence-equipped stereomicroscope (485-nm excitation; 520-nm emission). All individuals that fluoresced brightly in at least half of their chambers were considered as live individuals, picked wet and placed on micropalaeontological slides (Fig. 4). Additionally, after selecting all green individuals from CellHunt Green labelled sediments, the residue was subsequently stained with Rose Bengal for approximately 24h. Samples stained with Rose Bengal were examined using reflected-light microscopy (Fig. 4). Foraminifera which stained dark magenta in at least half of their chambers were picked and mounted on micropaleontological slides. All collected foraminifera were identified, counted and sorted by species.

In Article 3 and 4, the Rose-Bengal stained foraminifera from the >100-µm fraction were examined under reflected-light microscopy. All benthic foraminiferal individuals that stained dark magenta and were fully filled with cytoplasm were considered to be 'living' foraminifera i.e., live + recently dead individuals, still containing cytoplasm, and individuals showing no colorization were considered as unstained, empty (dead) individuals. Specimens of the planktic foraminiferal species *Neogloboquadrina pachyderma* from each core were picked and investigated using Scanning Electron Microscopy (SEM) to detect presence of authigenic overgrowth on the outer surface of the test.

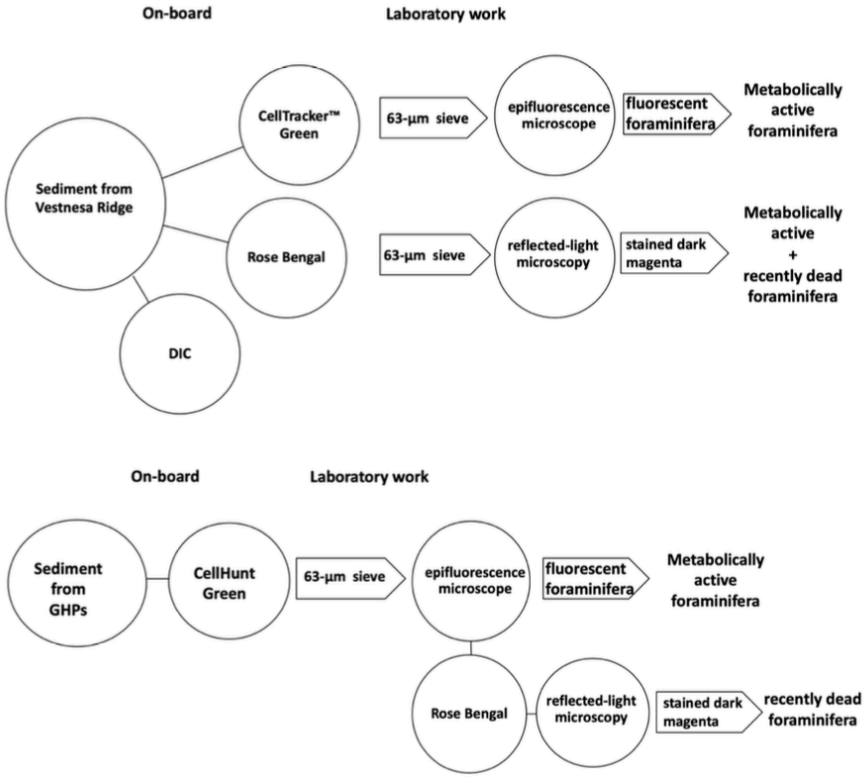

Figure 4. Onboard and laboratory processing of the sediment collected by multicorer from Vestnesa Ridge and from Storfjordrenna pingos.

3.2.4 Stable isotope analysis ($\delta^{13}C$ and $\delta^{18}O$)

For stable isotope measurements (Article 2), the most frequently occurring species such as *Melonis barleeanus*, *Cassidulina neoteretis, Nonionellina labradorica* and planktic foraminiferal species *Neogloboquadrina pachyderma* were picked, selecting approximately 10 CellTracker™ Green/ CellHunt Green labelled, Rose Bengal and empty specimens. Carbon-13 compositions of calcium carbonate tests of benthic foraminifera were determined on a MAT 253 Isotope Ratio Mass Spectrometer (Department of Geoscience, UiT) with analytical precision estimated to be better than 0.07 ‰ for $\delta^{13}C$ by measuring a certified standard NBS-19. For Article 3, stable isotope analyses were performed on both Rose Bengal stained and empty specimens of *M. barleeanus*, *C. neoteretis*, *C. wuellerstorfi*, and *N. pachyderm*a in separate analyses. When present, approximately 10 specimens of each species were taken from each sample. Isotopic measurements were performed at Woods Hole Oceanographic Institution (WHOI). Data are reported in standard notation ($\delta^{13}C$, $\delta^{18}O$), according to the Pee Dee Belemnite (PDB) standard. In both cases isotopic values were expressed as conventional δ notation against the Vienna Pee Dee Belemnite (V-PDB) standard (1.96‰, -10.21‰ and -48.95‰ for $\delta^{13}C$) and reported in parts per thousand (per mil, ‰).

4 SUMMARY OF MANUSCRIPTS/ ARTICLES

Article 1

Katarzyna Melaniuk, Joan M. Bernhard, Morten Hald, Giuliana Panieri. **Impact of hypoxia and high *p*CO_2 and diet on benthic foraminiferal growth: experiment with propagules.**

In this manuscript, we present the results of the laboratory experiment. The experimental set-up was designed to investigate the impact of environmental parameters, such as oxygen and *p*CO_2, and diet (methanotrophs vs algal diet) on benthic foraminiferal growth. To establish natural assemblages, sediments were collected from the western Barents Sea and the North Norwegian continental margin and further processed following the propagule method (Goldstein and Alve, 2011). The method is used to treat experimental assemblages in their original sediments, which helps to optimally mimic their natural conditions (Goldstein and Alve, 2011). To test the response of juvenile foraminifera to different environmental conditions, foraminifera-bearing sediment was split into 64 microcosms (translucent plastic containers), and evenly divided between the four experimental treatments, hosted in Biospherix C-Chambers. Each of the treatments represented different environmental parameters, including saturated oxygen to hypoxia (0.7 ml/L), modern-day *p*CO_2 (400 ppm) to elevated *p*CO_2 (2000 ppm), and dual stressors of hypoxia and elevated *p*CO_2. Once a week, half of each treatment was fed methanotrophic bacterium (*Methyloprofundus sedimenti* PKF-14), while the other half was fed a mix of marine microalgae (*Dunaliella tertiolecta* and *Isochrysis galbana*).

Results of the experiment imply that, at least to some extent, that the benthic foraminifera are able to calcify during exposure to hypoxia and/or elevated *p*CO_2 conditions. However, the responses of the foraminifera were different depending on the source of the sediment. Overall, dual-stress treatment (IV) had the strongest effect on the foraminifera. The dietary comparison shows that the methanotrophic bacteria diet did neither promote nor inhibit foraminiferal growth in the experimental conditions. To confidently conclude about an eventual impact of methanotrophs diet on foraminifera further dedicated studies are required.

Article 2

Katarzyna Melaniuk. **Effectiveness of fluorescent viability assays in studies of cold seep foraminifera.**

Article 2 presents the results of a study on live benthic foraminifera from two active methane seepage sites in the Lomvi pockmark at the Vestnesa Ridge, and from shallow cold-seep sites in Storfjordrenna, SW Svalbard on the western Barents Sea shelf (Fig. 2). Storfjordrenna hosts the so-called 'pingo' sites, where methane is released from pingo-like mounds on the seafloor, many of which contain gas hydrates. One of the investigated gas hydrate pingos (GHPs) is active (GHP1), while the other is presently inactive (GHP5) and considered 'post-active'. In order to distinguish live foraminifera, as an alternative to the commonly used Rose Bengal staining method, we used CellTracker™ Green CMFDA or CellHunt Green green-fluorescent probes, thus indicating only metabolically active foraminifera. To determine whether methane seepage has any effects on the carbon isotopic signatures of primary calcite of live benthic foraminifera, the $\delta^{13}C$ measured in CellTracker™ Green or CellHunt Green labelled (metabolically active), Rose Bengal stained (recently dead + dead individuals from Vestnesa Ridge, or recently dead foraminifera from Storfjordrenna), and unstained ('certified' dead) have been compared. The study showed a presence of metabolically active foraminifera in methane affected sediment from both Vestnesa Ridge and Storfjordrenna.

The results confirmed that Rose Bengal overestimated the number of live foraminifera when compared to the numbers obtained with fluorescent probes. The dominant calcareous species were *Melonis barleeanus* and *Cassidulina neoteretis* at Vestnesa Ridge and *M. barleeanus* and *Nonionelina labradorica* at Storfjordrenna. No endemic species were observed in this study. Except, for the foraminifera from the core MC 919 (Storfjordrenna) there is no clear evidence that $\delta^{13}C$ in tests of live foraminifera has been significantly affected by methane-derived carbon during biomineralization in any of the investigated sites. The combined use of the fluorogenic probe and the conventional Rose Bengal staining revealed minor shifts in species compositions and differences in ratios between live and recently dead foraminifera from the investigated pingo sites (active versus inactive).

Article 3

Katarzyna Melaniuk, Kamila Sztybor, Tina Treude, Stefan Sommer, Tine L. Rasmussen. **Evidence for influence of methane seepage on isotopic signatures in living deep-sea foraminifera, 79 °N**.

Article 3 reports on a study of isotopic signatures ($\delta^{13}C$ and $\delta^{18}O$) measured in of benthic foraminifera, together with biogeochemical data from sediments at Arctic seep sites from Vestnesa Ridge (79°N, Fram Strait) at c. 1200 m water depth. Here, we studied the informally named 'Lunde' pockmark focusing on three benthic species: *Melonis barleeanus* (intermediate to deep-infaunal species), *Cassidulina neoteretis* (shallow infaunal species) and *Cibicidoides wuellerstorfi* (epibenthic, suspension-feeding species) and their isotope signals. The upper 5 cm of the sediment of multicores from three different types of seep environments (bacterial mat, *Siboglinidae* worm field and non-seep control sites) were sliced into 1-cm think samples and stained. Stable isotopes were measured in both tests of Rose Bengal stained specimens and empty tests of the three species. Also, specimens the planktic foraminiferal species *Neogloboquadrina pachyderma* (dead specimens) were measured. Our study confirms that living benthic foraminifera are able to incorporate methane-derived carbon into their shells during their lifespan, most likely via feeding on methanotrophic bacteria. Methane-derived carbon can shift the $\delta^{13}C$ signature of living (Rose Bengal-stained) foraminifera towards lower $\delta^{13}C$ values. We observed that the $\delta^{13}C$ signature of foraminiferal tests is linked to methane-related processes, such as aerobic (MOx) and anaerobic methane oxidation (AOM). The $\delta^{13}C$ recorded in tests of RB -stained *M. barleeanus* was as low as -5.21‰ from the *Siboglinidae* field (the site dominated by MOx) indicating methane influence on the signature in the primary calcite of the foraminifera. Under other conditions, at the sediment dominated by AOM and covered by bacterial mats, the $\delta^{13}C$ signature of empty tests were influenced by methane-derived authigenic carbonates (MDAC). The $\delta^{13}C$ reach values as low as -6.48‰ (*M. barleeanus*), and even -6.17‰ for the epibenthic species *C. wuellerstorfi.* Because, AOM is a strong contributor to authigenic carbonate overgrowth, MDAC precipitation may severely overprint the initial isotopic signature of foraminiferal tests, even at shallow depth such a 3–4 cm (in this study). Additionally, we show a connection between the presence of overgrowth of MDAC and high $\delta^{18}O$ values in tests of dead specimens of benthic foraminiferal species *C. neoteretis.*

Article 4

Katarzyna Melaniuk, Kamila Sztybor, Tina Treude, Stefan Sommer, Marek Zajączkowski, Tine L. Rasmussen. **Response of benthic foraminifera to ecological succession in cold seeps from Vestnesa Ridge; implications for interpretations of paleo-seepage environments**

Manuscript 4 presents the result of a study on the response of living benthic foraminifera to progressing ecological succession in the development of a cold seep environment. Sediment samples used herein are the same as for Articles 2 and 3, with a greater focus on the samples from Vestnesa Ridge: the 'Lomvi' and 'Lunde' pockmarks. The distribution and species composition of metabolically active (CellTracker™Green labelled) and live (Rose Bengal-stained) foraminifera were analyzed in relation to the geochemical properties of the pore water, presence of bacterial mats, and distribution of macrofaunas (e.g., *Siboglinidae* tubeworms) in comparison to non-seep environments.

Ecological succession is a term used to describe the natural process of change in the faunal structures of an ecological community over time. At cold seeps, ecological succession refers to the duration of methane seepage and is linked to changes in biochemistry of the sediment and benthic faunal communities. Bergquist et al. (2003) suggest a general pattern of ecological successions in the seep environments i.e., stages 1, 2, and 3: from a patchy distribution of bacterial mats and initial seepage at stage 1, to dense microbial mats with H_2S production at stage 2, to authigenic rock formation and increasing tubeworms aggregations at stage 3, and eventually formation of long-lasting coral reefs after the seepage declines, as an eventual stage 4. The results of the study show that the distribution patterns of benthic foraminifera change accordingly to the progressing ecological succession of the seep environment. For example, at the initial stage (stage 1), oxygen is still available to the foraminifera, and as a result the species composition is similar to control sites, the main species being *Melonis barleeanus* and *Cassidulina neoteretis*. At stage 2 (with maximum seepage), high concentrations of H_2S create hostile conditions for benthic foraminifera. As a result, the samples were almost barren of foraminifera. At stage 3, moderate methane seepage supports a foraminiferal community of both calcareous and agglutinated species. The presence of chemosynthetic *Siboglinidae* tube worms may potentially support epibenthic *Cibicidoides wuellerstorfi* communities by generating a secondary hard bottom.

Despite the differences between each stage of faunal and environmental successions, none of the faunal characteristics can be used as an exclusive indicator of methane emission or stages of its environments in palaeoceanographic interpretations.

5 SYNTHESIS AND FUTURE WORK

The emphasis of this thesis is on improving the understanding of the distribution of living benthic foraminifera and carbon isotopic signatures in their tests in relation to methane seepage in the Fram Strait and Storfjordrenna (Barents Sea). This work consists of four research articles. In Article 1, the results of a laboratory experiment are presented. The second and fourth articles show the results of an analysis of modern foraminifera assemblages from surface sediments collected from two Arctic locations: pockmarks Lunde and Lomvi at Vestnesa Ridge (~1200m depth), and active and post-active gas hydrate pingos at a relatively shallow methane seep in Storfjordrenna (~400m depth; western Barents Sea; Fig. 2). The articles 2 and 3 show the result of isotopic analyses ($\delta^{13}C$ and $\delta^{18}O$) of cold seep associated foraminifera. The main conclusions based on the results of this work are presented below:

5.1 Laboratory experiment

The experiment was an approach to study the response of benthic foraminifera to environmental stress and dual-stress conditions (combined low oxygen and high pCO_2), as well as the first study in which foraminifera were fed with a methanotroph bacterium *Methyloprofundus sedimenti* PKF-14 in controlled laboratory conditions, using natural sediment from the Nordic Seas and Barents Sea. This experiment demonstrates, the ability of benthic foraminifera to both grow and calcify, at least to some extent, under potentially challenging conditions of hypoxia (O_2, 0.7ml/L) and elevated-pCO_2 (2000 ppm) showing that foraminifera are very much adaptable to temporary stress conditions.

Depending on the sources of sediment the response of the benthic foraminifera was different. Overall, the dual-stress treatment had the most significant impact on the foraminifera reducing the yield size by about 50% compared to modern-day treatments (I) or inhibiting the calcification completely, which was manifested by barren replicates. The most notable exception was the foraminiferal yield from Norwegian Sea B sediments where individuals seemed to be more resistant to the combined effect of both stressors. Analogously to the experiment, we can expect that the response of a benthic foraminiferal population to the same stressors will depend on the original species composition (pre-seep species composition) within the given methane seep. Some of the species,

particularly those adapted to high organic content (e.g., Akimoto et al., 1994, Rathburn et al., 2000, 2003, Bernhard et al., 2001) are also pre-adapted to cold-seep conditions and have the potential to thrive while other species might completely die out. Overall, environmental conditions seem to impact the growth of foraminifera more than the type of food offered. This means that within cold seeps, even when food is available, geochemical properties of the sediment might put limits on the distribution of the foraminifera. However, further dedicated studies are required to confidently conclude the impact of the methanotroph diet on foraminifera.

The results of the experiment highlight the importance of multi-factor laboratory experiments in studies on foraminiferal ecology. Should the experiment be repeated in the future, I suggest some improvements be made. First of all, the propagule method worked quite well as a set up to study the response of the foraminifera to environmental parameters, but it is not a suitable approach to study the dietary preferences of these organisms. The natural sediments used as a source of propagules (small/juvenile foraminifera) was not sterile and was thus contaminated by pre-experimental organic matter, which could potentially have served as a food source for some of the foraminifera. Therefore, to avoid such contamination, a future feeding experiment should either use pre-labelled microbes to facilitate the recognition of the experimental source of carbon, or the foraminifera should be picked from the sediment and transferred to a sterile environment. In addition, it would be beneficial to use for example Calcein (a cell-permeant dye) in order to mark experimental calcite (i.e., part of the tests built during the experiment).

5.2 Foraminiferal faunas

The study presented in Article 2 and 4 show that the distribution patterns of benthic foraminiferal species are influenced by seepage of methane, and results in uneven distribution of specimens within in the same seep. At Storfjordrenna pingos the density of metabolically active (Cell Tracker Green™ labelled) foraminifera gradually decreases from 12/10cc at the edge of the active gas hydrate pingo 1 (GHP1) with moderate influence of methane to almost barren sediment at the top of the pingo where the gas seeps out (Article 2). Similarly, at Vestnesa Ridge the distribution patterns and the species composition of the benthic foraminiferal faunas change according to the intensity of methane seepage and follow the progressing ecological succession model suggested by Bergquist et al., 2003 (Article 4).

In both cases it seems that foraminifera are indeed attracted to bacterial mats as a potential food source, as suggested earlier (Hill et al., 2005; Bernhard et al., 2010), but only when methane seepage is moderate or low and aerobic methane oxidation (MOx) is the dominant process e.g., ecological succession stage 1 or 3 (Article 4), and as at the edge of the active GHP1 (Storfjordrenna; Article 2). In sediments affected by AOM, with strong methane seepage (stage 2) or top of the GHP1,

even when potential food is available (i.e., bacterial mats are present), geochemistry of the sediment e.g., low oxygen concentration and presence of hydrogen sulfide, as well as sediment movements (in case of the top of GHP1), create unstable and hostile conditions for benthic foraminifera.

Both investigated sites are characterized by a comparable faunal pattern, with no endemic species and the observed species are similar to those from other nearby non-seep locations. No particular species or group of species potentially could indicate methane seepage. The foraminiferal fauna was dominated by species adapted to high organic content and low oxygen conditions. At Storfjordrenna, the main species were *Melonis barleeanus* and *Nonionellina labradorica,* and at Vestnesa Ridge *Melonis barleeanus*, *Cassidulina neoteretis*, and *Reophax* spp., predominated. All of the species are common in the Arctic. Especially, the higher abundance of opportunistic species at Storfjordrenna pingos can reflect both methane seepage and/or the Arctic spring bloom. Interestingly, it seems that at Vestnesa Ridge presence of *Siboglinidae* tube aggregations promotes *Cibicidoides wuellerstorfi* communities by generating secondary hard bottom.

Based on results of this thesis is it difficult if not impossible to find the link between methane seepage and distribution patterns of benthic foraminiferal species that could be further utilised as a template in reconstructions of the strength of past methane emissions. Cold seeps are ephemeral environments that can change rapidly over time, thus more high-resolution studies, preferably by seasonal sampling, in combination with analysis of the geochemistry of the sediment and pore water is recommended in order to obtain a detailed picture of the ecology of modern foraminiferal faunas within methane seeps. Such measures are thus recommended in order to further elucidate the link between methane seepage and foraminiferal distribution patterns.

5.3 Fluorescence viability in the study of living foraminiferal assemblages

This study confirmed that Rose Bengal staining overestimates the number of live benthic foraminifera in a sample. Rose Bengal always indicates a higher number of 'live' foraminifera when compared to CellTracker™ Green or CellHunt Green labelling (Article 2). Studies of benthic foraminiferal assemblages from Vestnesa Ridge show that a) there significantly less live (CellTracker™ Green labelled) foraminifera when compared to live + recently dead (Rose Bengal- stained) individuals; b) in some of the samples, despite the lack of live foraminifera, Rose Bengal still indicated the presence of cytoplasm, which would normally be considered as a ‘live’ individual; c) there is no significant difference between the $\delta^{13}C$ measured in the CellTracker™ Green labelled and the Rose Bengal stained foraminifera.

Samples from the Storfjordrenna pingos site were processed differently. Collected sediment was first labelled with CellHunt Green, live foraminifera were selected, and only afterwards the residue

was stained with a Rose Bengal solution. This approach allowed a) to distinguish metabolically active (CellHunt Green labelled) foraminifera from recently dead individuals (Rose Bengal- stained); b) observe minor changes in foraminiferal populations, which would otherwise be overlooked, c) observe a variation in the ratio between live and recently dead foraminifera. In geochemically active habitats (the active GHP1), approximately 40% of picked foraminifera were actually alive at the time of collection, whereas the other 60% were recently dead individuals. In the post-active GHP5, this percentage is the opposite. This difference in populations might indeed reflect a more unstable and variable habitat, probably associated with methane seepage. Alternatively, because of lower decomposition rates in cold low-oxygen environments, the Rose Bengal stained individuals may have been dead for a relatively longer period of time at the active GHP1 (e.g., Jorissen et al., 1995; Bernhard et al., 2001), which could explain their over-abundance compared to non-seep sites. A notable surprise is the presence of a high abundance of fluorescent labelled *Buccella frigida* in samples from the active GHP1 with lack of Rose Bengal-stained individuals. This implies that the presence of live *B. frigida* might actually reflect a relatively recent appearance of bacterial mats associated with methane seepage.

Our current understanding of ecology of foraminifera from cold seeps is based on studies that have applied the Rose Bengal staining method. As mentioned above, not all Rose Bengal-stained foraminifera are actually alive during the sampling. It was documented that staining of recently dead specimens may occur several weeks after their death (e.g., Jorissen et al., 1995; Bernhard et al., 2001). Thus, it is controversial if, in earlier published papers, foraminifera indicated as living were actually metabolically active or that Rose Bengal indicated dead cytoplasm as well. From the palaeoceanographically perspective, poor understanding of the ecology of foraminifera might result in inaccurate interpretations. For example, individuals that recently died out due to methane seepage could potentially still be stained by Rose Bengal, while simultaneously due to partly decomposed cytoplasm, the exposed surface of the tests have been affected by Methane-Derived Authigenic Carbonates (MDAC) precipitation (Mackensen et al., 2006). As a result, a depleted $\delta^{13}C$ signal can be misinterpreted as the incorporation of methane derived carbon during biomineralization, when in fact it was the result of post-mortem deposition in methane-charged sediment. Fossil assemblages that represent a wide time range of foraminifera may thus reflect a mix of several smaller methane seepage events and/or changes in foraminiferal populations due to local environmental variations.

Despite the more time-consuming protocol and higher costs compared to Rose Bengal, both CellHunt Green and CellTracker™ Green are valuable tools in studies of the ecology of benthic foraminiferal species. In order to obtain a better picture of the modern fauna, it is recommended to use fluorescence viability assays in studies of foraminiferal assemblages. CellHunt Green and CellTracker™ Green are equally good indicators, with the former being the more affordable option.

5.4 Carbon isotope signatures in tests of live foraminifera

Results reported in Article 2 show no substantial influence of methane-derived carbon on primary calcite in metabolically active foraminifera. This is most likely because the ambient pore water (microhabitat in which foraminifera lives) was not saturated enough in depleted C-13 to influence the isotopic signature of the benthic foraminifera. There were also no signs of methane-derived authigenic carbonates (MDAC) precipitation on empty foraminiferal tests. This supports the hypothesis previously reported from other studies that low $\delta^{13}C$ values measured in fossil foraminiferal tests are due to authigenic overgrowth and reflect processes that took place after foraminiferal tests have been deposited in the methane charged sediment.

Nevertheless, since the $\delta^{13}C$ was measured on pools of specimens (N=10), it is possible that at least some of the live individuals had more negative $\delta^{13}C$ signatures than others, or that some chambers indeed incorporated methane-derived carbon. To obtain more accurate $\delta^{13}C$ values and to draw a more robust conclusion, analysis of single CellTracker™ Green or CellHunt Green labelled foraminifera, or more advanced techniques, such as for example secondary-ion mass spectrometry (SIMS), are recommended.

Contrasting results are presented in Article 3, were data shows that, at the *Siboglinidae* field with moderate seepage of methane, dominance of MOx, and low concentrations of sulfide, the live benthic foraminifera (RB-stained) incorporate methane-derived carbon, most likely by feeding on methane-oxidizing bacteria or by direct intake of $^{12}CO_2$ produced during MOx. Additionally, primary signals measured in empty foraminiferal tests of benthic and planktic foraminifera from bacterial mats (MUC12) were overprinted by MDAC precipitation. MDAC represents strong methane seepage, and indicate sediment oversaturated in HCO^{3-} derived from sulfate-reducing and methane-oxidizing microbial consortiums in the sulfate-methane stability zone (SMTZ). Overgrowth starts coating the tests at relatively shallow depth 2–3 cm in the multicores from bacterial mats, causing a $\delta^{13}C$ signature shifts of tests towards low values down to -6.48‰ for fossil *Melonis barleeanus*, 6.18‰ for *Cassidulina neoteretis*, and -6.17‰ for *Cibicides wuellerstorfi*.

MDAC overprints seem to affect the $\delta^{18}O$ signature of fossil *C. neoteretis*. The $\delta^{18}O$ have a relatively heavy signature, and reach up to 5.17‰. It was already suggested that high $\delta^{18}O$ measured in fossil records indicated gas hydrate dissociation. Nevertheless, considering that the sediment collected was in a deep-sea Arctic setting and represents modern sediment, the presence of high $\delta^{18}O$ is due to gas hydrate dynamics (dissipation, production as well as an AOM activity), it may not result exclusively from gas hydrate dissociation due to the present climate change and warming of deep waters. Which has to be considered while interpreting fossil data.

Similar to the species distribution, the carbon isotopic signature measured in both living and empty foraminiferal tests depend on intensity of MOx and AOM and it changes depending on methane flux (i.e., methane seep intensity). Fossil records reflect the cumulative history of methane seepage which took place during the lifespan of the benthic foraminifera as well as post mortem processes affecting it shell. Therefore, in context of palaeoceanographic studies it seems that depletions in $\delta^{13}C$ measured in fossil foraminiferal records can only provide qualitative information about presence of seepage as it was suggested by Martin et al., (2004). Additionally, under certain geochemical conditions, the cold seep environment is hostile for benthic foraminifera i.e., there are no foraminifera for isotopic measurements at all. It is however, promising that the SMTZ-zone is close to sediment surface when methane seepage is strong (Borowski et al., 1996) (2–3 cm at the bacterial mat site); which depending on the sedimentation rates at the time will allow at least timing of when paleo-methane seepage was at its strongest at a given site.

6 REFERENCES

Akimoto, K., Tanaka, T., Hattori, M., Hotta, H., 1994. Recent benthic foraminiferal assemblages from the cold seep communities}a contribution to the methane gas indicator. In: Tsuchi, R. (Ed.), Pacific Neogene Events in Time and Space. University of Tokyo Press. 11–25.

Allison, N., W. Austin, D. Paterson, and H. Austin. 2010. "Culture studies of the benthic foraminifera Elphidium williamsoni: Evaluating pH, Δ[CO32−] and inter-individual effects on test Mg/Ca." *Chemical Geology* 274 (1): 87-93. .

Alve, Elisabeth, and Susan T. Goldstein. 2010. "Dispersal, survival and delayed growth of benthic foraminiferal propagules." *Journal of Sea Research* 63 (1): 36-51. https://www.sciencedirect.com/science/article/pii/S1385110109000951.

Alve E, Goldstein ST (2014) The propagule method as an experimental tool in foraminiferal ecology. In: Kitazato H, Bernhard JM (eds) Approaches to Study Living Foraminifera. Environmental Science and Engineering. Springer, Tokyo. DOI: 10.1007/978-4-431-54388-6

Archer D., Buffett B., Brovkin V. 2009. "Ocean methane hydrates as a slow tipping point in the global carbon cycle." *Proceedings of the National Academy of Sciences* 106: 20596-20601. https://doi.org/https://doi.org/10.1073/pnas.0800885105.

Åström, E. K. L., M. L. Carroll, W. G. Ambrose, Jr., and J. Carroll. 2016. "Arctic cold seeps in marine methane hydrate environments: impacts on shelf macrobenthic community structure offshore Svalbard." *Marine Ecology Progress Series* 552: 1-18. https://www.int-res.com/abstracts/meps/v552/p1-18/.

Åström, E. K. L., Carroll, M. L., Ambrose, W. G., and Carroll, J. 2016. Arctic cold seeps in marine methane hydrate environments: Impacts on shelf macrobenthic community structure offshore Svalbard. Marine Ecology Progres Series. 552, 1–18. doi: 10.3354/meps11773.

Barry, J. P., R. E. Kochevar, and C. H. Baxter. 1997. "The influence of pore-water chemistry and physiology on the distribution of vesicomyid clams at cold seeps in Monterey Bay: Implications for patterns of chemosynthetic community organization." *Limnology and Oceanography* 42 (2): 318-328. https://aslopubs.onlinelibrary.wiley.com/doi/abs/10.4319/lo.1997.42.2.0318.

Bernhard, Joan M., Kurt R. Buck, and James P. Barry. 2001. "Monterey Bay cold-seep biota: Assemblages, abundance, and ultrastructure of living foraminifera." *Deep Sea Research Part I: Oceanographic Research Papers* 48 (10): 2233-2249.

https://www.sciencedirect.com/science/article/pii/S0967063701000176.
Bernhard, Joan M., Jonathan B. Martin, and Anthony E. Rathburn. 2010. "Combined carbonate carbon isotopic and cellular ultrastructural studies of individual benthic foraminifera: 2. Toward an understanding of apparent disequilibrium in hydrocarbon seeps." *Paleoceanography* 25 (4). https://agupubs.onlinelibrary.wiley.com/doi/abs/10.1029/2010PA001930.
Bernhard, Joan M., Dorinda R. Ostermann, David S. Williams, and Jessica K. Blanks. 2006. "Comparison of two methods to identify live benthic foraminifera: A test between Rose Bengal and CellTracker Green with implications for stable isotope paleoreconstructions." *Paleoceanography* 21 (4). https://agupubs.onlinelibrary.wiley.com/doi/abs/10.1029/2006PA001290.
Boetius, Antje, Katrin Ravenschlag, Carsten J. Schubert, Dirk Rickert, Friedrich Widdel, Armin Gieseke, Rudolf Amann, Bo Barker Jørgensen, Ursula Witte, and Olaf Pfannkuche. 2000. "A marine microbial consortium apparently mediating anaerobic oxidation of methane." *Nature* 407 (6804): 623-626. https://doi.org/10.1038/35036572.
Consolaro, C., T. L. Rasmussen, G. Panieri, J. Mienert, S. Bünz, and K. Sztybor. 2015. "Carbon isotope (δ¹³C) excursions suggest times of major methane release during the last 14 kyr in Fram Strait, the deep-water gateway to the Arctic." *Clim. Past* 11 (4): 669-685. https://cp.copernicus.org/articles/11/669/2015/.
Coleman, D.F. & Ballard, R.D. 2001. A highly concentrated region of cold hydrocarbon seeps in the south- eastern Mediterranean Sea. Geo-Marine Letters 21, 162–167.
Dickens, Gerald R., Maria M. Castillo, and James C. G. Walker. 1997. "A blast of gas in the latest Paleocene: Simulating first-order effects of massive dissociation of oceanic methane hydrate." *Geology* 25 (3): 259-262. https://doi.org/10.1130/0091-7613(1997)025.
Etiope, G., G. Panieri, D. Fattorini, F. Regoli, P. Vannoli, F. Italiano, M. Locritani, and C. Carmisciano. 2014. "A thermogenic hydrocarbon seep in shallow Adriatic Sea (Italy): Gas origin, sediment contamination and benthic foraminifera." *Marine and Petroleum Geology* 57: 283-293. https://doi.org/https://doi.org/10.1016/j.marpetgeo.2014.06.006.
Fontanier, C., K. A. Koho, M. S. Goñi-Urriza, B. Deflandre, S. Galaup, A. Ivanovsky, N. Gayet, B. Dennielou, A. Grémare, S. Bichon, C. Gassie, P. Anschutz, R. Duran, and G. J. Reichart. 2014. "Benthic foraminifera from the deep-water Niger delta (Gulf of Guinea): Assessing present-day and past activity of hydrate pockmarks." *Deep Sea Research Part I: Oceanographic Research Papers* 94: 87-106. https://www.sciencedirect.com/science/article/pii/S0967063714001666.
Goldstein, S. T., and E. Alve. 2011. "Experimental assembly of foraminiferal communities from coastal propagule banks." *Marine Ecology Progress Series* 437: 1-11. https://www.int-res.com/abstracts/meps/v437/p1-11/.
Hansen Jesper, Hoff Ulrike, Sztybor Kamila, Rasmussen Tine L. 2017. Taxonomy and palaeoecology of two Late Pleistocene species of vesicomyid bivalves from cold methane seeps at Svalbard (79°N), Journal of Molluscan Studies, Volume 83, Issue 3. Pages 270–279.
Heinz, Petra, and Emmanuelle Geslin. 2012. "Ecological and Biological Response of Benthic Foraminifera Under Oxygen-Depleted Conditions: Evidence from Laboratory Approaches." In *Anoxia: Evidence for Eukaryote Survival and Paleontological Strategies*, edited by Alexander V. Altenbach, Joan M. Bernhard and Joseph Seckbach, 287-303. Dordrecht: Springer Netherlands.
Heinz, Petra; Sommer, Stefan; Pfannkuche Olaf, Hemleben, Christoph. 2005. "Living benthic foraminifera in sediments influenced by gas hydrates at the Cascadia convergent margin, NE Pacific." *Marine Ecology Progress Series* 304: 77-89. https://www.int-res.com/abstracts/meps/v304/p77-89/.
Herguera, J. C., C. K. Paull, E. Perez, W. Ussler III, and E. Peltzer. 2014. "Limits to the sensitivity of living benthic foraminifera to pore water carbon isotope anomalies in methane vent environments." *Paleoceanography* 29 (3): 273-289. https://agupubs.onlinelibrary.wiley.com/doi/abs/10.1002/2013PA002457.
Hill, T. M., J. P. Kennett, and H. J. Spero. 2003. "Foraminifera as indicators of methane-rich environments: A study of modern methane seeps in Santa Barbara Channel, California." *Marine*

Micropaleontology 49 (1): 123-138. https://www.sciencedirect.com/science/article/pii/S037783980300032X.

Hill, T. M., J. P. Kennett, and D. L. Valentine. 2004. "Isotopic evidence for the incorporation of methane-derived carbon into foraminifera from modern methane seeps, Hydrate Ridge, Northeast Pacific." *Geochimica et Cosmochimica Acta* 68 (22): 4619-4627. https://www.sciencedirect.com/science/article/pii/S0016703704005654.

Himmler Tobias, Sahy Diana, Martma Tonu, Bohrmann Gerhard, Plaza-Faverola Andrea, Bunz Stefan, Daniel J. Condon, Knies Jochen, Lepland Aivo. 2019. A 160,000-year-old history of tectonically controlled methane seepage in the Arctic. Sci Adv, 5 (8). 10.1126/sciadv.aaw1450eaaw1450

Hong, W.-L., M. E. Torres, A. Portnov, M. Waage, B. Haley, and A. Lepland. 2018. "Variations in Gas and Water Pulses at an Arctic Seep: Fluid Sources and Methane Transport." *Geophysical Research Letters* 45 (9): 4153-4162. https://agupubs.onlinelibrary.wiley.com/doi/abs/10.1029/2018GL077309.

IPCC. 2007. Climate Change 2007: The Physical Basis. New York, NY: Cambridge University Press.

Jahren, A. Hope, Nan Crystal Arens, Gustavo Sarmiento, Javier Guerrero, and Ronald Amundson. 2001. "Terrestrial record of methane hydrate dissociation in the Early Cretaceous." *Geology* 29 (2): 159-162.

Jorissen, Frans J., Henko C. de Stigter, and Joen G. V. Widmark. 1995. "A conceptual model explaining benthic foraminiferal microhabitats." *Marine Micropaleontology* 26 (1): 3-15. https://www.sciencedirect.com/science/article/pii/037783989500047X.

Katz, Miriam E., Dorothy K. Pak, Gerald R. Dickens, and Kenneth G. Miller. 1999. "The Source and Fate of Massive Carbon Input During the Latest Paleocene Thermal Maximum." *Science* 286 (5444): 1531-1533. https://science.sciencemag.org/content/sci/286/5444/1531.full.pdf.

Kennett, J. P., and L. D. Stott. 1991. "Abrupt deep-sea warming, palaeoceanographic changes and benthic extinctions at the end of the Palaeocene." *Nature* 353 (6341): 225-229. https://doi.org/10.1038/353225a0.

Knittel, Katrin, and Antje Boetius. 2009. "Anaerobic Oxidation of Methane: Progress with an Unknown Process." *Annual Review of Microbiology* 63 (1): 311-334. https://www.annualreviews.org/doi/abs/10.1146/annurev.micro.61.080706.093130.

Knittel, Katrin, Tina Lösekann, Antje Boetius, Renate Kort, and Rudolf Amann. 2005. "Diversity and Distribution of Methanotrophic Archaea at Cold Seeps." *Applied and Environmental Microbiology* 71 (1): 467-479. https://journals.asm.org/doi/abs/10.1128/AEM.71.1.467-479.2005.

Levin Lisa, A. 2005. Ecology of cold seep sediments: Interactions of fauna with flow, chemistry and microbes. In: Oceanography and Marine Biology: An Annual Review, Gibson RN, Atkinson RJA, Gordon JDM (eds) CRC Press-Taylor & Francis Group, Boca Raton, 1–46.

Mackensen, Andreas, Jutta Wollenburg, and Laetitia Licari. 2006. "Low δ13C in tests of live epibenthic and endobenthic foraminifera at a site of active methane seepage." *Paleoceanography* 21 (2). https://agupubs.onlinelibrary.wiley.com/doi/abs/10.1029/2005PA001196.

Martin, Jonathan B., Shelley A. Day, Anthony E. Rathburn, M. Elena Perez, Chris Mahn, and Joris Gieskes. 2004. "Relationships between the stable isotopic signatures of living and fossil foraminifera in Monterey Bay, California." *Geochemistry, Geophysics, Geosystems* 5 (4). https://agupubs.onlinelibrary.wiley.com/doi/abs/10.1029/2003GC000629.

Martin, Ruth A., Elizabeth A. Nesbitt, and Kathleen A. Campbell. 2010. "The effects of anaerobic methane oxidation on benthic foraminiferal assemblages and stable isotopes on the Hikurangi Margin of eastern New Zealand." *Marine Geology* 272 (1): 270-284. https://www.sciencedirect.com/science/article/pii/S0025322709000759.

Maslin, M., Owen, M., Betts, R., Day, S., Dunkley Jones, T., Ridgwell, A. 2010. "Gas hydrates: past and future geohazard?" *Philos Trans A Math Phys Eng Sci* 368 (1919): 2369-93. https://doi.org/10.1098/rsta.2010.0065.

Melaniuk, Katarzyna. 2021. "Effectiveness of Fluorescent Viability Assays in Studies of Arctic Cold Seep Foraminifera." *Frontiers in Marine Science* 8 (198). https://www.frontiersin.org/article/10.3389/fmars.2021.587748.

Millo, Christian, Michael Sarnthein, Helmut Erlenkeuser, Pieter M. Grootes, and Nils Andersen. 2005. "Methane-induced early diagenesis of foraminiferal tests in the southwestern Greenland Sea." *Marine Micropaleontology* 58 (1): 1-12. https://www.sciencedirect.com/science/article/pii/S0377839805000885.

Milucka, Jana, Timothy G. Ferdelman, Lubos Polerecky, Daniela Franzke, Gunter Wegener, Markus Schmid, Ingo Lieberwirth, Michael Wagner, Friedrich Widdel, and Marcel M. M. Kuypers. 2012. "Zero-valent sulphur is a key intermediate in marine methane oxidation." *Nature* 491 (7425): 541-546. https://doi.org/10.1038/nature11656.

Olu, Karine, Sophie Lance, Myriam Sibuet, Pierre Henry, Aline Fiala-Médioni, and Alain Dinet. 1997. "Cold seep communities as indicators of fluid expulsion patterns through mud volcanoes seaward of the Barbados accretionary prism." *Deep Sea Research Part I: Oceanographic Research Papers* 44 (5): 811-841. https://www.sciencedirect.com/science/article/pii/S0967063796001239.

Orphan, Victoria J., Christopher H. House, Kai-Uwe Hinrichs, Kevin D. McKeegan, and Edward F. DeLong. 2001. "Methane-Consuming Archaea Revealed by Directly Coupled Isotopic and Phylogenetic Analysis." *Science* 293 (5529): 484-487. https://doi.org/10.1126/science.1061338.

Panieri, Giuliana. 2006. "THE EFFECT OF SHALLOW MARINE HYDROTHERMAL VENT ACTIVITY ON BENTHIC FORAMINIFERA (AEOLIAN ARC, TYRRHENIAN SEA)." *Journal of Foraminiferal Research* 36 (1): 3-14. https://doi.org/10.2113/36.1.3. https://doi.org/10.2113/36.1.3.

Panieri, Giuliana, and Barun K. Sen Gupta. 2008. "Benthic Foraminifera of the Blake Ridge hydrate mound, Western North Atlantic Ocean." *Marine Micropaleontology* 66 (2): 91-102. https://www.sciencedirect.com/science/article/pii/S0377839807000862.

Phrampus Benjamin , Hornbach, Matthew J. 2012. "Recent changes to the Gulf Stream causing widespread gas hydrate destabilization." *Nature* 490: 527–530.

Phrampus, Benjamin J., and Matthew J. Hornbach. 2012. "Recent changes to the Gulf Stream causing widespread gas hydrate destabilization." *Nature* 490 (7421): 527-530. https://doi.org/10.1038/nature11528.

Pierre-Antoine Dessandier, Chiara Borrelli, Dimitri Kalenitchenko, Giuliana Panieri. 2019. "Benthic Foraminifera in Arctic Methane Hydrate Bearing Sediments." *Frontiers in Marine Science* 6: 765.

Rathburn, A. E., Lisa A. Levin, Zachary Held, and K. C. Lohmann. 2000. "Benthic foraminifera associated with cold methane seeps on the northern California margin: Ecology and stable isotopic composition." *Marine Micropaleontology* 38 (3): 247-266. https://www.sciencedirect.com/science/article/pii/S0377839800000050.

Rathburn, Anthony E., M. Elena Pérez, Jonathan B. Martin, Shelley A. Day, Chris Mahn, Joris Gieskes, Wiebke Ziebis, David Williams, and Amanda Bahls. 2003. "Relationships between the distribution and stable isotopic composition of living benthic foraminifera and cold methane seep biogeochemistry in Monterey Bay, California." *Geochemistry, Geophysics, Geosystems* 4 (12). https://agupubs.onlinelibrary.wiley.com/doi/abs/10.1029/2003GC000595.

Reeburgh, William S. 2007. "Oceanic Methane Biogeochemistry." *Chemical Reviews* 107 (2): 486-513. https://doi.org/10.1021/cr050362v.

Ruppel, Carolyn D., and John D. Kessler. 2017. "The interaction of climate change and methane hydrates." *Reviews of Geophysics* 55 (1): 126-168. https://agupubs.onlinelibrary.wiley.com/doi/abs/10.1002/2016RG000534.

Sahling, Heiko, Sergey V. Galkin, Anatoly Salyuk, Jens Greinert, Hilmar Foerstel, Dieter Piepenburg, and Erwin Suess. 2003. "Depth-related structure and ecological significance of cold-seep communities—a case study from the Sea of Okhotsk." *Deep Sea Research Part I: Oceanographic Research Papers* 50 (12): 1391-1409. https://www.sciencedirect.com/science/article/pii/S096706370300147X.

Schneider, Andrea, Antoine Crémière, Giuliana Panieri, Aivo Lepland, and Jochen Knies. 2017. "Diagenetic alteration of benthic foraminifera from a methane seep site on Vestnesa Ridge (NW Svalbard)." *Deep Sea Research Part I: Oceanographic Research Papers* 123: 22-34. https://www.sciencedirect.com/science/article/pii/S0967063716301996.

Sen Gupta, B.K., Platon, E., Bernhard, J.M. & Aharon, P. 1997. Foraminiferal colonization of hydrocarbon- seep bacterial mats and underlying sediment, Gulf of Mexico Slope. Journal of Foraminiferal Research 27, 292–300

Sen, A., E. K. L. Åström, W. L. Hong, A. Portnov, M. Waage, P. Serov, M. L. Carroll, and J. Carroll. 2018. "Geophysical and geochemical controls on the megafaunal community of a high Arctic cold seep." *Biogeosciences* 15 (14): 4533-4559. https://bg.copernicus.org/articles/15/4533/2018/.

Sen Gupta, Barun K., Lorene E. Smith, and Melissa K. Lobegeier. 2007. "Attachment of Foraminifera to vestimentiferan tubeworms at cold seeps: Refuge from seafloor hypoxia and sulfide toxicity." *Marine Micropaleontology* 62 (1): 1-6. https://www.sciencedirect.com/science/article/pii/S0377839806001101.

Serov, Pavel, Sunil Vadakkepuliyambatta, Jürgen Mienert, Henry Patton, Alexey Portnov, Anna Silyakova, Giuliana Panieri, Michael L. Carroll, JoLynn Carroll, Karin Andreassen, and Alun Hubbard. 2017. "Postglacial response of Arctic Ocean gas hydrates to climatic amelioration." *Proceedings of the National Academy of Sciences* 114 (24): 6215-6220. https://www.pnas.org/content/pnas/114/24/6215.full.pdf.

Smith, L. M., J. P. Sachs, A. E. Jennings, D. M. Anderson, and A. deVernal. 2001. "Light δ13C events during deglaciation of the East Greenland Continental Shelf attributed to methane release from gas hydrates." *Geophysical Research Letters* 28 (11): 2217-2220. https://agupubs.onlinelibrary.wiley.com/doi/abs/10.1029/2000GL012627.

Sloan, E.D.D. 1990. Clathrate Hydrates of Natural Gases. New York: Marcel Dekker.

Somero, G.N., Childress, J.J. & Anderson, A.E. 1989. Transport, metabolism, and detoxification of hydrogen sulfide in animals from sulfide-rich marine environments. Aquatic Sciences 1, 591–614.

Strąpoć, Dariusz, Benjamin Jacquet, Oscar Torres, Shahnawaz Khan, Esra Inan Villegas, Heidi Albrecht, Bruno Okoh, and Daniel McKinney. 2020. "Deep biogenic methane and drilling-associated gas artifacts: Influence on gas-based characterization of petroleum fluids." *AAPG Bulletin* 104 (4): 887-912.. https://doi.org/10.1306/08301918011.

Sztybor, Kamila, and Tine L. Rasmussen. 2017. "Diagenetic disturbances of marine sedimentary records from methane-influenced environments in the Fram Strait as indications of variation in seep intensity during the last 35 000 years." *Boreas* 46 (2): 212-228. https://onlinelibrary.wiley.com/doi/abs/10.1111/bor.12202.

Thomsen Elsebeth, Rasmussen, Tine L., Sztybor Kamila, Hanken, Nils-Martin, Tendal, Ole Secher & Uchman Alfred. 2019. Cold-seep macrofaunal assemblages in cores from Vestnesa Ridge, eastern Fram Strait, during the past 45000 years. Polar Research, 38, 3310. https://doi.org/10.33265/polar.v38.3310

Torres, M. E., Mix, A. C., Kinports, K., Haley, B., Klinkhammer, G. P., McManus, J., de Angelis, M. A. 2003. "Is methane venting at the seafloor recorded by δ13C of benthic foraminifera shells?" *Paleoceanography* 18 (3). https://agupubs.onlinelibrary.wiley.com/doi/abs/10.1029/2002PA000824.

Treude, Tina, Victoria Orphan, Katrin Knittel, Armin Gieseke, Christopher H. House, and Antje Boetius. 2007. "Consumption of Methane and CO₂ by Methanotrophic Microbial Mats from Gas Seeps of the Anoxic Black Sea." *Applied and Environmental Microbiology* 73 (7): 2271-2283. https://journals.asm.org/doi/abs/10.1128/AEM.02685-06 .

Tryon, Michael D., and Kevin M. Brown. 2001. "Complex flow patterns through Hydrate Ridge and their impact on seep biota." *Geophysical Research Letters* 28 (14): 2863-2866. https://agupubs.onlinelibrary.wiley.com/doi/abs/10.1029/2000GL012566.

Tryon, Michael D., Brown, Kevin M. and Torres, Marta E. 2002. Fluid and chemical fluxes in and out of sediments hosting hydrate deposits on Hydrate Ridge, OR, II: hydrological processes. Earth and Planetary Science Letters 201, 541–557.

Valentine, David L. 2002. "Biogeochemistry and microbial ecology of methane oxidation in anoxic environments: a review." *Antonie van Leeuwenhoek* 81 (1): 271-282. https://doi.org/10.1023/A:1020587206351.

Wefer, G., P. M. Heinze, and W. H. Berger. 1994. "Clues to ancient methane release." *Nature* 369 (6478): 282-282. https://doi.org/10.1038/369282a0.

Whiticar, Michael J. 1999. "Carbon and hydrogen isotope systematics of bacterial formation and oxidation of methane." *Chemical Geology* 161 (1): 291-314. https://www.sciencedirect.com/science/article/pii/S0009254199000923.

Wollenburg, J. E., and A. Mackensen. 2009. "The ecology and distribution of benthic foraminifera at the Håkon Mosby mud volcano (SW Barents Sea slope)." *Deep Sea Research Part I: Oceanographic Research Papers* 56 (8): 1336-1370.. https://www.sciencedirect.com/science/article/pii/S0967063709000363.

Wollenburg, Jutta E., Markus Raitzsch, and Ralf Tiedemann. 2015. "Novel high-pressure culture experiments on deep-sea benthic foraminifera — Evidence for methane seepage-related δ13C of Cibicides wuellerstorfi." *Marine Micropaleontology* 117: 47-64. https://www.sciencedirect.com/science/article/pii/S0377839815000341.

Article 1.

Impact of hypoxia and high pCO_2 and diet on benthic foraminiferal growth: experiment with propagules.

Impact of hypoxia and high pCO_2 and diet on benthic foraminiferal growth: experiment with propagules.

Katarzyna Melaniuk[1], Joan M. Bernhard[2], Morten Hald[3], Giuliana Panieri[1]

1. Centre of Arctic Gas Hydrate, Environment and Climate CAGE, Department of Geosciences, UiT The Arctic University of Norway, 9010 Tromsø, Norway
2. Geology & Geophysics Department, Woods Hole Oceanographic Institution, Woods Hole, MA 02543, USA
3. Department of Geosciences, UiT The Arctic University of Norway, Tromsø

Under revision *Marine Micropaleontology*

Abstract

Benthic foraminifera, one of the largest groups of marine calcifiers, are limited in their distribution by oxygen, organic matter, and carbonate bioavailability. For this reason, they can be severely affected by processes associated with the ongoing climate changes, such as Ocean Acidification (OA), amplified methane seepage or ocean warming, which cause a decrease in oxygen concentration and pH of seawater. Despite the fact that in natural conditions environmental parameters are interlinked and foraminifera might be affected by more than one stressor at the same time, only a few laboratory studies have tested the simultaneous effects of oxygen deficiency and elevated pCO_2 on benthic foraminifera. Here, we present the results of a 5-month laboratory experiment. Small 'juvenile' benthic foraminifera collected from four location at the Barents Sea and Norwegian Sea were incubated in one of four experimental treatments designed to simulate different environmental conditions, including saturated oxygen to hypoxia, modern-day pCO_2 to elevated pCO_2, and dual stressors of hypoxia and elevated pCO_2. Additionally, foraminifera were fed a methanotroph

(*Methyloprofundus sedimenti* PKF-14) or a mix of algae (*Dunaliella tertiolecta* and *Isochrysis galbana*). Our experiment demonstrated the ability of juvenile foraminifera to calcify under induced hypoxia (O_2, 0.7ml/L) and elevated pCO_2 (2000 ppm). Overall, foraminiferal yields were most affected by the dual-stress treatment and their growth was more susceptible to environmental stressors than the organic matter offered. Except for the foraminiferal yield from Norwegian Sea sediments where foraminifera were more resistant to the combined effect of hypoxia and elevated pCO_2 compared to modern-day treatment.

Keywords: climate change; methanotrophic bacteria; dual-stress; ocean acidification; cold seep

1. Introduction

Benthic foraminifera (Protista) commonly occur in a range of marine environments and constitute the major group of marine organisms that precipice calcium carbonate ($CaCO_3$). For this reason, foraminifera play a significant part in both the oceanic carbon cycle and benthic food webs (Murray 2006). Distribution of foraminifera is mainly determined by abiotic factors, such as temperature, salinity, and oxygen availability. Particular species have been defined for certain environments, thus the tests (shells) of foraminifera are a well-established proxy in palaeoceanography, used to reconstruct past environmental conditions, e.g. temperature or ocean productivity (e.g. Murray 2006, Gooday and Jorissen 2011).

Most foraminifera are considered to be aerobes for which oxygen is crucial for efficient generation of cellular energy (Heinz and Geslin 2012). Prolonged hypoxia can cause stress on their physiological processes, as well as potentially alter the community's species composition (e.g. Alve and Bernhard 1995, Jorissen *et al.* 1995, Pucci *et al.* 2009). Similarly, life under elevated pCO_2 is often associated with high energy expenditure, since it requires physiological

adaptations to supports growth and biocalcification under elevated pCO_2 conditions (e.g. de Nooijer *et al.* 2009, Allison *et al.* 2010, Stumpp *et al.* 2012). In a vast majority of oceanic environments, only the top centimetres or millimetres of the sediment is oxygenated (e.g. Jørgensen and Revsbech, 1989). Permanent low-oxygen conditions occur naturally below the oxygen minimum zone (OMZ) extended along the continental margins, and seasonal hypoxia or anoxia develop in fjords or coastal environments (Helly and Levin 2004). Similar to oxygen content, pCO_2 concentration varies within marine sediments and can be as high as 3324ppm (Haynert *et al.* 2012). Currently, due to climatic changes, poorly-oxygenated / high pCO_2 environments might become more common (e.g. Sarmiento *et al.*, 1998; Keeling and Garcia, 2002; Meier *et al.*, 2011). For example, the ongoing process of Ocean Acidification (OA) caused by absorption of atmospheric carbon dioxide (CO_2) by the oceans can lead to a decrease in the pH of seawater and of the carbonate bioavailability for marine calcifiers, including foraminifera. Analogously, climate change can amplify methane seepage at cold seeps. Input of methane stimulates the growth of methane oxidizing bacteria (methanotrophs) and simultaneously, during aerobic methane oxidation (MOx) close to the sediment-water interface, these bacteria use oxygen and release carbon dioxide (CO_2). In the long-term, these processes lead to oxygen-depletion (i.e., hypoxia) and an increase of pCO_2, decreasing the pH of the pore water (e.g. Levin 2005, Treude *et al.* 2007).

Foraminiferal response to environmental stressors has been the subject of numerous laboratory studies, most of which were focused on the response to single environmental parameters such as oxygen (e.g. Moodley and Hess, 1992, 1998; Bernhard and Alve, 1996; Ernst *et al.*, 2005; Geslin *et al.*, 2004; Pucci *et al.*, 2009) or carbon dioxide (e.g. Haynert *et al.*, 2012, 2014; Vogel and Uthicke 2012; Keul *et al.*, 2013; McIntyre-Wressnig *et al.*, 2013). Despite the fact that environmental parameters are interlinked and the effects of stressors can be

cumulative, greater than cumulative (synergistic) or less than cumulative (antagonistic; Gobler *et al.* 2014, Breitburg *et al.* 2015), and foraminifera might be affected by more than one stressor at the same time, relatively few studies have investigated the simultaneous effects of oxygen deficiency and elevated pCO_2 on foraminifera, i.e. dual-stressor impact (Glas *et al.*, 2012; Wit *et al.* 2016, van Dijk van *et al.* 2017).

In this paper, we present the results of a 5-month laboratory experiment, in which we investigated the impact of three environmental variables: pCO_2, oxygen and diet, on small 'juvenile' benthic foraminifera. The foraminifera were incubated in one of four experimental treatments designed to simulate different environmental conditions, including saturated oxygen to hypoxia, modern-day pCO_2 to elevated pCO_2, and dual stressors of hypoxia and elevated pCO_2. A *Methyloprofundus sedimenti* PKF-14 or a mix of algae (*Dunaliella tertiolecta* and *Isochrysis galbana*) was offered weekly as a food source to the foraminifera.

2. Materials and Methods

2.1. Sampling

In order to obtain a living benthic foraminiferal assemblage, sediment samples were collected from the western Barents Sea and the North Norwegian continental margin (Fig. 1) on board the R/V *Helmer Hanssen* in October 2016. Sediments were collected using a box core (50x50x50cm) at water depths of 800 m (sample BSA) and 803 m (sample BSB) from the Barents Sea and at water depths of 993 m (sample NSA) and 354 m (sample NSB) from the Norwegian Sea (Table 1; Fig. 1).

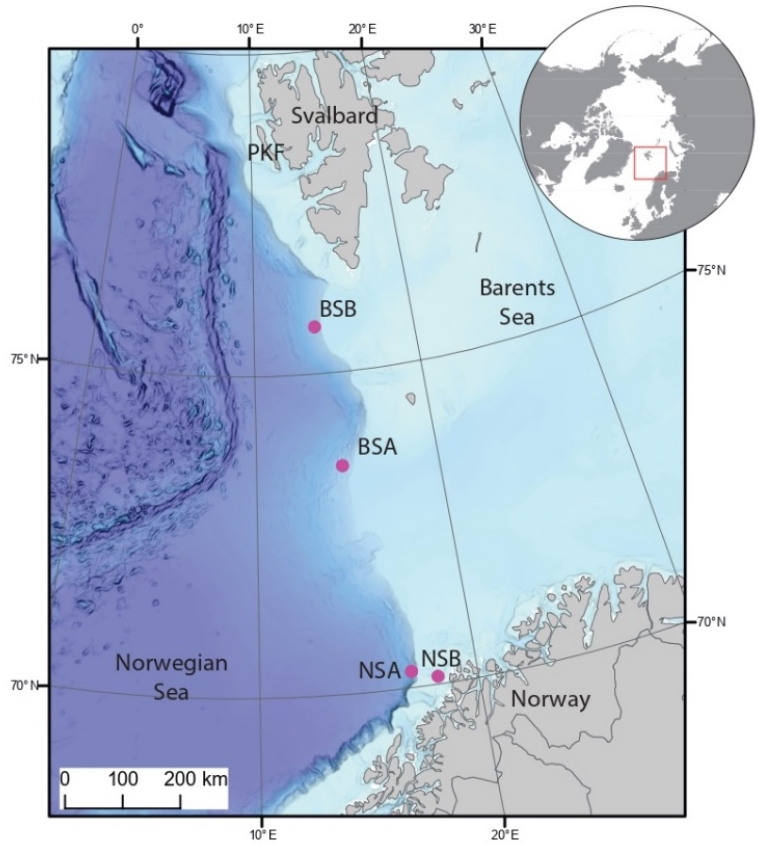

Figure 1. Map of the Barents Sea and surrounding region with sediment sampling locations (pink dots); BSA- Barents Sea A, BSB- Barents Sea B, NSA- Norwegian Sea A, NSB- Norwegian Sea B, PKF- Prins Karls Forland. Map is from IBCAO (Jaccobson et al., 2012).

Table.1. Geographic position, coordinates, water-depth information and date of collection for all samples.

Station	Location	Coordinates	Water Depth (m)	Date of collection
BSA	Barents Sea A	73.55° N, 14.72°E	800	October 7th 2016
BSB	Barents Sea B	75.73 ° N, 13.84°E	803	October 24th 2016
NSA	Norwegian Sea A	70.25 ° N, 16.98°E	993	October 9th2016
NSB	Norwegian Sea B	70.12 ° N, 18.15°E	354	October 9th 2016

The upper ~2 cm of the sediment was collected using a spoon and transferred to plastic containers containing ambient seawater. The samples were then stored on board in a temperature-controlled room at ~4°C. One day after the cruise, all the sediment samples were

washed through a 63 µm mesh using chilled seawater. To avoid contamination and to remove living organisms, e.g. phytoplankton, the seawater was filtered through a 0.45 µm filter. The remaining <63 µm fraction of the sediment was sieved again over a 53-µm mesh. The three sediment fractions (<53 µm, 53-63 µm, >63 µm) were kept with seawater in plastic containers with lids. All containers were stored in near ambient conditons (in dark , 4°C) and within 3 days transported in a cooler to Woods Hole Oceanographic Institution (WHOI), where the experiment was conducted.

2.2. Treatments

The experiment with four different treatments (named I, II, III, IV), was conducted in a darkened, climate-controlled room maintained at 6°C. Each treatment was housed in a separate Biospherix C-Chamber incubator, each with a unique atmospheric pCO_2 and [O_2] combination (Table 2). We applied the experimental set-up previously used by Wit *et al.* (2016) and van Dijk van *et al.* (2017) with modifications. The elevated atmospheric pCO_2 (2000 ppm) was maintained using a feedback controlled infrared CO_2-sensor and controller (Biospherix ProCO_2 system). Oxygen concentration was maintained by an O_2-sensor and controller (Biospherix *ProOx system; Table 2). Each* controller was connected to an external gas source: nitrogen gas (N_2) to maintain hypoxic conditions, 400 ppmCO_2 and/or 1% CO_2 in 99% N_2 to establish CO_2 concentration as noted in Table 2.

Table. 2. Experimental treatments (I, II, III, IV), O_2 (ml/L) and CO_2 (ppm) concentration, gas sources (400 ppm CO_2, 1% CO_2 /99% N_2, and N_2), gas sensors and controllers used for the experiment.

Treatment	O_2 (ml/L)	pCO_2 (ppm)	Gas source	Gas sensors and controllers	Imitated environmental conditions
I	saturated	400	400 ppmCO_2	No controllers	Modern atmospheric conditions
II	0.7	400	1% CO_2 in N_2; N_2	ProCO_2, ProOx	Hypoxia, modern pCO_2
III	saturated	2000	1% CO_2in N_2	ProCO_2	Oxygenated, elevated-pCO_2
IV	0.7	2000	1% CO_2 in N_2; N_2	ProCO_2, ProOx	´Dual stress´ combined hypoxia and elevated-pCO_2

2.3. Experimental setting

In each Biospherix C-Chamber, we placed 16 translucent plastic containers filled with 80 ml of filtered (0.2 µm) natural seawater obtained from the Environmental Systems Laboratory (WHOI). To establish equilibrium between experiment seawater and the atmosphere inside the Biospherix C-Chambers, we left containers for one week to equilibrate. A previous study determined that the atmosphere and seawater are in equilibrium within ~40 h after introduction to the controlled atmosphere within the chamber (McIntyre-Wressnig *et al.* 2014). The water level was marked on each translucent tub and monitored during the experiment; to minimize potential water evaporation, an open container with distilled water was placed in each C-chamber to maintain humidity. After seawater equilibration, foraminifera-bearing sediment (<53 µm) was introduced into each container where we gently mixed the sediment (<53 µm fraction) to create a homogeneous sample; a syringe was used to transfer 20 ml of propagule-bearing sediment into each plastic container (Rubbermaid™ 120 ml), which was filled with pre-equilibrated filtered seawater (0.45 µm). After the sediment settled (~24 h), 20 ml of water was removed from each container so that there was 80 ml of water and a sediment depth of

~1 cm. To mimic the sub-photic zone, the microcosms were kept in darkness. For the experiment, we used four sources of sediment (Table 1). Three days before the start of the experiment, the sediments were sieved once again over a 53 μm screen, to ensure that no foraminifera >53 μm were included in the inoculum. Because sufficient material was available from site BSA, it was divided between 4 tubs (i.e. replicates named BSA1, BSA2, BSA3, BSA4) for each diet in each treatment. The sediment from site BSB was divided between 2 replicates (named BSB1, BSB2) for each diet, in each treatment, resulting in a total of 16 samples. The sediment from sites NSA and NSB was split equally between 16 containers, no replicates. Altogether, we created 64 microcosms divided between 4 treatments (16 replicates in each treatment; Fig. 2).

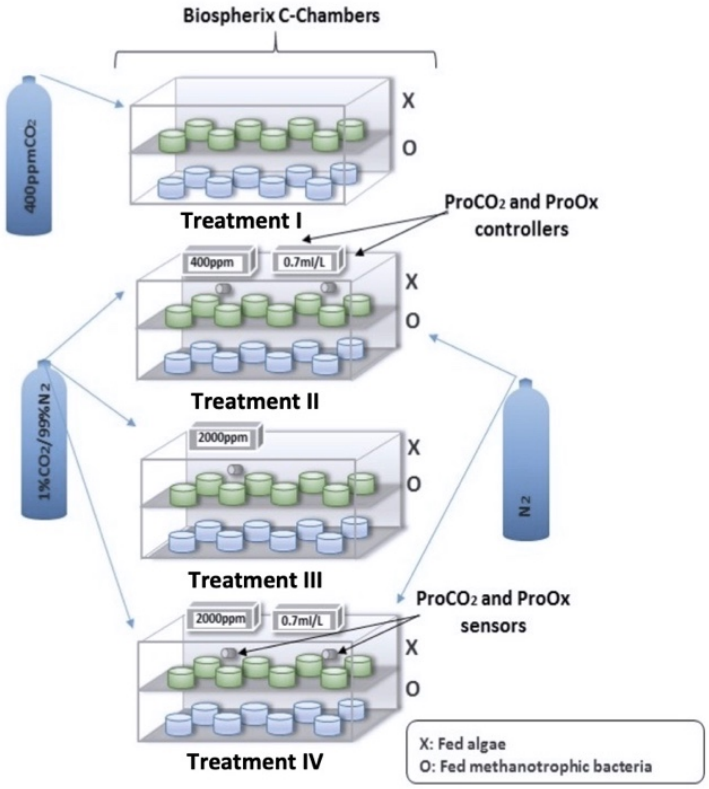

Figure 2. Schematic presentation of experiment: treatment I: saturated oxygen, 400 ppmCO_2, treatment II: 0.7ml/L [O_2], 400 ppmCO_2, treatment III: saturated oxygen, 2000 ppmCO_2, treatment IV: 0.7ml/L [O_2], 2000 ppmCO_2. Biospherix ProCO_2-sensors and controllers maintained atmospheric *p*CO_2. Biospherix ProOx sensors and controllers-maintained oxygen concentrations. External gas source: nitrogen gas (N_2), 400 ppmCO_2 and/or 1% CO_2 in 99% N_2.

2.4. Feeding

In each of the treatments, 8 microcosms were fed weekly 1 ml of the methanotroph bacterium Methyloprofundus *sedimenti, and the other 8 microcosms with* 1 ml of a mixture of marine green algae *Dunaliella tertiolecta* and brown algae *Isochrysis galbana*, prepared as described below. Methyloprofundus *sedimenti strain PKF-14 was isolated from a sea water at Prins Karls Forland, west of Svalbard (Fig. 1). The bacteria were cultured in* a medium made of two parts *sterile filtered seawater and one-part NMS pH 6.8 (Nitrate mineral salt, DSMZ medium 921) under a headspace of 20% methane at 5°C, in 100 ml serum vials with butyl rubber septa and aluminium crimp caps. Dunaliella tertiolecta* Butcher and *Isochrysis galbana* Parke were cultured in f/2 medium (Guillard and Ryther 1962). To concentrate cells, each harvested algal culture was centrifuged at 4150 rpm for 20 min and the supernatant was carefully removed. The remaining fractions containing algae cells were stored at -20 °C before use. Algae were kept frozen to prevent potential growth in the experiment, which could negatively affect the growth of the foraminifera, e.g., by producing and releasing metabolic products into the water (Arnold 1974). Bacteria were dosed directly from the culture. Due to the lack of methane as an experiment variable, the risk of methanotrophic bacterial overgrowth was negligible.

2.5. Foraminiferal analysis

The experiment was terminated after 5 months. On the day prior to termination, each replicate was incubated for 24 h in the viability indicator CellTracker™ Green CMFDA (5-chloromethyl fluorescein diacetate; Thermo Fisher) with a final concentration of 1 µM in seawater (Bernhard et al. 2006) in order to isolate living foraminifera. After incubation, samples were sieved through a 53-µm screen with filtered seawater (0.45 µm). To identify specimens that grew during the experiment and were living at the end of the experiment, the

>53-µm fraction was examined for labeled foraminifera using a Leica MZ FLIII epifluorescence stereomicroscope equipped with optics for fluorescein detection (480 nm excitation; 520 nm emission). Following examination with epifluorescence microscopy, in order to detect the presence of cytoplasm (viable or otherwise), each sample was exposed to a Rose Bengal-seawater solution (2 mg/L). After 24 hours, the samples were sieved again over the 53-µm mesh and the >53-µm fraction was investigated with reflected-light microscopy. All specimens were counted and preserved in ethanol. To determine whether hypoxia, elevated pCO_2, and combined effect of both parameters had significant effect on the number of foraminifera in the >53-µm fraction, a one-way analysis of variance (one-way ANOVA) with probability value p=0.05 was used. The same statistic was used to determine whether there was a significant difference between the yields obtained from the bacterial and algal diet.

3. Results

At the end of the experiment, foraminifera were present in each replicate of each treatment and both diets from BSA samples (Barents Sea A; Table 3). The foraminiferal yields (number of tests) in replicates varied from 17 to 90 individuals. Foraminifera were also present in some replicates from the NSA (Norwegian Sea A), samples but only in the hypoxic treatment (II) and dual-stress treatment (IV), with 13 and 26 individuals, respectively (Table 3). Both calcareous and agglutinated foraminifera were observed (Fig. 3). CellTracker™ Green and Rose Bengal results indicate a lack of living or cytoplasm-bearing foraminifera. Taxonomic identification was impossible due to the small size of most of the specimens, therefore the interpretations are based on direct counts of foraminiferal tests present in the experiment after termination.

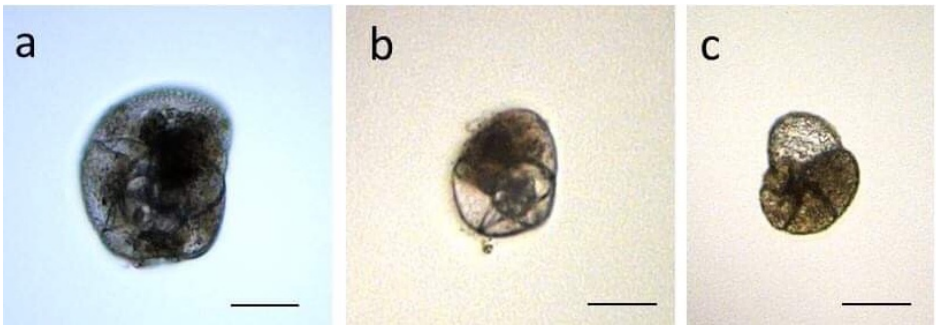

Figure 3. Examples of benthic foraminifera obtained from the experiment; a- *Rosalina* sp.; b- *Epistominella arctica,* c- *Paratrochammina* sp. Scale bars = 50 µm.

Table. 3. The number of foraminiferal tests in the >53-µm fraction of each replicate of each experimental treatment (I, II, III, IV) at the end of the experiment. Values determined by direct counts of foraminiferal tests. Treatment I = saturated oxygen and 400 ppmCO_2; treatment II = *0.7 ml/L* [O_2] and 400 ppmCO_2; treatment III = saturated oxygen and 2000 ppmCO_2; treatment IV = *0.7 ml/L* [O_2] and 2000 ppmCO_2.

	Treatment I		Treatment II		Treatment III		Treatment IV	
Site ID	Bacteria	Algae	Bacteria	Algae	Bacteria	Algae	Bacteria	Algae
BSA 1	41	50	30	39	53	60	20	18
BSA 2	52	42	40	46	61	52	26	36
BSA3	70	63	26	45	67	28	23	19
BSA4	90	50	35	50	49	57	25	17
Sum	253	205	131	180	230	197	94	90
Mean	63,25	51,25	32,75	45	57,5	49,25	23,5	22,5
SD	21.46	8.69	6.07	4.54	8.06	15.54	2.64	9.03
BSB1	0	0	0	0	0	0	0	0
BSB2	0	0	0	0	0	0	0	0
NSA	0	0	10	16	0	0	5	8
NSB	0	0	0	0	0	0	0	0

Data obtained from BSA replicates show no significant difference between the foraminiferal yields of high atmospheric pCO_2 (2000 ppm) treatments versus atmospheric pCO_2 (400 ppm) treatments within the saturated oxygen treatments (I and III; p=0.59; Fig. 4). In total, 458 individuals were obtained from treatment I and 427 from treatment III (Table 3). Conversely, there was a significant difference for hypoxic treatments (II, IV; p<0.001; Fig. 4), where the higher pCO_2 treatment IV had a lower yield (184 individuals) than treatment II (311 individuals; Table 3). Treatments with the same pCO_2 had significantly different yields: the hypoxic treatment had lower yields than the oxygen saturated treatments (p=0.01, 400 ppmCO_2; p<0.001, 2000 ppmCO_2; Fig.4). Results obtained from NSA replicates show that the foraminifera grew in the hypoxic treatment (II) and the dual-stress treatment (IV), whereas the sediments in treatments I (modern day) and III (elevated pCO_2) were barren (i.e. zero foraminifera; Table 3).

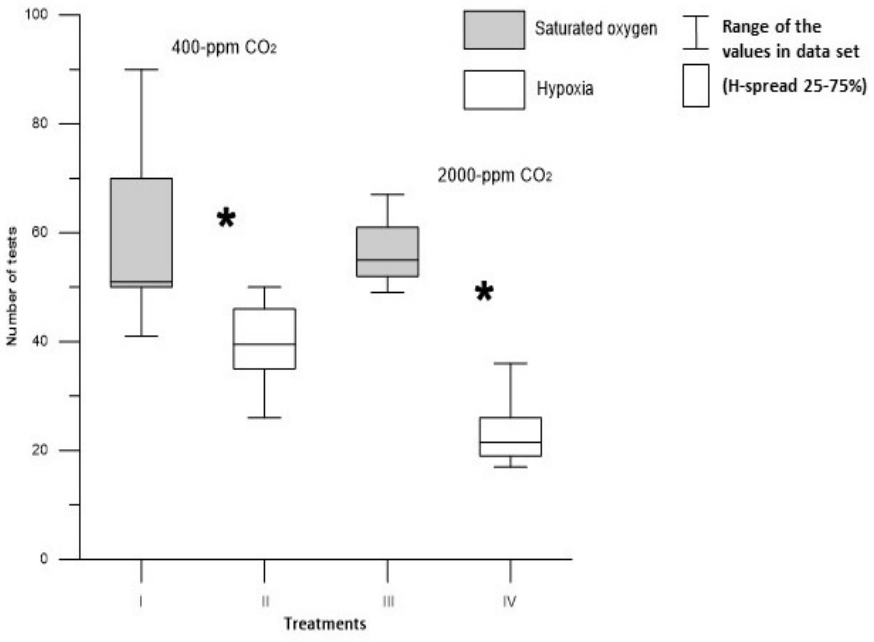

Figure 4. Box-and-whisker plot showing the comparison between the total number of foraminiferal tests from different oxygen conditions (saturated and hypoxia) under the same pCO_2 concentration (400 ppm or

2000 ppmCO_2) from BSA replicates. Asterisks indicates significant differences between the yields from saturated versus hypoxic treatments (p=0.014, 400 ppm CO_2; p=0.001, 2000 ppmCO_2). The upper and lower whiskers indicate the maximum and a minimum number of foraminiferal tests obtained in each treatment. The top and bottom of the box is indicated by upper and lower quartiles, respectively. The horizontal line represents the median.

The average yield obtained from BSA replicates of exposure to 400 ppmCO_2 was 57.25 individuals (treatment I) and 38.88 (treatment II), and the average yield for treatments with 2000 ppmCO_2 was 53.3 individuals (treatment III) and 23.0 individuals (treatment IV). Across all treatments, there was no significant difference between foraminifera yields for the different diets (p=0.72; Fig. 5). In total, 708 tests were obtained from the methanotroph diet and 673 tests from the algal diet (Table 3).

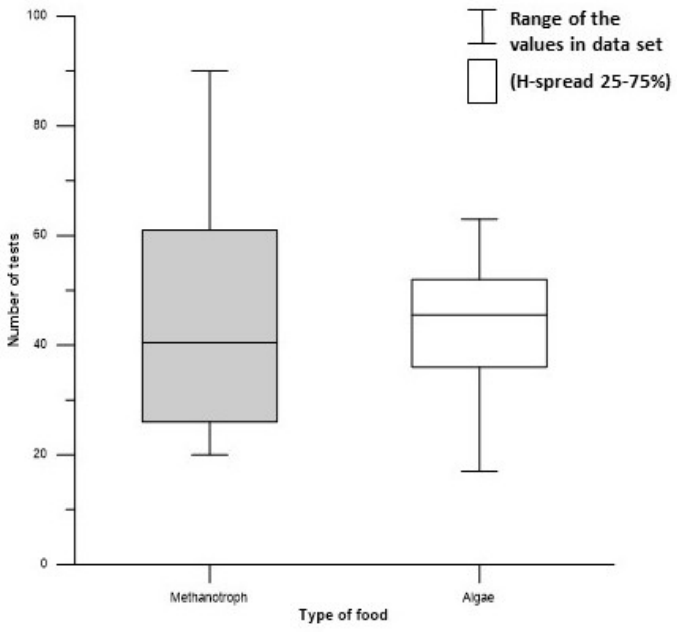

Figure 5. Box and whiskers plot showing the total number of foraminifera obtained for each diet from all BSA replicates from all four treatments. As assessed by one-way ANOVA (p<0.05), there was no statistical difference between the sizes of yields from methanotrophic bacterial and algal diets (p= 0.72). See Fig.4 for plot description.

Comparisons of the number of foraminifera for each diet in each treatment varied, with no significant differences between diets in treatments I, III, and IV (p=0.43, treatment I; p=0.29, treatment III; p=0.87; treatment IV), but a significant difference in treatment II (p=0.02) (Fig. 6).

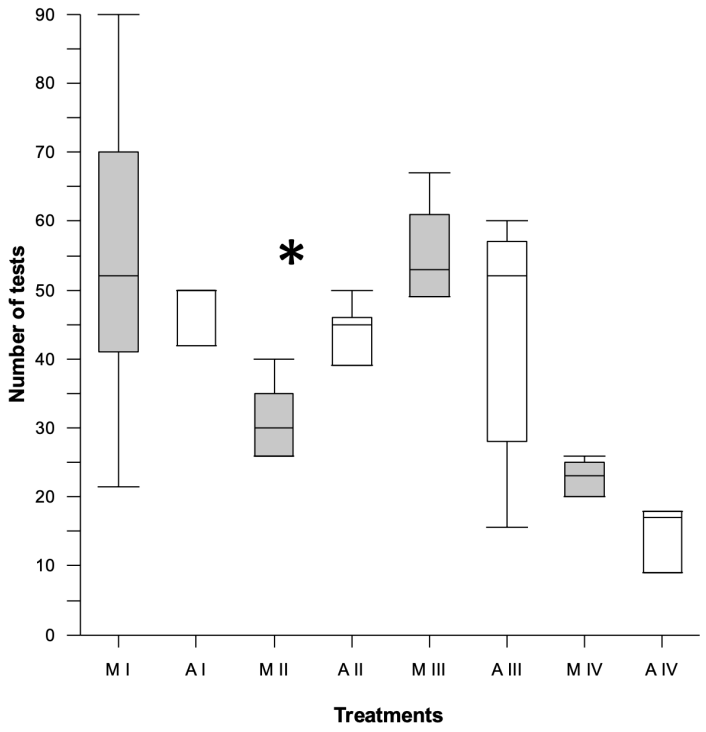

Figure 1. The number of foraminiferal tests obtained from methanotroph (M) versus algal (A) diet for each treatment (I, II, III, IV). The asterisk indicates a significant difference in yields within the same treatment for BSA replicates (one-way ANOVA; p=0.02).

4. Discussion

4.1. Impact of environmental parameters

During the five months of incubation, we were able to successfully grow foraminifera in all four treatments and with both diets (BSA sediment). Although no living individuals remained at experiment termination, due to the design of the study we are confident that foraminifera grew during its course. We separated the small foraminifera from adult

individuals by sieving sediment over a 53-µm sieve, and only the fine fraction containing juvenile foraminifera was used as inoculum. At the end of the experiment, we sieved the sediment once more over a 53-µm sieve, but this time we collected the coarse fraction (>53 µm), which was considered to contain individuals that grew during the experiment. In experiments with propagules, the response of the foraminifera is measured by the individuals' ability to grow under the experimental conditions; all specimens, both live and dead, harvested at the end of an experiment, have responded to the treatments (Alve and Goldstein, 2014).

Due to the long course of this experiment, it is challenging to recognise when the foraminifera died. Nevertheless, considering the fact that each experimental assemblage was homogeneous and originally from the same propagule bank (i.e., BSA, BSB, NSA or NSB), the number of propagules in each of the replicates for a particular propagule bank is expected to be roughly equal. Obtained data show that foraminifera did not grow in all of the sediments, and that some microcosms (replicates) remained empty. For example, NSB and BSB sediments were barren, whereas in the replicates from BSA the foraminifera grew to be larger than the screen size. Therefore, we are confident that the foraminifera did not die simultaneously. Rather, due to the different yields (abundances) between treatments we assert that the populations died over time in response to experimental variables (hypoxia, elevated pCO_2, or both).

While previous experiments in this field were short-term and based on selected species, our experiment was conducted over five months and used juvenile multi-species assemblages, making direct comparisons difficult. Nevertheless, some similarities in the results are apparent. Overall, in our experiment both prolonged hypoxia and elevated pCO_2 had adverse effects on the resilience of our juvenile foraminiferal community in BSA sediments. Within the

same oxygen conditions, despite the differences in pCO_2, there were no significant differences between the sizes of the yields (i.e. foraminifera harvested from the experiment). In contrast, there was a significant difference between the numbers of foraminifera in treatments with different oxygen concentrations. A culturing experiment previously performed on *Ammonia aomoriensis* showed, that the species was negatively affected by CO_2 concentration up to 3130 µatm, which resulted in an increased mortality and a significant reduction of the test size (Haynert *et al.*, 2012). No significant impact of elevated pCO_2 was reported for *Ammonia* sp. (Keul *et al.*, 2013; Dissard *et al.*, 2010) and the symbiont-bearing foraminifer *Amphistegina gibbosa* (McIntyre-Wressnig *et al.*, 2013). A short experiment on *Globobulimina turgida* suggested that certain species may even be positively affected by an increase in ambient pCO_2 (Witt *et al.*, 2016). The resilience of foraminifera to an increase in ambient pCO_2 has been explained by the fact that the pore waters in which foraminifera live in is higher than atmospheric pCO_2 (Haynert *et al.*, 2012). Alternatively, foraminifera are capable of manipulating the inorganic carbon speciation by elevating their intracellular pH during calcification (de Nooijer *et al.*, 2009).

Benthic foraminifera are known to have lower respiration rates and relatively low oxygen demand compared to other groups of meiofauna (Piña-Ochoa *et al.* 2010). This may be advantageous when foraminifera are exposed to environmental stress (Theede *et al.* 1969). There is no uniform response pattern to low oxygen conditions (i.e. 0.1–1 ml/L) in foraminifera. Prior laboratory studies showed that certain species can manage hypoxia quite well: *Ammonia tepida*, *Melonis barleeanus* (Geslin *et al.*, 2014), *Nouria polymorphinoides* and *Nonionella turgida* (Pucci *et al.*, 2009) were not negatively affected by low oxygen conditions. A decrease in the yield size in our hypoxic treatments might be explained by the fact that the stress response of any individual depends on its current life stage, and juveniles are typically

more sensitive to changing habitats and more metabolically active compared to adult individuals (Pandori & Sorte 2019).

The smallest yield was harvested from the dual-stressor treatment of hypoxia and high pCO_2. In response to combined hypoxia and elevated pCO_2, the number of foraminifera was reduced to about a half when compared to the aerated 400 ppmCO_2 treatment. A similar experimental set-up has been applied previously by Wit *et al.* (2016) and van Dijk *et al.* (2017). Both studies demonstrated that the cumulative effect of dual stressors always had a negative impact on foraminifera, affecting their survival and individual growth in the calcareous *Globobulimina turgida* (Wit *et al.*, 2016) and the agglutinated *Miliammina fusca* (van Dijk *et al.*, 2017). Foraminifera have several adaptations that allow them to cope with seemingly adverse conditions, but simultaneous effects of several stress factors can trigger molecular and cellular responses, that lead to high energy expenditures and a decrease in the organism's resilience (Melzner *et al.* 2013).

In contrast, the data obtained from the NSA sediment show the opposite pattern to the BSA replicates. Foraminifera from the NSA replicates grew better in the hypoxic treatment (II) and the dual-stress treatment (IV) when compared to the two other treatments: modern day treatment (I) and elevated pCO_2 treatment (III), in which there was no discernable growth. This is surpising, since treatments I and III are considered to represent mild conditions. Foraminiferal fauna from the NSA sediment seemed to be better adapted to low O_2 conditions compared to foraminifera from BSA replicates. Despite the fact that all replicates were kept in the same conditions, foraminiferal assemblages of different origins responded differently, demonstrating that not every deep-sea foraminifera assemblage will react in the same way.

It is noteworthy that the temperature used in the experiment was approximately ~2°C higher than the *in situ* temperature (~4°C). Laboratory studies indicate that foraminiferal

growth is positively correlated with temperature (Barras *et al.*, 2009; Dong *et al.*, 2019). Since the sediment used in this experiment originated from the Arctic region, the temperature increase of about 2°C could potentially be an additional stressor for the Arctic foraminifera causing increase in metabolic rates, and as a result amplify the effect of the other two experimental variables. Similar conclusions have been reached by Bernhard *et al.* (2016), who suggested that compound (triple-stress) impact of warmth, hypoxia and high pCO_2 significantly affects foraminiferal communities.

Consequently, in the future, in response to the ongoing processes related to climate change such as Ocean Acidification, amplified methane seepage or deoxygenation caused by ocean warming, benthic foraminifera may face significant challenges. Oxygen loss combined with a drop in the pH of seawater might decrease the size of foraminiferal populations, lower their diversity and promote the expansion of more resistant opportunitic species.

4.3. Impact of diet

The propagule method is well adapted to investigations of the effects of environmental parameters on benthic foraminiferal populations. However, the method has its limitations e.g., natural, non-sterile sediment used as inoculum might contain unknown bacteria, very small metazoans or algae, which may interact with the foraminifera as predators or prey, via competition for space or food, or by modifying the microenvironment (Goldstein and Alve 2011; Duffield *et al.*, 2014). Utilizing a reasonably homogenous fine sediment fraction and using replicates minimizes the impact of natural sediment on results from experiments using propagules (Goldstein and Alve 2011). Since relatively equal foraminiferal yields were obtained from each tested diet, our results suggest that the type of diet did not significantly impact the juvenile foraminifera. Also, to some extent, our results suggest that methanotrophs might potentially serve as a food source for foraminifera. Similarly,

Wollenburg *et al.* (2015) proposed that methanotrophs present in a pre-experimental sediment were consumed by foraminifera during the experiment.

To our knowledge, foraminiferal dietary preferences towards methanotrophs have not been experimentally tested, so our results cannot be compared with the existing literature. However, evidence from field studies suggests that foraminifera feed on methanotrophs; for example, higher foraminiferal absolute abundances at seep sites compared to surrounding non-seep sites indirectly indicates that cold seeps might be richer in food than surrounding sites (e.g. Heinz *et al.* 2005, Panieri 2006, Torres *et al.* 2010). Additionally, transmission electron microscopy (TEM) micrographs reveal a presence of a methanotrophs close to the apertural region in seep-dwelling benthic foraminiferal specimens of *Melonis barleeanus* (Bernhard and Panieri 2018).

5. Conclusion and implications for future research

The experiment demonstrated the ability of juvenile foraminifera to grow at least to some extent (as evidenced by increased test sizes) under the potentially challenging environmental conditions of hypoxia (O_2; 0.7 ml/L) and elevated pCO_2 (2000 ppm). Our dual-stress treatment had the most significant impact on foraminifera reducing the yield size by about a half compared to modern day treatments (I). Except for the foraminiferal yield from NSB sediments where foraminifera seem to be more resistant to the combined effect of hypoxia and elevated pCO_2. Overall, dual or single-stressor environmental conditions affected the growth of foraminifera more than the type of the organic matter offered. Further dedicated studies are required to confidently conclude on the impact of methanotroph diet on foraminifera.

Acknowledgements

We gratefully acknowledge Daniel McCorkle from Woods Hole Oceanographic Institution for professional advice during the experiment, Mette M. Svenning and Anne Grethe Hestnes for *M. sediment* strain PKF14 and support for cultivation of it, and the captain and crew of the R/V *Helmer Hanssen* for help with sampling. Funding of this project was provided by the Research Council of Norway through its Centers of Excellence funding scheme grant 287 no. 223259, the NORCRUST project, The Loeblich and Tappan Student Research Award from the Cushman Foundation for Foraminiferal Research, and a Travel grant from The Norwegian Research School in Climate Dynamics (ResClim). JMB's participation was partially supported by US NSF grant OCE-1634469.

References

Allison N, Austin W, Paterson D, Austin H (2010) Culture studies of the benthic foraminifera *Elphidium williamsoni*: Evaluating pH, $\Delta[CO_3^{2-}]$ and inter-individual effects on test Mg/Ca. Chemical Geology 274: 87–93. DOI: 10.1016/j.chemgeo.2010.03.019

Alve E, Bernhard J (1995) Vertical migratory response of benthic foraminifera to controlled oxygen concentrations in an experimental mesocosm. Marine Ecology Progress Series 116:137–151. DOI: 10.3354/meps116137

Alve E, Goldstein ST (2014) The propagule method as an experimental tool in foraminiferal ecology. In: Kitazato H, Bernhard JM (eds) Approaches to Study Living Foraminifera. Environmental Science and Engineering. Springer, Tokyo. DOI: 10.1007/978-4-431-54388-6

Arnold ZM (1974) Field and laboratory techniques for the study of living Foraminifera. In: Hedley RH, Adams CG (eds) Foraminifera, vol. 1. London: Academic Press, 153–206.

Barras C, Geslin E, Duplessy JC, Jorissen F (2009) Reproduction and growth of the deep-sea benthic foraminifer *Bulimina marginata* under different laboratory conditions. Journal of Foraminiferal Research, 39: 155–165.

Bernhard JM, Alve, E (1996) Survival, ATP pool, and ultrastructural characterization of benthic foraminifera from Drammensfjord (Norway): response to anoxia. Marine Micropaleontology, 28: 5–17. DOI: 10.1016/0377-8398(95)00036-4

Bernhard JM, Ostermann DR, Williams DS, Blanks JK (2006) Comparison of two methods to identify live benthic foraminifera: A test between Rose Bengal and CellTracker Green with implications for

stable isotope paleoreconstructions. Paleoceanography, 21: 4210. DOI: 10.1029/2006PA001290

Bernhard JM, Panieri G (2018) Keystone Arctic paleoceanographic proxy association with putative methanotrophic bacteria. Scientific Reports, 8: 10610. DOI: 10.1038/s41598-018-28871-3

Breitburg DL, Salisbury J, Bernhard JM, Cai WJ, Dupont S, Doney SC, Kroeker KJ, Levin LA, Long WC, Milke LM, Miller SH, Phelan B, Passow U, Seibel BA, Todgham AE, and Tarrant AM (2015) And on top of all that… Coping with ocean acidification in the midst of many stressors. Oceanography 28(2): 48–61.

de Nooijer LJ, Toyofuku T, Kitazato H (2009) Foraminifera promote calcification by elevating their intracellular pH. Proceedings of the National Academy of Sciences, 106: 15374–15378. DOI: 10.1073/pnas.0904306106

Dong S, Lei Y, Li T, Jian (2019) Responses of benthic foraminifera to changes of temperature and salinity: Results from a laboratory culture experiment. Science China Earth Sciences, 62: 459–472. DOI: 10.1007/s11430-017-9269-3

Duffield C, Edvardsen B, Eikrem W, Alve E (2014) Effects of different potential food sources on upper-bathyal benthic foraminifera: An Experiment with Propagules. The Journal of Foraminiferal Research, 44: 427–44. DOI: 10.2113/gsjfr.44.4.416

Geslin E, Barras C, Langlet D, Nardelli MP, Kim JH, Bonnin J, Metzger E, Jorissen FJ (2014) Survival, reproduction and calcification of three Benthic Foraminiferal Species in Response to Experimentally Induced Hypoxia. In: Kitazato H., M. Bernhard J. (eds) Approaches to Study Living Foraminifera. Environmental Science and Engineering. Springer, Tokyo. DOI:10.1371%2Fjournal.pone.0177604

Geslin E, Heinz P, Jorissen F, Hemleben C (2004). Migratory responses of deep-sea benthic foraminifera to variable oxygen conditions: laboratory investigations. Marine Micropaleontology, 53: 227–243. DOI: 10.1016/j.marmicro.2004.05.010

Glas MS, Langer G, Keul N (2012) Calcification acidifies the microenvironment of a benthic foraminifer (*Ammonia* sp.). Journal of Experimental Marine Biology and Ecology, 424–425: 53–58.

Gobler CJ, DePasquale EL, Griffith AW, Baumann H (2014) Hypoxia and acidification have additive and synergistic negative effects on the growth, survival, and metamorphosis of early life stage bivalves. PLOS One 9:1–10. DOI: 10.1371/journal.pone.0083648

Goldstein ST, Alve E (2011) Experimental assembly of foraminiferal communities from coastal propagule banks. Marine Ecology Progress Series, 437:1–11. DOI:10.3354/meps09296

Gooday AJ, Jorissen FJ (2011) Benthic Foraminiferal Biogeography: controls on global distribution patterns in deep-water settings. Annual Review of Marine Science, 4: 237–262. DOI: 10.1146/annurev-marine-120709-142737

Guillard RR, Ryther JH (1962) Studies of marine planktonic diatoms. I. *Cyclotella nana* Hustedt, and *Detonula confervacea* (cleve) Gran. Canadian Journal of Microbiology, 8:229–239. DOI: 10.1139/m62-029

Haynert K, Schönfeld J, Polovodova-Asteman I, Thomsen J (2012) The benthic foraminiferal community in a naturally CO_2-rich coastal habitat in the southwestern Baltic Sea. Biogeosciences, 9: 4421–4440. DOI: 10.5194/bg-9-4421-2012

Haynert K, Schönfeld J, Schiebel R, Wilson B, Thomsen J (2014) Response of benthic foraminifera to ocean acidification in their natural sediment environment: a long-term culturing experiment. Biogeosciences, 11: 1582–1597. DOI: 10.5194/bg-11-1581-2014

Heinz P, Geslin E (2012) Ecological and Biological Response of Benthic Foraminifera Under Oxygen-Depleted Conditions: Evidence from Laboratory Approaches. In: Altenbach A Bernhard JM, Seckbach J (eds) Anoxia. Cellular Origin, Life in Extreme Habitats and Astrobiology, 21: 287–303 Springer, Dordrecht.

Heinz P, Sommer S, Pfannkuche O (2005) Living benthic foraminifera in sediments influenced by gas hydrates at the Cascadia convergent margin, NE Pacific. Marine Ecology Progress Series, 304: 77–89. DOI: 10.3354/meps304077

Helly, J.J., Levin, L.A., (2004). Global distribution of naturally occurring marine hypoxia on continental margins. Deep Sea Research Part I: Oceanographic Research Papers, 51: 1159–1168. DOI: 10.1016/j.dsr.2004.03.009

Jakobsson M, Mayer L, Coakley B, Dowdeswell JA, Forbes S, Fridman B, Hodnesdal H, Noormets R, Pedersen R, Rebesco M, Werner Schenke HW, Zarayskaya Y, Accettella D, Armstrong A, Anderson RM, Bienhoff P, Camerlenghi A, Church I, Edwards M, Gardner JV, Hall JK, Hell B, Hestvik O, Kristoffersen Y, Marcussen C, Mohammad R, Mosher D, Nghiem SV, Pedrosa MT, Travaglini PG, Weatherall P (2012) The International Bathymetric Chart of the Arctic Ocean (IBCAO) Version 3.0. Geophysical Research Letters, 39 (12): 609.

Jørgensen BB, Revsbech, NP (1989) Oxygen uptake, bacterial distribution, and carbon-nitrogen-sulfur cycling in sediments from the baltic sea - North sea transition. Ophelia, 31 (1): 29–49. DOI: 10.1080/00785326.1989.10430849

Jorissen FJ, de Stigter HC, Widmark JG V (1995) A conceptual model explaining benthic foraminiferal microhabitats. Marine Micropaleontology, 26: 3–15. DOI: 10.1016/0377-8398(95)00047-X

Keeling RF, Garcia HE (2002) The change in oceanic O_2 inventory associated with recent global warming. Proceedings of the National Academy of Sciences, 99 (12) 7848–7853. DOI: 10.1073/pnas.122154899

Keul N, Langer G, de Nooijer LJ, Bijma J (2013) Effect of Ocean Acidification on the Benthic Foraminifera Ammonia Sp. Is Caused by a Decrease in Carbonate Ion Concentration. Biogeosciences, 10 (10): 6185–98. DOI: 10.5194/bg-10-6185-2013

Levin LA (2005) Ecology of cold seep sediments: Interactions of fauna with flow, chemistry and microbes. In: Oceanography and Marine Biology: An Annual Review, Gibson RN, Atkinson RJA, Gordon JDM (eds) CRC Press-Taylor & Francis Group, Boca Raton, 1–46. DOI: 10.1201/9781420037449.ch1

McIntyre-Wressnig A, Bernhard JM, Wit JC, McCorkle DC (2014) Ocean acidification not likely to affect the survival and fitness of two temperate benthic foraminiferal species: results from culture experiment . Journal of Foraminiferal Research 44: 341–351. DOI: 10.2113/gsjfr.44.4.341

Melzner F, Thomsen J, Koeve W, Oschlies A, Gutowska MA, Bange HW, Hansen HP, Körtzinger A (2013) Future ocean acidification will be amplified by hypoxia in coastal habitats. Marine Biology, 160: 1875–1888. DOI: 10.1007/s00227-012-1954-1

Moodley L, Hess C (1992) Tolerance of infaunal benthic foraminifera for low and high oxygen

concentrations. The Biological Bulletin. 183 (1): 94–98. DOI: 10.2307/1542410

Murray JW (2006) Ecology and Applications of Benthic Foraminifera. Cambridge University Press, Cambridge.

Pandori LLM, Sorte CJB (2019) The weakest link: sensitivity to climate extremes across life stages of marine invertebrates. Oikos 128: 621–629. DOI: 10.1111/oik.05886

Panieri G (2006) Foraminiferal response to an active methane seep environment: A case study from the Adriatic Sea. Marine Micropaleontology 61: 116–130. DOI: 10.1016/j.marmicro.2006.05.008

Piña-Ochoa E, Høgslund S, Geslin E, Cedhagen T, Revsbech NP, Nielsen LP, Schweizer M, Jorissen F, Rysgaard S, Risgaard-Petersen N (2010) Widespread occurrence of nitrate storage and denitrification among foraminifera and gromiids. Proceedings of the National Academy of Sciences, 107: 1148–1153. DOI: 10.1073/pnas.0908440107

Pucci F, Geslin E, Barras C, Morigi C, Sabbatini A, Negri A, Jorissen FJ (2009) Survival of benthic foraminifera under hypoxic conditions: Results of an experimental study using the CellTracker Green method. Marine Pollution Bulletin, 59 (8–12): 336–351. DOI: 10.1016/j.marpolbul.2009.08.015

Sarmiento J, Hughes T, Stouffer R, Manabe S (1998) Simulated response of the ocean carbon cycle to anthropogenic climate warming. Nature, 393: 245–249. DOI: 10.1038/30455

Stumpp M, Hu MY, Melzner F, Gutowska MA, Dorey N, Himmerkus N, Holtmann WC, Dupont ST, Thorndyke MC, Bleich M (2012) Acidified seawater impacts sea urchin larvae pH regulatory systems relevant for calcification. Proceedings of the National Academy of Sciences, 109: 18192–18197. DOI: 10.1073/pnas.1209174109

Theede H, Ponat A., Hiroki K, Sclieper C (1969) Studies on the resistance of marine bottom invertebrates to oxygen-deficiency and hydrogen sulphide. Marine Biology, 2: 325–337. DOI: 10.1007/BF00355712

Torres ME, Martin RA, Klinkhammer GP, Nesbitt EA (2010) Post depositional alteration of foraminiferal shells in cold seep settings: New insights from flow-through time-resolved analyses of biogenic and inorganic seep carbonates. Earth and Planetary Science Letters, 299: 10–22. DOI: 10.1016/j.epsl.2010.07.048

Treude T, Orphan V, Knittel K, Gieseke A, House CH, Boetius A (2007) Consumption of methane and CO_2 by methanotrophic microbial mats from gas seeps of the anoxic Black Sea. Applied and Environmental Microbiology, 73: 2271–2283. DOI: 10.1128/AEM.02685-06

van Dijk I, Bernhard JM, de Nooijer LJ, Nehrke G, Wit JC, Reichart G-J (2017) Combined impacts of ocean acidification and dysoxia on survival and growth of four agglutinating foraminifera. Journal of Foraminiferal Research, 47: 294–303. DOI: 10.2113/gsjfr.47.3.294

Vogel N, Uthicke S (2012) Calcification and photobiology in symbiont-bearing benthic foraminifera and responses to a high CO_2 environment. Journal of Experimental Marine Biology and Ecology, 424–425: 15–24. DOI: 10.1016/jembe.2012.05.008

Wit JC, Davis MM, McCorkle DC, Bernhard JM (2016) A short-term survival experiment assessing impacts of ocean acidification and hypoxia on the benthic foraminifera *Globulimina turgida*. Journal of Foraminiferal Research, 46: 25–33.

Wollenburg JE, Raitzsch M, Tiedemann R (2015) Novel high-pressure culture experiments on deep-sea benthic foraminifera — Evidence for methane seepage-related $\delta^{13}C$ of *Cibicides wuellerstorfi*. Marine Micropaleontology, 117: 47–64. DOI: 10.1016/j.marmicro.2015.04.003

Article 2

Effectiveness of Fluorescent Viability Assays in Studies of Arctic Cold Seep Foraminifera.

frontiers in Marine Science

ORIGINAL RESEARCH
published: 09 March 2021
doi: 10.3389/fmars.2021.587748

Effectiveness of Fluorescent Viability Assays in Studies of Arctic Cold Seep Foraminifera

*Katarzyna Melaniuk**

Centre for Arctic Gas Hydrate, Environment, and Climate CAGE, Department of Geosciences, UiT The Arctic University of Norway, Tromsø, Norway

Highly negative $\delta^{13}C$ values in fossil foraminifera from methane cold seeps have been proposed to reflect episodes of methane release from gas hydrate dissociation or free gas reservoirs triggered by climatic changes in the past. Because most studies on live foraminifera are based on the presence of Rose Bengal staining, that colors the cytoplasm of both live and recently dead individuals it remains unclear if, and to what extent live foraminifera incorporate methane-derived carbon during biomineralization, or whether the isotopic signature is mostly affected by authigenic overgrowth. In this paper, modern foraminiferal assemblages from a gas hydrate province Vestnesa Ridge (~1,200 m water depth, northeastern Fram Strait) and from Storfjordrenna (~400 m water depth in the western Barents Sea) is presented. By using the fluorescent viability assays CellTracker^{TM} Green (CTG) CMFDA and CellHunt Green (CHG) together with conventional Rose Bengal, it was possible to examine live and recently dead foraminifera separately. Metabolically active foraminifera were shown to inhabit methane-enriched sediments at both investigated locations. The benthic foraminiferal faunas were dominated by common Arctic species such as *Melonis barleeanus*, *Cassidulina neoteretis*, and *Nonionellina labradorica*. The combined usage of the fluorescence probe and Rose Bengal revealed only minor shifts in species compositions and differences in ratios between live and recently dead foraminifera from Storfjordrenna. There was no clear evidence that methane significantly affected the $\delta^{13}C$ signature of the calcite of living specimens.

Keywords: CellTracker^{TM} Green CMFDA, Rose Bengal, gas hydrate, Vestnesa Ridge, Storfjordrenna, cold seep, Arctic

OPEN ACCESS

Edited by:
Daniela Zeppilli, Institut Français de Recherche pour l'Exploitation de la Mer (IFREMER), France

Reviewed by:
Clara F. Rodrigues, University of Aveiro, Portugal
Alessandra Asioli, Institute of Marine Sciences (CNR), Italy

***Correspondence:**
Katarzyna Melaniuk
Katarzyna.Melaniuk@uit.no

Specialty section:
This article was submitted to Deep-Sea Environments and Ecology, a section of the journal Frontiers in Marine Science

Received: *27 July 2020*
Accepted: *15 February 2021*
Published: *09 March 2021*

Citation:
Melaniuk K (2021) Effectiveness of Fluorescent Viability Assays in Studies of Arctic Cold Seep Foraminifera. Front. Mar. Sci. 8:587748. doi: 10.3389/fmars.2021.587748

INTRODUCTION

Due to the present climate warming, the Arctic region is undergoing remarkably rapid environmental changes, termed the Arctic amplification (IPCC, 2013; Box et al., 2019). The increase in global temperature and atmospheric CO_2 has severe consequences for the Arctic Ocean, causing among others ocean acidification (Amap Assessment, 2018), loss of sea ice (Stroeve et al., 2012), and increase in primary production (Arrigo and van Dijken, 2011). The ocean warming also impose

a high risk of release of methane from geological reservoirs (IPCC, 2007; Phrampus and Hornbach, 2012) as large amounts of methane are stored on Arctic continental margins in the form of pressure-temperature sensitive gas hydrates (e.g., Maslin et al., 2010; Ruppel and Kessler, 2017). Gas hydrate is a widespread, ice-like substance formed when water and methane or other hydrocarbon gases combine in marine sediments under high pressure (3–5 MPa) and temperatures below ∼25°C (e.g., Kvenvolden, 1993). Pressure release and/or increase in temperature can cause destabilization of gas hydrate reservoirs, resulting in a release of free methane gas into the sediment and/or water column (e.g., Archer et al., 2009; Maslin et al., 2010). Several studies have implied a link between the release of methane from geological reservoirs and climate change during the Quaternary and the Paleocene periods (e.g., Wefer et al., 1994; Dickens et al., 1997; Smith et al., 2001). It is feared that ongoing climate change can trigger destabilization of gas hydrate reservoirs and methane release into the water column and eventually to atmosphere (Ruppel and Kessler, 2017). Therefore, it is crucial to understand the fate of methane in marine sediments in order to understand the potential impact of methane release to future climate and Arctic ecosystems.

For the last decades, the carbon isotopic signature $\delta^{13}C$ of benthic foraminifera has been commonly used as a proxy in the reconstruction of productivity and origin and ventilation of water masses in the past (e.g., Gooday, 1994, 2003; Smart et al., 1994; Rohling and Cooke, 1999; Murray, 2006; Ravelo and Hillaire-Marcel, 2007). Recent studies have shown that the $\delta^{13}C$ incorporated into the calcareous ($CaCO_3$) tests of benthic foraminifera can record episodes of release of methane in the past (e.g., Torres et al., 2003; Millo et al., 2005; Martin et al., 2010; Schneider et al., 2017; Sztybor and Rasmussen, 2017). The $\delta^{13}C$ in the shells of some fossil benthic foraminifera can be lower than −10‰ (e.g., Hill et al., 2004; Schneider et al., 2017; Sztybor and Rasmussen, 2017), while the signature of calcite of living foraminifera generally do not exceed −7.5‰ (Mackensen et al., 2006; Wollenburg et al., 2015), it remains unclear if, and to what extent live benthic foraminifera incorporate methane-derived carbon during biomineralization, or whether the isotopic signature is mostly affected by authigenic overgrowth from carbonate precipitation.

Modern methane cold seeps can provide valuable information about changes in seepage intensity and the possible effects of methane seepage on the distribution patterns of live foraminifera and the isotopic composition of their tests. The $\delta^{13}C$ of calcareous benthic foraminifera is determined by species-specific vital effects (i.e., intracellular metabolic processes; e.g., Grossman, 1987; McCorkle et al., 1990; Mackensen et al., 2006) and their microhabitat (e.g., sedimentary organic matter, dissolved inorganic carbon content, temperature, and re-mineralization; e.g., McCorkle et al., 1985; Fontanier et al., 2006). Within cold seeps, the release of methane from the seafloor is partly controlled by sulfate-dependent anaerobic oxidation of methane (AOM) and aerobic methane oxidation (MOx; Treude et al., 2007; Knittel and Boetius, 2009). Thus, as a product of these microbial activities, ^{13}C-depleted carbon is released in the form of carbon dioxide (CO_2) or bicarbonate (HCO_3^{2-}), causing changes in the carbon isotopic signature of pore water i.e., changes in the microhabitat (e.g., Whiticar, 1999; Rathburn et al., 2003; Treude et al., 2007).

Since benthic foraminifera construct their tests by incorporating carbon from the surrounding pore water or bottom water and from the intracellular storage of inorganic carbon (e.g., de Nooijer et al., 2009; Toyofuku et al., 2017), the foraminiferal calcite supposedly records the isotopic signal of ambient waters (i.e., pore water or interstitial water in which the foraminifera live) at the time of calcification (e.g., Rathburn et al., 2003; Panieri and Sen Gupta, 2008). Alternatively, foraminifera might absorb the ^{13}C-depleted carbon *via* the food web (Panieri, 2006) or by feeding on, or living in symbiosis with, methanotrophic bacteria, as suggested by Hill et al. (2004). Some studies show that the $\delta^{13}C$ measured in tests of living foraminifera collected from active seeps are not markedly lower than those from non-seep sites, indicating that living foraminifera might not be able to record the episodes of methane release (e.g., Rathburn et al., 2003; Torres et al., 2003; Etiope et al., 2014; Herguera et al., 2014; Dessandier et al., 2020). Simultaneously, numerous other studies indicate that methane has an effect on isotopic signatures of "live" foraminifera (Rose Bengal stained; e.g., Hill et al., 2004; Mackensen et al., 2006; Panieri, 2006; Wollenburg and Mackensen, 2009; Wollenburg et al., 2015).

Studies of live foraminiferal assemblages are commonly based on Rose Bengal staining, presumably marking specimens that were alive at the sampling time. Stained specimens can include both live and recently dead individuals (Bernhard et al., 2006; Figueira et al., 2012) thus, it is still not clear if live foraminifera have recorded the ^{13}C signal that comes from incorporation of carbon from methane in their shells during calcification. Compared to the conventional Rose Bengal, the CellTracker^{TM} Green (CTG) CMFDA (5-chloromethylfluorescein diacetate; Thermo Fisher Scientific) and CellHunt Green (CHG) (SETAREH biotech, LLC) probes are reactive with internal cell components and gives a green-fluorescent coloring of the cytoplasm, indicating metabolically active foraminiferal specimens. The combined usage of the fluorogenic probes together with the Rose Bengal staining can be used to separate live foraminifera from recently dead individuals, and thus be a useful tool to build up a more detailed picture of benthic foraminiferal distribution patterns and ecology. It might be especially useful in studies of heterogeneous and variable environments such as cold seeps, which depend on the highly variable flux of methane and can evolve and change rapidly over time (Levin, 2005; Cordes et al., 2006; Åström et al., 2020).

This paper presents results of a study of live benthic foraminifera from a gas hydrate province on Vestnesa Ridge (∼1,200 m water depth; western Svalbard margin) and from gas hydrate "pingo" structures from Storfjordrenna (∼400 m water depth) in the western Barents Sea (**Figure 1**). The aims of the study are to (1) identify species compositions of the benthic foraminiferal faunas in these Arctic methane seeps and (2) to compare the carbon isotopic signature ($\delta^{13}C$) in the tests of

metabolically active (CTG or CHG labeled) foraminifera, with Rose Bengal stained and with unstained tests (empty tests), to determine if methane seepage has any significant effects on the isotopic signatures of calcite of live benthic foraminifera.

MATERIALS AND METHODS

Study Area

Vestnesa Ridge is located northwest of Svalbard in the eastern Fram Strait and is an approximately 100 km long sediment drift at water depths of ∼1,200–1,300 m. The Fram Strait forms the gateway between the North Atlantic Ocean and the Arctic Ocean. This region is characterized by large annual fluctuations in sea-ice cover. Relatively warm (3–6°C), saline (S < 35.4 psu), and nutrient-rich Atlantic water pass through the Fram Strait into the Arctic Ocean carried by the West Spitzbergen Current (WSC) (e.g., Manley, 1995; Rudels et al., 2000; Walczowski et al., 2005). The southwestern part of the Vestnesa Ridge is characterized by the presence of several active pockmarks (i.e., shallow seabed depressions) where methane-rich fluids seep from gas hydrate and free gas reservoirs (Bünz et al., 2012; **Figure 1B**). The most active pockmarks, "Lomvi" and "Lunde," are approximately 10–15 m deep depressions with diameters

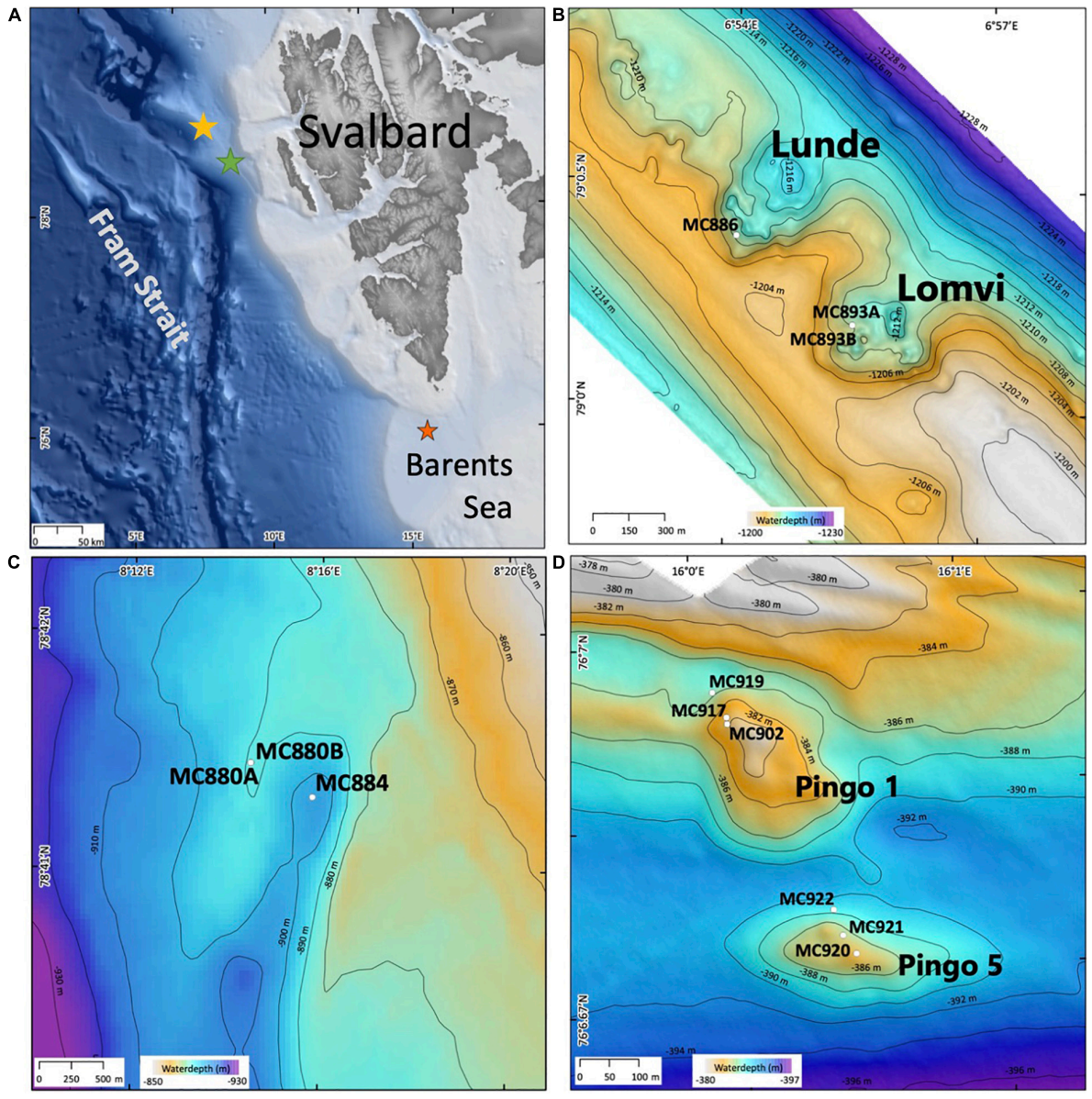

FIGURE 1 | Maps showing **(A)** sampling location, indicated by stars: yellow- Vestnesa Ridge; green- Control site 7,808; orange- Storfjordrenna pingos; **(B)** bathymetry of Vestnesa Ridge (swath bathymetry from Hustoft et al., 2009); control site **(C)** and bathymetry of Storfjordrenna pingos [**(D)**; swath bathymetry from Serov et al. (2017)].

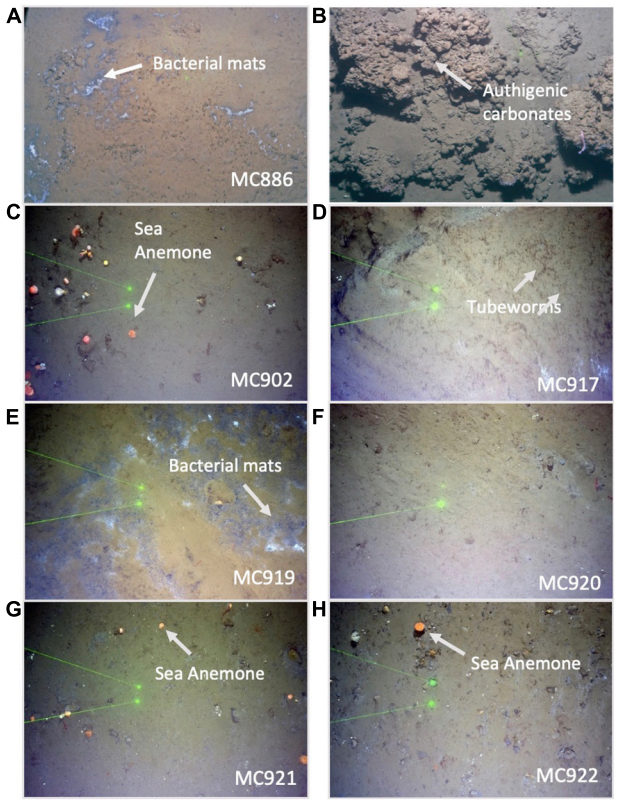

FIGURE 2 | Seafloor images from the Vestnesa Ridge MC886 Lunde pockmark, MC893 Lomvi pockmark showing gray bacterial mats **(A)** and authigenic carbonates **(B)**, and from Storfjordrenna pingos site from active site gas hydrate pingo 1 (GHP1; MC902—MC919) showing tubeworms **(D)**, gray bacterial mats **(E)** and sea anemones **(C)**, and from the inactive site GHP 5 (MC920—MC922) showing sea anemones **(G,H)**. Distance between laser dots (green dots) = 20 cm. **(F)** regular marine sediment.

of 400–600 m. The TowCam−guided multicore investigation of the Vestnesa Ridge shows heterogeneity of the site and presence of macrofauna and seafloor structures associated with the occurrence of methane seepage. These include, e.g., bacterial mats and tubeworm fields (*Siboglinidae*) within the Lunde pockmark, and Methane-Derived Authigenic Carbonate (MDAC) outcrops at the seafloor within the Lomvi pockmark (e.g., Sztybor and Rasmussen, 2017; Åström et al., 2018; **Figure 2**). The $\delta^{13}C_{DIC}$ values of pore water for the Lomvi pockmark have been reported to range between −25.1 and −37.7‰ and for the Lunde pockmark −22.4‰ to −39.4‰ in surface sediments (Dessandier et al., 2019).

The Storfjordrenna hydrate mound "pingo" area is located ∼400 m water depth on the Arctic continental shelf, south of the Svalbard archipelago in the north-western Barents Sea (**Figure 1D**). Similar to the Vestnesa Ridge, Storfjordrenna is under influence of relatively warm Atlantic water (Loeng, 1991). The area is characterized by five gas hydrates mounds (pingo-like features) spread within an area of 2 km^2. The gas hydrate pingos (GHPs) are between 8 and 12 m high, with diameters between 280 and 450 m. Four of the five GHPs are presently active and show active methane seepage in the form of acoustically detected gas/bubble streams (i.e., acoustic flares) around the summits and one is in a "post-active stage" and presently inactive (Hong et al., 2017; Serov et al., 2017). Elevated concentrations of methane (mostly of thermogenic origin) have been detected in both sediments and bottom waters at GHP1, and gas hydrates were recovered in sediment cores (Hong et al., 2017; Carrier et al., 2020). The $\delta^{13}C_{DIC}$ values of pore water for the top of GHP1 (MC902) reached −24.2‰ (Dessandier et al., 2020). Seabed images acquired with a Multicorer-TowCam during the CAGE17-2 cruise revealed the presence of white and gray bacterial mats as well as sediments colonized by chemosynthetic *Siboglinidae* tubeworms, biota well known to indicate active hydrocarbon seepage (Niemann et al., 2006; Treude et al., 2007; **Figure 2**). The megafauna community associated with cold seeps has been previously documented at the Storfjordrenna by Åström et al. (2016) and Sen et al. (2018).

Sampling

Sediment samples were collected during the CAGE 15-2 cruise in May 2015 to Vestnesa Ridge from the sites of active methane emission, the Lomvi and Lunde pockmarks, and at site 7,808 located south-east from the Vestnesa Ridge as a control site where no methane seepage occurs (**Figures 1B,C**). During CAGE cruise 17-2 in June 2017 to Storfjordrenna pingo area, several samples were taken from the active gas hydrates pingo (GHP1) along a transect from the top the pingo toward its edge (**Figure 1D**). For comparison, the inactive GHP5 was sampled in a similar manner (**Figure 1D**).

The samples from both Vestnesa Ridge and the pingo area in Storfjordrenna (**Table 1** and **Figure 1**) were collected with a multicorer equipped with six tubes (10 cm diameter) and combined with a Towed Digital Camera (TowCam) developed at the Woods Hole Oceanographic Institution's Multidisciplinary Instrumentation in Support of Oceanographic (MISO) Facility onboard the R/V *Helmer Hanssen*. The live-stream feed from the TowCam system were used to identify the different seafloor environments and to locate active methane vents, authigenic carbonates, and bacterial mats for targeted accurate sampling locations (**Figure 2**).

After recovery, undisturbed cores were selected for this study. The uppermost core section of each selected core was subsampled using a flat spatula slicing the sediment into 1-cm thick, horizontal intervals (0–1, 1–2, and 2–3 cm). Sediment samples from Vestnesa Ridge were processed as follows: One-third of each slice designated for different treatments, (1) labeling with CTG, (2) staining with Rose Bengal, and (3) extraction of dissolved inorganic carbon (DIC) from pore waters. Each sample was transferred into plastic containers (125-ml HDPE). The CTG solution was prepared beforehand as follows: 1.4 ml of DMSO (dimethyl sulfoxide; not anhydrous) was added to 1 mg CTG, mixed gently, and kept in the original plastic vial from the supplier at −20°C. The solution was thawed approximately 20 min before the sampling. CTG was added to 20 ml of seawater sampled in the multicore tube and added to the sediment immediately after sampling and giving a final concentration of

TABLE 1 | Core numbers, location, coordinates, water depths, and dates of sampling.

Core number	Location	Coordinates	Water depth (m)	Sampling date
MC893A and MC893B	Vestnesa Ridge (Lomvi pockmark)	79.18N, 00.44E	1200	20 May 2015
MC886	Vestnesa Ridge (Lunde pockmark)	79.38N, 00.04E	1200	20 May 2015
MC880A and MC880B	Site 7808 (Control site)	78.44N, 00.50E	889	19 May 2015
MC884	Site 7808 (Control site)	78.30N, 00.82E	900	19 May 2015
MC902	Storfjordrenna Active GHP1	76.91N, 16.08E	377	22 June 2017
MC917	Storfjordrenna Active GHP1	76.93N, 16.02E	377	23 June 2017
MC919	Storfjordrenna Active GHP1	76.96N, 15.98E	378	23 June 2017
MC920	Storfjordrenna Inactive GHP5	76.70N, 16.00E	379	23 June 2017
MC921	Storfjordrenna Inactive GHP5	76.72N, 16.40E	380	23 June 2017
MC922	Storfjordrenna Inactive GHP5	76.74N, 16.37E	386	23 June 2017

GHP, gas hydrates pingo.

CTG of 1 μM in seawater (Bernhard et al., 2006). Samples were incubated in a temperature-controlled room at 4°C for approximately 12 h. Rose Bengal solution was made prior to sampling by dissolving Rose Bengal powder in distilled water (2 g/L). The solution was added to the designated sediment samples, agitated gently, and kept in plastic containers (250 ml). Sediment labeled with CTG and stained with Rose Bengal was preserved with 36% formaldehyde (to final concentration 5.5%) and kept at 4°C.

The sediment collected from Storfjordrenna pingo area was treated differently when compared to samples from the Vestnesa Ridge. Each 1-cm slice of sediment taken from GHP multicores was directly transferred into a 125 ml HDPE bottle. The whole sediment was treated with the CHG solution. The CHG solution was prepared beforehand (following the protocol for CTG). Samples were incubated in CHG onboard in a dark, temperature-controlled room at 4°C for approximately 12 h. Hereafter, the samples were preserved in ethanol with final concentration 70%.

Foraminiferal Fauna Analysis

Rose Bengal stained and CTG labeled (i.e., fluorescently labeled) samples from Vestnesa Ridge were washed over a 63-μm sieve using filtered seawater (0.45 μm); the >63 μm fraction was kept in filtered seawater and further analyzed. The fluorescently labeled samples were examined using an epifluorescence-equipped stereomicroscope (Leica MZ FLIII; 485 nm excitation; 520 nm emission). All individuals that fluoresced brightly in at least half of their chambers were considered as live (**Figure 6**). They were picked wet and placed on micropaleontology slides. The Rose Bengal stained samples were examined with reflected-light microscopy using a Zeiss Stemi SV6. All foraminifera that stained dark magenta in at least half of their chambers were picked and mounted on micropaleontology slides (**Figure 3**). All collected foraminifera were sorted by species and counted and identified to species level (**Tables 2**, **3**).

The CHG labeled (i.e., fluorescently labeled) sediment samples from GHPs were processed in the same manner as CTG labeled, except that individuals that did not show any green coloration were subsequently incubated in a Rose Bengal-ethanol solution (2 g/L). After approximately 24 h, samples were re-sieved over a 63-μm sieve. Obtained Rose Bengal stained foraminifera were wet picked (**Figure 3**). Unstained tests have been omitted and not counted in this study.

The density of foraminifera was normalized per unit volume at the number of specimens per 10 cm^3. The Shannon index S(H) of diversity, Evenness index, and Chao1 index (**Tables 2**, **3**) was calculated for each sample. The number of CTG labeled and Rose Bengal stained foraminifera, as well as the CHG labeled and Rose Bengal stained foraminifera, were compared by chi-square testing. Assuming that CHG foraminifera would have stained with Rose Bengal, the number of Rose Bengal stained foraminifera was determined as a sum of CHG labeled (living) and Rose Bengal stained (recently dead) individuals. For our chi-square test, the Rose Bengal stained individuals were treated as the expected values, whereas the CTG or CHG labeled individuals were treated as the observed values; this approach is adapted from Bernhard et al. (2006). The percentage of CHG labeled (living) faunal assemblages from GHP sites were calculated relative to total foraminiferal abundance (CHG labeled + Rose Bengal stained, i.e., foraminifera containing cytoplasm; **Figure 7**). Due to similar properties, further in the text CTG and CHG labeled foraminifera are interchangeably referred to as "fluorescently labeled."

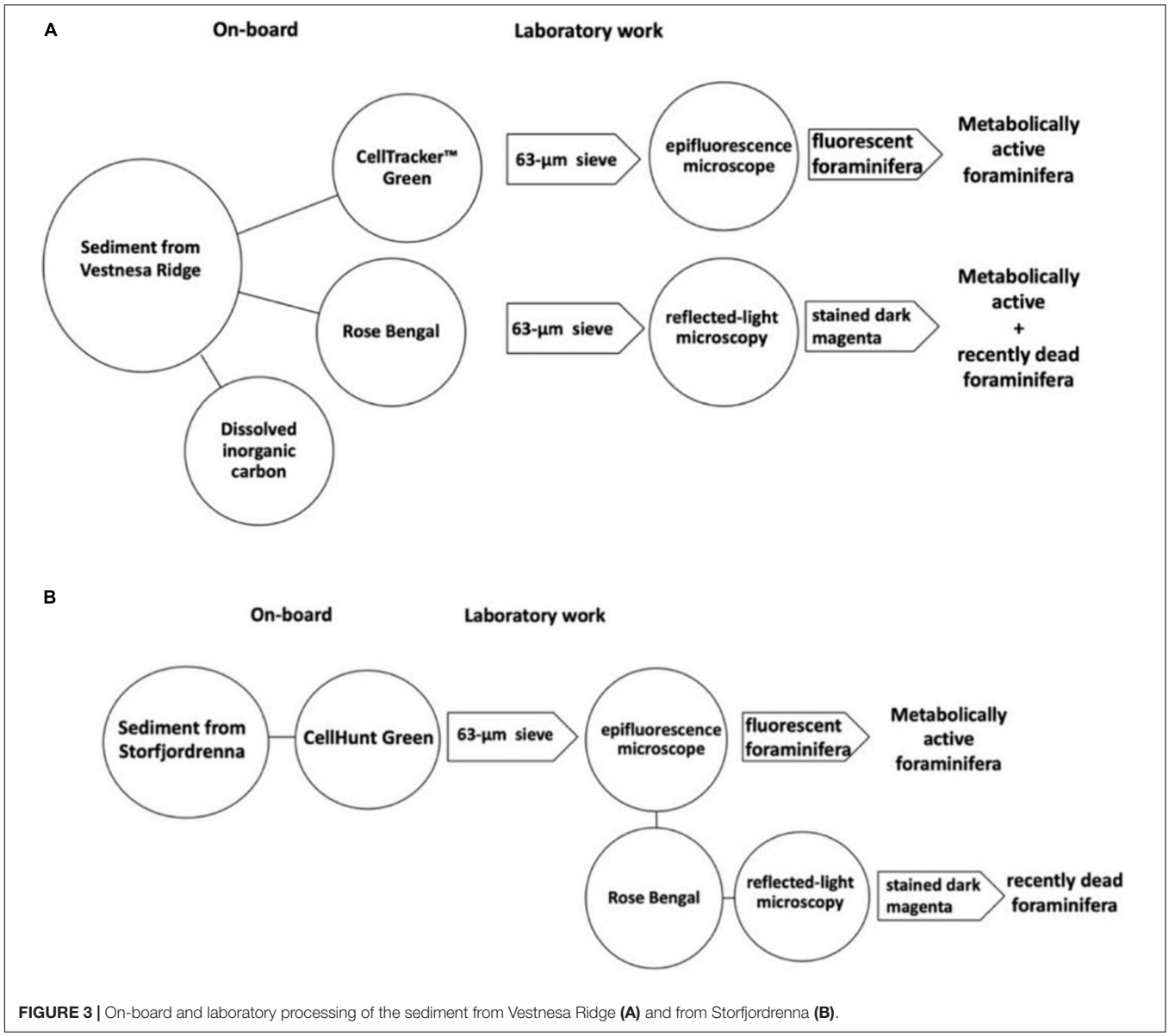

FIGURE 3 | On-board and laboratory processing of the sediment from Vestnesa Ridge **(A)** and from Storfjordrenna **(B)**.

Stable Isotopes Analyses

For carbon ($\delta^{13}C$) stable isotope analyses of Vestnesa Ridge samples, the most numerous individuals of species indicated as a metabolically active (CTG labeled; live) and individuals "live + recently dead" (Rose Bengal stained) were selected. Due to the small size of most specimens, between 8 and 10 specimens of *Melonis barleeanus* and *Cassidulina neoteretis* (when present) and 10 unstained tests of the planktonic foraminiferal species *Neogloboquadrina pachyderma* were picked from each sample. In case of foraminifera from GHPs, $\delta^{13}C$ measurements were performed on metabolically active (CHG labeled) foraminifera and recently dead (Rose Bengal stained) foraminifera of the two most numerous species *M. barleeanus* and *Nonionellina labradorica* (between eight and 10 specimens). Some "dead" (unstained tests) were picked for isotope analyses for comparison. Whenever possible, replicates were processed and analyzed.

Isotopic measurements were performed on a MAT 253 Isotope Ratio Mass Spectrometer (Department of Geosciences, UiT The Arctic University of Norway). Carbon isotopic compositions are expressed in conventional δ notation against the Vienna Pee Dee Belemnite (V-PDB) standard (1.96, −10.21, and −48.95‰ for $\delta^{13}C$) and reported in parts per thousand (per mil, ‰). Analytical precision was estimated to be better than 0.07‰ for $\delta^{13}C$ by measuring the certified standard NBS-19.

RESULTS

Foraminiferal Assemblages

Vestnesa Ridge

Fluorescently labeled (living) individuals were present in the sediment from core MC893A (Lomvi pockmark) at 0–1 cm and

TABLE 2 | Direct counts of CellTracker™ Green labeled foraminifera from all samples.

	Control site									**Vestnesa Ridge**								
Core number	**MC880A**			**MC880B**			**MC884**			**MC886**			**MC893A**			**MC893B**		
Depth (cm)	0–1	1–2	2–3	0–1	1–2	2–3	0–1	1–2	2–3	0–1	1–2	2–3	0–1	1–2	2–3	0–1	1–2	2–3
Cassidulina laevigata	4						1											
Cassidulina neoteretis	22	1		21	7		4	1					13	2				
Cassidulina reniforme				3	1		4						2					
Cibicides lobatulus				3									1	1				
Melonis barleeanus	4	3		6	7		8	7					10	9				
Nonionellina labradorica								3					1					
Pullenia bulloides	1			4			2	5					2					
Total number/sample	31	4		37	15		19	16					29	12				
SD	9,60	1,41		7,7	3,46		2,68	2,584					5,26	4,35				
Number/10 cm^3	11.9	1.5		14.2	5.7		7.7	6.2					11.15	5				
#Taxa	4	2		5	3		5	4					6	3				
Shannon's H index	0.88	0.56		1.03	1.22		1.41	1.21					1.33	0.72				
Evenness index	0.60	0.87		0.70	0.81		0.82	0.84					0.62	0.58				
Chao1 index	4	2		5	3		5	4					6.3	3				

TABLE 3 | Direct counts of Rose Bengal stained foraminifera from all samples.

	Control site									Vestnesa Ridge								
Core number	**MC880A**			**MC880B**			**MC884**			**MC886**			**MC893A**			**MC893B**		
Depth (cm)	0–1	1–2	2–3	0–1	1–2	2–3	0–1	1–2	2–3	0–1	1–2	2–3	0–1	1–2	2–3	0–1	1–2	2–3
Adercotryma glomeratum		3																
Buccella frigida		7		5				1					14	6				
Cassidulina laevigata	1							1	1	1								
Cassidulina neoteretis	44	24		11	12	17	9	13	3				9	2				
Cassidulina reniforme		3		1	1		3	1					8	1	1			
Cibicides lobatulus	4						2	2					2					
Elphidium excavatum									1							3		
Fissurina sp.				2														
Labrospira crassimargo										7								
Lagena sp. 1		1						1										
Lagena sp. 2		1							1				1					
Melonis barleeanus	16			10	31	23	8	28	12	1			52	16	5	16	14	3
Nonionellina labradorica					1	3		1	1				1					
Pullenia bulloides	4	3			2	2	2	8	3	1			1	1		2		
Reophax guttifer		3						4	2					1				
Reophax fusiformis							2						12					
Reophax sp.				2	5	1			1				1	2		7		
Stainforthia loeblichi		1						2		1								
Spiroplectammina earlandi				1						4			1					
Trifarina angulosa	1			2			2											
Triloculina sp.				1			1		2									
Total number/sample	70	46		35	52	46	29	62	27	15			102	29	6	28	14	3
SD	17.83	7.32		3.95	11.70	10.10	3.06	8.34	3.36	2.5			15	5.52	2.82	6.37	0	0
Number/10 cm^3	27	18		13 >4	20	17.6	11.2	23.8	10.4	5.8			39.2	11.2	2.3	10.7	5.4	1.2
#Taxa	6	9		9	6	5	8	11	10	6			11	7	2	4	1	1
Shannon's H index	1.08	1.55		1.79	1.15	1.04	1.80	1.62	1.75	1.43			1.6	1.37	0.45	1.09	0	0
Evenness index	0.55	0.54		0.66	0.52	0.60	0.76	0.48	0.63	0.69			0.44	0.56	0.78	0.74	1	1
Chao1 index	5	12		9.75	6.5	5	8	14.33	13.33	12			16	8	2	4	1	1

1–2 cm core depths, but not in the 2–3 cm interval. None of the individuals in cores MC886 and MC893B were metabolically active. At the control site, fluorescently labeled foraminifera were found in all samples from 0–1 cm and 1–2 cm intervals, while again no living foraminifera were observed in the 2–3 cm interval (**Figure 4** and **Table 2**). Rose Bengal stained aliquots indicated presence of foraminifera (live + recently dead) in cores MC893A, MC893B, MC884, MC880A, and MC880B in all sampling intervals. No Rose Bengal stained individuals were observed in the 1–2 cm and 2–3 cm samples at site MC886 (**Figure 4** and **Table 3**). Both the chi-square (p = 1, α = 0.05) and Student's t-test (p = 0.44, α = 0.05) test show significant differences between number of fluorescently labeled and Rose Bengal stained specimens, within any given sediment interval. In general, there was a lower number of foraminifera in the cold-seep samples than in the control samples. Density of fluorescently labeled foraminifera at Vestnesa Ridge ranged from 0 to 11.1 individuals per 10 m^3 in the 0–1 cm intervals, and from zero to five individuals per 10 cm^3 in the 1–2 cm intervals. Density of live foraminifera at control sites ranged from 7.7 to 14.2 individuals per 10 cm^3 in the 0–1 cm intervals, and from 1.5 to 6.1 in the 1–2 cm intervals (**Figure 4**). The number of Rose Bengal stained

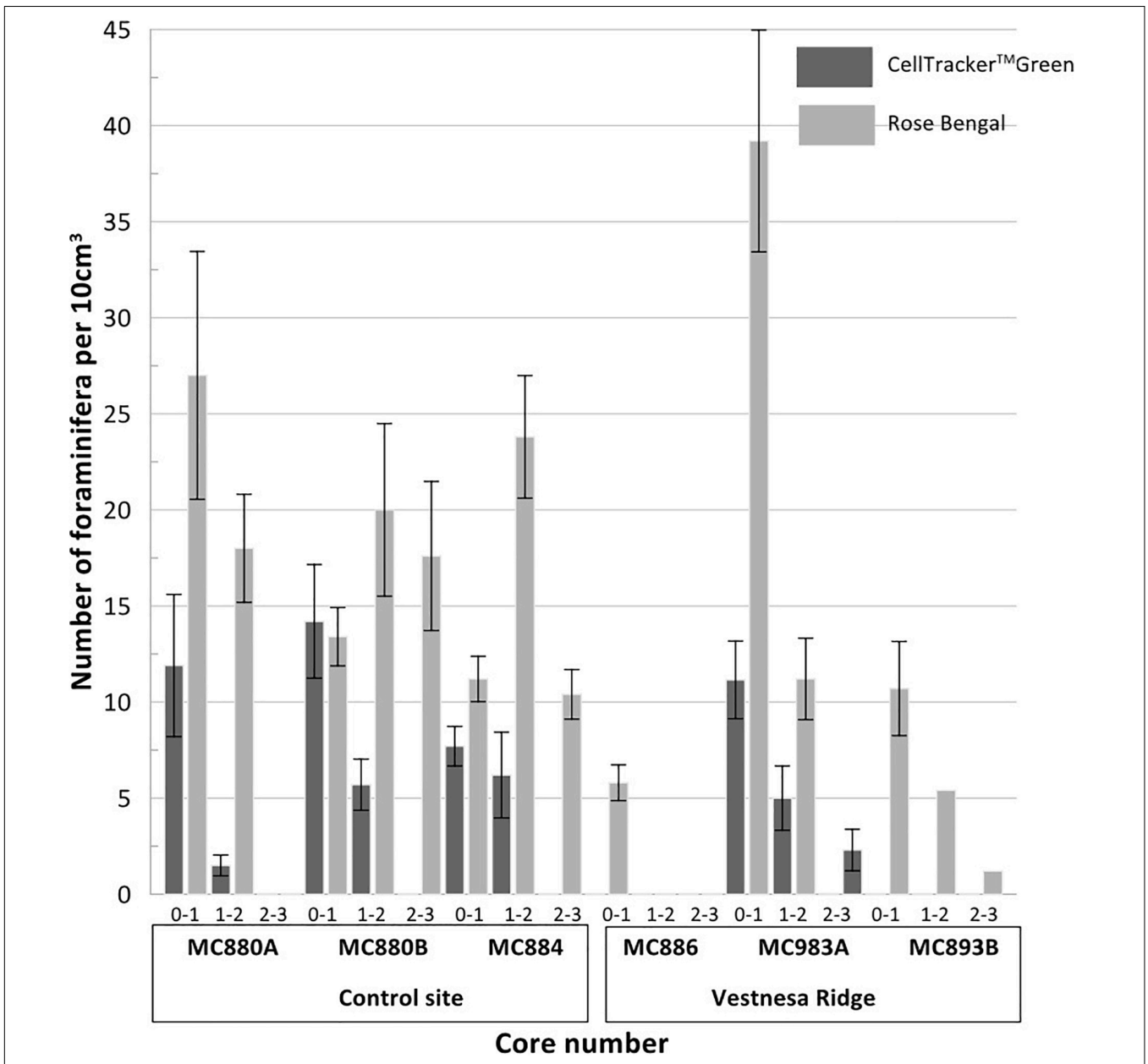

FIGURE 4 | Plots presenting the number (per 10 cm^3) of CellTracker™ Green CMFDA labeled (live) and Rose Bengal stained (live + recently dead) foraminifera from aliquots of Vestnesa Ridge and the nearby control site. Numbers 0–1, 1–2, and 2–3 next to the core number refer to the depth: 0–1, 1–2, and 2-3 cm respectively.

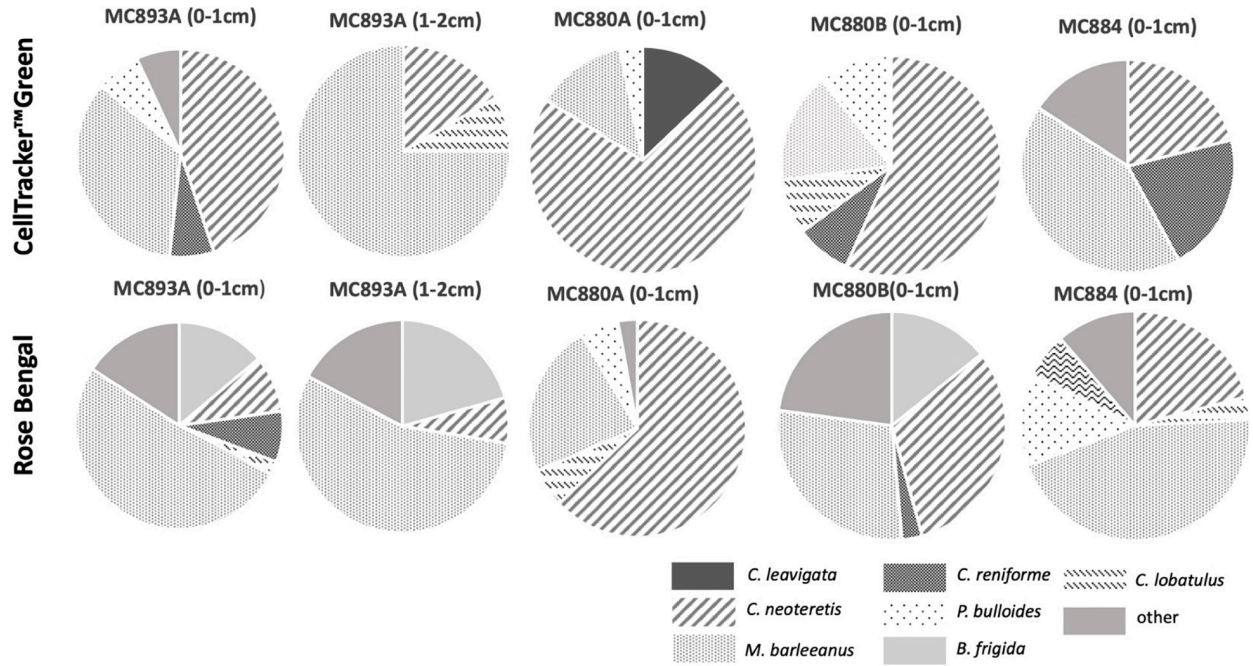

FIGURE 5 | Foraminiferal species composition at Lomvi pockmark (Vestnesa Ridge) and control site using CellTracker^{TM}Green (live) and Rose Bengal (live + recently dead). Plots are based on direct counts (**Tables 2**, **3**).

foraminifera in samples from Vestnesa Ridge active sites ranged from 5.8 to 39.2 individuals per 10 cm^3 in the 0–1 cm interval, from 0 to 11.2 in the 1–2 cm interval, and from 0 to 2.3 in the 2–3 cm interval (**Figure 4**). In the sediment from the control site, the abundance of Rose Bengal stained (live + recently dead) foraminifera ranged from 11.3 to 27 specimens per 10 cm^3 in the 0–1 cm interval, from 20 to 46 foraminifera in the 1–2 cm interval and from 0 to 17.2 in the 2–3 cm interval (**Figure 4**).

CTG and Rose Bengal show that dominant and most common species were the same in the assemblages from active seep sites at Vestnesa Ridge (**Tables 2**, **3** and **Figure 5**). The S(H) index in CTG labeled samples from Vestnesa Ridge range from 0 (empty samples) to 1.33, and from 0.56 to 1.41 in samples from the control site. The S(H) index in Rose Bengal stained samples from Vestnesa Ridge range from 0 (empty sample) to 1.33, and from 1.04 to 1.8 in control site. The Pielou evenness index in CTG labeled samples from Vestnesa Ridge range from 0.58 to 0.88 and from 0.60 to 0.87 in samples from the control site (**Table 2**). In Rose Bengal stained samples the same index varies from 0.44 to 0.78 for Vestnesa Ridge and from 0.48 to 0.76 for the control site (**Table 3**).

In the fluorescently labeled samples from Vestnesa Ridge the foraminiferal faunas are dominated by *M. barleeanus* (34% of total fauna in the 0–1 cm interval and 69% in the 1–2 cm interval) and *C. neoteretis* (45% of total fauna in the 0–1 cm interval and 15% in the 1–2 cm interval) (**Table 2**). Similarly, in Rose Bengal-stained samples the most abundant species were *M. barleeanus* (51% of total fauna in the 0–1 cm interval and 55% in the 1–2 cm interval), *C. neoteretis* (9% of total fauna in the 0–1 cm interval and 7% in the 1–2 cm interval) and *Buccella frigida* (14% of the total fauna in the 0–1 cm interval and 6% in the 1–2 cm interval) (**Table 3**). No apparent endemic foraminiferal species were observed in the Vestnesa Ridge seep sediment samples (**Tables 2**, **3**).

Storfjordrenna Pingos

Metabolically active (fluorescently labeled) benthic foraminifera were present in both the active GHP1 and the inactive GHP5, except at site MC902 taken at the top of the active GHP1 (**Table 4**). In addition to live, metabolically active foraminifera, Rose Bengal staining shows presence of recently dead individuals, i.e., foraminiferal tests that still contain cytoplasm, but were not metabolically active at the time of collection, which could lead to a significant overestimation of the number of live foraminifera ($p = 0.01$, $\alpha = 0.05$; chi-square test) (**Figure 7**).

The ratio between fluorescently labeled and Rose Bengal-stained foraminifera differed between the active and inactive GHP1 and GHP5. A higher proportion of live to recently dead individuals was found in the inactive GHP5, and in GHP1 (except for the sample MC902, which appeared to be barren; **Figure 7**). The ratio between live vs. recently dead foraminifera was approximately 2:3 in the active GHP1, and 3:2 in the inactive GHP5 (**Figure 7**).

At GHP1, the density of live individuals increased along the transect from 0 individuals at the top of GHP1 to 11.84 (per 10 cm^3) at the edge of the pingo. At GHP5 (the non-active site), the foraminifera were relatively evenly distributed compared to the active GHP1. Similarly, to GHP1, the lowest density 3.43 (per 10 cm^3) of metabolically active foraminifera was observed in the sediment from the summit of GHP5 (**Table 4**). The S(H) index

TABLE 4 | Number per sample of CellHunt Green labeled (CHG) and Rose Bengal stained (RB) foraminifera (direct count), and Shannon diversity index from active GHP1 and inactive GHP5.

	MC902		MC917		MC919		MC920		MC921		MC922	
	CHG	RB	CHG	RB	CHG	RB	CHG	RB	CHG	RB	CHG	RB
Buccella frigida			4		6	14	2		2		3	
Cassidulina laevigata			2	1			1	1			1	
Cassidulina neoteretis					2	37		5		5		9
Cassidulina reniforme				4	1	6						3
Cibicides lobatulus			3	14	1	4	1	13	1	10		
Elphidium excavatum			1		8				3		8	
Globobulimina turgida				2	1	4	4	5	2	1	1	2
Melonis barleeanus			8	8	22	31	9	12	30	22	24	2
Nonionellina labradorica			6	3	18	18	10	5		1	3	
Pullenia bulloides				2		5		1	1	3	2	3
Stainforthia loeblichi						1						
Triloculina sp.				1								1
Uvigerina sp.				1	3	2		1				
Total number/sample			24	36	62	122	27	43	39	42	42	20
#Taxa			6	9	9	10	6	8	6	6	7	6
Shannon index			1.53		1.75		1.3		1.08		1.26	
Evenness index			0.83	0.65	0.59	0.63	0.71	0.70	0.40	0.61	0.54	0.77
Chao1 index			6	10	10.5	10	6.5	11	6.3	7	7.5	6

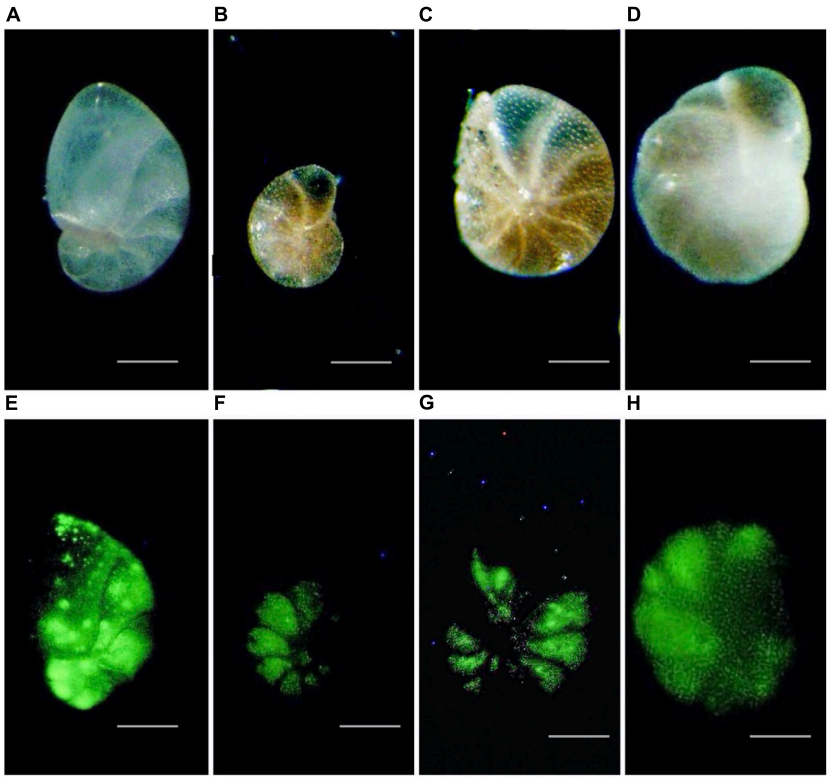

FIGURE 6 | Reflected light **(A–D)** and corresponding epifluorescence (green coloration from CellTracker™ Green) **(E–H)** micrographs of foraminifera collected at Vestnesa Ridge (core 893A); **(A,E)** *Nonionellina labradorica*; **(B,C,G,F)** *Melonis barleeanus*; **(D,H)** *Cassidulina neoteretis*. Scales: panels **(A–D)** = 30 μm; panels **(B,C,F,G)** = 25 μm.

in samples from GHP1 ranged from 0 closer to the center to 1.75 at the edge, and in GHP5 from 1.08 to 1.26 (**Table 4**). The Pielou evenness index in CHG labeled samples from GHP1 varies from 0.59 to 0.83 and between 0.40 and 0.71 in GHP5 (**Table 4**).

Both the active and the post-active pingo were characterized by presence of the same dominant CHG labeled species: *M. barleeanus* (35% of total living fauna in GHP1, and 52% in GHP5), *N. labradorica* (28% in GHP1, and 11% in GHP5), *Elphidium excavatum* (11% in GHP1, and 9% in GHP5) and, to some extent, *B. frigida* (12% in GHP1; **Figure 8**). In the Rose Bengal-stained (i.e., recently dead) samples, the dominant species were *M. barleeanus* (25% of the total living fauna in GHP1, and 34% in GHP5), *C. neoteretis* (23% in GHP1, and 18% in GHP5), *C. lobatulus* (22% in GHP5), and to some extent *N. labradorica* (13% in GHP1, and 6% in GHP5) (**Figure 8**). No endemic species were found in any of the samples from GHP1 or GHP5 (**Figure 8**).

Isotopic Signatures

CellTracker™ Green labeled foraminifera tend to have less negative $\delta^{13}C$ signatures compared to Rose Bengal stained pools and empty tests of their conspecifics, both at Vestnesa Ridge (core MC893A) and at the control site (core MC880A and MC880B; **Figure 9**). The difference between $\delta^{13}C$ measured in CTG labeled individuals and Rose Bengal-stained specimens is 0.22‰ in samples from Vestnesa Ridge, whereas in samples from the control site the difference is 0.41 and 0.15‰. The difference between $\delta^{13}C$ measured in CTG labeled and empty tests is 0.29 and 0.22‰ at Vestnesa Ridge, and between 0.04 and 0.27‰ at the control site (**Table 5**).

In contrast, in both GHP1 and GHP5 the $\delta^{13}C$ values measured in CHG labeled pools are always considerably more depleted compared to values measured in Rose Bengal-stained specimens (**Figure 8**). The difference in $\delta^{13}C$ values in CHG labeled foraminifera is 0.08‰ (at GHP1) and 0.20 and 0.49‰ (at GHP5; **Table 5**). The difference between $\delta^{13}C$ values measured in CHG labeled foraminifera and unstained tests is 0.88 and 1.46‰ at GHP1 and range between 0.14 and 0.58‰ at GHP5. The most pronounced difference is found in samples from the active GHP1 (MC919), where the isotopic signature of live *M. barleeanus* is more depleted compared to the signature of dead individuals (about 1.46‰; **Table 5** and **Figure 8**).

DISCUSSION

Foraminiferal Fauna

The study shows presence of living foraminifera in sediments from active methane emission sites from pockmarks at Vestnesa Ridge and from hydrate mounds ("pingos") in Storfjordrenna.

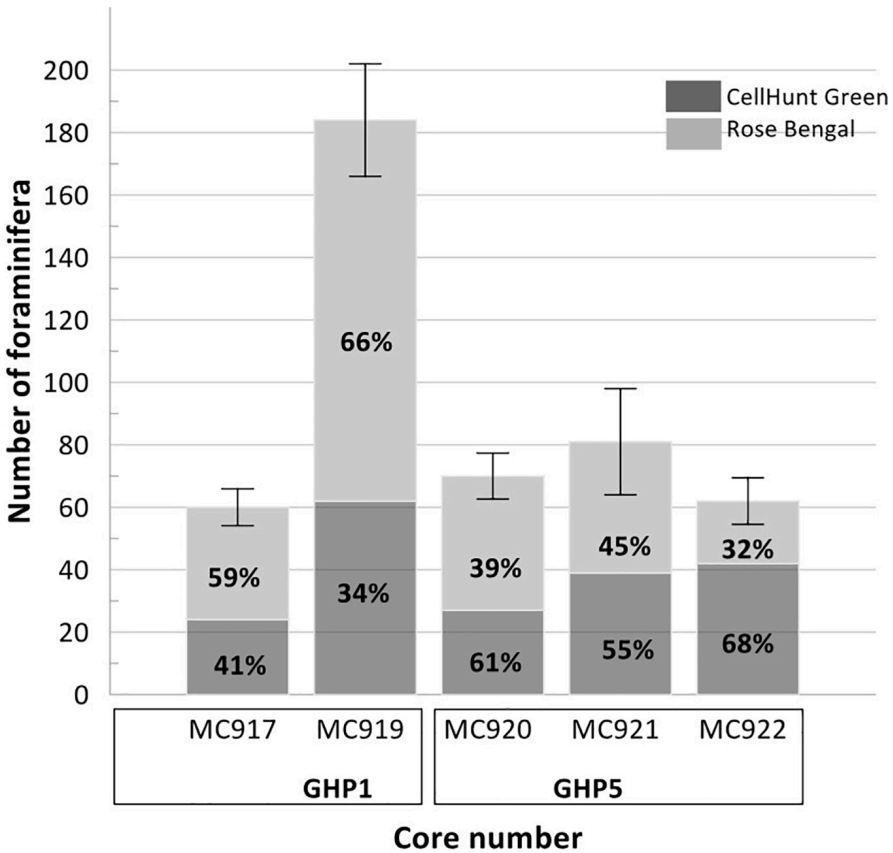

FIGURE 7 | Percentages of benthic foraminifera labeled with CellHunt Green (CHG) = live, and individuals subsequently stained with Rose Bengal (RB) = recently dead (direct count) from Storfjordrenna pingo. The number of foraminifera represents the sum of CHG (dark gray) and RB (light gray) individuals. Plot based on direct counts.

Results imply that, despite the hostile conditions (e.g., low oxygen, high carbon dioxide concentrations and potentially also hydrogen sulfide), which are a result of anaerobic methane oxidation (Herguera et al., 2014), the benthic foraminifera were metabolically active. Furthermore, the results confirmed a previous observation that Rose Bengal staining overestimated the number of live foraminifera (Bernhard et al., 2006). This is manifested for example by the presence of Rose Bengal stained foraminifera in samples with no fluorescently labeled individuals, or by a higher number of Rose Bengal stained foraminifera compared to fluorescently labeled individuals (see samples MC917 and MC919 from Storfjordrenna; **Figure 7**).

Considering the sampling location and previously published studies from Vestnesa Ridge (e.g., Panieri et al., 2017; Sztybor and Rasmussen, 2017; Åström et al., 2018; Dessandier et al., 2019, 2020; Yao et al., 2019), the uneven distribution of foraminifera is most likely a result of the horizontal distribution of geochemically diverse microhabitats within the Vestnesa sediments. The TowCam imaging survey during the sampling campaign revealed a patchy distribution of organisms, such as white and gray bacterial mats and tubeworms (**Figure 2**), which correspond to geochemically different microhabitats (e.g., Niemann et al., 2006; Treude et al., 2007). For example, gray bacterial mats (*Arcobacter* spp., *Thiomargarita* spp.) are common in unstable environments, whereas white bacterial mats (*Beggiatoa* spp.) and tubeworms fields indicate stable sulfide conditions (e.g., Sahling et al., 2002; Niemann et al., 2006; Treude et al., 2007). It has been previously observed that in response to a heterogeneous distribution of methane-dependent microbial and macrofaunal biota, the foraminiferal species composition and absolute abundance (density) may show great variability within the same seep area (e.g., Rathburn et al., 2000; Wollenburg and Mackensen, 2009; Dessandier et al., 2019).

In this study, CTG shows the lowest number or absence of metabolically active foraminifera in some of the assemblages from Vestnesa Ridge, which indeed can be interpreted as an environment being inhospitable for foraminifera. At the same time, in the samples from the MC886 site with no fluorescently labeled individuals, Rose Bengal stained foraminifera (mostly agglutinated taxa) are still present. This observation suggests that "inhospitable" conditions are temporary variations rather than permanent constraints. Instability/variability of the environment can be related to the ephemeral nature of methane seeps, which are strongly dependent on methane

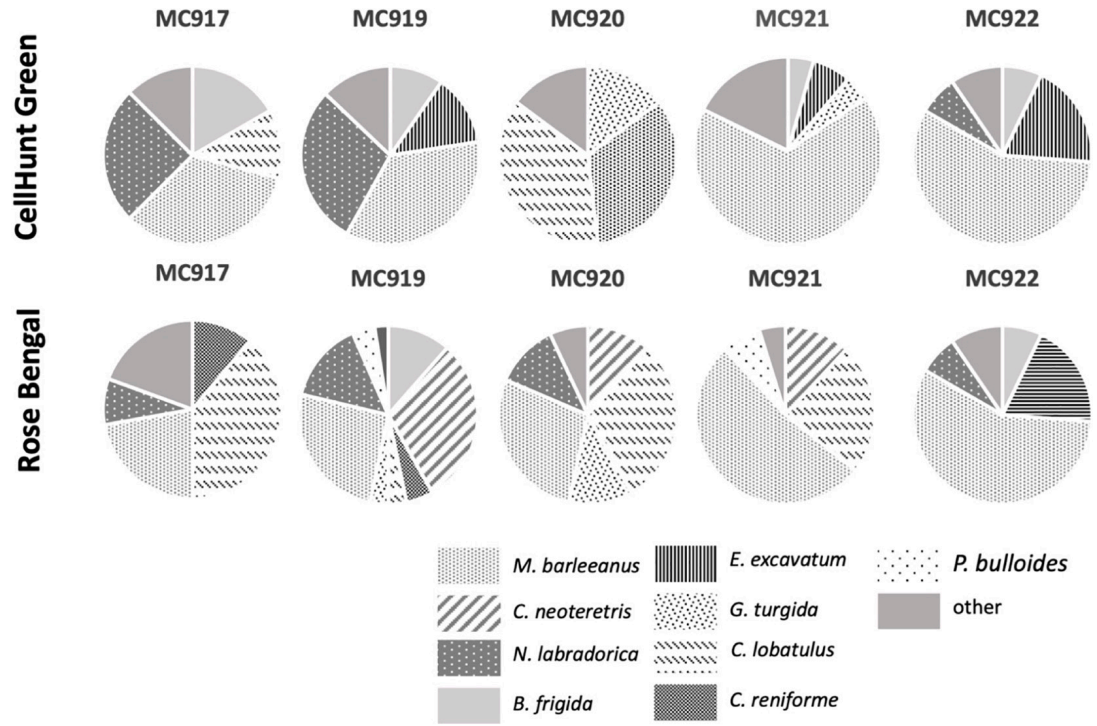

FIGURE 8 | Foraminiferal species composition within the active GHP1 (MC917 and MC919) and post- active GHP5 (MC920, MC921, and MC922). CellHunt Green labeled samples **(upper panel)** and Rose Bengal stained **(lower panel)**.

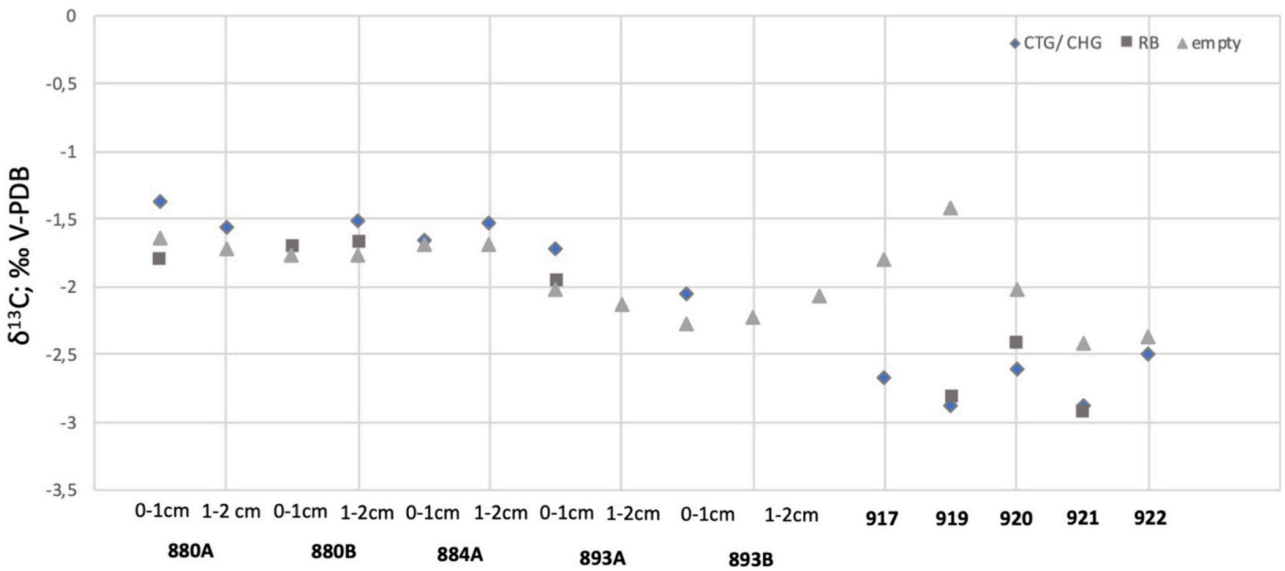

FIGURE 9 | The $\delta^{13}C$ values measured in CellTracker™ Green labeled (CTG), CellHunt Green labeled (CHG), Rose Bengal stained (RB), and empty tests of *Melonis barleeanus*.

flux (Levin, 2005; Åström et al., 2020). As shown by Yao et al. (2019), the Lomvi (MC893) and Lunde (MC886) pockmarks are characterized by two different types of methane transport: advective and dominated by methane diffusion (Lomvi and Lunde, respectively). Additionally, sulfate and methane profiles within the MC886 core indicate non-steady-state conditions (Yao et al., 2019). Those unstable conditions could explain the lack of metabolically active foraminifera with a presence

of Rose Bengal stained specimens in the samples from Lunde pockmark (MC886) at the time of sampling. Similar observations were made by Dessandier et al. (2019): the authors suggested a correlation between low density of foraminifera and methane-diffusive areas due to high sulfide concentration, and decreased or lack of agglutinated foraminifera in cold seep assamblagdes as a result of an increase in organic matter content due to methane related microbial mass, and stronger competition from calcareous species.

Similarly to Vestnesa Ridge, the benthic foraminiferal distribution pattern within the active GHP1 shows a greater variability along the analyzed transect compared to the transect along the inactive GHP5. The highest density of foraminifera is observed at the edge of GHP1, where white and gray bacterial mats are present, with a small difference in density toward the center of GHP1, and reaching zero individuals approximately at the top, where most of the methane flares are located (Serov et al., 2017; Carrier et al., 2020). The $\delta^{13}C_{DIC}$ value at the top of the active GHP reached −24.2‰, which can be linked to methane-related microbial activity (Dessandier et al., 2019). The absence of foraminifera at the summit is thus most likely due to the combined effect of disturbance caused by gas bubbles passing though the sediment and geochemical constraints related to microbial activity (e.g., low oxygen or presence of hydrogen sulfide; Herguera et al., 2014; Carrier et al., 2020). The Shannon index shows that the suite of samples from GHP 5 has less variability compared to the samples from GHP1. The highest density and diversity are observed at the edge of GHP1 (MC919), in bacterial mats. Similarly to other methane cold seeps, the microbial community at the active GHP1 might serve as a food source and support benthic foraminiferal growth (e.g., Rathburn et al., 2000; Panieri, 2006; Fontanier et al., 2014; Herguera et al., 2014).

It is widely accepted that the distribution of benthic foraminiferal faunas at cold seeps is mainly controlled by oxygen levels and organic content, and that species preferring organic-rich environments and reduced oxygen are well adapted to live in the environmental conditions of seep sites (e.g., Akimoto et al., 1994; Rathburn et al., 2000, 2003; Bernhard et al., 2001; Fontanier et al., 2014). In fact, the living foraminiferal fauna at Vestnesa Ridge is dominated by *M. barleeanus* and *C. neoteretis,* and by *M. barleeanus* and *N. labradorica* at the active GHP1. *M. barleeanus* is described as an intermediate to deep infaunal species associated with high-nutrient conditions and resistant to environmental stress due to organic matter degradation (e.g., Wollenburg and Mackensen, 1998; Alve et al., 2016). Both *M. barleeanus* and *C. neoteretis* have been previously observed as the most abundant species in methane-charged sediments at Vestnesa Ridge (Dessandier et al., 2019). Additionally, the TEM (transmission electron microscopy) analyses of *M. barleeanus* from Lomvi pockmark (MC893) at Vestnesa Ridge revealed presence of methanotrophic-like bacteria located outside the test, but very close to their apertural region (Bernhard and Panieri, 2018). Although a possible symbiosis between *M. barleeanus* and methanotrophs remains unconfirmed, the potential influence of seep-related bacteria on *M. barleeanus* cannot be excluded. Similarly, to *M. barleeanus, C. neoteretis* (Rose Bengal stained) was found to be dominant in the top layers of the dysoxic (low oxygen) sediments of the Håkon Mosby Mud Volcano (Wollenburg and Mackensen, 2009) and was one of the most numerous species at Vestnesa Ridge (Dessandier et al., 2019). As in other investigated methane seep sites, to date, there are no endemic species found at Vestnesa Ridge and Storfjordrenna pingos, but only well-known species represented in a wide range of environments (e.g., Rathburn et al., 2000; Bernhard et al., 2001; Herguera et al., 2014; Dessandier et al., 2019).

The combined use of CHG and Rose Bengal allows to distinguish live and recently dead foraminifera from the Storfjordrenna area, which reveals major shifts in species compositions in both the active GHP1 and the inactive GHP5. In live foraminiferal assemblages, the most common species after *M. barleeanus* are *N. labradorica* and *E. excavatum,* whereas in Rose Bengal stained samples *C. neoteretis* and *C. lobatulus* are of high relative abundance. Because species which tolerate high organic concentration and low oxygen conditions are associated both with spring bloom and methane seepage, it is challenging to distinguish precisely to what extent the switch in population is due to methane availability. Particularly, the relatively high number of live *N. labradorica* both in the active GHP1 and inactive GHP5, as well as appearance of *E. excavatum*, might indicate the influence of the seasonal algae bloom. *E. excavatum* is an opportunistic species, with the ability to respond rapidly to deposition of food (pulsed food supply; Corliss, 1991; Altenbach, 1992) and colonize harsh environments (Korsun and Hald, 2000). It almost completely replaces other species, such as *C. lobatulus*, which is an epifaunal species that prefers low food supply and high oxygen concentration (e.g., Hald and Steinsund, 1996; Klitgaard-Kristensen et al., 2002). The significant number of *N. labradorica* and *B. frigida* in samples MC919 from GHP1 is puzzling. Although *N. labradorica* is known to feed on fresh phytodetritus, and is an indicator species of high primary productivity as a result of the retreating summer sea-ice margin or Arctic Front (Cedhagen, 1991; Corliss, 1991), this species also has a potential to thrive at methane seepage sites. *N. labradorica* (Rose Bengal stained) have been found previously in the sediment from the top of the GHP1 (Dessandier et al., 2020). Kleptoplasts present in cell of *N. labradorica* might be involved in ammonium or sulfate assimilation pathways and might potentially support life under adverse conditions (Jauffrais et al., 2019). Alike *N. labradorica,* the distribution of *B. frigida* is related to seasonal sea-ice retreat and appearance of fresh algae (Seidenkrantz, 2013). From all investigated samples from Storfjordrenna, *B. frigida* occurs most frequently in the MC919 samples, where bacterial mats are present. In previous studies from Vestnesa Ridge, it was suggested that the species potentially can feed on microbial food sources, i.e., methane related bacterial mats (Dessandier et al., 2019). Interestingly, in this study *B. frigida* occur in CTG labeled samples, but there were no Rose Bengal stained individuals. This suggests that presence of live *B. frigida* might reflect a relatively recent appearance of bacterial mats associated with methane seepage.

Additionally, the use of both CHG and Rose Bengal reveals a difference in the percentage of living vs. recently dead

TABLE 5 | Carbon isotope values ($\delta^{13}C$; ‰ V-PDB) of *Melonis barleeanus*, *Cassidulina neoteretis*, and *Neogloboquadrina pachyderma*, and dissolved inorganic carbon (DIC; *Bernhard and Panieri, 2018) from Vestnesa Ridge and control site; and *Melonis barleeanus* and *Nonionellina labradorica* from Storfjordrenna pingo from active GHP1 and inactive GHP5; CellTracker™ Green CMFDA (CTG), CellHunt Green (CHG), Rose Bengal (RB) individuals, and empty tests.

			M. barleeanus			*C. neoteretis*			*N. pachyderma*	*N. labradorica*			DIC*
	Core number	**Depth (cm)**	**CTG/CHG δ ^{13}C**	**RB δ ^{13}C**	**Empty δ ^{13}C**	**CTG δ ^{13}C**	**RB δ ^{13}C**	**Empty δ ^{13}C**	**Empty δ ^{13}C**	**CHG δ ^{13}C**	**RB δ ^{13}C**	**Empty δ ^{13}C**	**δ ^{13}C**
Vestnesa Ridge	MC893A	0–1	−1.73	−1.95	−2.02	−0.26			−0.63				
					−2.14				−0.22				
		1–2	−2.06		−2.28			−0.66					
	MC893B	0–1			−2.24								−3.34
		1–2			−2.08								−14.25
Control site	MC880A	0–1	−1.38	−1.79	−1.65				−0.33				
		1–2	−1.57		−1.72								−0.79
	MC880B	0–1		−1.70	−1.77	−0.38							
		1–2	−1.52	−1.67	−1.78	−0.35							−0.64
	MC884	0–1	−1.66		−1.70				−0.84				
		1–2	−1.54		−1.70								
GHP 1	MC917	0–1	−2.68		−1.80								
	MC919	0–1	−2.89	−2.81	−1.43					−4.34	−4.34		
GHP5	MC920	0–1	−2.61	−2.41	−2.03					−4.21	−3.38		
	MC921	0–1	−2.89	−2.92	−2.43					−3.38			
	MC922	0–1	−2.51		−2.37								

foraminifera within each of the investigated GHP types. The active GHP1 is characterized by a greater percentage of recently dead (Rose Bengal stained) individuals, compared to living (CHG labeled) specimens, whereas in the inactive GHP5 pingo this ratio is reversed with more live than dead foraminifera. This difference between the active GHP1 and inactive GHP5 implies more unstable and variable environmental conditions at GHP1, potentially related to methane emissions, rather than general seasonal environmental changes (Carrier et al., 2020). On average, CHG labeling showed that approximately 40% of the benthic foraminifera in GHP1 and approximately 54% in GHP5 were alive at the time of collection.

Interestingly, despite the highest number of living foraminifera in GHP5 the Pielou evenness index in CHG labeled samples shows fairly low values (from 0.40 to 0.71) compared to samples from GHP1 (from 0.59 to 0.83) (**Table 4**). It indicates the presence of dominant, well-adapted species in the foraminiferal population within the post-active GHP, most likely due to the recent environmental changes. Because, the Pielou evenness index is relatively low in the post-active GHP5 compared to GHP1, we can exclude methane influence. It is possible the evenness index decreased due to the influence of the spring bloom. In the literature methane cold seeps are described as a biological oasis in the high−Arctic deep sea (Åström et al., 2018) due to the presence of microbial communities seeps provide enough food to sustain foraminiferal populations (e.g., Rathburn et al., 2000; Torres et al., 2003; Heinz et al., 2005; Panieri, 2006; Panieri and Sen Gupta,2008). In contrast, sediments outside the seeps are impoverished in organic substrates for most of the year and depend on benthic-pelagic coupling (Gooday, 1988). Thus, the benthic communities in the Arctic, which experience low food are likely more sensitive to food input from primary production (e.g., Gooday, 1988, 1993; Sander and van der Zwaan, 2004; Nomaki et al., 2005; Schönfeld and Numberger, 2007; Braeckman et al., 2018). After the episode of strong food pulses, a population of specific opportunistic species increased, which can quickly utilize large amounts of detritus (e.g., Gooday, 1988; Nomaki et al., 2005; Braeckman et al., 2018). In fact, samples from GHP5 are dominated by *M. barleeanus*, an opportunistic species well adapted to high organic content (e.g., Wollenburg and Mackensen, 1998; Alve et al., 2016) and shows a relatively high number of *E. excavatum*. A " bloom-feeding" behavior of *E. excavatum* was previously described by Schönfeld and Numberger (2007). In comparison, the foraminiferal fauna from the active GHP consists mainly of species such as *B. frigida* and *N. labradorica*, species that thrive in cold seeps and can feed on bacteria (e.g., Dessandier et al., 2019; Jauffrais et al., 2019).

The $\delta^{13}C$ Signature in Foraminiferal Tests

Within methane cold seeps, the geochemistry of pore water is influenced by aerobic and/or anaerobic methane oxidation (Treude et al., 2007). Because methane-derived carbon is characterized by very low carbon isotopic signatures (from −50 to −20‰ for thermogenic methane, and from −110‰ to −60‰ for microbial methane) (Whiticar, 1999), the ambient DIC pool is enriched in isotopically light carbon in the form of either carbon dioxide (CO_2) or bicarbonate (HCO_3^-) resulting from microbial activity. If foraminifera incorporate methane-derived carbon from the ambient seawater during biomineralization, we would expect to see more negative $\delta^{13}C$ values in their tests compared to $\delta^{13}C$ values in tests of foraminifera from the non-seep sites. At Lomvi pockmark (Vestnesa Ridge), the $\delta^{13}C$ measured on CTG labeled, Rose Bengal stained, and unstained tests of *M. barleeanus* have values within the same range as of its conspecifics in "normal" (non-seep) marine environments, i.e., approximately −2‰ (e.g., Wollenburg et al., 2001; Dessandier et al., 2020). Likewise, the $\delta^{13}C$ measured on live *C. neoteretis* showed values within the expected range for specimens from non-seep environments, i.e., approximately −0.3‰ to −1‰ (Wollenburg et al., 2001), and was not as depleted as previously reported values (−7.5‰ $\delta^{13}C$) measured on Rose Bengal stained *C. neoteretis* from Håkon Mosby Mud Volcano (Mackensen et al., 2006). Therefore, the data provide no clear evidence that *M. barleeanus* and *C. neoteretis* from Vestnesa Ridge incorporate significant amounts of methane-derived carbon during test formation that would markedly affect the isotopic signature of their carbonate tests. The difference between $\delta^{13}C$ signatures of *M. barleeanus* and *C. neoteretis* most likely reflects different microhabitat preferences of these species. Infaunal species, such as *M. barleeanus,* tend to have more negative $\delta^{13}C$ compared to, for example, epifaunal or shallow infaunal species, such as *C. neoteretis* (e.g., Grossman, 1984; McCorkle et al., 1985; Fontanier et al., 2006).

The $\delta^{13}C$ measured in both metabolically active (CHG labeled) and recently dead (Rose Bengal stained) foraminifera from Storfjordrenna pingos is not straightforward to interpret. Although the $\delta^{13}C$ in tests of fluorescently labeled foraminifera from the active GHP1 have values slightly more depleted than the values exhibited by the same species in the post-active GHP5, still the $\delta^{13}C$ values measure in *M. barleeanus* from both GHPs are not much more depleted compared to Rose Bengal stained conspecific from near non-seep site (i.e., lower than −2.1‰; Dessandier et al., 2019). Overall, the $\delta^{13}C$ measured in *M. barleeanus* from Storfjordrenna are not significantly depleted compared to isotopic signatures of other seep-site foraminifera, e.g., *Uvigerina peregrina* with measured $\delta^{13}C$ values down to −5.64‰ (Hill et al., 2004), or *C. neoteretis* with $\delta^{13}C$ values of −7.5‰ (Mackensen et al., 2006). Storfjordrenna is at a relatively shallow water depth (∼400 m) and the sediment samples were collected in June. Thus, the negative $\delta^{13}C$ signature in foraminiferal tests could originate from a greater flux of particulate organic matter produced during the spring bloom and only potentially partly from methane seepage. A shift of approximately 0–4‰ toward a more negative $\delta^{13}C$ is shown to have an origin in local organic matter degradation (e.g., Torres et al., 2003; Martin et al., 2004).

It is generally believed that more negative $\delta^{13}C$ signatures in unstained and/or fossil foraminifera compared to those of "living" (Rose Bengal stained) specimens result from an authigenic overgrowth layer covering the tests. Foraminiferal tests deposited in methane-charged sediments might be coated by precipitates from highly ^{13}C-depleted pore water or

bacterially mediated methane oxidation and associated carbonate precipitation (e.g., Rathburn et al., 2003; Torres et al., 2003; Schneider et al., 2017; Sztybor and Rasmussen, 2017). A similar interpretation can be applied to explain the offset in $\delta^{13}C$ values between Rose Bengal stained and fluorescently labeled *M. barleeanus* from Vestnesa Ridge. Since Rose Bengal stained foraminifera represent both live and recently dead individuals, it is possible that in some of the specimens the organic lining was already partially decomposed, and that this surface of the tests had authigenic carbonate overgrowths (Mackensen et al., 2006). Considering the fact that isotopic offset occurred both in samples from Lomvi and the control site, and the isotopic variation is relatively low (∼0.20‰ Vestnesa Ridge, 0.15 and 0.41‰ at the control site), the offset could be due to dissolution of biogenic calcite and re-precipitation of inorganic calcite (overgrowth and recrystallization) or other early diagenetic processes that occur in normal non-seep sediments (Ravelo and Hillaire-Marcel, 2007), and as such not necessarily the effect of Methane-Derived Authigenic Carbonates (MDAC) overgrowth. Additionally, $\delta^{13}C$ values recorded in unstained tests of the planktonic foraminifera *N. pachyderma* from Vestnesa Ridge are close to the expected $\delta^{13}C$ values for normal "Holocene" marine environments (−0.5 to 0.5‰; Zamelczyk et al., 2014; Werner et al., 2016). Because planktic foraminifera live and calcify in the water column, significantly depleted $\delta^{13}C$ signature (−7‰ or higher; Torres et al., 2003) in their unstained tests results from diagenetic overgrowth by authigenic carbonates associated with aerobic methane oxidation (AOM; Torres et al., 2003; Uchida et al., 2004; Martin et al., 2010; Schneider et al., 2017). Values obtained for *N. pachyderma* from Vestnesa Ridge support the inference that benthic foraminiferal assemblages have not been significantly overprinted by MDAC.

Unlike Vestnesa Ridge, in GHP1 and GPH 5 the $\delta^{13}C$ values in the fluorescently labeled *M. barleeanus* are always more negative compared to the $\delta^{13}C$ in Rose Bengal stained and unstained tests. This could suggest that living foraminifera did incorporate methane-derived carbon during biomineralization. Mackensen et al. (2006) suggested that more depleted isotopic $\delta^{13}C$ signatures in living (Rose Bengal stained) foraminifera compared to unstained tests can be interpreted as a result of methane influence. In sample MC919 the difference between $\delta^{13}C$ measured in live *M. barleeanum* compared to value in empty tests is pronounced (about 1.55‰), whereas the difference between $\delta^{13}C$ in live foraminifera and empty tests in the post-active GHP5 does not exceed 0.4‰. Most likely, foraminifera absorbed methane-derived carbon *via* the food web by feeding on methanotrophic bacteria (see section "Foraminiferal Fauna").

Although the $\delta^{13}C$ signatures in tests of live foraminifera from the study areas are not significantly depleted to determine the influence of methane, it should be noted that the $\delta^{13}C$ are measured on pools of specimens (N = ∼10). It is possible that at least some of the individuals had more negative $\delta^{13}C$ signatures than others, or that some chambers indeed incorporated methane-derived carbon, as suggested by Bernhard et al. (2010). However, even if the foraminifera calcified during episodes of high methane flux, it is likely that only parts of the tests were constructed under intense seepage conditions, while the major part of the tests had a pre-seep or post-seep signatures (i.e., carbon isotopes incorporated before or after a seepage event). Methane is only one of the potential carbon sources at cold seeps. In surface sediments, the biological degradation of marine snow contributes to the local DIC pool and might explain the negative signature of the $\delta^{13}C_{DIC}$ (e.g,„ Alldredge and Silver, 1988; Bauer and Druffel, 1998; Torres et al., 2003). As an example, a previous study of the $\delta^{13}C_{TOC}$ values for Vestnesa Ridge showed presence of both classical marine $\delta^{13}C_{TOC}$ and depleted $\delta^{13}C_{TOC}$ related to methane seepage (Dessandier et al., 2019). Thus, if the foraminifera use carbon both from ambient water and intracellular storage (i.e., resulting from respiration and diet; de Nooijer et al., 2009; Toyofuku et al., 2017), it seems unlikely that the isotopic signature of foraminifera only reflects the methane-derived carbon; rather, it may be a result of both non-seep and seep carbon. To obtain more accurate $\delta^{13}C$ values, analysis of single specimens, or more advanced techniques, e.g., secondary-ion mass spectrometry (SIMS) is recommended.

CONCLUSION

1. Labeling with fluorescence probes showed that metabolically active foraminifera were present in methane-influenced sediments both at Vestnesa Ridge and Storfjordrenna. Both sites were characterized by comparable faunal patterns, with no endemic species, and the observed species were similar to those from other non-seep locations within the Arctic Ocean. At Vestnesa Ridge, and at the non-seep control site off Vestnesa Ridge, the most abundant calcareous species were *M. barleeanus* and *C. neoteretis*. In Storfjordrenna in both GHP environments, the foraminiferal faunas were dominated by *M. barleeanus* and *N. labradorica*.
2. Methane seepage did not markedly affect the isotopic signature ($\delta^{13}C$) of primary calcite in metabolically active foraminifera. One exception was sample MC919, where a more negative isotopic signature of *M. barleeanus* could potentially reflect methane influence.
3. The results of this study show the effectiveness of fluorescent probes in ecological studies. At Vestnesa Ridge, Rose Bengal staining overestimated the number of living foraminifera, indicating a higher number of live foraminifera compared to the CTG labeled specimens (23% of foraminifera were live at Vestnesa Ridge and 34% at the control site).
4. The is no significant difference between $\delta^{13}C$ measured in fluorescent labeled foraminifera and Rose Bengal stained.
5. At Storfjordrenna, the combined use of CHG and Rose Bengal allowed to distinguish between living and recently dead benthic foraminifera. This demonstrated a marked change in the foraminiferal population from a *C. neoteretis/Cibicides lobatulus* dominated assemblage to an assemblage dominated by *M. barleeanus* and *N. labradorica,* which otherwise would have been overlooked. Despite the more time-consuming protocol compared to Rose Bengal staining, the fluorescent viability

assays such as CHG and CTG CMFDA have a great advantage and it is advised that they be applied more often in studies of the ecology of benthic foraminifera.

DATA AVAILABILITY STATEMENT

The original contributions presented in the study are included in the article/supplementary material, further inquiries can be directed to the corresponding author/s.

AUTHOR CONTRIBUTIONS

KM collected and processed the samples, analyzed data, and wrote the manuscript.

FUNDING

This work was supported by the Research Council of Norway through its Centers of Excellence funding scheme grant 287 no. 2232.

ACKNOWLEDGMENTS

The author would like to thank the captain and crew of the R/V *Helmer Hansen* and chief scientist G. Panieri during CAGE15-2 cruise and AMGG CAGE17-2 cruise, A.G. Hestnes for support assistance in work with a fluorescence microscope, and A. N. Osiecka for linguistic assistance and J. M. Bernhard for comments that greatly improved the manuscript.

REFERENCES

Akimoto, K., Tanaka, T., Hattori, M., and Hotta, H. (1994). "Recent benthic foraminiferal assemblages from the cold seep communities}a contribution to the methane gas indicator," in *Pacific Neogene Events in Time and Space*, ed. R. Tsuchi (Tokyo: University of Tokyo Press), 11–25.

Alldredge, A. L., and Silver, M. W. (1988). Characteristics, dynamics and significance of marine snow. *Prog. Oceanogr.* 20y, 41–82. doi: 10.1016/0079-6611(88)90053-5

Altenbach, A. V. (1992). Short term processes and patterns in the foraminiferal response to organic flux rates. *Mar. Micropaleontol.* 19, 119–129. doi: 10.1016/0377-8398(92)90024-E

Alve, E., Korsun, S., Schönfeld, J., Dijkstra, N., Golikova, E., Hess, S., et al. (2016). Foram-AMBI: A sensitivity index based on benthic foraminiferal faunas from North-East Atlantic and Arctic fjords, continental shelves and slopes. *Mar. Micropaleontol.* 122, 1–12. doi: 10.1016/j.marmicro.2015.11.001

Amap Assessment (2018). *Arctic Ocean Acidification, Arctic Monitoring and Assessment Programme (AMAP)*. Tromsø: AMAP Assessment.

Archer, D., Buffett, B., and Brovkin, V. (2009). Ocean methane hydrates as a slow tipping point in the global carbon cycle. *Proc. Natl. Acad. Sci. U S A.* 106, 20596–20601. doi: 10.1073/pnas.0800885105

Arrigo, K. R., and van Dijken, G. L. (2011). Continued increases in Arctic Ocean primary production. *Prog. Oceanogr.* 136, 60–70. doi: 10.1016/j.pocean.2015.05.002

Åström, E. K. L., Carroll, M. L., Ambrose, W. G. Jr., Sen, A., Silyakova, A., and Carroll, J. (2018). Methane cold seeps as biological oases in the high-Arctic deep sea. *Limnol. Oceanogr.* 63, 209–231. doi: 10.1002/lno.10732

Åström, E. K. L., Carroll, M. L., Ambrose, W. G., and Carroll, J. (2016). Arctic cold seeps in marine methane hydrate environments: Impacts on shelf macrobenthic community structure offshore Svalbard. *Mar. Ecol. Prog. Ser.* 552, 1–18. doi: 10.3354/meps11773

Åström, E. K. L., Sen, A., Carroll, M. L., and Carroll, J. (2020). Cold Seeps in a Warming Arctic: Insights for Benthic Ecology. *Front. Mar. Sci.* 7:244. doi: 10.3389/fmars.2020.00244

Bauer, J., and Druffel, E. (1998). Ocean margins as a significant source of organic matter to the deep open ocean. *Nature* 392, 482–485.

Bernhard, J. M., and Panieri, G. (2018). Keystone Arctic paleoceanographic proxy association with putative methanotrophic bacteria. *Sci. Rep.* 8:10610. doi: 10.1038/s41598-018-28871-3

Bernhard, J. M., Buck, K. R., and Barry, J. P. (2001). Monterey Bay cold-seep biota: Assemblages, abundance, and ultrastructure of living foraminifera. *Deep Sea Res. Part I Oceanogr. Res. Papers* 48, 2233–2249.

Bernhard, J. M., Martin, J. B., and Rathburn, A. E. (2010). Combined carbonate carbon isotopic and cellular ultrastructural studies of individual benthic foraminifera: 2. Toward an understanding of apparent disequilibrium in hydrocarbon seeps. *Paleoceanography* 25:4206. doi: 10.1029/2009PA001846

Bernhard, J. M., Ostermann, D. R., Williams, D. S., and Blanks, J. K. (2006). Comparison of two methods to identify live benthic foraminifera: A test between Rose Bengal and CellTracker Green with implications for stable isotope paleoreconstructions. *Paleoceanography* 21:4210. doi: 10.1029/2006PA001290

Box, J. E., Colgon, W. T., Christensen, T. R., Schmidt, N. M., Lund, M., and Parmentier, F. W. (2019). Key indicators of Arctic climate change: 1971-2017. *Environ. Res. Lett.* 14:045010.

Braeckman, U., Janssen, F., Lavik, G., Elvert, M., Marchant, H., Buckner, C., et al. (2018). Carbon and nitrogen turnover in the Arctic deep-sea: in situ benthic community response to diatom and coccolithophorid phytodetritus. *Biogeosciences* 15, 6537–6557. doi: 10.5194/bg-15-6537-2018

Bünz, S., Polyanov, S., Vadakkepuliyambatta, S., Consolaro, C., and Mienert, J. (2012). Active gas venting through hydrate-bearing sediments on the Vestnesa Ridge, offshore W-Svalbard. *Mar. Geol.* 332-334, 189–197. doi: 10.1016/j.margeo.2012.09.012

Carrier, V., Svenning, M. M., Gründger, F., Niemann, H., Dessandier, P.-A., Panieri, G., et al. (2020). The Impact of Methane on Microbial Communities at Marine Arctic Gas Hydrate Bearing Sediment. *Front. Microbiol.* 11:1932. doi: 10.3389/fmicb.2020.01932

Cedhagen, T. (1991). Retention of chloroplasts and bathymetric distribution in the sublittoral foraminiferan Nonionellina labradorica. *Ophelia* 33, 17–30.

Cordes, E., Bergquist, D., Predmore, B., Dienes, P., Jones, C., Telesnicki, G., et al. (2006). Alternate unstable states: convergent paths of succession in hydrocarbon-seep tubeworm-associated communities. *J. Exp. Mar. Biol. Ecol.* 339, 159–176. doi: 10.1016/j.jembe.2006.07.017

Corliss, B. H. (1991). Morphology and microhabitat preferences of benthic foraminifera from the northwest Atlantic Ocean. *Mar. Micropaleontol.* 17, 195–236. doi: 10.1016/0377-8398(91)90014-W

de Nooijer, L. J., Langer, G., Nehrke, G., and Bijma, J. (2009). Physiological controls on seawater uptake and calcification in the benthic foraminifer *Ammonia tepida*. *Biogeosciences* 6, 2669–2675. doi: 10.5194/bg-6-2669-2009

Dessandier, P. A., Borrelli, C., Kalenitchenko, D., and Panieri, G. (2019). Benthic Foraminifera in Arctic Methane Hydrate Bearing Sediments. *Front. Mar. Sci.* 6:765. doi: 10.3389/fmars.2019.00765

Dessandier, P., Borrelli, C., Yao, H., Sauer, S., Hong, W. L., and Panieri, G. (2020). Foraminiferal $\delta^{18}O$ reveals gas hydrate dissociation in Arctic and North Atlantic Ocean sediments. *Geo Mar. Lett.* 40, 507–523. doi: 10.1007/s00367-019-00635-6

Dickens, G. R., Castillo, M. M., and Walker, J. C. G. (1997). A blast of gas in the latest Paleocene: Simulating first-order effects of massive dissociation of oceanic methane hydrate. *Geology* 25, 259–262. doi: 10.1130/0091-76131997025<0259:abogit<2.3.co;2

Etiope, G., Panieri, G., Fattorini, D., Regoli, F., Vannoli, F. P., Italiano, F., et al. (2014). A thermogenic hydrocarbon seep in shallow Adriatic Sea (Italy): Gas origin, sediment contamination and benthic foraminifera. *Mar. Petroleum Geol.* 57, 283–293.

Figueira, B., Grenfell, Hugh, Hayward, B., and Alfaro, A. (2012). Comparison of rose bengal and CellTracker^{TM} green staining for identification of live salt-marsh foraminifera. *J. Foraminiferal Res.* 42, 206–215.

Fontanier, C., Duros, P., Toyofuku, T., Oguri, K., Koho, K. A., Buscail, R., et al. (2014). Living (stained) deep-sea foraminifera off hachinohe (NE Japan, western Pa- cific): Environmental interplay in oxygen-depleted ecosystems. *J. Foraminiferal Res.* 44, 281–299.

Fontanier, C., Mackensen, A., Jorissen, F. J., Anschutz, P., Licari, L., and Griveaud, C. (2006). Stable oxygen and carbon isotopes of live benthic foraminifera from the Bay of Biscay: Microhabitat impact and seasonal variability. *Mar. Micropaleontol.* 58, 159–183.

Gooday, A. J. (1988). A response by benthic Foraminifera to the deposition of phytodetritus in the deep-sea. *Nature* 332, 70–73.

Gooday, A. J. (1993). Deep-sea benthic foraminifera species which exploit phytodetritus: Characteristic features and controls on distribution. *Mar. Micropaleontol.* 22, 187–205.

Gooday, A. J. (1994). The biology of deep-sea foraminifera: a review of some advances and their applications. *Paleoceanography* 9, 14–31.

Gooday, A. J. (2003). Benthic foraminifera (Protista) as tools in deep-water palaeoceanography: a review of environmental influences on fau- nal characteristics. *Adv. Mar. Biol.* 46, 1–90.

Grossman, E. L. (1984). Stable isotope fractionation in live benthic foraminifera from the southern California Borderland. *Palaeogeogr. Palaeoclimatol. Palaeoecol.* 47, 301–327. doi: 10.1016/0031-0182(84)90100-7

Grossman, E. L. (1987). Stable isotopes in modern benthic foraminifera: a study of vital effect. *J. Foraminifera Res.* 17, 48–61.

Hald, M., and Steinsund, P. I. (1996). "Benthic foraminifera and carbonate dissolution in surface sediments of the Barents-and Kara Seas," in *Surface sediment composition and sedimentary processes in the central Arctic Ocean and along the Eurasian Continental Margin. Berichte zur Polarforschung*, Vol. 212, eds R. Stein, G. I. Ivanov, M. A. Levitan, and K. Fahl (Bremerhaven: Wegener Inst. Polar Meeresforsch), 285–307.

Heinz, P., Sommer, S., and Pfannkuche, O. (2005). Living benthic foraminifera in sediments influenced by gas hydrates at the Cascadia convergent margin, NE Pacific. *Mar. Ecol. Prog. Ser.* 304, 77–89.

Herguera, J. C., Paull, C. K., Perez, E., Ussler, W., and Peltzer, E. (2014). Limits to the sensitivity of living benthic foraminifera to pore water carbon isotope anomalies in methane vent environments. *Paleoceanography* 29, 273–289. doi: 10.1002/2013PA002457

Hill, T. M., Kennett, J. P., and Valentine, D. L. (2004). Isotopic evidence for the incorporation of methane-derived carbon into foraminifera from modern methane seeps, Hydrate Ridge, Northeast Pacific. *Geochim. Cosmochim. Acta* 68, 4619–4627. doi: 10.1016/j.gca.2004.07.012

Hong, W.-L., Torres, M. E., Carroll, J., Cremiere, A., Panieri, G., Yao, H., et al. (2017). Seepage from an Arctic shallow marine gas hydrate reservoir is insensitive to momentary ocean warming. *Nat. Commun.* 8, 1–14. doi: 10.1038/ncomms15745

Hustoft, S., Bünz, S., Mienert, J., and Chand, S. (2009). Gas hydrate reservoir and active methane-venting province in sediments on <20 Ma young oceanic crust in the Fram Strait, offshore NW-Svalbard. *Earth Planetary Sci. Lett.* 284, 12–24. doi: 10.1016/j.epsl.2009.03.038

IPCC (2007). *Climate Change 2007: The Physical Basis*. New York, NY: Cambridge University Press.

IPCC (2013). "The physical science basis," in *Contribution of Working Group I to the Fifth Assessment Report of the Intergovernmental Panel on Climate Change*, eds T. F. Stocker, D. Qin, G.-K. Plattner, M. Tignor, S. K. Allen, J. Boschung, et al. (Cambridge: Cambridge University Press), 1535.

Jauffrais, T., LeKieffre, C., Schweizer, M., Geslin, E., Metzger, E., Bernhard, J. M., et al. (2019). Kleptoplastidic benthic foraminifera from aphotic habitats: insights into assimilation of inorganic C, N and S studied with sub-cellular resolution. *Environ. Microbiol.* 21, 125–141. doi: 10.1111/1462-2920.14433

Klitgaard-Kristensen, D., Sejrup, H., and Haflidason, H. (2002). Distribution of recent calcareous benthic foraminifera in the northern North Sea and relation to the environment. *Polar Res.* 21, 275–282. doi: 10.1111/j.1751-8369.2002.tb00081.x

Knittel, K., and Boetius, A. (2009). Anaerobic Oxidation of Methane: Progress with an Unknown Process. *Annu. Rev. Microbiol.* 63, 311–334. doi: 10.1146/annurev.micro.61.080706.093130

Korsun, S., and Hald, M. (2000). Seasonal dynamics of benthic foraminifera in a glacially fed fjord of Svalbard, European Arctic. *J. Foraminifer Res.* 30, 251–271.

Kvenvolden, K. A. (1993). Gas hydrates geological perspective and global change. *Rev. Geophys.* 31, 173–187. doi: 10.1029/93RG00268

Levin, L. A. (2005). "Ecology of cold seep sediments: Interactions of fauna with flow, chemistry and microbes," in *Oceanography and Marine Biology: An Annual Review*, eds R. N. Gibson, R. J. A. Atkinson, and J. D. M. Gordon (Boca Raton: CRC Press-Taylor & Francis Group), 1–46.

Loeng, H. (1991). Features of the physical oceanographic conditions of the Barents Sea. *Polar Res.* 10, 5–18. doi: 10.3402/polar.v10i1.6723

Mackensen, A., Wollenburg, J., and Licari, L. (2006). Low $\delta^{13}C$ in tests of live epibenthic and endobenthic foraminifera at a site of active methane seepage. *Paleoceanography* 21, 1–12. doi: 10.1029/2005PA001196

Manley, T. O. (1995). Branching of Atlantic Water within the Greenland-Spitsbergen Passage: An estimate of recirculation. *J. Geophys. Res.* 100, 20627–20634. doi: 10.1029/95JC01251

Martin, J. B., Day, S. A., Rathburn, A. E., Perez, M. E., Mahn, C., and Gieskes, J. (2004). Relationships between the stable isotopic signatures of living and fossil foraminifera in Monterey Bay, California. *Geochem. Geophys. Geosyst.* 5:Q04004. doi: 10.1029/2003GC000629

Martin, R. A., Nesbitt, E. A., and Campbell, K. A. (2010). The effects of anaerobic methane oxidation on benthic foraminiferal assemblages and stable isotopes on the Hikurangi Margin of eastern New Zealand. *Mar. Geol.* 272, 270–284. doi: 10.1016/j.margeo.2009.03.024

Maslin, M., Owen, M., Betts, R., Day, S., Dunkley, J. T., and Ridgwell, A. (2010). Gas hydrates: Past and future geohazard? *Philosoph. Transact. R. Soc. A* 368, 2369–2393. doi: 10.1098/rsta.2010.0065

McCorkle, D. C., Emerson, S. R., and Quay, P. D. (1985). Stable carbon isotopes in marine pore waters. *Earth Planetary Sci. Lett.* 74, 13–26. doi: 10.1016/0012-821X(85)90162-1

McCorkle, D. C., Keigwin, L. D., Corliss, B. H., and Emerson, S. R. (1990). The influence of microhabitats on the carbon isotopic composition of deep-sea benthic foraminifera. *Paleoceanography* 5, 161–185. doi: 10.1029/PA005i002p00161

Millo, C., Sarnthein, M., Erlenkeuser, H., and Frederichs, T. (2005). Methane-driven late Pleistocene δ13C minima and overflow reversals in the southwestern Greenland Sea. *Geology* 33, 873–876. doi: 10.1130/G21790.1

Murray, J. W. (2006). *Ecology and Applications of Benthic Foraminifera*. Cambridge: Cambridge University Press.

Niemann, H., Lösekann, T., de Beer, D., Elvert, M., Nadalig, T., Knittel, K., et al. (2006). Novel microbial communities of the Haakon Mosby mud volcano and their role as a methane sink. *Nature* 443, 854–858. doi: 10.1038/nature05227

Nomaki, H., Heinz, P., Hemleben, C., and Kitazato, H. (2005). Behaviour and response of deep-sea benthic foraminifera to freshly supplied organic matter: A laboratory feeding experiment in microcosm environments. *J. Foraminiferal Res.* 35, 103–113.

Panieri, G. (2006). Foraminiferal response to an active methane seep environment: A case study from the Adriatic Sea. *Mar. Micropaleontol.* 61, 116–130. doi: 10.1016/j.marmicro.2006.05.008

Panieri, G., and Sen Gupta, B. K. (2008). Benthic Foraminifera of the Blake Ridge hydrate mound, Western North Atlantic Ocean. *Mar. Micropaleontol.* 66, 91–102.

Panieri, G., Bünz, S., Fornari, D. J., Escartin, J., Serov, P., Jansson, P., et al. (2017). An integrated view of the methane system in the pockmarks at Vestnesa Ridge, 79°N. *Mar. Geol.* 390, 282–300. doi: 10.1016/j.margeo.2017.06.006

Phrampus, B., and Hornbach, M. (2012). Recent changes to the Gulf Stream causing widespread gas hydrate destabilization. *Nature* 490, 527–530. doi: 10.1038/nature11528

Rathburn, A. E., Levin, L. A., Held, Z., and Lohmann, K. C. (2000). Benthic foraminifera associated with cold methane seeps on the northern California margin: ecology and stable isotopic composition. *Mar. Micropaleontol.* 38, 247–266.

Rathburn, A. E., Pérez, M. E., Martin, J. B., Day, S. A., Mahn, C., Gieskes, J., et al. (2003). Relationships between the distribution and stable isotopic composition of living benthic foraminifera and cold methane seep biogeochemistry in Monterey Bay, California. *Geochem. Geophys. Geosyst.* 4:1106. doi: 10.1029/2003GC000595

Ravelo, A. C., and Hillaire-Marcel, C. (2007). Chapter Eighteen: The Use of Oxygen and Carbon Isotopes of Foraminifera in Paleoceanography. *Dev. Mar. Geol.* 1, 735–764.

Rohling, E. J., and Cooke, S. (1999). "Stable oxygen and carbon isotopes in foraminiferal carbonate shells," in *Modern Foraminifera*, ed. B. K. Sen Gupta (Dordrecht: Springer), doi: 10.1007/0-306-48104-9_14

Rudels, B., Muench, R. D., Gunn, J., Schauer, U., and Friedrich, H. J. (2000). Evolution of the Arctic Ocean boundary current north of the Siberian shelves. *J. Mar. Syst.* 25, 77–99. doi: 10.1016/S0924-7963(00)00009-9

Ruppel, C. D., and Kessler, J. D. (2017). The interaction of climate change and methane hydrates. *Rev. Geophys.* 55, 126–168. doi: 10.1002/2016RG000534

Sahling, H., Rickert, D., Link, P., Suess, E., and Lee, R. W. (2002). Community structure at gas hydrate deposits at the Cascadia convergent margin, NE Pacific. *Mar. Ecol. Prog. Ser.* 231, 121–138. doi: 10.3354/meps231121

Sander, E., and van der Zwaan, B. (2004). Effects of experimentally induced raised levels of organic flux and oxygen depletion on a continental slope benthic foraminiferal community. *Deep Sea Res. Part I Oceanogr. Res. Papers* 51, 1709–1739. doi: 10.1016/j.dsr.2004.06.003

Schneider, A., Crémière, A., Panieri, G., Lepland, A., and Knies, J. (2017). Diagenetic alteration of benthic foraminifera from a methane seep site on Vestnesa Ridge (NW Svalbard). *Deep Sea Res. Part I Oceanogr. Res. Papers* 123, 22–34. doi: 10.1016/j.dsr.2017.03.001

Schönfeld, J., and Numberger, L. (2007). The benthic foraminiferal response to the 2004 spring bloom inthe western Baltic Sea. *Mar. Micropaleontol.* 65, 78–95. doi: 10.1016/j.marmicro.2007.06.003

Seidenkrantz, M. S. (2013). Benthic foraminifera as paleo sea-ice indicators in the subarctic realm - examples from the Labrador Sea-Baffin Bay region. *Q. Sci. Rev.* 79, 135–144. doi: 10.1016/j.quascirev.2013.03.014

Sen, A., Åström, E. K. L., Hong, W.-L., Portnov, A., Waage, M., and Serov, P. (2018). Geophysical and geochemical controls on the megafaunal community of a high Arctic cold seep. *Biogeosciences* 15, 4533–4559.

Serov, P., Vadakkepuliyambatta, S., Mienert, J., Patton, H., Portnov, A. D., Silyakova, A., et al. (2017). Postglacial response of Arctic Ocean gas hydrates to climatic amelioration. *Proc. Natl. Acad. Sci. U S A.* 114, 6215–6220. doi: 10.1073/pnas.1619288114

Smart, C. M., Gooday, A. J., Murray, J. W., and Thomas, E. (1994). A benthic foraminiferal proxy for pulsed organic matter palaeofluxes. *Mar. Micropaleontol.* 23, 89–99.

Smith, L. M., Sachs, J. P., Jennings, A. E., Anderson, D. M., and de Vernal, A. (2001). Light $\delta^{13}C$ events during deglaciation of the East Greenland continental shelf attributed to methane release from gas hydrate. *Geophys. Res. Lett.* 28, 2217–2220. doi: 10.1029/2000GL012627

Stroeve, J. C., Serreze, M. C., Holland, M. M., Kay, J. E., Malanik, J., and Barrett, A. P. (2012). The Arctic's rapidly shrinking sea ice cover: A research synthesis. *Clim. Change* 110, 1005–1027. doi: 10.1007/s10584-011-0101-1

Sztybor, K., and Rasmussen, T. L. (2017). Diagenetic disturbances of marine sedimentary records from methane-influenced environments in the Fram Strait as indications of variation in seep intensity during the last 35 000 years. *Boreas* 46, 212–228.

Torres, M. E., Mix, A. C., Kinports, K., Haley, B., Klinkhammer, G. P., McManus, J., et al. (2003). Is methane venting at the seafloor recorded by $\delta^{13}C$ of benthic foraminifera shells? *Paleoceanography* 18:1062. doi: 10.1029/2002PA000824

Toyofuku, T., Matsuo, M. Y., de Nooijer, L. J., Nagai, Y., Kawada, S., Fujita, K., et al. (2017). Proton pumping accompanies calcification in foraminifera. *Nat. Commun.* 8, 1–6. doi: 10.1038/ncomms14145

Treude, T., Orphan, V., Knittel, K., Gieseke, A., House, C. H., and Boetius, A. (2007). Consumption of methane and CO_2 by methanotrophic microbial mats from gas seeps of the anoxic Black Sea. *Appl. Environ. Microbiol.* 73, 2271–2283. doi: 10.1128/AEM.02685-06

Uchida, M., Shibata, Y., Ohkushi, K., Ahagon, N., and Hoshiba, M. (2004). Episodic methane release events from Last Glacial marginal sediments in the western North Pacific. *Geochem. Geophys. Geosyst.* 5:Q08005. doi: 10.1029/2004GC000699

Walczowski, W., Piechura, J., Osinski, R., and Wieczorek, P. (2005). The West Spitsbergen Current volume and heat transport from synoptic observations in summer. *Deep Sea Res. Part I Oceanogr. Res. Papers* 52, 1374–1391. doi: 10.1016/j.dsr.2005.03.009

Wefer, G., Heinze, P. M., and Berger, W. H. (1994). Clues to ancient methane release. *Nature* 369:282. doi: 10.1038/369282a0

Werner, K., Müller, J., Husum, K., Spielhagen, R. F., Kandiano, E. S., and Polyak, L. (2016). Holocene sea subsurface and surface water masses in the Fram Strait. Comparisons of temperature and sea-ice reconstructions. *Quaternary Sci. Rev.* 147, 194–209. doi: 10.1016/j.quascirev.2015.09.007

Whiticar, M. J. (1999). Carbon and hydrogen isotope systematics of bacterial formation and oxidation of methane. *Chem. Geol.* 161, 291–314. doi: 10.1016/S0009-2541(99)00092-3

Wollenburg, J. E., and Mackensen, A. (1998). Living benthic foraminifers from the central Arctic Ocean: faunal composition, standing stock and diversity. *Mar. Micropaleontol.* 34, 153–185.

Wollenburg, J. E., and Mackensen, A. (2009). The ecology and distribution of benthic foraminifera at the Håkon Mosby mud volcano (SW Barents Sea slope). *Deep Sea Res. Part I Oceanogr. Res. Papers* 56, 1336–1370. doi: 10.1016/j.dsr.2009.02.004

Wollenburg, J. E., Kuhnt, W., and Mackensen, A. (2001). Changes in Arctic Ocean paleoproductivity and hydrography during the last 145 kyr: The benthic foraminiferal record. *Paleoceanography* 16, 65–77. doi: 10.1029/1999PA000454

Wollenburg, J. E., Raitzsch, M., and Tiedemann, R. (2015). Novel high-pressure culture experiments on deep-sea benthic foraminifera — Evidence for methane seepage-related δ13C of Cibicides wuellerstorfi. *Mar. Micropaleontol.* 117, 47–64. doi: 10.1016/j.marmicro.2015.04.003

Yao, H., Hong, W.-L., Panieri, G., Sauer, S., Torres, M. E., Lehmann, M. F., et al. (2019). Fracture-controlled fluid transport supports microbial methane-oxidizing communities at the Vestnesa ridge. *Biogeosciences* 16, 2221–2232.

Zamelczyk, K., Rasmussen, T. L., Husum, K., Godtliebsen, F., and Hald, M. (2014). Surface water conditions and calcium carbonate preservation in the Fram Strait during marine isotope stage 2, 28.8–15.4 kyr. *Paleoceanography* 29, 1–12. doi: 10.1002/2012PA002448

Conflict of Interest: The author declares that the research was conducted in the absence of any commercial or financial relationships that could be construed as a potential conflict of interest.

Article 3

Evidence for influence of methane seepage on isotopic signatures in living deep-sea foraminifera, 79 °N.

Evidence for influence of methane seepage on isotopic signatures in living deep-sea foraminifera, 79 °N.

Katarzyna Melaniuk [1], Kamila Sztybor [2], Tina Treude [3, 4], Stefan Sommer [5], Tine L. Rasmussen [1]

1. Centre of Arctic Gas Hydrate, Environment and Climate CAGE, Department of Geosciences, UiT The Arctic University of Norway, 9010 Tromsø, Norway.
2. Akvaplan-niva AS, Fram Centre, 9296 Tromsø, Norway.
3. Department of Earth, Planetary, and Space Sciences, University of California Los Angeles, Los Angeles, USA.
4. Department of Atmospheric and Oceanic Sciences, University of California Los Angeles, Los Angeles, USA.
5. GEOMAR Helmholtz Centre for Ocean Research Kiel, 24148 Kiel, Germany.

Key words: Arctic gas hydrate, cold seeps, carbon and oxygen isotopes; Svalbard margin

Fossil foraminifera have a high potential as a tool for tracing past methane release linked to climate change in the geological past. However, it is still debated whether the isotopic signatures of living foraminifera from methane-charged sediment reflect incorporation of methane-derived carbon. A deeper understanding of isotopic signatures of living foraminifera from methane-rich environments will help to improve reconstruction of methane release in the past and to better predict the impact of climate warming on methane seepage in the future. Here, we present a study on isotopic signatures ($\delta^{13}C$ and $\delta^{18}O$) of foraminiferal calcite together with biogeochemical data from Arctic seep sites from Vestnesa Ridge (79°N, Fram Strait) at c. 1200 m water depth. We confirm that living foraminifera incorporate methane-derived carbon into its test during their lifespan, most likely via feeding on methanotrophic bacteria. Lowest $\delta^{13}C$ values were recorded in shells of *Melonis barleeanus*, i.e., -5.21‰ in live specimens and -6.48‰ in empty shells, from sediments dominated by either aerobic or anaerobic oxidation of methane, respectively. Our data indicate that foraminifera actively incorporate methane-derived carbon into their shells in sediments with lower seepage activity, while sediments with high seepage activity become poisonous due to sulfide buildup and lead to overgrowth of shells by methane-derived authigenic carbonates.

INTRODUCTION

One of the consequences of the ongoing climate warming is an increase in ocean temperature[1]. The Arctic is already warming about twice as fast as the global average, because of a process called 'the polar amplification' caused by decline in sea-ice cover and increased atmospheric heat transport from the equator to the Arctic. As large amounts of methane are stored on Arctic continental margins in the form of gas hydrates (pressure-temperature sensitive methane captured in ice[2,3,4]), concern has increased that ongoing ocean warming will trigger destabilization of the gas hydrate reservoirs and cause further release of methane in the future[1,3,5,6]. Because methane is a *~25 times more potent* greenhouse gas than CO_2, a significant increase in the atmosphere can cause further amplification of the global warming. In the geological past, methane released from marine reservoirs has been linked to pronounced paleoclimatic and palaeoceanographic changes during the Quaternary[7], Late Paleocene[8], Cretaceous[9] and linked to the Permian-Triassic extinction event[10]. In methane-rich environments such as cold seeps, the carbon pool available for benthic foraminifera is enriched in inorganic methane-derived $^{12}CO_2$ and $H^{12}CO_3^-$, and organic carbon in form of the methane related microbial communities characterized by low $\delta^{13}C$ values. It has been hypothesized that benthic foraminifera are able to record past methane seepage events by incorporating the low $\delta^{13}C$ values derived from methane into their shells called tests, and that they thus have a high potential to record variations in past seabed methane release[11–12]. Although $\delta^{13}C$ values of benthic foraminifera are a widely used proxy in paleoceanography, it is still disputed how methane-derived carbon enters foraminiferal shells, which might be via consumption of ^{13}C-depleted microbes, the presence of microbial symbionts[13,14], active incorporation of dissolved inorganic carbon (DIC) from ambient seawater, or as a result of passive diagenetic alteration via deposition of methane-derived authigenic carbonates (MDAC) from anaerobic oxidation of methane (AOM)[15]. Improved understanding of isotopic signatures of benthic foraminifera as a consequence of methane-related biological processes is necessary to develop more robust models for the interpretation of past as well as the prediction of future methane releases and their impact on climate. Modern cold seeps, i.e., methane-fuelled chemosynthetic ecosystems[16] , are reasonable analogs of past methane-rich environments[17] , and thus are perfect environments to study the impact of methane seepage on the isotopic signatures of living benthic foraminifera.

For this study, we investigated the stable isotopes ($\delta^{13}C$ and $\delta^{18}O$) of modern and fossil foraminiferal assemblages from gas hydrate-bearing sediment of Vestnesa Ridge, ~79 °N, 6°E, northwestern Svalbard margin in the eastern Fram Strait. Our results confirm[18,19] that methane-derived carbon has the potential to shift the $\delta^{13}C$ signature of live (Rose Bengal-stained) benthic

foraminifera towards lower values of up to -5.21‰ in the species *Melonis barleeanus* and that the $\delta^{13}C$ of benthic foraminifera are closely linked to aerobic (MOx) and anaerobic oxidation of methane (AOM). Additionally, we show a connection between the presence of overgrowth of MDAC and high $\delta^{18}O$ values in tests of dead specimens of benthic foraminiferal species *Cassidulina neoteretis*.

STUDY AREA

Vestnesa Ridge is located at water depths of ~1200–1300 m at ~79 °N, 6°E in the eastern Fram Strait, NW of Svalbard (Fig. 1a). It is ~100 km long and surrounded by ~1-km thick sediment drifts of Pliocene-Pleistocene age. The crest of the ridge shows a series of pockmarks (i.e., shallow seabed depressions) through which methane-rich fluids actively seep from gas-hydrate and deep free-gas reservoirs[20,21]. The two most active pockmarks at Vestnesa Ridge are informally referred to as 'Lomvi' and 'Lunde'[20] (Fig. 1b). Fluid flow and methane seepage probably started in the early Pleistocene[22]. Previous paleo-studies from Lomvi pockmark at Vestnesa Ridge revealed fossil macrofaunal communities related to the seep environment[23] (and references therein), and studies of fossil foraminifera showed diagenetic alterations of their tests[15,12]. Biological investigations documented the presence of species-rich live macro- and megafaunas[24,25] and carbonate outcrops[12,26] associated with methane emission.

For this study, two multicorer (MUC) stations from Lunde Pockmark were selected by video guidance. MUC 10 targeted a dense field of *Siboglinidae* tube worms and MUC 12 targeted a sulfur-bacteria mat (Fig. 1; Table S2). A third MUC station (MUC 11) was selected outside the pockmark to serve as reference site without methane seepage (see methods for details). Pore water chemistry was measured in MUC 10 and 12.

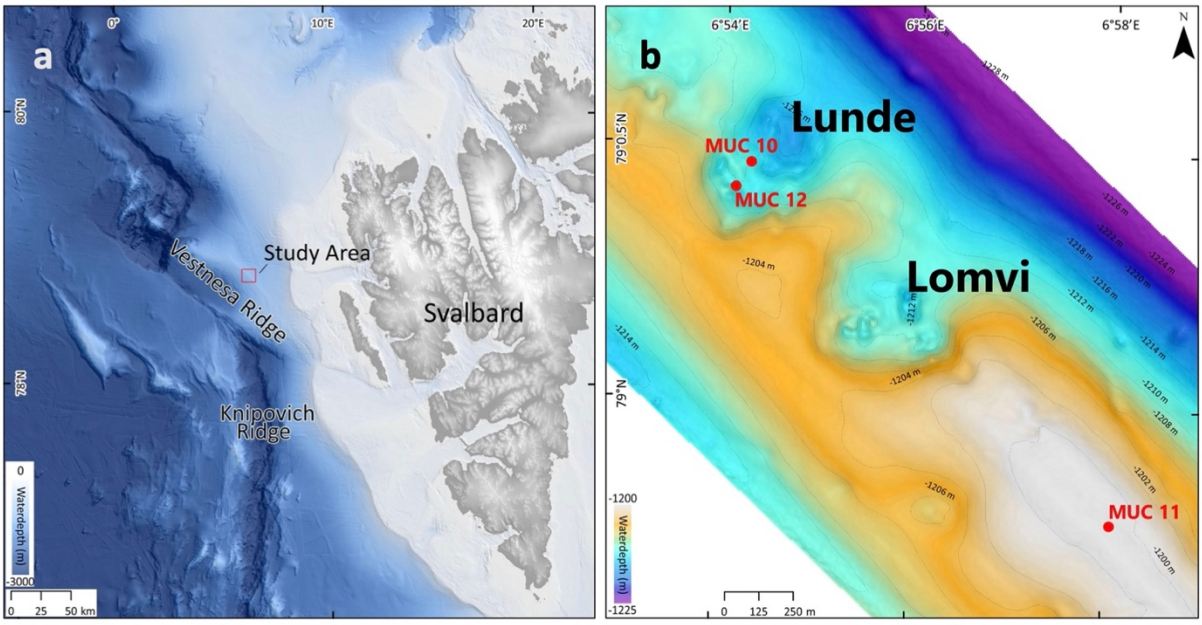

Figure 1. (a) Svalbard margin in the Eastern Fram Strait (bathymetry Jakobsson et al. [27] 2020. (b) Detail of Vestnesa Ridge (modified from Bünz et al.,[20]). Red dots indicate multicorer locations.

RESULTS

Sediment biogeochemistry

Sediments of the *Siboglinidae* field (MUC 10) showed strong indications for bio-irrigation by the tubeworms (Fig. 2a, b). Sulfate (~28 mmol L^{-1}), total alkalinity (~3 mmol L^{-1}), sulfide (<0.2 mmol L^{-1}, except 3 mmol L^{-1} at 3–4 cm), and methane concentrations (<0.1 mmol L^{-1}) remained relatively unchanged in the topmost 4–6 cm. Irrigation was further suggested by the bright brown coloring of the top sediment layers (Fig. S1) indicative of oxidized sediment. Below 4-6 cm, sulfate decreased while total alkalinity, sulfide, and methane increased (Fig. 2a, b). Sulfate declined to a minimum of 16.8 mmol L^{-1} at the bottom of the core, while total alkalinity and methane increased to 18.5 and 1.1 mmol L^{-1}, respectively. Sulfide peaked with 7 mmol L^{-1} at 9 cm and then declined with depth to reach 1.5 mmol L^{-1} at the bottom of the core. Accordingly, sediment color changed to black and (deeper in the core) grey indicating reducing conditions (Fig. S1a, b). In all three replicates, the majority of methane oxidation occurred in the top 4 cm of the sediment with rates up to 196 nmol cm^{-3} d^{-1} in the top (0–1 cm) sediment layer (Fig. 2c). This activity showed no match with sulfate reduction (Fig. 2d), neither in the profile, nor in magnitude, and suggests that it was coupled to MOx. Methane oxidation reached a minimum (~0.4 nmol cm^{-3} d^{-3}) at 5–6 cm, below which rates increased again (see insert in Fig. 2c) reaching a maximum of 4.8 nmol cm^{-3} d^{-1} at 7–8 cm (Fig. 2c). The double peaking of methane oxidation

suggests a change from an aerobic to an anaerobic methane oxidation pathway likely coupled to sulfate reduction below 6 cm, i.e., below the bio-irrigation activity of the tubeworms. Methane oxidation declined below the second peak to values ~1 nmol cm^{-3} d^{-3} at the bottom of the core. Sulfate reduction was low (<3 nmol cm^{-3} d^{-3}) in the top 0–1 cm, but steeply increased in all three replicates reaching values between 11 and 23 nmol cm^{-3} d^{-3} at 2–3 cm (Fig. 2d). Below 3 cm, sulfate reduction steadily declined reaching values ~1 nmol cm^{-3} d^{-3} at 10 cm, which remained consistently low down to the bottom of the core. The decoupling of methane oxidation and sulfate reduction in the surface sediment suggest that sulfate reduction was coupled to organic matter degradation in the top 6 cm, while part of it was likely also coupled to AOM below 6 cm.

Sediment covered by bacterial mats (MUC 12) showed steep geochemical gradients in the top 3–4 cm of the sediment: pore water sulfate and sulfide concentration declined from 28 to 2 and from 6.5 to 0.8 mmol L^{-1}, respectively, while total alkalinity increased from 2.5 to 35 mmol L^{-1} (Fig. 2e, f). Methane peaked with concentrations ~11 mmol L^{-1} at 2-4 and 28.5 cm and varied between 2-5 mmol L^{-1} in other depths with no clear trend (Fig. 2f). It is likely that measured concentrations were below in-situ levels and that the true methane profile was blurred due to degassing after sample recovery from depth. Degassing was clearly noticeable during core handling (Fig. S1 c-d). Methane oxidation was low at the surface (<13 nmol cm^{-3} d^{-1}) and steeply increased in all three replicates to a maximum of up to 181 nmol cm^{-3} d^{-1} between 2–5 cm (Fig. 2g). Below the peaks, methane oxidation in all three replicates sharply declined and reached values around 1–4 nmol cm^{-3} d^{-1} below 7 cm. Profiles of all three sulfate reduction samples showed a general alignment with methane oxidation (Fig. 2h), suggesting a coupling to AOM. However, sulfate reduction was about two times higher than methane oxidation in the surface sediment (maximum 408 nmol cm^{-3} d^{-1}) and therefore likely also coupled to other processes, most reasonably organic matter degradation.

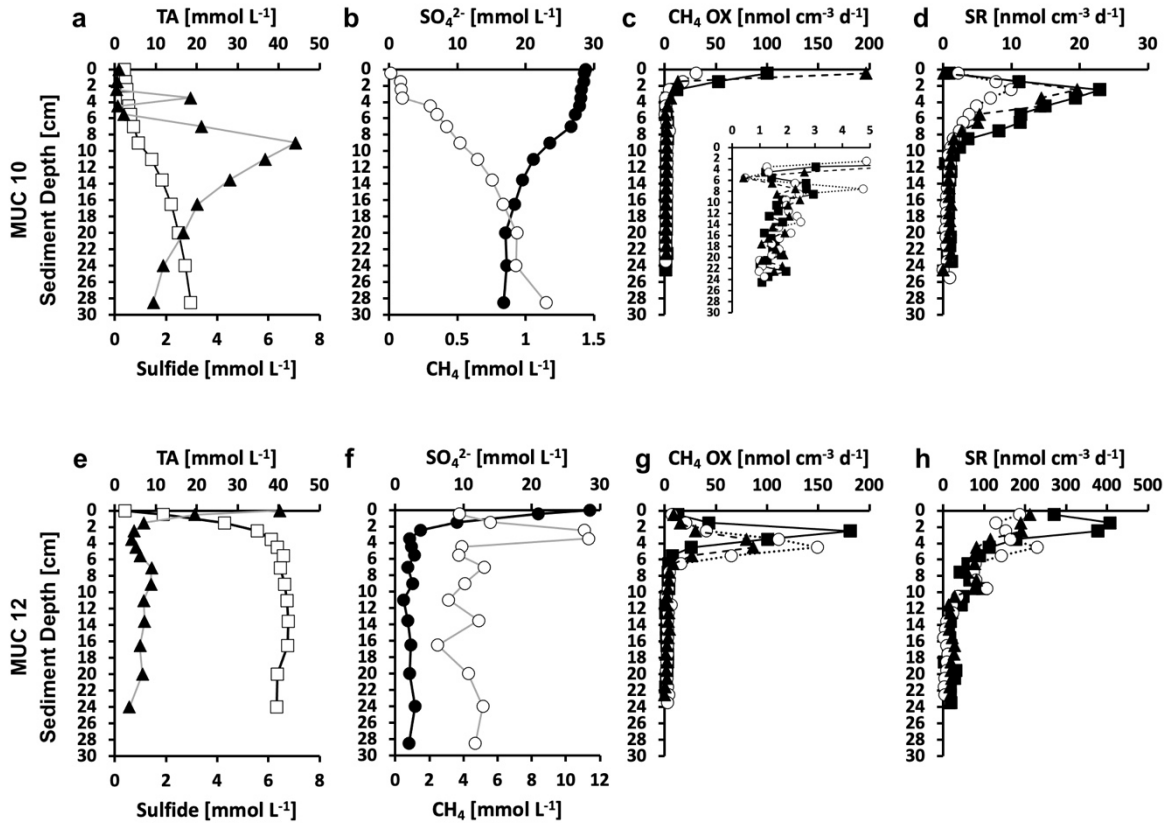

Figure 2. Biogeochemical data of sediment from MUC 10 (*Siboglinidae* field*,* a-d) and MUC 12 (bacterial mat, e-h). a, e: Concentrations of pore-water total alkalinity (TA, open squares), and sulfide (solid triangles). b, f: Concentrations of pore-water sulfate (SO_4^{2-}, solid circles) and sediment methane (CH_4, open circles). Note the different x-axes for methane. c, g: Methane oxidation rates (CH_4 OX, symbols represent three replicates). Note that c includes an insert that focusses on rates <5 nmol cm^{-3} d^{-1}. d, h: Sulfate reduction rates (SR, symbols represent three replicates).

FORAMINIFERAL ISOTOPIC SIGNATURES

Carbon isotopic signatures ($\delta^{13}C$) of Rose Bengal stained (RB-stained) foraminifera specimens from the *Siboglinidae* field (MUC 10) showed the lowest values (Table S2) for the benthic foraminiferal species *M. barleeanus* and *C. neoteretis,* reaching values as low as -5.21 and -1.83‰, respectively, as compared to non-stained specimens (i.e., empty tests) (Fig. 4). No RB-stained specimens occurred in sediment from the bacterial mat (MUC 12). At this station, the lowest $\delta^{13}C$ was detected, with values as low as -6.48, -6.17, and -6.18 ‰, were found in empty specimens of *M. barleeanus*, *C. wuellerstorfi,* and *C. neoteretis*, respectively (Table S2). Similarly, empty specimens of the planktonic foraminiferal species *N. pachyderma* show the lowest values, reaching -6.18‰ (Table S2).

It is notable that the $\delta^{13}C$ of RB-stained specimens of *M. barleeanus*, C. *wuellerstorfi,* and *C. neoteretis* were lower in samples from MUC 10A compared to MUC 10B from the *Siboglinidae* field (Figs. 3–5). The carbon isotopic signature of RB-stained *M. barleeanus* and *C. wuellerstorfi* displayed a wide range of values (0.18–1.13‰, and -2.80 – -5.21‰, respectively; Figs. 3,5). Overall, RB-stained *M. barleeanus* had lower $\delta^{13}C$ values in comparison to empty specimens of its conspecifics from the same interval (Fig. 3). RB-stained and empty tests of *M. barleeanus* were more depleted in ^{13}C in deeper parts of the sediment. The most pronounced negative excursion in $\delta^{13}C$ was recorded in empty specimens M. *barleeanus* from the bacterial mats (MUC 12; Fig. 3) reaching -6.48‰. SEM investigations of empty specimens of *N. pachyderma* (MUC 12B) revealed authigenic overgrowth of carbonate on the surface of their tests (Fig. 6).

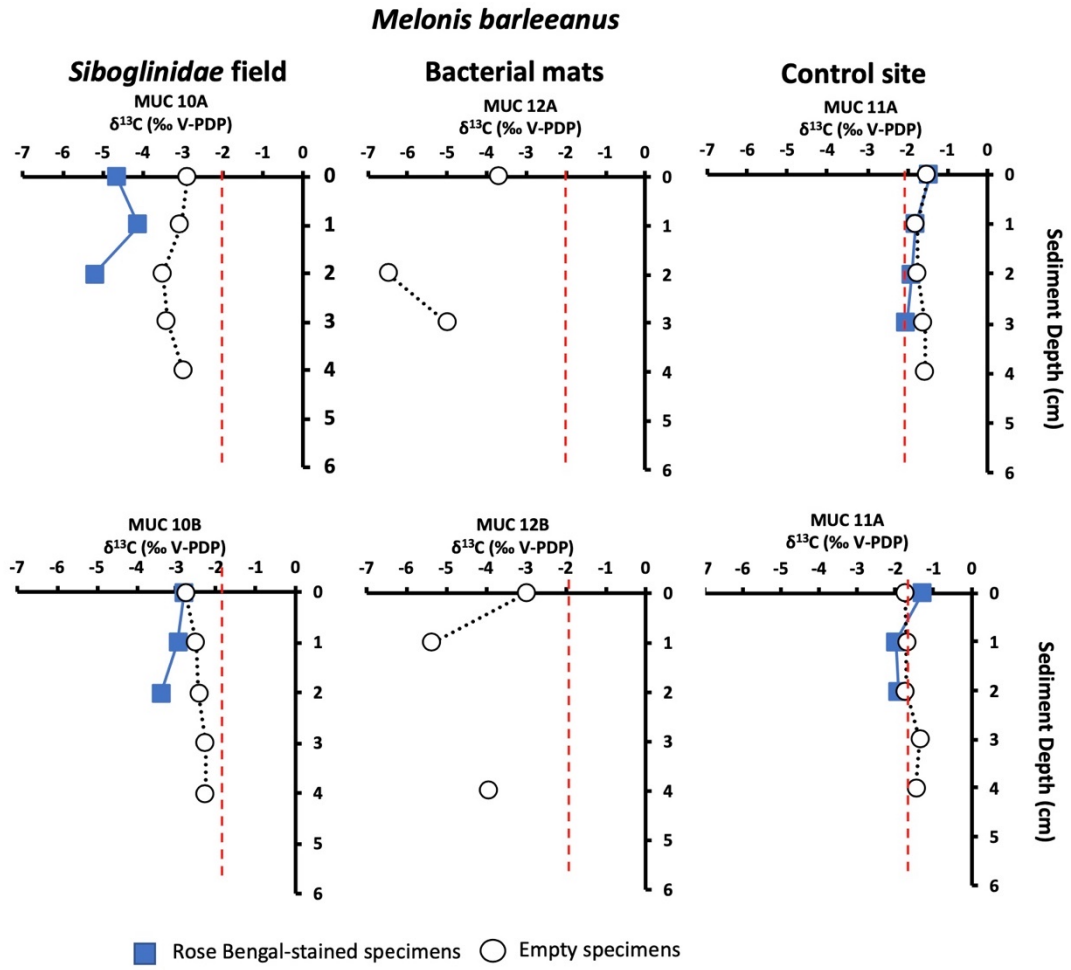

Figure 3. Carbon isotope values ($\delta^{13}C$) of *Melonis barleeanus* in sediment from the *Siboglinidae* field (MUC 10A and MUC 10B), bacterial mats (MUC 12A and MUC 12B), and control site (MUC 11A and MUC 11B). The vertical red line indicates the $\delta^{13}C$ minimum value for non-seep conditions [28].

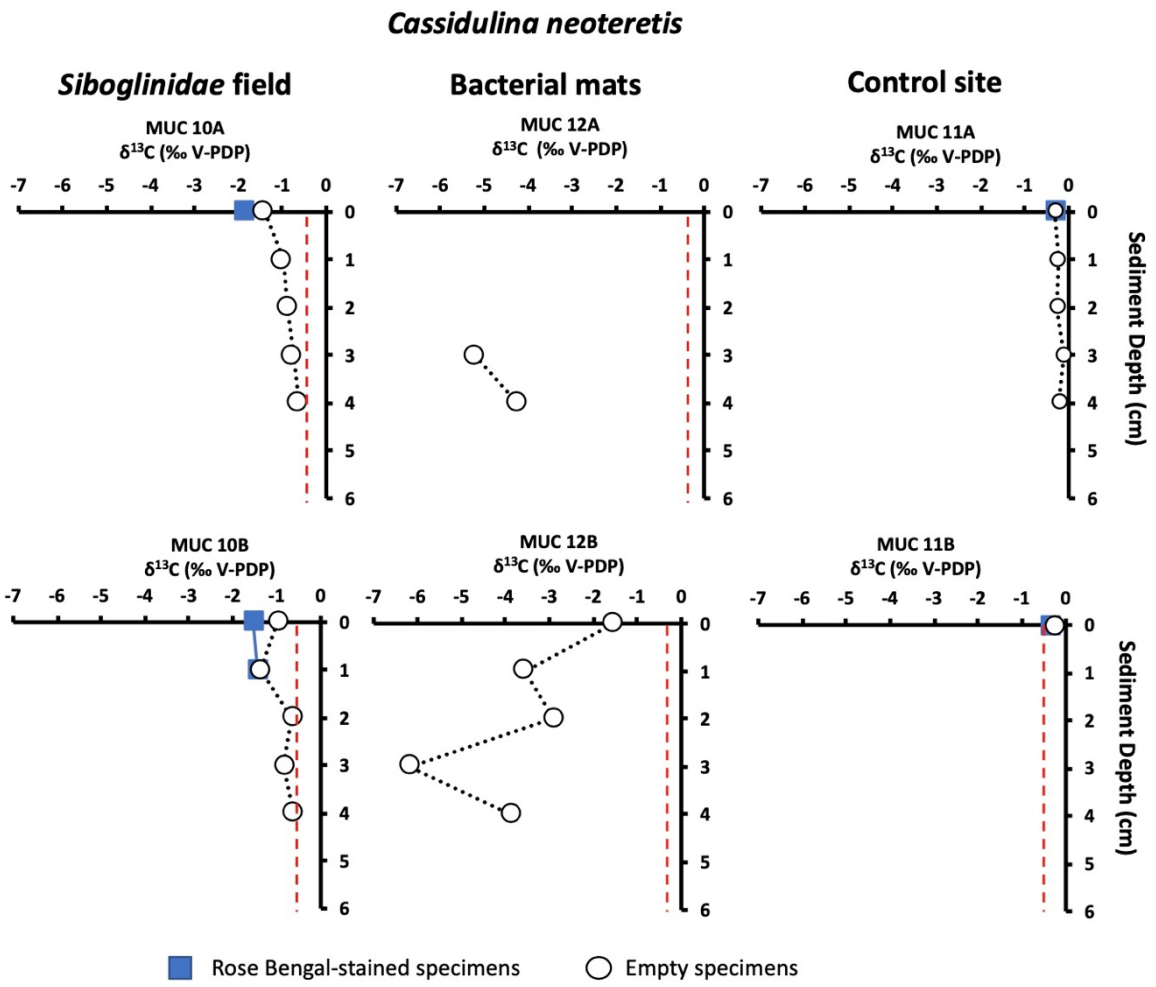

Figure 4. Carbon isotope values ($\delta^{13}C$) of *Cassidulina neoteretis* in sediment from the *Siboglinidae* field (MUC 10A and MUC 10B), bacterial mats (MUC 12A and MUC 12B), and control site (MUC 11A and MUC 11B). The vertical red line indicates the $\delta^{13}C$ minimum value for conditions[28].

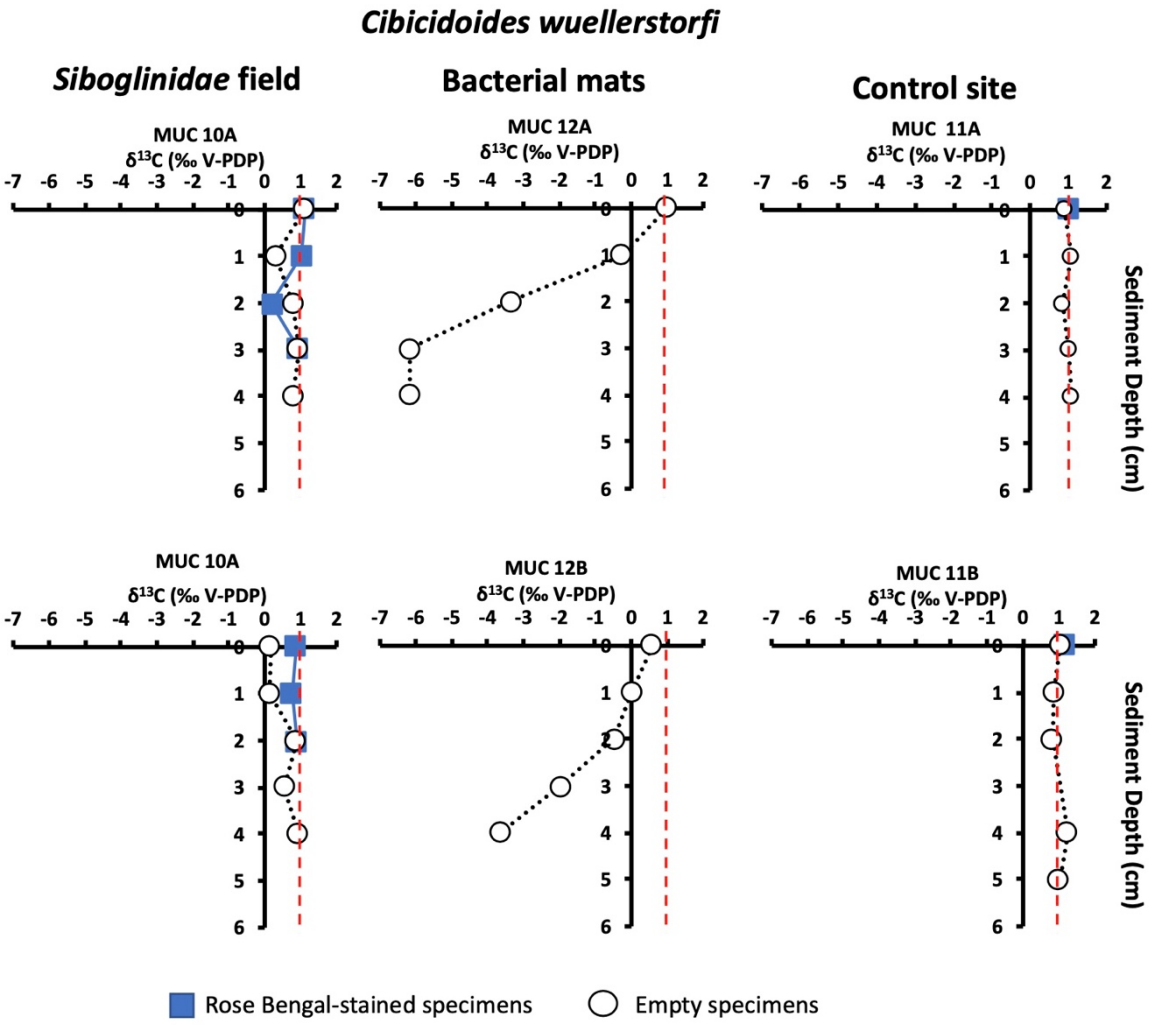

Figure 5. Carbon isotope values ($\delta^{13}C$) of *Cibicidoides wuellerstorfi* from the *Siboglinidae* field (MUC 10 and MUC 10B), bacterial mats (MUC 12A and MUC 12B), and control site (MUC 11A and MUC 11B). The vertical red line indicates the $\delta^{13}C$ minimum value for non-seep conditions[28].

Highest oxygen isotopic values ($\delta^{18}O$) were recorded in empty specimens of *C. neoteretis* from MUC 12A, reaching 5.24‰ (Table S2; Fig. 6). The $\delta^{18}O$ values recorded in the RB-stained foraminifera assemblages from the *Siboglinidae* field (corrected for vital effects; see Methods) varied between 4.23–4.35‰ for *M. barleeanus* (Table S2), 4.22–4.43‰ for *C. wuellerstorfi*, and 4.17–4-26‰ for *C. neoteretis*. At the control site, values for RB-stained foraminifera ranged between 4.22–4.43, 4.19–4.41, and 4.14–4.23‰. The $\delta^{18}O$ values for empty foraminifera from the *Siboglinidae* field range between 4.32–4.59‰, 4.38–4.55‰, and 2.21–4.59‰ for *M. barleeanus*, *C. wuellerstorfi,* and *C. neoteretis,* respectively. At the bacterial mat site, the $\delta^{18}O$ signature was between 4.09–4.41‰, 4.15–4.63‰, and 4.32–5.17‰, respectively. Similarly, the $\delta^{18}O$ values for the empty conspecifics from the

control site ranged 4.21– 4.52‰, 4.25–4.48‰, and 4.29–4.35 ‰ for *M. barleeanus*, *C. wuellerstorfi,* and *C. neoteretis* (Table S2).

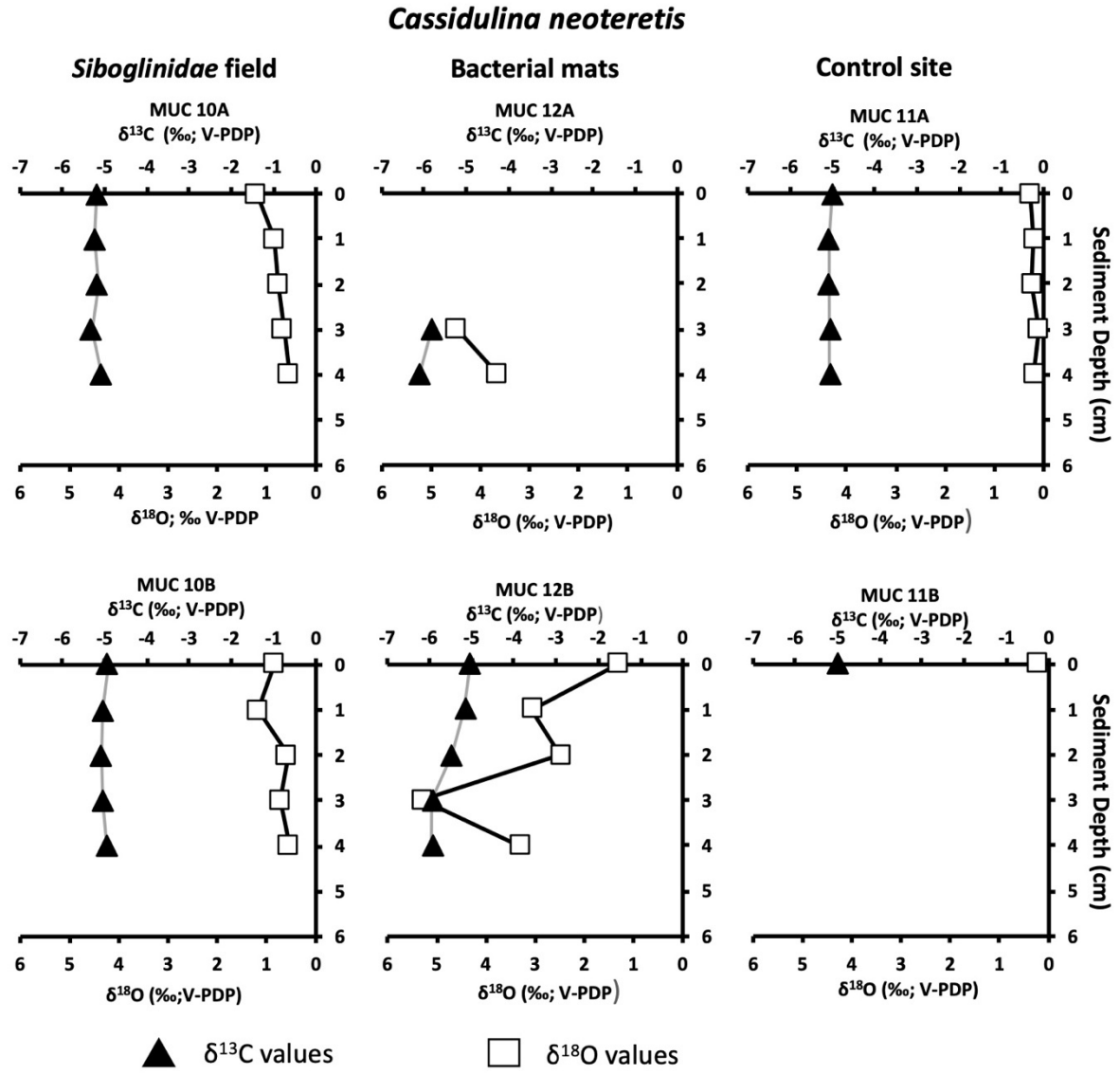

Figure 6. Oxygen isotope values ($\delta^{18}O$) of empty tests of *Cassidulina neoteretis* in sediment from the *Siboglinidae* field (MUC 10A and MUC 10B), bacterial mats (MUC 12A and MUC 12B), and control site (MUC 11A and MUC 11B).

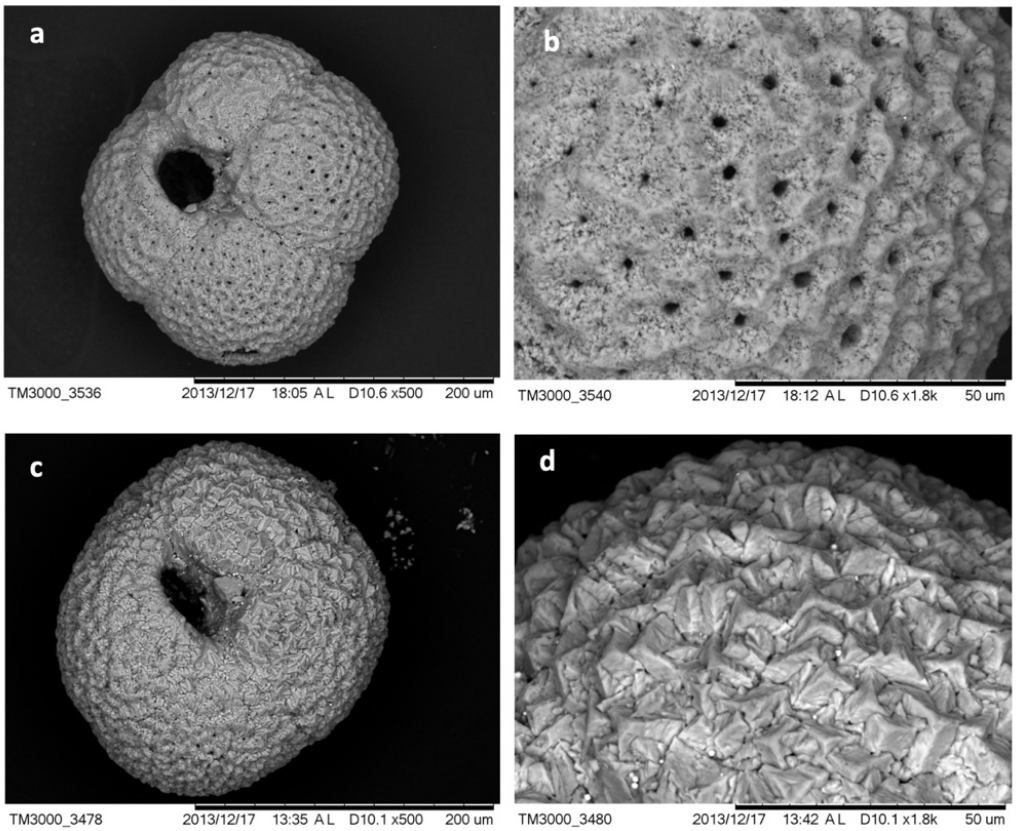

Figure 6. Scanning electron microscopy (SEM) micrography of *N. pachyderma* from MUC 10B 4-5 cm depth (a, b) and MUC 12B 3-4 cm depth (c, d). Micrographs c and d show authigenic overgrowth on the outer surface of the test, while a, b, show a pristine shell with no coating.

DISCUSSION

Siboglinidae field - moderate methane seepage

Biogeochemical data of the pore water from the *Siboglinidae* field indicate moderate methane seepage activity [16,29,30]. The bio-irrigation activity of the *Siboglinidae* tubeworms might cause oxidation of the top layer of the sediment[31] and potentially presence of free oxygen, resulting in the consumption of methane by aerobic methanotrophic microorganisms (top 4 cm of the sediment, Fig. 2). As a result of methane oxidation, the pore water is likely enriched in methane-derived $^{12}CO_2$ and $H^{12}CO_3^-$ [32] as well as microbial biomass, which provides a carbon source for the benthic foraminifera during construction of their tests by biocalcification. To build its test foraminifera use carbon both from ambient DIC pool and intracellular storage (i.e., resulting from respiration and diet [33,34]). Consequently, isotopically light carbon is likely incorporated by the benthic foraminifera, not only as an inorganic carbon from pore water but also via nutrition (i.e., by consumption of methanotrophic microbes). Presumably, during biocalcification CO_2 is preferred as CO_2 diffuses more efficiently across

cell membranes compared to HCO_3^- and/or CO_3^{2-}[33]. In fact, the $\delta^{13}C$ values of RB-stained *M. barleeanus* (–4.10 to -5.21‰, MUC 10A) from the *Siboglinidae* field are more negative compared to its conspecific from the control site (-1.30 to -2.01‰, MUC 11), as well as compared to other non-seep (i.e., normal) environments in the Arctic Ocean (min. -2‰)[35]. In contrast, $\delta^{13}C$ of RB-stained *M. barleeanus* from the active 'Lomvi' pockmark did not indicate any influence of methane (-1.95‰)[36]. Similar to *M. barleeanus*, $\delta^{13}C$ of RB-stained *C. neoteretis* from the *Siboglinidae* field showed fairly negative values (from -1.44‰ to -1.83‰) compared to the non-seep site MUC 11A, and -B (from -0.32‰ to -0.34‰) (Fig. 4), and to other non-seep sites from the Arctic Ocean (from -0.3‰ to -1‰)[35]. The $\delta^{13}C$ values of *C. neoteretis* from this study are also much lower than values (-0.26‰) from the active 'Lomvi' pockmark[36]. 'Lomvi' pockmark is characterized by advective methane transport i.e., methane escape in the gas phase through cracks; thus not affecting the foraminifera[37].

The $\delta^{13}C$ of calcareous benthic foraminifera is conditioned by vital effects (i.e., species-specific intracellular metabolic processes[38,28]) and their microhabitat (e.g., sedimentary organic matter, dissolved inorganic carbon content)[39, 40]. Vital effects can cause differences in the $\delta^{13}C$ values of ~1–2 ‰ between foraminiferal specimens from the same species. In the present study, $\delta^{13}C$ vary from -5.21 to -1.3‰ between specimens of RB-stained *M. barleeanus* from the *Siboglinidae* field and from the control site. The differences between RB-stained specimens of *C. neoteretis* range from -0.32 to -1.83‰. These large differences between methane-influenced sites and non-methane sites cannot be attributed to vital effects alone. We suggest that the major factor controlling the $\delta^{13}C$ in the foraminiferal tests of RB-stained *M. barleeanus* and *C. neoteretis* in the seep samples comes from methane, i.e., from microhabitat effects.

The $\delta^{13}C$ of RB-stained *C. wuellerstorfi* from the *Siboglinidae* field vary between 0.73‰ and 1.13‰, which is similar to the $\delta^{13}C$ values of their conspecifics from the control site (from 1.05‰ to 1.20‰), and within the range of 'normal' values for the species[18]. Thus, there is no considerable influence of carbon-derived methane on their isotopic signature. This 'normal' carbon isotopic signature could be related to the epibenthic lifestyle of *C. wuellerstorfi,* which tend to attach itself to structures extending above the seafloor, e.g., tubes of *Siboglinidae* worms[41, 18, 42]. They do so to avoid hostile environmental conditions, such as oxygen depletion and toxicity of sulfide, both common at cold seeps[43, 42] (Fig. 2). In the *Siboglinidae* field, samples showed specimens of *C. wuellerstorfi* attached to *Siboglinidae* tubes (Fig. 7). However, due to the absence of hostile environmental conditions, we suggest that *C. wuellerstorfi* is more likely attached to the tubes to support its feeding behavior.

Figure 7. Rose Bengal stained *Cibicidoides wuellerstorfi* attached to a Siboglinidae tube, MUC 10A. Photo: K. Sztybor.

A laboratory culturing experiment performed by Wollenburg et al.[44] showed that artificially injecting ^{13}C-enriched methane to the water altered not only the $\delta^{13}C$ signatures of the ambient DIC pool, but also the $\delta^{13}C$ of the foraminiferal offspring of the epifaunal species *C. wuellerstorfi* and the shallow infaunal species *C. neoteretis*. These findings indicate that the $\delta^{13}C$ values of *C. wuellerstorfi* can become more negative with low $\delta^{13}C_{DIC}$ in the ambient water. The experiments resulted in mean $\delta^{13}C$ values of −1.44‰ for *C. wuellerstorfi* and −2.24‰ for *C. neoteretis* under controlled culturing conditions[44]. Since the $\delta^{13}C$ measured in *C. neoteretis* (offspring) has values similar to those obtained from an in-situ reference site from the Håkon Mosby Mud Volcano[18], the authors suggested that the $\delta^{13}C$ of this shallow infaunal species mainly reflect their dietary preferences, i.e., feeding on bacteria[44], whereas the epifaunal species *C. wuellerstorfi* reflects the $\delta^{13}C$ of the bottom water DIC[44]. Thus, the $\delta^{13}C$ signatures of *M. barleeanus*, *C. neoteretis,* and *C. wuellerstorfi* from the same sample might reflect the different microhabitat preferences of these species. Foraminifera that calcify deeper in the sediment (intermediate infaunal and deep-infaunal species), for example *M. barleeanus,* often have low isotopic values when compared to shallow infaunal or epifaunal species, such as *C. neoteretis* or *C. wuellerstorfi*, respectively [38,39]. Our results from the *Siboglinidae* field indicate that the proportion of depleted ^{13}C in the ambient bottom water was not sufficient to considerably affect the isotopic signature of the epifaunal *C. wuellerstorfi* in comparison to the species that live deeper in the sediment, i.e., *M. barleeanus* and *C. neoteretis,* that are more susceptible to the effects of methane. These infaunal species are probably affected by feeding on the ^{13}C-depleted methanotrophic microbial communities within the sediment and incorporating ^{13}C-depleted DIC from the porewater during

calcification. Food sources of ^{13}C-depleted microbes (archaea, bacteria) can contribute to up to a 5 to 6 ‰ decrease of the $\delta^{13}C$ values of foraminiferal tests at seep sites[19].

Bacterial mats - strong methane seepage

It has been suggested that due to the hostility of environments severely influenced by methane seepage with presence of H_2S , benthic foraminifera do not calcify, and consequently their $\delta^{13}C$ values do not record methane seepage[45]. Our results on the pore water biogeochemistry of the bacterial mats site (MUC 12) indicate a strong methane seepage regime, which is dominated by AOM and sulfate reduction activity and high concentrations of H_2S just below the sediment surface (Fig. 2). Although foraminifera have a high tolerance to short-term exposure to H_2S (up to 21 days) the prolonged exposure to H_2S (>66 day, with final concentration of H_2S 12 µM), results in a significant reduction of the living population[46]. Indeed, no RB-stained foraminifera are found in samples from the bacterial mat (MUC 12A and MUC 12B). Nevertheless, the $\delta^{13}C$ of empty tests from the bacterial mat reached values as low as -6.48‰ (*M. barleeanus*), and -6.18‰ (*C. neoteretis*) (Table S2) and even -6.17‰ for *C. wuellerstorfi*. These values are considerably lower compared to $\delta^{13}C$ values of empty tests from its conspecifics from the control site, which show 'normal' values and are also lower than in empty foraminiferal shells from the *Siboglinidae* field (Figs. 3–5). We believe the low $\delta^{13}C$ values are related to MDAC, which may severely overprint the initial isotopic signatures of the foraminiferal tests. In support of this hypothesis, the SEM investigation of the planktonic foraminiferal species *N. pachyderma* from the bacterial mat revealed signs of authigenic precipitation of carbonate on the outer surface (Fig. 6 c, d), and the $\delta^{13}C$ signature is considerably more negative (-0.9 to -4.23‰) compared to 'normal' values in surface water environments (-0.5‰ to 0.5‰)[47].

AOM is a strong contributor to authigenic carbonate overgrowth due to its production of HCO_3^- and increase in alkalinity [12,15]. Overprinting by authigenic carbonate on foraminiferal shells can cause a lowering of the $\delta^{13}C$ values of >10‰[15]. In the MUC 12 samples, overgrowth was detected at relatively shallow sediment depth, i.e., 2–3 cm below the sediment surface (MUC 12A). Hence, the measured low values are most likely the result of a minor degree of a very recent overgrowth and are therefore less depleted in ^{13}C compared to values previously recorded in Vestnesa Ridge studies [12,15].

The $\delta^{18}O$ ratio in calcareous foraminiferal tests is influenced by several factors, including bottom water temperature, isotopic composition of the ambient seawater, and vital effects[48]. Gas hydrate dissociation at cold seeps, for example, enriches the pore water ^{18}O [49,50]. Thus, foraminiferal tests affected by methane-derived carbon might record higher $\delta^{18}O$ values[12] (and references therein). Our data show that the $\delta^{18}O$ signature in empty tests of *C. neoteretis* from the bacterial mat (MUC 12A

and MUC 12B) display low $\delta^{13}C$ values and a high $\delta^{18}O$ signature (up to 5.17‰). There was no such pattern in *C. neoteretis* from the *Siboglinidae* field or the control site (Fig. 6). We suggest that the higher ^{18}O results from the precipitation of ^{18}O-enriched MDAC. Similarly, $\delta^{18}O$ in *N. pachyderma* show relatively high values (3.05–4.05‰)[47] (Table S2). In accordance with these observations, authigenic carbonates from seep sites in the 'Lomvi' pockmark displayed relatively high $\delta^{18}O$ values (4.53 to 5.90 ‰ VPDB)[12]. Given the more positive values, *C. neoteretis* might have a high predisposition for authigenic overgrowth, likely due to its test structure[15], which may explain why only this species showed high $\delta^{18}O$ values compared to others from the same samples.

CONCLUSION

The $\delta^{13}C$ values measured in both RB-stained benthic foraminifera and and empty tests of both planktic and benthic foraminifera from Vestnesa Ridge together with biogeochemical datasets of pore water conditions showed a large degree of variation between different habitats (*Siboglinidae* field, bacterial mat, and control site). At the *Siboglinidae* field with moderate seepage of methane, dominance of MOx, and low concentrations of sulfide, the live benthic foraminifera (RB-stained) incorporate methane-derived carbon, most likely by feeding on methane-oxidizing bacteria or by direct intake of $^{12}CO_2$ produced during MOx. The response, however, differed between species: the epifaunal species *Cibicidoides wuellerstorfi* appeared to be less susceptible to methane influence, while the intermediate infaunal species *Melonis barleeanus* responded more strongly by reaching $\delta^{13}C$ values down to -5.21‰. In bacterial mats sediment with strong methane seepage, high activity of AOM and sulfate reduction produced high levels of sulfide and total alkalinity, which killed living specimens and lead to the lowest $\delta^{13}C$ values recorded in dead specimens due to postmortem MDAC overgrowth, respectively. Overgrowth may have started coating the fossil foraminiferal tests at relatively shallow depth in the sediment (2–3 cm), causing $\delta^{13}C$ signatures shifts of tests towards low values (down to -6.48‰ for fossil *M. barleeanus).* Higher $\delta^{18}O$ values in fossil *C. neoteretis* (5.17‰) from the bacterial mats combined with low $\delta^{13}C$ values (-6.18) suggest the MDAC formation was affected by gas hydrates.

METHODS

Sediment sampling

Sediment samples were collected from a pockmark on Vestnesa Ridge, NW Svalbard margin in August 2011 during the POS419 expedition of the RV Poseidon. Using a TV-guided multicorer, sediment samples were taken from a *Siboglinidae* field (chemosymbiotic tubeworms), from a sulfur-bacterial mat, and from far outside of the pockmark as a control site, where no methane seepage occurs (Table S1). The TV-guided multicorer system enables visual localization of active methane seeps based on the presence of cold-seep related structures, such as bacterial mats and authigenic carbonate crusts for targeted, designated sampling spots. The multicorer collected 6 cores of 10 cm in diameter at each location. After recovery of the multicorer, two cores (labelled A, B) were selected from each site for the study of foraminifera and subsampled onboard into 1-cm thick horizontal slices down to 10 cm core depth. The samples were transferred into plastic containers, and stained with Rose Bengal-ethanol solution following the FOBIMO protocol (2 g\l)[51]. Samples were kept onboard in a dark, cool room at 4 °C until further processing. A third core was sectioned in 1, 2, 3, and 5 cm increments (from top to bottom) for sediment porewater analyses. A fourth core was sectioned in 1, 2, 3, and 5 cm increments (from top to bottom) for sediment methane analyses. A fifth core was subsampled with a total of six mini polycarbonate cores (inner diameter 26 mm, length 30 cm) for the determination of methane concentration, methane oxidation, and sulfate reduction. All sediment sampling procedures were conducted at +4 °C inside a cooled laboratory.

Porewater analyses

Porewater was extracted onboard at +4 °C using a low-pressure squeezer (argon at 1–5 bar). While squeezing, porewater was filtered through 0.2 µm cellulose acetate nuclepore filters and collected in argon-flushed recipient vessels. Onboard, the collected porewater samples were analyzed for their content of dissolved total sulfides (in the following referred to as "sulfide")[52]. A 1 ml sample was added to 50 µl of zinc acetate solution. Subsequently, 10 µl of N,N-dimethyl-1,4-phenylenediamine-dihydrochloride color reagent solution and 10 µl of the $FeCl_3$ catalyst were added and mixed. After 1 hr of reaction time, the absorbance was measured at 670 nm. Total alkalinity (TA) was determined by direct titration of 1 mL pore water with 0.02 M HCl using a mixture of methyl red and methylene blue as an indicator and bubbling the titration vessel with argon gas to strip CO_2 and hydrogen sulfide. The analysis was calibrated using IAPSO seawater standard, with a precision and detection limit of 0.05

mmol L^{-1}.Porewater samples for sulfate (SO_4^{2-}) analyses were stored in 2-ml glass vials at +4 °C and analyzed onshore. Sulfate was determined by ion chromatography (Metrohm, IC Compact 761). Analytical precision based on repeated analysis of IAPSO standards (dilution series) was <1%.

Methane measurements

According to Sommer et al.[53] methane concentrations in sediment cores were determined in 1 cm intervals down to a depth of 6 cm followed by 2 cm intervals down to 12, 3 cm intervals down to 18 cm and 5 cm interval deeper than 18 cm. From each depth horizon, a 2 ml sub-sample was transferred into a septum-stoppered glass vial (21.8 ml) containing 6 ml of saturated NaCl solution and 1.5 g of NaCl in excess. The volume of headspace was 13.76 ml. Within 24 h, the methane concentration in the headspace was determined using a Shimadzu GC 14A gas chromatograph fitted with a flame ionization detector and a 4 m × 1⁄8-inch Poraplot Q (mesh 50/80) packed column. Prior to the measurements the samples were equilibrated for 2 h on a shaking table. Precision to reproduce a methane standard of 9.98 ppm was 2%.

Microbial methane oxidation rates

On board, radioactive methane ($^{14}CH_4$ dissolved in water, injection volume 15 µl, activity ~5 kBq, specific activity 2.28 GBq $mmol^{-1}$) was injected into three replicate mini cores at 1-cm intervals according to the whole-core injection method[54]. The mini cores were incubated at in-situ temperature for ~24 h in the dark. To stop bacterial activity, the sediment cores were sectioned into 1-cm intervals and transferred into 50-ml crimp glass vials filled with 25 ml sodium hydroxide (2.5% w/w). After crimp-sealing, glass vials were shaken thoroughly to equilibrate the pore-water methane between the aqueous and gaseous phase. Control samples were first terminated before addition of tracer. In the home laboratory, methane oxidation rates and methane concentrations in the sample vials were determined according to Treude et al.[55].

Microbial sulfate reduction rates

Sampling, injection, and incubation procedures were identical to methane oxidation samples. The injected radiotracer was carrier-free $^{35}SO_4^{2-}$ (dissolved in water, injection volume 6 µl, activity 200 kBq, specific activity 37 TBq $mmol^{-1}$). To stop bacterial activity after incubation, sediment cores were sectioned into 1-cm intervals and transferred into 50 ml plastic centrifuge vials filled with 20 ml zinc acetate (20% w/w) and frozen. Control sediment was first terminated before addition of tracer. In the home laboratory, sulfate reduction rates were determined according to the cold-chromium distillation method[56].

Foraminiferal analyses

Rose-Bengal stained samples were sieved over a 100-µm sieve. The >100-µm fraction was kept wet and further examined under reflected-light microscopy. All benthic foraminiferal individuals that stained dark magenta and were fully filled with cytoplasm were considered to be 'living' foraminifera i.e., live + recently dead individuals, still containing cytoplasm. Foraminifera showing no colorization were considered as unstained, empty (dead) individuals. The foraminifera were wet picked, sorted by species and placed on micropaleontology slides. For carbon ($\delta^{13}C$) and oxygen ($\delta^{18}O$) stable isotope analyses, both Rose Bengal stained and unstained (empty) specimens of benthic foraminiferal species *Melonis barleeanus*, *Cassidulina neoteretis* and *Cibicidoides wuellerstorfi* and empty specimens of the planktic foraminiferal species *Neogloboquadrina pachyderma* were picked. When present, approximately 10 specimens of each species were taken from each sample. Empty tests were obtained from the same samples as Rose-Bengal stained foraminifera. Isotopic measurements were performed at Woods Hole Oceanographic Institution (WHOI). Data are reported in standard notation ($\delta^{13}C$, $\delta^{18}O$), according to the Pee Dee Belemnite (PDB) standard. The $\delta^{18}O$ values were corrected for vital effects as follows: +0.4‰ for *M. barleeanus*[57] and + 0.64‰ for *C. wuellerstorfi*[58] . *Neogloboquadrina pachyderma*, two specimens from intervals 0–1 cm and 4–5 cm from each core were selected and investigated using Scanning Electron Microscopy (SEM). To make our data comparable with other studies on live foraminifera, we deliberately used the most widely used staining method, the Rose Bengal. Since Rose Bengal indicates both live and dead cytoplasm, even weeks to months after the death of an individual[59,36], we nevertheless refer here to Rose Bengal stained foraminifera as 'live' specimens, and empty, unstained tests as dead specimens.

Acknowledgment

Funding of this project was provided by Tromsø Research Foundation (Tromsø Forskningsstiftelse, TFS) to the Paleo-CIRCUS project 2010–2014. Further support was provided through the Cluster of Excellence "The Future Ocean" funded by the German Research Foundation and through the Alexander von Humboldt Foundation. We would like to thank the captain, crew, chief scientist (O. Pfannkuche) and scientific party of the RV *Poseidon* PO419 expedition for technical support. M. Veloso, V. Bertics, and K. Kretschmer are thanked for subsampling of sediment. J. Hommer and B. Dohmeyer are thanked for geochemical analyses. We also acknowledge J. M. Bernhard for hosting and guiding K. Sztybor at WHOI, and D. McCorkle and A. Gagnon for supervising isotope analyses. We thank Anna N. Osiecka for copy-editing and Sunil Vadakkepuliyambatta for his help with maps in Fig. 1.

SUPPLEMENTARY INFORMATION

Table S1. Sample coordinates and environmental information.

Station POS419	**Sample ID**	**Coordinates**	**Depth (cm)**	**Environment**	**Date**	**Analyses**
675	MUC 10	79° 00,466´N 06°54,279´E	1241	*Siboglinidae* field	25.08.2011	stable isotopes, SEM sulfide, SO_4^{2-}, total alkalinity, methane, AOM, sulfate reduction
676	MUC 11	78° 59,774´N 06° 58,064´E	1191	Control site, regular marine sediment	28.08. 2011	Stable isotopes, SEM
678	MUC 12	79° 00,417´N 06° 54,131´E	1235	Bacterial mats	29.08. 2011	stable isotopes, SEM; sulfide, SO_4^{2-}, total alkalinity, methane, AOM, sulfate reduction

Table S2. Stable isotope values ($\delta^{13}C$ and $\delta^{18}O$; ‰) of Rose Bengal- stained (RB) and empty (fossil) tests of benthic foraminiferal species *Melonis barleeanus*, *Cassidulina neoteretis*, *Cibicidoides wuellerstorfi*, and planktonic foraminiferal species *Neogloboquadrina* pachyderma from Vestnesa Ridge *Siboglinidae* field (MUC 10A, MUC 10B), bacterial mat (MUC 12A, MUC 12B) and control site (MUC 11A and MUC 11B). The * represent the $\delta^{18}O$ values corrected for vital effects: +0.4‰ for *M. barleeanus* and + 0.64‰ for *C. wuellerstorfi.*

		RB-stained			**Fossil**		
	Depth cm	$\delta^{13}C$‰	$\delta^{18}O$ ‰	$\delta^{18}O$‰*	$\delta^{13}C$‰	$\delta^{18}O$‰	$\delta^{18}O$‰*
MUC 10A							
	0-1	-4.65	3.95	4.35	-2.88	4.16	4.56
M. barleeanus	1-2	-4.10	3.91	4.31	-3.05	4.18	4.58
	2-3	-5.21	3.90	4.31	-3.50	4.16	4.56
	3-4	-	-	-	-3.38	4.19	4.59
	4-5	-	-	-	-2.99	4.05	4.45
	0-1	1.13	3.66	4.3	1.11	3.85	4.49
C. wuellerstorfi	1-2	1.04	3.73	4.37	0.30	3.91	4.55
	2-3	0.18	3.72	4.36	0.79	3.88	4.52
	3-4	0.93	3.79	4.43	0.94	3.83	4.47
	4-5	-	-	-	0.80	3.89	4.53
	0-1	-1.83	4.26	4.26	-1.40	4.45	4.45
	1-2	-	-	-	-0.98	4.48	4.48
C. neoteretis	2-3	-	-	-	-0.87	4.43	-
	3-4	-	-	-	-0.75	4.54	-
	4-5	-	-	-	-0.62	4.35	-

	0-1	-	-	-	-0.10	2.69	2.69
N. pachyderma	1-2	-	-	-	0.20	3.15	3.15
	2-3	-	-	-	-0.28	3.42	3.42
	3-4	-	-	-	0.06	2.93	2.93
	4-5	-	-	-	-	-	-
MUC 10B							
	0-1	-2.80	3.83	4.23	-2.78	3.96	4.36
M. barleeanus	1-2	-2.95	3.86	4.26	-2.52	3.92	4.32
	2-3	-3.28	3.88	4.28	-2.43	3.96	4.36
	3-4	-	-	-	-2.27	3.97	4.37
	4-5	-	-	-	-2.26	3.97	4.37
	0-1	0.88	3.77	4.36	0.15	3.76	4.4
C. wuellerstorfi	1-2	0.77	3.63	4.27	0.13	3.88	4.52
	2-3	0.87	3.58	4.22	0.87	3.75	4.38
	3-4	-	-	-	0.55	3.84	4.48
	4-5	-	-	-	0.95	3.80	4.44
	0-1	-1.54	4.26	4.26	-0.97	4.21	-
C. neoteretis	1-2	-1.44	4.17	4.17	-1.37	4.32	-
	2-3	-	-	-	-0.66	4.35	-
	3-4	-	-	-	-0.84	4.31	-
	4-5	-	-	-	-0.62	4.24	-

MUC 11A							
	0-1	-1.42	3.87	4.27	-1.46	4.05	4.45
M. barleeanus	1-2	-1.77	4.01	4.41	-1.75	4.08	4.48
	2-3	-1.91	4.03	4.43	-1.74	3.96	4.36
	3-4	-2.01	4.01	4.41	-1.56	4.04	4.44
	4-5	-	-	-	-1.55	4.12	4.52
	0-1	1.05	3.55	4.19	0.92	3.85	4.49
C. wuellerstorfi	1-2	-	-	-	1.08	3.73	4.37
	2-3	-	-	-	0.85	3.81	4.45
	3-4	-	-	-	1.02	3.69	4.33
	4-5	-	-	-	1.08	3.84	4.48
	0-1	-0.32	4.14	4.14	-0.32	4.29	-
C. neoteretis	1-2	-	-	-	-0.23	4.35	-
	2-3	-	-	-	-0.27	4.35	-
	3-4	-	-	-	-0.11	4.33	-
	4-5	-	-	-	-0.22	4.34	-
MUC 11B							
	0-1	-1.30	3.87	4.27	-1.75	3.93	4.33
M. barleeanus	1-2	-1.99	3.89	4.29	-1.71	4.02	4.42
	2-3	-1.93	3.82	4.22	-1.73	3.81	4.21
	3-4	-	-	-	-1.37	4.11	4.51
	4-5	-	-	-	-1.46	4.12	4.52

	0-1	1.20	3.77	4.41	1.05	3.61	4.25
C. wuellerstorfi	1-2	-	-	-	0.86	3.73	4.37
	2-3	-	-	-	0.83	3.59	4.23
	3-4	-	-	-	1.25	3.76	4.4
	4-5	-	-	-	1.02	3.73	4.37
C. neoteretis	0-1	-0.34	4.23	4.23	-0.22	4.29	-
MUC 12A							
	0-1	-	-	-	-3.68	3.92	4.32
M. barleeanus	1-2	-	-	-	-		-
	2-3	-	-	-	-6.48	3.70	4.1
	3-4	-	-	-	-4.99	4.01	4.41
	4-5	-	-	-	-	-	-
	0-1	-	-	-	0.98	3.99	4.63
C. wuellerstorfi	1-2	-	-	-	-0.27	3.67	4.31
	2-3	-	-	-	-3.35	3.54	4.18
	3-4	-	-	-	-6.17	3.51	4.15
	4-5	-	-	-	-6.17	3,67	4.31
	0-1	-	-	-	-	-	-
C. neoteretis	1-2	-	-	-	-	-	-
	2-3	-	-	-	-	-	-

	3-4	-	-	-	-5.22	4.99	-
	4-5	-	-	-	-4.25	5.24	-
	0-1	-	-	-	-0.92	3.26	3.26
N. pachyderma	1-2	-	-	-	-3.07	3.13	3.13
	2-3	-	-	-	-3.30	3.05	3.05
	3-4	-	-	-	-4.23	4.03	4.03
	4-5	-	-	-	-3.07	3.71	3.71
MUC 12B							
	0-1	-	-	-	-2.98	3.79	4.19
M. barleeanus	1-2	-	-	-	-5.32	3.69	4.09
	2-3	-	-	-	-5.54	3.83	4.23
	3-4	-	-	-	-	-	-
	4-5cm	-		-	-3.90	3.84	4.24
	0-1	-	-	-	0.59	3.63	4.33
C. wuellerstorfi	1-2	-	-	-	-0.004	3.60	4.24
	2-3	-	-	-	-0.46	3.61	4.25
	3-4	-	-	-	-1.97	3.61	4.25
	4-5	-	-	-	-3.65	3.67	4.31
	0-1	-	-	-	-1.54	4.32	-
C. neoteretis	1-2	-	-	-	-3.57	4.44	-
	2-3	-	-	-	-2.91	4.72	-

	3-4	-	-	-	-6.18	5.17	-
	4-5	-	-	-	-3.87	5.09	-

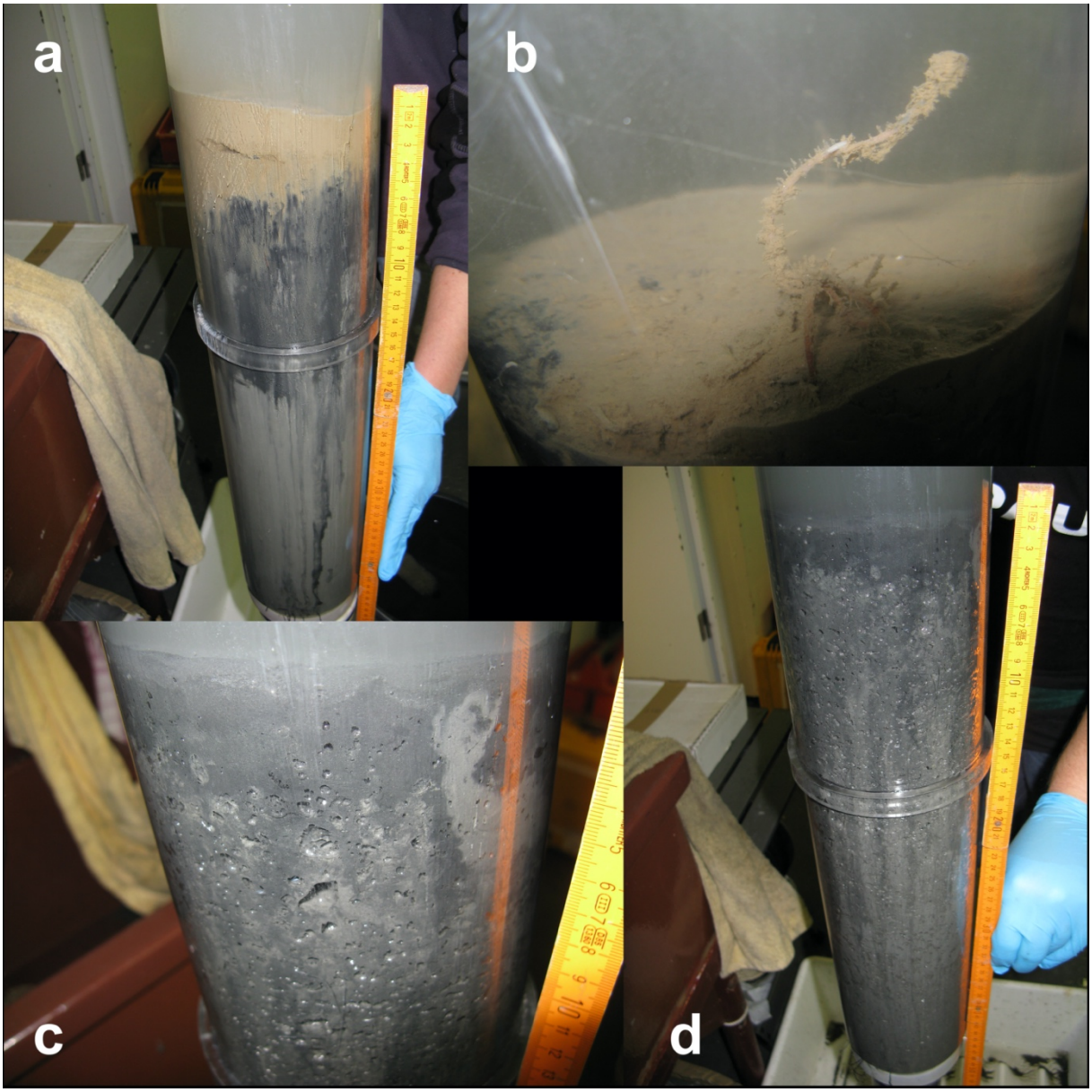

Figure S1. Selected sediment cores from MUC 10 (*Siboglinidae* field, a and b) and MUC 12 (bacteria mat, c and d). Note that a *Siboglinidae* tube is shown in b and the degassing of methane is visible in c and d (foamy sediment consistency).

REFERENCES

1 Stocker, T. F., D. Qin, G.-K. Plattner, M. Tignor, S.K. Allen, J. Boschung, A. Nauels, Y. Xia, V. Bex and P.M. Midgley (eds.). IPCC, 2013: Climate Change 2013: The Physical Science Basis. Contribution of Working Group I to the Fifth Assessment Report of the Intergovernmental Panel on Climate Change *Cambridge University Press, Cambridge, United Kingdom and New York, NY, USA,*, 1535 (2013).

2 Maslin, M., Owen, M., Betts, R., Day, S., Dunkley Jones, T., Ridgwell, A. Gas hydrates: past and future geohazard? *Philos Trans A Math Phys Eng Sci* **368**, 2369-2393, doi:10.1098/rsta.2010.0065 (2010).

3 Ruppel, C. D. & Kessler, J. D. The interaction of climate change and methane hydrates. *Reviews of Geophysics* **55**, 126-168, doi:https://doi.org/10.1002/2016RG000534 (2017).

4 David Archer, B. B., Victor Brovkin. Ocean methane hydrates as a slow tipping point in the global carbon cycle. *Proceedings of the National Academy of Sciences* **106**, 20596-20601, doi:https://doi.org/10.1073/pnas.0800885105 (2009).

5 Biastoch, A., Treude, T., Rüpke, L. H., Riebesell, U., Roth, C., Burwicz, E. B., Park, W., Latif, M., Böning, C. W., Madec, G., Wallmann, K. Rising Arctic Ocean temperatures cause gas hydrate destabilization and ocean acidification. *Geophysical Research Letters* **38**, doi:https://doi.org/10.1029/2011GL047222 (2011).

6 Phrampus, B. J. & Hornbach, M. J. Recent changes to the Gulf Stream causing widespread gas hydrate destabilization. *Nature* **490**, 527-530, doi:10.1038/nature11528 (2012).

7 Wefer, G., Heinze, P. M. & Berger, W. H. Clues to ancient methane release. *Nature* **369**, 282-282, doi:10.1038/369282a0 (1994).

8 Dickens, G. R., O'Neil, J. R., Rea, D. K. & Owen, R. M. Dissociation of oceanic methane hydrate as a cause of the carbon isotope excursion at the end of the Paleocene. *Paleoceanography* **10**, 965-971, doi:https://doi.org/10.1029/95PA02087 (1995).

9 Jahren, A. H., Arens, N. C., Sarmiento, G., Guerrero, J. & Amundson, R. Terrestrial record of methane hydrate dissociation in the Early Cretaceous. *Geology* **29**, 159-162, doi:10.1130/0091-7613(2001)029<0159:Tromhd>2.0.Co;2 (2001).

10 Brand, U. *et al.* Methane Hydrate: Killer cause of Earth's greatest mass extinction. *Palaeoworld* **25**, 496-507, doi:https://doi.org/10.1016/j.palwor.2016.06.002 (2016).

11 Torres, M. E., Mix, A. C., Kinports, K., Haley, B., Klinkhammer, G. P., McManus, J., de Angelis, M. A. Is methane venting at the seafloor recorded by δ13C of benthic foraminifera shells? *Paleoceanography* **18**, doi:https://doi.org/10.1029/2002PA000824 (2003).

12 Sztybor, K. & Rasmussen, T. L. Diagenetic disturbances of marine sedimentary records from methane-influenced environments in the Fram Strait as indications of variation in seep intensity during the last 35 000 years. *Boreas* **46**, 212-228, doi:https://doi.org/10.1111/bor.12202 (2017).

13 Rathburn, A. E., Levin, L. A., Held, Z. & Lohmann, K. C. Benthic foraminifera associated with cold methane seeps on the northern California margin: Ecology and stable isotopic composition. *Marine Micropaleontology* **38**, 247-266, doi:https://doi.org/10.1016/S0377-8398(00)00005-0 (2000).

14 Bernhard, J. M., Martin, J. B. & Rathburn, A. E. Combined carbonate carbon isotopic and cellular ultrastructural studies of individual benthic foraminifera: 2. Toward an understanding of apparent disequilibrium in hydrocarbon seeps. *Paleoceanography* **25**, doi:https://doi.org/10.1029/2010PA001930 (2010).

15 Schneider, A., Crémière, A., Panieri, G., Lepland, A. & Knies, J. Diagenetic alteration of benthic foraminifera from a methane seep site on Vestnesa Ridge (NW Svalbard). *Deep Sea Research Part I: Oceanographic Research Papers* **123**, 22-34, doi:https://doi.org/10.1016/j.dsr.2017.03.001 (2017).

16 Heiko, S., Dirk, R., Raymond, W. L., Peter, L. & Erwin, S. Macrofaunal community structure and sulfide flux at gas hydrate deposits from the Cascadia convergent margin, NE Pacific. *Marine Ecology Progress Series* **231**, 121-138 (2002).

17 Van Dover, C. L., German, C. R., Speer, K. G., Parson, L. M. & Vrijenhoek, R. C. Evolution and Biogeography of Deep-Sea Vent and Seep Invertebrates. *Science* **295**, 1253-1257, doi:10.1126/science.1067361 (2002).

18 Mackensen, A., Wollenburg, J. & Licari, L. Low δ13C in tests of live epibenthic and endobenthic foraminifera at a site of active methane seepage. *Paleoceanography* **21**, doi:https://doi.org/10.1029/2005PA001196 (2006).

19 Hill, T. M., Kennett, J. P. & Spero, H. J. Foraminifera as indicators of methane-rich environments: A study of modern methane seeps in Santa Barbara Channel, California. *Marine Micropaleontology* **49**, 123-138, doi:https://doi.org/10.1016/S0377-8398(03)00032-X (2003).

20 Bünz, S., Polyanov, S., Vadakkepuliyambatta, S., Consolaro, C. & Mienert, J. Active gas venting through hydrate-bearing sediments on the Vestnesa Ridge, offshore W-Svalbard. *Marine Geology* **332-334**, 189-197, doi:https://doi.org/10.1016/j.margeo.2012.09.012 (2012).

21 Plaza-Faverola, A., Bünz, S., Johnson, J. E., Chand, S., Knies, J., Mienert, J., Franek, P. Role of tectonic stress in seepage evolution along the gas hydrate-charged Vestnesa Ridge, Fram Strait. *Geophysical Research Letters* **42**, 733-742, doi:https://doi.org/10.1002/2014GL062474 (2015).

22 Knies, J. *et al.* Modelling persistent methane seepage offshore western Svalbard since early Pleistocene. *Marine and Petroleum Geology* **91**, 800-811, doi:https://doi.org/10.1016/j.marpetgeo.2018.01.020 (2018).

23 Thomsen, E., Rasmussen, T.L., Sztybor, K., Hanken, N.M., Secher Tendal, O., Uchman, A. Cold-seep fossil macrofaunal assemblages from Vestnesa Ridge, eastern Fram Strait, during the past 45 000 years. *Polar Research* **38**, doi:10.33265/polar.v38.3310 (2019).

24 Åström, E. K. L., Carroll, M. L., Ambrose, W. G., Jr. & Carroll, J. Arctic cold seeps in marine methane hydrate environments: impacts on shelf macrobenthic community structure offshore Svalbard. *Marine Ecology Progress Series* **552**, 1-18 (2016).

25 Åström, E. K. L., Carroll, M. L., Ambrose Jr., W. G., Sen, A., Silyakova, A., Carroll, J. Methane cold seeps as biological oases in the high-Arctic deep sea. *Limnology and Oceanography* **63**, S209-S231, doi:https://doi.org/10.1002/lno.10732 (2018).

26 Himmler, T. *et al.* Stromatolites below the photic zone in the northern Arabian Sea formed by calcifying chemotrophic microbial mats. *Geology* **46**, 339-342, doi:10.1130/g39890.1 (2018).

27 Jakobsson M, M. L., Bringensparr C, et al. . The International Bathymetric Chart of the Arctic Ocean Version 4.0. . *Scientific Data* **7(1):176**, doi:10.1038/s41597-020-0520-9. (2020).
28 McCorkle, D. C., Keigwin, L. D., Corliss, B. H. & Emerson, S. R. The influence of microhabitats on the carbon isotopic composition of deep-sea benthic foraminifera. *Paleoceanography* **5**, 161-185, doi:https://doi.org/10.1029/PA005i002p00161 (1990).
29 Torres, M. E. *et al.* Fluid and chemical fluxes in and out of sediments hosting methane hydrate deposits on Hydrate Ridge, OR, I: Hydrological provinces. *Earth and Planetary Science Letters* **201**, 525-540, doi:https://doi.org/10.1016/S0012-821X(02)00733-1 (2002).
30 Tina, T., Antje, B., Katrin, K., Klaus, W. & Bo Barker, J. Â. r. Anaerobic oxidation of methane above gas hydrates at Hydrate Ridge, NE Pacific Ocean. *Marine Ecology Progress Series* **264**, 1-14 (2003).
31 Niemann, H. *et al.* Novel microbial communities of the Haakon Mosby mud volcano and their role as a methane sink. *Nature* **443**, 854-858, doi:10.1038/nature05227 (2006).
32 Krause, S., Aloisi, G., Engel, A., Liebetrau, V. & Treude, T. Enhanced Calcite Dissolution in the Presence of the Aerobic Methanotroph Methylosinus trichosporium. *Geomicrobiology Journal* **31**, 325-337, doi:10.1080/01490451.2013.834007 (2014).
33 Toyofuku, T. *et al.* Proton pumping accompanies calcification in foraminifera. *Nature Communications* **8**, 14145, doi:10.1038/ncomms14145 (2017).
34 Bentov, S., Brownlee, C. & Erez, J. The role of seawater endocytosis in the biomineralization process in calcareous foraminifera. *Proceedings of the National Academy of Sciences* **106**, 21500-21504, doi:10.1073/pnas.0906636106 (2009).
35 Wollenburg, J. E., Kuhnt, W. & Mackensen, A. Changes in Arctic Ocean paleoproductivity and hydrography during the last 145 kyr: The benthic foraminiferal record. *Paleoceanography* **16**, 65-77, doi:https://doi.org/10.1029/1999PA000454 (2001).
36 Melaniuk, K. Effectiveness of Fluorescent Viability Assays in Studies of Arctic Cold Seep Foraminifera. *Frontiers in Marine Science* **8**, doi:10.3389/fmars.2021.587748 (2021).
37 Yao, H. *et al.* Fracture-controlled fluid transport supports microbial methane-oxidizing communities at Vestnesa Ridge. *Biogeosciences* **16**, 2221-2232, doi:10.5194/bg-16-2221-2019 (2019).
38 Grossman, E. L. Carbon isotopic fractionation in live benthic foraminifera—comparison with inorganic precipitate studies. *Geochimica et Cosmochimica Acta* **48**, 1505-1512, doi:https://doi.org/10.1016/0016-7037(84)90406-X (1984).
39 McCorkle, D. C., Emerson, S. R. & Quay, P. D. Stable carbon isotopes in marine porewaters. *Earth and Planetary Science Letters* **74**, 13-26, doi:https://doi.org/10.1016/0012-821X(85)90162-1 (1985).
40 Christofer Fontanier, A. M., Frasns J. Jorissen, Pierre Anschutz, Laetitia Licari, Clémentine. Griveaud. Stable oxygen and carbon isotopes of live benthic foraminifera from the Bay of Biscay: Microhabitat impact and seasonal variability. *Marine Micropaleontology* **58**, 159-183, doi:https://doi.org/10.1016/j.marmicro.2005.09.004 (2006).

41 Lutze, G. F. & Thiel, H. Epibenthic foraminifera from elevated microhabitats; Cibicidoides wuellerstorfi and Planulina ariminensis. *Journal of Foraminiferal Research* **19**, 153-158, doi:10.2113/gsjfr.19.2.153 (1989).
42 Wollenburg, J. E. & Mackensen, A. The ecology and distribution of benthic foraminifera at the Håkon Mosby mud volcano (SW Barents Sea slope). *Deep Sea Research Part I: Oceanographic Research Papers* **56**, 1336-1370, doi:https://doi.org/10.1016/j.dsr.2009.02.004 (2009).
43 Sen Gupta, B. K., Smith, L. E. & Lobegeier, M. K. Attachment of Foraminifera to vestimentiferan tubeworms at cold seeps: Refuge from seafloor hypoxia and sulfide toxicity. *Marine Micropaleontology* **62**, 1-6, doi:https://doi.org/10.1016/j.marmicro.2006.06.007 (2007).
44 Wollenburg, J. E., Raitzsch, M. & Tiedemann, R. Novel high-pressure culture experiments on deep-sea benthic foraminifera — Evidence for methane seepage-related δ13C of Cibicides wuellerstorfi. *Marine Micropaleontology* **117**, 47-64, doi:https://doi.org/10.1016/j.marmicro.2015.04.003 (2015).
45 Herguera, J. C., Paull, C. K., Perez, E., Ussler III, W. & Peltzer, E. Limits to the sensitivity of living benthic foraminifera to pore water carbon isotope anomalies in methane vent environments. *Paleoceanography* **29**, 273-289, doi:https://doi.org/10.1002/2013PA002457 (2014).
46 Moodley, L., Schaub, B. E. M., Zwaan, G. J. v. d. & Herman, P. M. J. Tolerance of benthic foraminifera (Protista: Sarcodina) to hydrogen sulphide. *Marine Ecology Progress Series* **169**, 77-86 (1998).
47 Werner, K., Müller, J., Husum, K., Spielhagen, R.F., Kandiano, E. S., Polyak, L. Holocene sea subsurface and surface water masses in the Fram Strait – Comparisons of temperature and sea-ice reconstructions. *Quaternary Science Reviews* **147**, 194-209, doi:https://doi.org/10.1016/j.quascirev.2015.09.007 (2016).
48 Ravelo, A. C. & Hillaire-Marcel, C. in *Developments in Marine Geology* Vol. 1 (eds Claude Hillaire–Marcel & Anne De Vernal) 735-764 (Elsevier, 2007).
49 Feng, D., Chen, D., Peckmann, J. & Bohrmann, G. Authigenic carbonates from methane seeps of the northern Congo fan: Microbial formation mechanism. *Marine and Petroleum Geology* **27**, 748-756, doi:https://doi.org/10.1016/j.marpetgeo.2009.08.006 (2010).
50 Haas, A., Peckmann, J., Elvert, M., Sahling, H. & Bohrmann, G. Patterns of carbonate authigenesis at the Kouilou pockmarks on the Congo deep-sea fan. *Marine Geology* **268**, 129-136, doi:https://doi.org/10.1016/j.margeo.2009.10.027 (2010).
51 Schönfeld, J., Alve, E., Geslin, E., Jorissen, F., Korsun, S., Spezzaferri, S. The FOBIMO (FOraminiferal BIo-MOnitoring) initiative—Towards a standardised protocol for soft-bottom benthic foraminiferal monitoring studies. *Marine Micropaleontology* **94-95**, 1-13, doi:https://doi.org/10.1016/j.marmicro.2012.06.001 (2012).
52 CLINE, J. D. SPECTROPHOTOMETRIC DETERMINATION OF HYDROGEN SULFIDE IN NATURAL WATERS1. *Limnology and Oceanography* **14**, 454-458, doi:https://doi.org/10.4319/lo.1969.14.3.0454 (1969).
53 Sommer, S. *et al.* Seabed methane emissions and the habitat of frenulate tubeworms on the Captain Arutyunov mud volcano (Gulf of Cadiz). *Marine Ecology Progress Series* **382**, 69-86 (2009).
54 Jørgensen, B. A comparison of methods for the quantification of bacterial sulfate reduction in coastal marine sediments. (1978).

55 Treude, T. *et al.* Biogeochemical Consequences of Nonvertical Methane Transport in Sediment Offshore Northwestern Svalbard. *Journal of Geophysical Research: Biogeosciences* **125**, e2019JG005371, doi:https://doi.org/10.1029/2019JG005371 (2020).

56 Kallmeyer, J., Ferdelman, T. G., Weber, A., Fossing, H. & Jørgensen, B. B. A cold chromium distillation procedure for radiolabeled sulfide applied to sulfate reduction measurements. *Limnology and Oceanography: Methods* **2**, 171-180, doi:https://doi.org/10.4319/lom.2004.2.171 (2004).

57 Duplessy, J.-C. *et al.* 13C Record of benthic foraminifera in the last interglacial ocean: Implications for the carbon cycle and the global deep water circulation. *Quaternary Research* **21**, 225-243, doi:https://doi.org/10.1016/0033-5894(84)90099-1 (1984).

58 Shackleton, N. J. Attainment of isotopic equilibrium between ocean water and the benthonic foraminifera genus Unigerina : isotopic changes in the ocean during the last glacial. *Centre Natl. Rech. Sci. Coll. Inter.* **219**, 203-209 (1974).

59 Bernhard, J. M., Ostermann, D. R., Williams, D. S. & Blanks, J. K. Comparison of two methods to identify live benthic foraminifera: A test between Rose Bengal and CellTracker Green with implications for stable isotope paleoreconstructions. *Paleoceanography* **21**, doi:https://doi.org/10.1029/2006PA001290 (2006).

Manuscript 4

Response of benthic foraminifera to ecological succession of cold seeps from Vestnesa Ridge, Svalbard: implications for interpretations of paleo-seepage environments.

Response of benthic foraminifera to ecological succession of cold seeps from Vestnesa Ridge, Svalbard: implications for interpretations of paleo-seepage environments.

Melaniuk, K., Sztybor, K., Treude, T., Sommer, S., Zajączkowski, M., Rasmussen, T.L.

Key words: Arctic, gas hydrate, methane, benthic ecology, Protista

Abstract

This paper presents the result of a study on the response of living benthic foraminifera to progressing ecological successions of environments in a cold-seep ecosystem. Sediment samples were collected from two pockmarks on Vestnesa Ridge (79°N, Fram Strait) at c. 1200 m water depth. The downcore distribution of metabolically active (CellTracker™ Green labelled) and live (Rose Bengal-stained) foraminifera were analyzed in the upper 5 cm of sediment in relation to pore water biogeochemical data together with the distribution of bacterial mats and *Siboglinidae* tubeworms. At methane cold seeps, the process of ecological succession is strongly connected to the duration of seepage and the intensity of methane-related biological processes. e.g., aerobic and anaerobic oxidation of methane. The results show that the distribution pattern of benthic foraminifera changes according to the progressing ecological succession of the seep environments. The benthic foraminifera seem to thrive in sediments with a moderate activity of seepage i.e., initial seepage or when seepage decreases at a late stage. The species composition is similar to the control sites (outside pockmarks), the main species being *Melonis barleeanus* and *Cassidulina neoteretis*. In sediments with high seepage activity the hostile environmental conditions due to the presence of toxic sulfide, caused a reduction in the foraminiferal population, and as a result, the samples were almost barren of foraminifera. Additionally, in environments of moderate methane seepage the presence of chemosynthetic *Siboglinidae* tube worms potentially support communities of the epibenthic species *Cibicidoides wuellerstorfi*. Nevertheless, none of the faunal characteristics seems to be suited as an exclusive indicator of methane release or stages of its environmental development in palaeoceanographic interpretations.

1. Introduction

Benthic foraminifera are a unicellular organism, commonly occurring in a variety of marine environments. Information about the distribution and abundance of foraminiferal species carry a valuable record of past oceanic conditions, thus they are commonly used as tools in paleoclimatic and –oceanographic reconstructions (Murray 2006, Gooday and Jorissen, 2012). In recent years, cold seep benthic foraminifera have gained increased attention due to their potential to record changes in past degree of methane seepage (Torres, 2003; Millo et al. 2005; Bernhard et al. 2010; Martin et al. 2010; Schneider et al. 2017; Consolaro et al. 2015). There is existing evidence showing a link between the release of methane from geological reservoirs and climate change, e.g., during the Quaternary and the Paleocene periods (Wefer et al. 1994; Dickens et al. 1997; Smith et al. 2001). Among others places a large amount of natural gas is stored in Arctic marine sediments in the form of gas hydrate (i.e., ice-like structure). It is speculated that ongoing climate change can trigger destabilization of gas hydrate reservoirs and cause release of methane into the water column and eventually to atmosphere (IPCC, 2007; Ruppel and Kessler 2017). Therefore, it is crucial to understand the fate of methane in marine sediments to understand the potential impact of methane release on future climate and Arctic ecosystems.

Methane seepage from subseafloor reservoirs is manifested by the presence of cold seep ecosystems, i.e., methane-dependent, chemosynthetic ecosystems at the seabed. Although knowledge of the ecology and distribution patterns of cold-seep-associated benthic foraminiferal species remains one key to improve the interpretation of past records, the ecology and distribution patterns of living foraminiferal species in relation to different types of seep environments are still poorly studied. It is commonly accepted that the distribution of benthic foraminifera is mainly determined by environmental factors, such as oxygen, food availability, and pCO_2 (Jorissen et al. 1995; Corliss et al. 1986; Thomas et al. 1995; Rasmussen and Thomsen, 2017). Due to the ephemeral nature of cold seeps, the above-mentioned environmental factors change over time, and so does the microhabitat in which the foraminifera live. Natural processes of changes in the faunal structure of an ecological community over time is called ecological successions and can result from the combined effects of environmental factors and biological interactions, including among others commensalism and competition (Dayton and Hessler, 1972; Tanner et al. 1994; Chapman and Underwood,

1994) . At cold seeps, ecological succession is strongly connected to seepage of hydrocarbon fluids and methane-related biological processes such as aerobic and anaerobic oxidation of methane (MOx and AOM, respectively), which shape the biochemistry of the sediment. Seep community succession as modeled by (Bergquist et al. 2003) suggests a general succession pattern from bacterial mats in the initial stage 1 of seepage to authigenic rock formation to decreasing sulfide concentration and increasing tubeworms aggregations in stage 3. As seepage declines, cold-water corals can settle on authigenic carbonate rocks and eventually form large, long-lasting coral reefs that support a diverse coral-associated fauna in a stage 4 succession (Bergquist et al. 2003).

At the initial stage 1 of the ecological succession methane oxidizing bacteria may serve as a food source and stimulate growth of a foraminiferal community at rates far exceeding those of other deep-sea communities; however, prolonged aerobic methane oxidation causes increase in the partial pressure of carbon dioxide (pCO_2), and decrease in the concentration of oxygen, which eventually leads to anoxic conditions and release of toxic sulfides (H_2S). These conditions are lethal to many marine organisms including most benthic foraminiferal species (Herguera et al. 2014; Somero et al. 1989).

In this paper, we present the results of a study of the distribution patterns of metabolically active (CellTracker™ Green labelled) and living (Rose Bengal-stained) benthic foraminifera in the upper 5 cm of surface sediment from a cold seep ecosystem at Vestnesa Ridge together with the downcore distribution of pore water biogeochemical data. We show that the different types of seep environments present three stages of the seep environmental ecological succession: stages 1, 2, and 3. We observed that benthic foraminifera thrive in sediments with moderate activity of seepage i.e., initial seepage of an early stage or when seepage decreases at a late stage. In sediments with high seepage activity the toxic environmental conditions due to the presence of sulfide, caused a reduction in the foraminiferal population.

2. Materials and methods

2.1. Study area

Vestnesa Ridge is a deep-sea ridge (>1000 m), located in the Fram Strait, west of Svalbard in the Arctic Ocean (79°N, 5-7°E; Fig. 1). Vestnesa developed under the effect of

contour currents (Eiken and Hinz, 1993; Hustoft et al. 2009) and it is estimated that periodic gas seepage has occurred since 2.7 Ma from the start of the Quaternary coinciding with glacial intensification at the western Svalbard margin (Plaza-Faverola et al. 2015). On the crest of Vestnesa Ridge a series of pockmarks occur (i.e., shallow seabed depressions where methane-rich fluids seep from the seabed), among which the two most active are informally referred to as 'Lomvi' and 'Lunde' (Bünz et al. 2012; Plaza-Faverola et al. 2015). In these pockmarks, TowCam video observations have revealed the presence of cold-seep related structures such as bacterial mats, megafaunas and methane-derived authigenic carbonate outcrops (Åström et al., 2016, 2018; Sztybor and Rasmussen, 2017; Dessandier et al. 2019; Melaniuk, 2021).

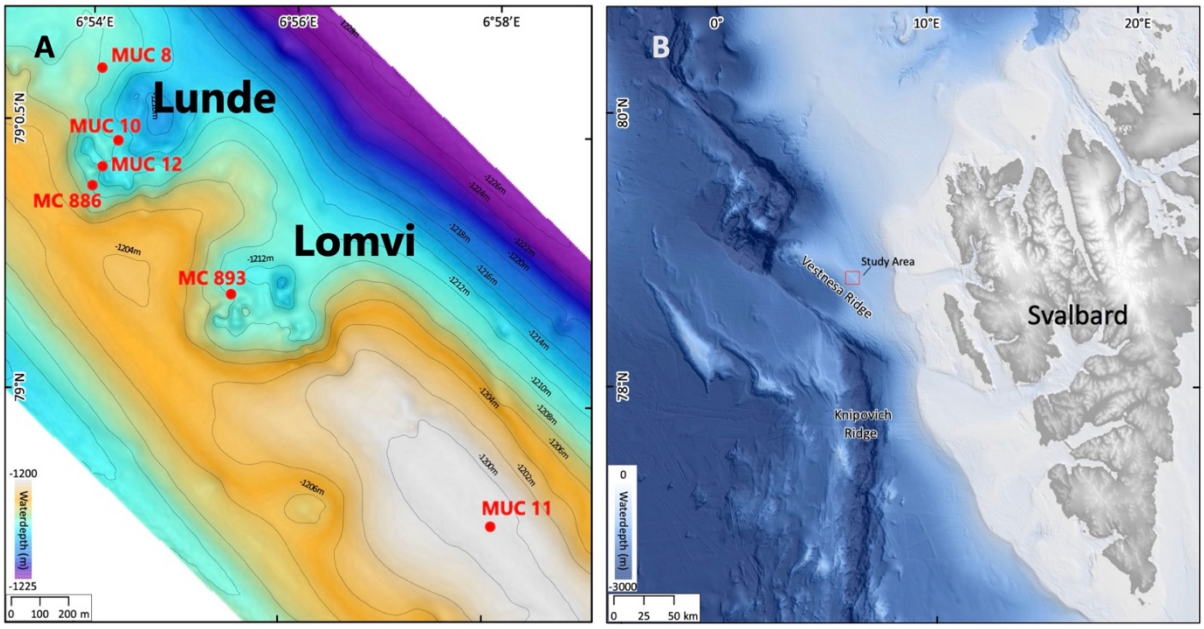

Figure 1.(A) Detail of Vestnesa Ridge (modified from Bünz et al. 2012). Red dots indicate multicorer locations. (B) Svalbard margin in the Eastern Fram Strait (bathymetry from (Jakobsson et al. 2020).

2.2. Sediment sampling

Sediment samples for this study were collected during the CAGE 15-2 cruise in May 2015 with RV *Helmer Hanssen* (Melaniuk, 2021) and during the POS419 expedition of RV *Poseidon* in August 2011 (Fig. 1; Table 1) from the 'Lomvi' and 'Lunde' pockmarks at Vestnesa Ridge. The samplings on both cruises were done using a TV-guided multicorer to visually localize active methane seep sites within the pockmarks to select sampling spots.

After recovery of the multicorer, selected cores were processed on board. Cores designated for benthic foraminiferal analyses were sampled in 1-cm thick slices, down to 3 cm

depth (CAGE 15-2) and down to 5 cm depth (POS419). Each 1-cm thick slice of sediment from CAGE15-2 was equally divided and subjected to two different staining methods; fluoresce probe Cell Tracker™ Green and Rose Bengal. (Melaniuk, 2021). The sediment from POS419 was transferred into plastic containers and stained with Rose Bengal-ethanol solution following the FOBIMO protocol (2 g\l). Rose Bengal was deliberately used in this study to make our results comparable with other studies. Samples were kept onboard in a dark, cool room at 4 °C until further processing (see for details Melaniuk, 2021, Melaniuk et al. submitted).

Three cores collected from each station of the POS419 cruise were designated for the analyses of 1) sediment pore water chemistry, 2) sediment methane concentration, 3) rates of microbial methane oxidation and sulfate reduction. All sediment sampling procedures were conducted at +4 °C inside a cooled laboratory (see for details Melaniuk et al. submitted).

Table 1. Sampling locations, coordinates, water depth, date of sampling, environmental characteristics and analyses performed at sampling sites. * = data from Melaniuk, 2021.

MUC ID	Location	Coordinates	Depth (m)	Data	Environment	Analyses
MUC 10	'Lunde' pockmark	79.46N 06.27E	1241	25.08.2011	*Siboglinidae* field	Foraminiferal faunas sulfide, SO_4^{2-}, total alkalinity, methane, AOM, sulfate reduction
MUC 8	'Lunde' pockmark	79. 60N 06.09E	1204	25.08.2011	*Siboglinidae* field	Foraminiferal faunas sulfide, SO_4^{2-}, total alkalinity, methane, AOM, sulfate reduction
MUC 12	'Lunde' pockmark	79.41N 06.13E	1235	29.08.2011	Bacterial mats	Foraminiferal faunas sulfide, SO_4^{2-}, total alkalinity, methane, AOM, sulfate reduction
MUC 11	Control site	78.77N 06.06E	1191	28.08. 2011	Non-seep	Foraminiferal faunas
MC 893*	'Lomvi' pockmark	79.18N, 00.44E	1200	20.05.2015	Bacterial mats	Foraminiferal faunas
MC 886*	'Lunde' pockmark	79.38N, 00.04E	1200	20.05.2015	Bacterial mats/ *Siboglinidae*	Foraminiferal faunas

2.3. Foraminiferal analyses

Sediment samples from MUC 10, 11, and 12 were washed through a 100-µm sieve. The >100-µm residue was kept wet and further examined under reflected-light microscopy. Rose Bengal-stained foraminifera representing both live + recently dead individuals, but still containing cytoplasm were wet picked, counted and identified. Individuals that stained dark magenta and were fully filled with cytoplasm were considered 'living' foraminifera (i.e., live + recently dead individuals). Empty, unstained tests were omitted and not counted in this study. Number of living (Rose Bengal stained) foraminifera were compared using Student's *t*-test ($\alpha = 0.05$). The Shannon index S(H) of diversity, Evenness index, and a Chao1 index (Table 1S) were calculated for each sample.

Cell Tracker™ Green labelled and Rose Bengal -stained sediment samples from MC 893 and MC 886 were washed through a 63-µm sieve**.** Cell Tracker™ Green labelled samples were examined using an epifluorescence-equipped stereomicroscope (Leica MZ FLIII; 485 nm excitation; 520 nm emission). All individuals that fluoresced brightly in at least half of their chambers were considered as a metabolically active foraminifer. Rose Bengal-stained samples were examined under reflected-light microscopy (see details in Melaniuk, 2021).

2.4. Porewater analyses

Porewater was extracted at +4 °C using a low-pressure squeezer (argon at 1–5 bar) onboard the vessel and right after sampling. While squeezing, porewater was filtered through 0.2 µm cellulose acetate nuclepore filters and collected in argon-flushed recipient vessels. The collected porewater samples were analyzed onboard for their content of dissolved total sulfides (in the following referred to as "sulfide") (Cline, 1969). 50 µl of zinc acetate solution was added to a 1-ml sample of pore water. Subsequently, 10 µl of N,N-dimethyl-1,4-phenylenediamine-dihydrochloride color reagent solution and 10 µl of the FeCl3 catalyst were added and mixed. After 1 hour of reaction time, the absorbance was measured at 670 nm. Total alkalinity (TA) was determined by direct titration of 1 mL pore water with 0.02 M HCl using a mixture of methyl red and methylene blue as an indicator. Bubbling the titration vessel with argon gas was performed to strip CO_2 and hydrogen sulfide. The analyses were calibrated using the IAPSO seawater standard, with a precision and detection limit of 0.05 mmol L^{-1}. Porewater samples for sulfate (SO_4^{2-}) analyses were stored in 2-ml glass vials at +4 °C and analyzed onshore. Sulfate was determined by ion chromatography (Metrohm, IC Compact

761). Analytical precision based on repeated analysis of IAPSO standards (dilution series) was <1%.

2.5. Methane measurements

Methane concentrations in sediment cores were determined in 1 cm intervals down to a depth of 6 cm followed by 2 cm intervals down to 12 cm, 3 cm intervals down to 18 cm and 5 cm intervals deeper than 18 cm (Sommer et al. 2009). From each level, a 2 mL sub-sample was transferred into a septum-stoppered glass vial (21.8 ml) containing 6 ml of saturated solution of NaCl and 1.5 g of NaCl in excess. The volume of headspace was 13.76 ml. Within 24 h, the methane concentration in the headspace was determined using a Shimadzu GC 14A gas chromatograph fitted with a flame ionization detector and a 4 m × 1⁄8-inch Poraplot Q (mesh 50/80) packed column. Prior to the measurements the samples were equilibrated for 2 h on a shaking table. The precision to reproduce a methane standard of 9.98 ppm was 2%.

2.6. Microbial methane oxidation rates

On board, radioactive methane ($^{14}CH_4$ dissolved in water, injection volume 15 µl, activity ~5 kBq, specific activity 2.28 GBq $mmol^{-1}$) was injected into three replicate mini cores at 1-cm intervals according to the whole-core injection method (Jørgensen, 1978). The mini cores were incubated at in-situ temperature for ~24 h in the dark. To stop bacterial activity, the sediment cores were sectioned into 1-cm intervals and transferred into 50-ml crimp glass vials filled with 25 ml of sodium hydroxide (2.5% w/w). After crimp-sealing, glass vials were shaken thoroughly to equilibrate the pore-water methane between the aqueous and gaseous phase. Control samples were first terminated before addition of tracer. In the home laboratory, methane oxidation rates and methane concentrations in the sample vials were determined according to (Treude et al. 2020).

2.7. Microbial sulfate reduction rates

Sampling, injection, and incubation procedures were the same as for the methane oxidation samples. The injected radiotracer here was carrier-free $^{35}SO_4^{2-}$ (dissolved in water, injection volume 6 µl, activity 200 kBq, specific activity 37 TBq $mmol^{-1}$). To stop bacterial activity after incubation, sediment cores were sectioned into 1-cm intervals and transferred into 50 ml plastic centrifuge vials filled with 20 ml zinc acetate (20% w/w) and frozen. Control

sediment was first terminated before addition of tracer. In the home laboratory, sulfate reduction rates were determined according to the cold-chromium distillation method (Kallmeyer et al. 2004).

3. Results

3.1. Habitat characteristics

Sediments of the *Siboglinidae* field from MUC 8 showed only modest signs of methane seepage activity. Total alkalinity increased only slightly, but steadily from seawater concentration (2.3 mM) to 3.9 mM at depth (Fig. 4M). Similarly, sulfate showed only a small but steady decline from seawater concentration (28.8 mM) to 27.5 mM at depth (Fig. 4J). The methane concentration profile showed two different slopes: a modest increase in concentration from the surface reaching 15 µM at 16.5 cm, and a steeper increase below 16.5 cm reaching 88 µM at depth (Fig. 4J). The change in slope could possibly marks the lower end of sediment irrigation by *Siboglinidae* tubes. Sulfide was generally low (<10 µM) with sporadic peaks at the surface, at 9 cm, and at 16.5 cm (Fig. 4J). No AOM data are available for MUC 8 and only one sulfate reduction replicate was obtained (Fig. 4G). Sulfate reduction was low (< 2 nmol cm^{-3} d^{-3}) throughout the core with no activity at the sediment-water interface and a distinct peak (max 1.6 nmol cm^{-3} d^{-3}) at 6.5 cm and a second, smaller peak (0.56 nmol cm^{-3} d^{-3}) at 14.5 cm. The fact that methane concentration steeply increased below 16.5 cm suggests that the second peak in sulfate reduction was related to methane-dependent AOM, while the shallower peak might be correlated to organoclastic sulfate reduction.

Biogeochemical data of MUC 10 and 12 were previously described in Melaniuk et al. (submitted)**.** Sediments of the *Siboglinidae* field from MUC 10 showed also strong indications for bio-irrigation by the tubeworms (Fig. 4B). Sulfate (~28 mmol L^{-1}), total alkalinity (~3 mmol L^{-1}), sulfide (<0.2 mmol L^{-1}, except 3 mmol L^{-1} at 3–4 cm), and methane concentrations (<0.1 mmol L^{-1}) remained relatively unchanged in the topmost 4–6 cm with a bright brown coloring (Fig. 4B) indicative of presence of oxidized sediment. Below 4–6 cm, sulfate decreased while total alkalinity, sulfide, and methane increased (Fig. 4K, N). Sulfate declined to a minimum of 16.8 mmol L^{-1} at the bottom of the core, while total alkalinity and methane increased to 18.5 and 1.1 mmol L^{-1}, respectively. Sulfide peaked with 7 mmol L^{-1} at 9 cm and then declined with depth to reach 1.5 mmol L^{-1} at the bottom of the core. Sediment color changed to black and deeper in the core to grey typical of reducing conditions (Fig. 4B). In all three replicates, the

majority of methane oxidation occurred in the top 4 cm of the sediment with high rates in the top (0–1 cm) sediment layer (Fig. 4E). Since this activity did not match with sulfate reduction (Fig. 4H), it was interpreted as coupled to MOx (Melaniuk et al. submitted). Methane oxidation reached a minimum (~0.4 nmol cm^{-3} d^{-3}) at 5–6 cm, below which rates increased again (see insert in Fig. 4E) to a maximum of 4.8 nmol cm^{-3} d^{-1} at 7–8 cm (Fig. 4E). This double peaking indicated a change from an aerobic to an anaerobic methane oxidation pathway likely coupled to sulfate reduction below the bio-irrigation activity of the tubeworms (Melaniuk et al. submitted). Methane oxidation declined below the second peak towards the bottom of the core. Sulfate reduction was low (<3 nmol cm^{-3} d^{-3}) in the top 0–1 cm, but steeply increased in all three replicates reaching values between 11 and 23 nmol cm^{-3} d^{-3} at 2–3 cm (Fig. 4E). Below 3 cm, sulfate reduction steadily declined reaching values ~1 nmol cm^{-3} d^{-3} at 10 cm, which remained consistently low down to the bottom of the core. The decoupling of methane oxidation and sulfate reduction in the surface sediment suggest that sulfate reduction was coupled to organic matter degradation in the top 6 cm, while part of it was likely also coupled to AOM below 6 cm.

Very steep geochemical gradients were found in the top 3–4 cm in the sediment covered by bacterial mats (MUC 12). Sulfate and sulfide concentration declined, respectively, while total alkalinity increased (Fig. 4O). Methane peaked with concentrations ~11 mmol L^{-1} at 2-4 and 28.5 cm and varied between 2 –5 mmol L^{-1} in other depths with no clear trend (Fig. 4L). Concentrations were most likely below in-situ levels and Melaniuk et al. (submitted) suggested that the true methane profile could have been blurred due to degassing after sample recovery. Degassing was clearly noticeable during core handling (Fig. 4C). Methane oxidation was low at the surface (<13 nmol cm^{-3} d^{-1}) and steeply increased in all three replicates to a maximum of up to 181 nmol cm^{-3} d^{-1} between 2–5 cm (Fig. 4F). Oxidation in all three replicates declined sharply below the maxima. Profiles of all three sulfate reduction samples showed a general alignment with methane oxidation (Fig. 4I), indicating a coupling to AOM (Melaniuk et al. submitted). The sulfate reduction was about two times higher than methane oxidation in the surface sediment (maximum 408 nmol cm^{-3} d^{-1}) and likely also coupled to other processes, probably organic matter degradation.

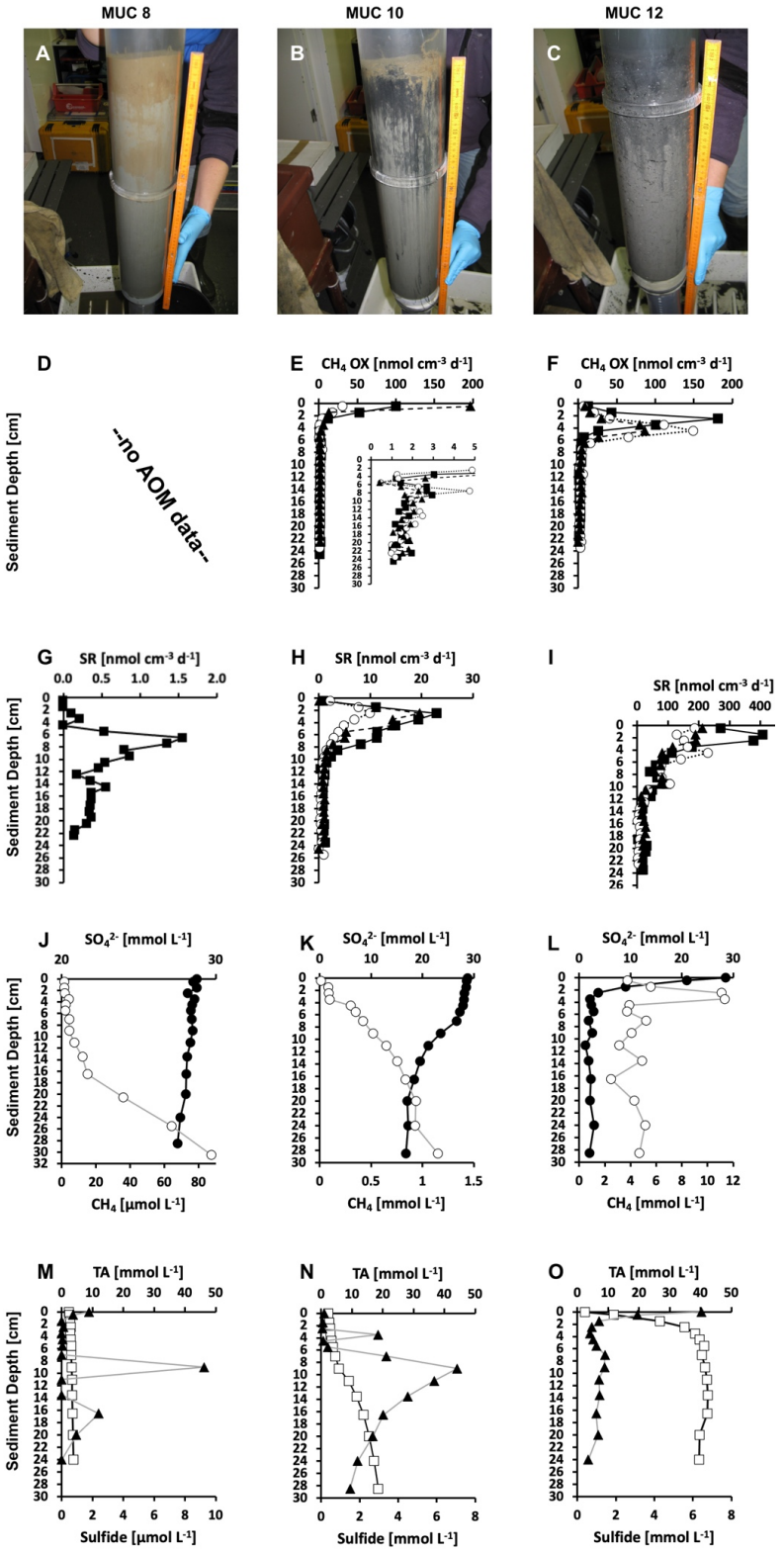

Figure 4. Selected sediment core photos and biogeochemical parameters of MUC 8 (*Siboglinidae* field, left panels, note the visible tubes at the surface), MUC 10 (*Siboglinidae* field, middle panels, note the visible tubes at the surface), and MUC 12 (bacterial mat, right panels, note the foamy sediment consistency caused by degassing). Note the different units for methane and sulfide in MUC 8.

3.2. Foraminiferal faunas from POS419

The results show a low number of living (Rose Bengal-stained) benthic foraminifera in the sediments from the bacterial mats, except for 10 specimens in the top 0–1 cm in MUC 12A and 4 specimens in MUC 12B (Table 1S). There was no significant difference in the total number of foraminifera (calcareous + agglutinated) (p=0.49; p<0.05) between the *Siboglinidae* field and the control site. There were further no significant differences in the number of calcareous foraminifera (p=0.40; p<0.05), and in the number of agglutinated foraminifera (p= 0.42, p<0.05) between the *Siboglinidae* field and the control site (Table 1S).

Rose Bengal-stained agglutinated foraminifera were most common in the upper sediment layer (0–1 cm), both in the *Siboglinidae* field and in the control site, and contributed to more than 50% of the total foraminiferal assemblage (Fig. 2). In deeper samples (below 3 cm) there was no Rose Bengal-stained agglutinated specimens in the core from the *Siboglinidae* field (Fig. 2).

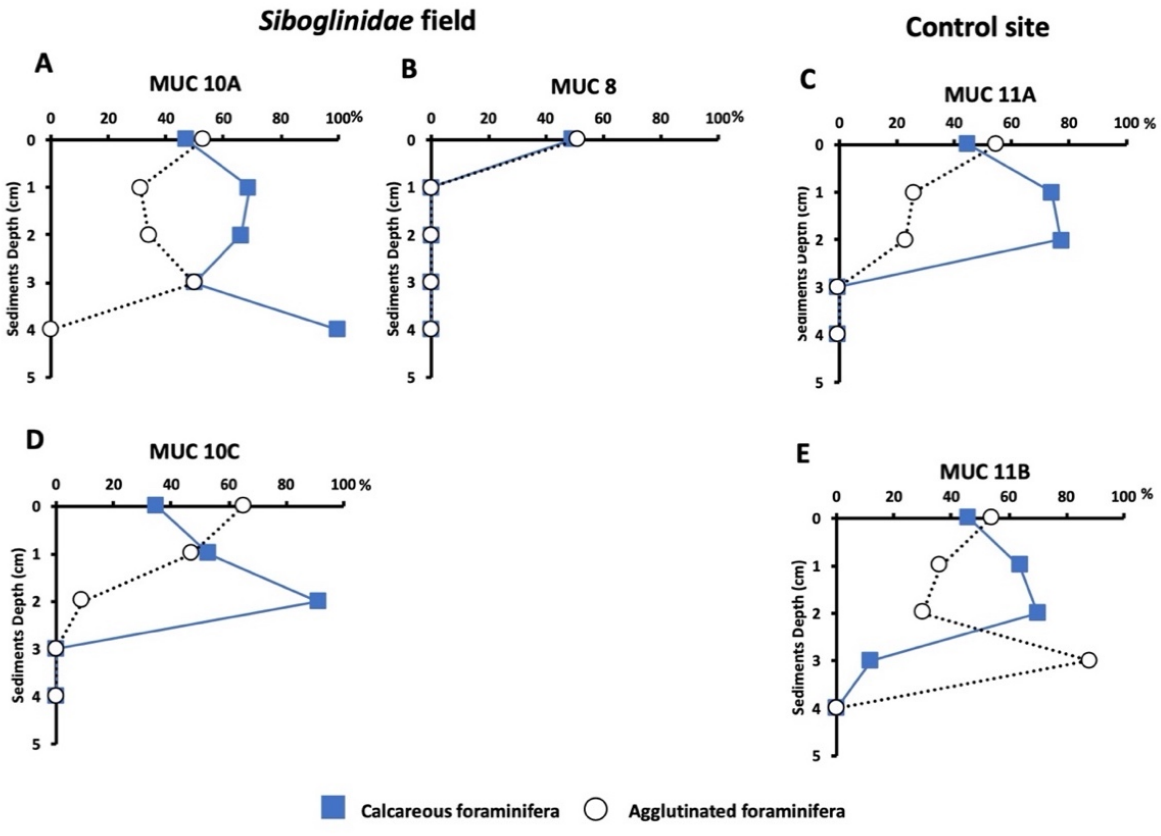

Figure 2. Percentage of Rose Bengal-stained benthic foraminifera. A, B, D: *Siboglinidae* field, C, E: Control site.

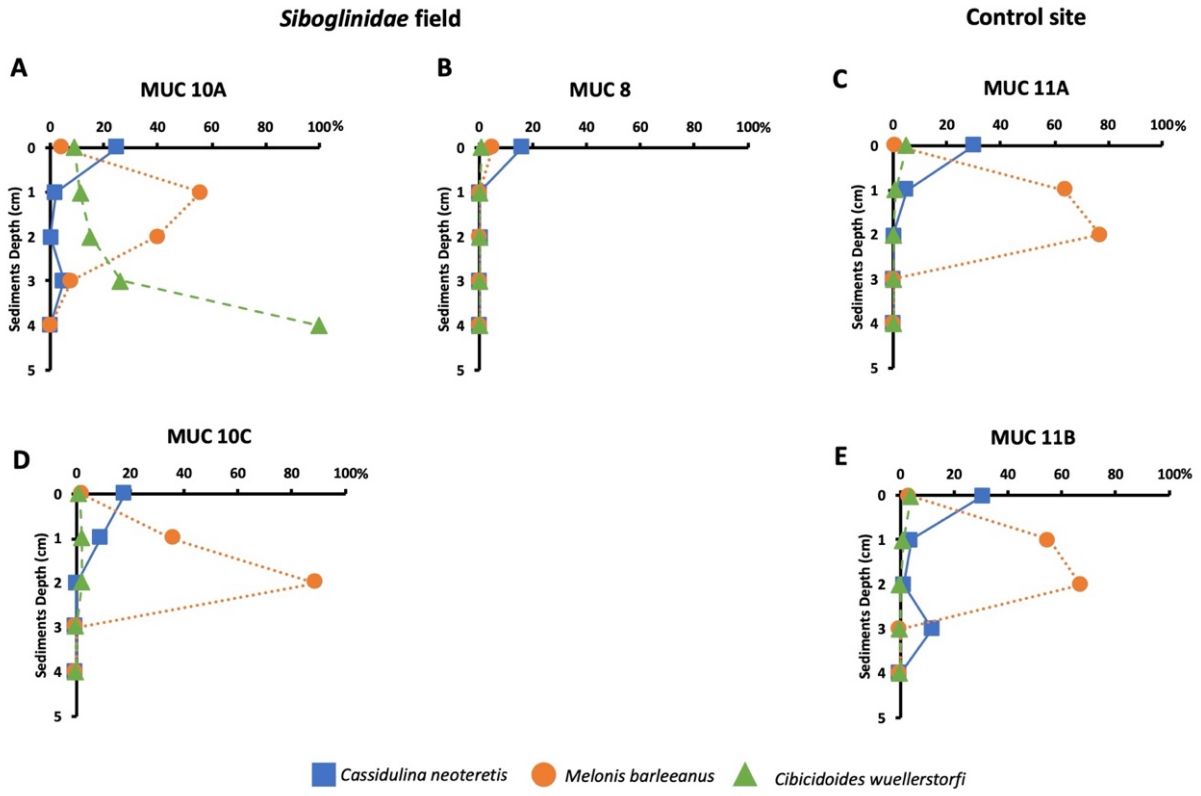

Figure 3. Percentage of most abundant calcareous species (*C. neoteretis*, *M. barleeanus*, and *C. wuellerstorfi*). A, B, D: *Siboglinidae* field, C, E: Control site.

In samples from the *Siboglinidae* field (MUC 10 and MUC 8) and the control site (MUC 11), the most common species was *Cassidulina neoteretis* (0–1 cm interval). The species constituted between 16 and 25% of the total number of foraminifera at the *Siboglinidae* field (Fig. 3). *Melonis barleeanus* was the most abundant species at the 1–2 cm interval and deeper intervals constituted up to 89% of the foraminifera (Fig. 3). Sediments from the *Siboglinidae* field were characterized by higher percentages of *Cibicidoides wuellerstorfi* compared to the control site (Fig. 3).

4. Discussion

4.1. Distribution patterns of living foraminiferal faunas

Samples collected at Vestnesa Ridge represent three potential stages of ecological succession of the seep environments according to the model suggested by Bergquist et al. (2003) (Fig. 5). The process depends on the intensity and duration of methane seepage and is manifested by changes in the distribution patterns of the benthic fauna. For example, appearance of sulfur-oxidizing bacteria (e.g., *Beggiatoa* sp.) characterizes the initial and second stage of succession, and symbiont-bearing animals (e.g., *Siboglinidae*) characterize the third stage, when seepage is slowing down and sulfide conditions are stable (Levin, 2005). We observed that the distribution patterns of the of benthic foraminifera are closely related to the properties of the different microhabitats and thus the species composition of the foraminiferal fauna changes according to the progressing ecological succession (Fig. 5.).

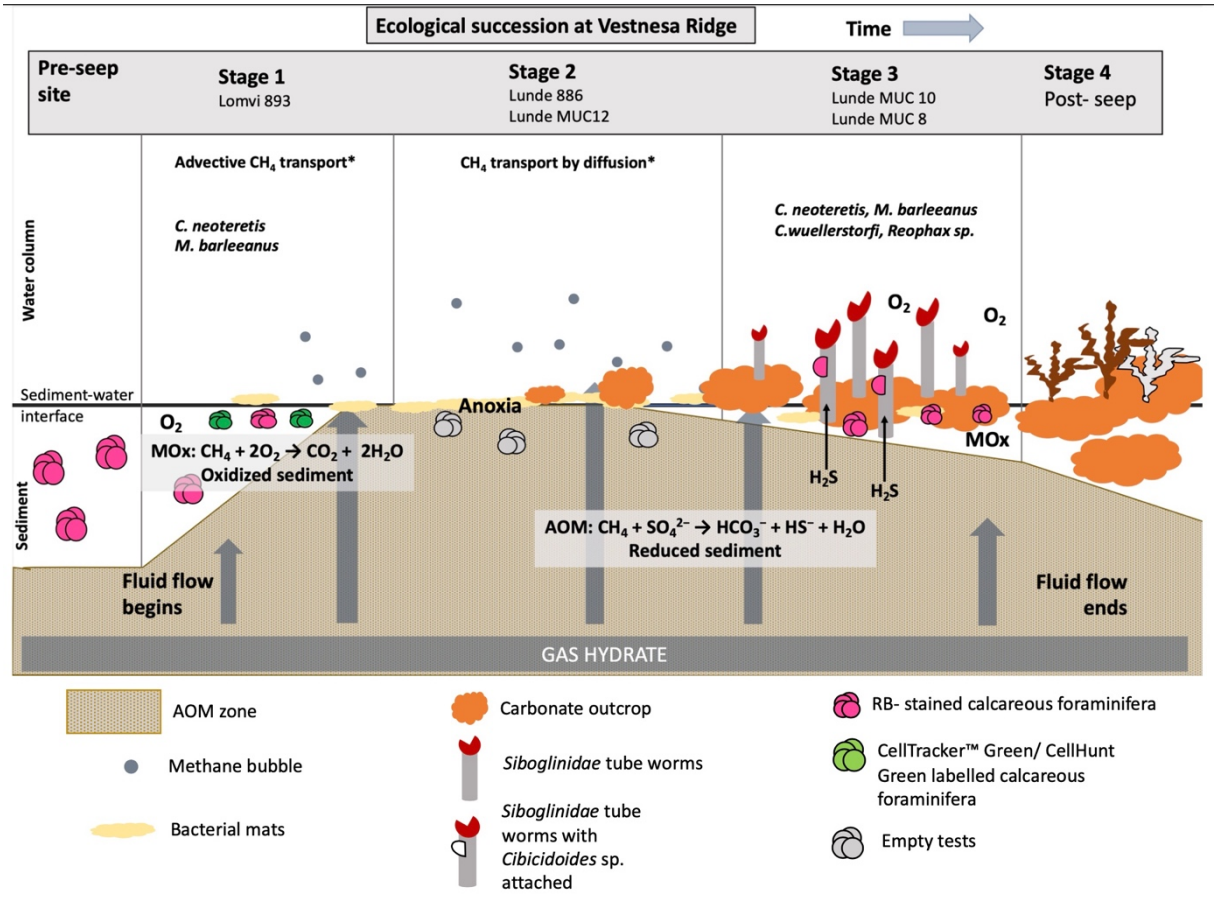

Figure 5. The proposed course of ecological succession at Vestnesa Ridge. *from (Yao et al. 2019). Stage 4 has not (yet) been observed at Vestnesa.

The sampling location of MC 893 represents the first i.e., the initial stage of ecological succession. The TowCam imaging survey during the sampling campaign of the CAGE 15-2 cruise showed that the sediment surface was covered by patchy distributed white and grey bacterial mats (*Beggiatoa* sp.) in areas where methane was leaking from the sediment (Yao et al. 2019; Dessandier et al. 2019; Melaniuk, 2021). The methanotrophic bacterial community at site MC 893 are not well developed yet, implying that the seepage by advective methane transport via mini-fractures at this location started relatively recently, most likely a year prior to the sampling (Yao et al. 2019). At the initial stage, metabolically active (CellTracker™ Green labelled) and Rose Bengal -stained foraminifera are still present and the density of the foraminiferal fauna is like the control site (Melaniuk, 2021). Similar to other foraminiferal faunas from cold-seeps, the fauna is dominated by species adapted to low oxygen and high organic content (Rathburn et al. 2000; Bernhard et al. 2001; Hill et al. 2003; Herguera et al. 2014; Etiope et al. 2014); here *M. barleeanus* and *C. neoteretis* (Fig. 3). These two species are common on the mid-slope in the Nordic Seas (Sejrup et al. 1989; Mackensen et al. 1985; Wollenburg and Mackensen, 1998), and are usually present within non-seep marine environments, and previously reported at both seep- and non-seep sites at Vestnesa Ridge (Sztybor and Rasmussen, 2017; Dessandier et al.2019; Melaniuk, 2021). *Melonis barleeanus* is an intermediate to deep infaunal species (i.e., species which live within the sediment) associated with high-nutrient conditions and resistant to environmental stress due to organic matter degradation (Wollenburg and Mackensen, 1998; Alve et al. 2016). Methanotrophic-like bacteria have previously been found in close proximity to the apertural region of living *M. barleeanus* suggesting that methane-related bacteria are a part of the diet of *M. barleeanus* (Bernhard and Panieri, 2018). *Cassidulina neoteretis* is a shallow infaunal species (i.e., species which lives within the sediment-water interface) , presently one of the most common species at Arctic cold seeps such as at Vestnesa Ridge (Dessandier et al. 2019; Melaniuk, 2021), Storfjordrenna pingo sites (Melaniuk, 2021), and Håkon Mosby Mud Volcano (Wollenburg and Mackensen, 2009).

Prolongated methane seepage causes oversaturation of methane in the sediment and lead to the development of a microbial AOM community. The ecological succession moves to stage 2, represented by MUC 12 and MC 886 in this study. The sediments become black to dark grey in color, release a strong smell of suphide, and are likely anoxic below the surface

(Fig. 4C). The sediment of MUC 12 was densely covered by sulfur bacteria mats and dominated by AOM and sulfate reduction developing high concentrations of H_2S just below the sediment surface (Figs. 4O; Melaniuk et al. submitted). The geochemistry of site MC 886 was described earlier by Yao et al. (2019). The authors estimated that methane seepage at site MC 886 started earlier compared to the seepage at site MC 893 and that the methane transport is characterized by diffusion (Yao et al. 2019). We suggest that the distribution of the benthic foraminifera at stage 2 in the ecological succession is mainly controlled by the presence of H_2S (a product of AOM). H_2S is considered highly toxic for marine organisms; it inhibits production of ATP (Adenozyno-5'-trifosforan) by binding to cytochrome c oxidase (CytOx; Somero et al. 1989). Compared to stage 1, food availability seems to play only a secondary role for the foraminiferal community. As a result of environmental constraints, samples from MUC 12 were almost completely barren of foraminifera. Except for a few live specimens in the top 1-cm layer, there were no living benthic foraminiferal specimens found either in MUC 12 or MC 886 (Melaniuk, 2021) (Table 1S). Considering that Rose Bengal stains both live and dead cytoplasm, even a few months after the death of the foraminifera, especially in anoxic conditions (Jorissen et al. 1995; Bernhard et al. 2001), it is possible that the few RB-stained individuals were already dead at the time of sampling. There is a growing body of evidence which prove the ability of some benthic foraminiferal species to use alternative metabolic processes, e.g., ammonium or sulfate assimilation pathways, and this might potentially support life under more episodic conditions of anoxia/H_2S surplus (LeKieffre et al. 2017, 2018, 2020; Jauffrais et al. 2018). Nevertheless, so far, no alternative respiration pathway has been observed in any benthic foraminifera from Vestnesa Ridge. If methane seepage and sulfidic conditions last long enough they can support the development of chemosynthetic invertebrate animals, e.g., *Siboglinidae* tubes worms and potentially also vesicomyid and solemyid clams (Niemann et al. 2006; Treude et al. 2007; Hansen et al. 2017, 2020). This corresponds to ecological succession stage 3**.** Clams, however have not been observed in modern assemblages from Vestnesa Ridge or other Arctic seep sites (Rybakova et al. 2013; Hansen et al. 2017, 2020; Thomsen et al. 2019; and references therein). There is fossil evidence confirming the presence of chemosynthetic bivalves at Vestnesa (Ambrose et al. 2015; Hansen et al. 2017, 2020; Thomsen et al. 2019). Additionally, AOM-induced increase in porewater alkalinity and sedimentary carbonate precipitation provides a secondary hard substrate for tubeworms to settle (Aharon and Fu, 2000; Boetius et al. 2000; Aloisi et al. 2002).

Siboglinidae worms were also recorded at site MC 886 (Yao et al. 2019; Melaniuk, 2021). The sediment at sampling site MUC 10 showed the typical bright brown coloring of the top sediment layers, indicating oxidized sediment from bio-irrigation by the tubeworms, which was further supported by biogeochemical profiles from the site (Figs. 4 A, B) (Melaniuk et al. submitted). Deeper in the core, sediment color changed to black and grey indicating reducing conditions (Fig. 4B). The majority of methane oxidation occurred in the top 4 cm and was decoupled from sulfate reduction, suggesting that MOx was the dominant biological process, while the lower parts of the core were subjected to AOM (Melaniuk et al. submitted). Thus, we assume that oxygen was present in the top layers of the core. Rose Bengal-stained foraminifera were present both in MUC 8 and MUC 10 (A and B). Similar to the initial stage 1, the fauna at stage 3 was dominated by *M. barleeanus* and *C. neoteretis*. *Cassidulina neoteretis* constitutes up to 16% of all foraminifera in MUC 10A (1–2 cm interval) and up to 25 % in MUC 10C (0–1 cm interval), and *M. barleeanus* constitutes up to 60% of the foraminifera in MUC 10A (1–2 cm interval) and up to 89% in MUC 10 C (2–3 cm interval) (Fig. 3).

Interestingly, there were many epibenthic species *Cibicides wuellerstorfi* at this site, compared to any other site presented in this study including the control site. *Cibicides wuellerstorfi* is an epifaunal species which tend to attach itself to structures extending above the seafloor. It prefers low food supply brought by currents and a high oxygen concentration (Lutze and Thiel, 1989; Hald and Steinsund, 1996; Klitgaard-Kristensen et al. 2002; Wollenburg and Mackensen, 2009). Apparently, the *Siboglinidae* tubeworm aggregations elevated high above the sediment provide a surface for attachment of *C. wuellerstorfi* (Melaniuk et al. submitted). Additionally, a position well above the sediment surface provides refuge from hostile environmental conditions, such as oxygen depletion and the toxicity of sulfide (Sen Gupta et al. 2007; Wollenburg and Mackensen, 2009).

The most abundant species among the agglutinated foraminifera are specimens which belong to the *Reophax* genus. They constitute up to 37% of the total benthic foraminiferal fauna (Table S1). It was previously suggested that agglutinated foraminifera are less abundant in sediments influenced by methane seepage than calcareous specimens (Dessandier et al. 2019; and references therein). Our study shows the opposite trend, in fact the sediment from the *Siboglinidae* field is more densely populated by agglutinated specimens compared to the samples from sulfur bacterial mats (MUC 12) and non-seep samples (MUC 11 A and B) (Fig. 2; Table 1S). In the upper 0–1 cm interval (MUC 8 and MUC 10A, B), living (RB-stained)

agglutinated specimens constitute more than 50% of the foraminiferal fauna (Fig. 2). The high number of agglutinated specimens may result from the elevated ambient pCO_2 from CO_2 produced during MOx. The elevated pCO_2 could create acidification of the pore water, which can inhibit calcification, eventually causing dissolution of the calcareous species and give agglutinated species a competitive advantage (Fig. 2.; Table 1S).

Although our interpretation is based on a limited number of samples similar patterns of ecological successions of seep environments has been found at Håkon Mosby Mud Volcano (Wollenburg and Mackensen, 2009). Sites from this area display strict horizontal and vertical distribution patterns according to microhabitat distributions i.e., the hummocky peripheral part with abundant *Siboglinidae* tube worms, the flat crater area with bacterial mats, and the active center with visible gas bubbles (Pimenov et al. 1999; Gebruk et al. 2003; Jerosch et al. 2007). Similar to our MUC 12, the authors observed that in the center of the seep, with the highest methane flux, the sediment is densely covered by bacterial mats, while the sediment is practically barren of foraminifera, only a few foraminifera have been found. In contrast, in areas where the seepage was lower, the sediment is patchily covered by white and grey sulfur bacteria mats, with an association of *C. neoteretis* populating dysoxic sediments in the upper 1-cm surface layer. This environment corresponds to the initial stage 1 of ecological succession of MC 893. Sediments at the periphery of the Håkon Mosby Mud Volcano were oxidized down to 10 cm depth and inhabited by tubeworms (Wollenburg and Mackensen, 2009). Similar to MUC 10 and 8 presented in this paper, Rose Bengal-stained *Fontbotia wuellerstorfi* (i.e., *C. wuellerstorfi*) were abundant and quite a large proportion of the individuals were attached to the *Siboglinidae* tubes.

Stage 4 has not been observed in our study as we have targeted the two most active pockmarks at Vestnesa Ridge. To find succession stage 4, formerly active, but presently inactive pockmarks found at the deeper part of the ridge at 1300 m water depth (Bünz et al. 2012; Consolaro et al.2015) should be sampled. In the study of Consolaro (2018) , the benthic foraminiferal faunas from an inactive pockmark near the core top (and not stained) consists of almost equal proportions of *C. neoteretis*, and *C. reniforme* (each c. 20%) accompanied by lower percentages of *M. barleeanus* (15%) and *C. wuellerstorfi* (10%). Agglutinated specimens constitute only 7% of the fauna.

4.2. Ecological succession and its significance in palaeoceanographic interpretation

Based on the results on this work, it becomes apparent that none of the faunal characteristics can be used exclusively as an indicator of methane emission as differences in composition of the faunas are small and the same species are dominant or there are no live foraminifera present, as a result of H_2S toxicity e.g., MUC 12 or MC 886 both from bacterial mats sites. It is difficult, if not impossible, to find the link between methane seepage and distribution of modern benthic foraminifera to use foraminiferal assemblage compositions as a tool for reconstructions of past methane emission. It seems that foraminifera are indeed attracted to methane oxidizing bacteria as a potential food source, as suggested earlier (e.g., Hill et al. 2005, Bernhard et al. 2010), but only when methane seepage is moderate or low as we show for MC 893 of ecological succession stage 1. Also, during high methane flux and intense AOM activity, oxygen is no longer available for foraminifera in addition to high levels of toxic H_2S within the sediment, and hence the foraminiferal population is radically reduced or samples are barren of foraminifera.

Furthermore, it was not possible to identify particular species or a group of species that could potentially indicate presence of methane seepage. All investigated sites were characterized by a similar faunal pattern, with no endemic species, and the observed species were similar to those from other non-seep locations within the Nordic Seas. Benthic foraminiferal fauna was dominated by species adapted to high organic carbon content and low oxygen conditions, and the key species were *M. barleeanus* and *C. neoteretis*, and *Reophax* sp.

Nevertheless, some subtle differences between seep and non-seep sites do exist, for example at the stage 3 of ecological succession presence of chemosynthetic macrofauna such as *Siboglinidae* tubes arguably support *Cibicides* sp. communities generating secondary hard substrates. Increased numbers of *Cibicidoides wuellerstorfi* were observed both at site MUC 8 and 10 as well in previously studies of the Håkon Mosby Mud Volcano (Wollenburg and Mackensen, 2009). Additionally, compared to other sites samples collected from *Siboglinidae* tubeworm fields (stage 3 of the ecological succession of seep environments) were characterized by a high number of agglutinated foraminifera. This characteristic, however, cannot be used as a methane seepage indicator. Many agglutinated foraminiferal species are often not preserved in fossil records due to the fragile structure, while calcareous species may

not preserve due to the elevated ambient pCO_2 (a high ratio of carbon dissolution is common in deep-sea settings including non-seep sites within the Arctic.

5. Conclusions

Our study shows that the distribution patterns and the species composition of the foraminiferal faunas change according to the progressing ecological succession model of seep environments suggested by Bergquist et al. 2003. Overall, progressing ecological succession result in patchy distribution of living benthic foraminifera; from barren samples from areas with dense bacterial mats in sediments affected by AOM (multicore MUC 10) to high density in sediment samples from *Siboglinidae* (tubeworm) fields with MOx as a dominant process (MUC 8 and 10). The main characteristic of each stage of methane seep environments are as follows:

- **At stage 1** with scattered patches of bacterial mats, the species composition of the benthic foraminiferal assemblages is similar to the non-seep locations in the Arctic and Nordic Seas with main dominant species *Cassidulina neoteretis*, and *Melonis barleeanus* being adapted to low oxygen and high organic content.
- **At stage 2** with presence of dense bacterial mats presence of H_2S produced by anaerobic methane oxidation is the main limiting factor controlling foraminiferal populations at Vestnesa Ridge with foraminifer-barren or almost barren samples.
- **At stage 3** moderate methane seepage with presence of numerous chemosynthetic Siboglinidae tube worms a rich foraminiferal community is found. Large numbers of *C. neoteretis*, *M. barleeanus*, and the agglutinated genus *Reophax* spp. were found and in high percentages. The presence of *Siboglinidae* tubes supports the epifaunal benthic foraminiferal species *Cibicides wuellerstorfi* by generating a secondary hard bottom.

Fossil assemblages represent a fairly wide time range of foraminiferal faunas as the result of that foraminifera from the same 1-cm depth interval in a sediment core may represent short-term changes in the foraminiferal population due to the different stages of succession and/or a mix of several different degrees of strengths of methane seepage events. Overall, none of the faunal characteristics can be used exclusively as an indicator of methane emission and stages of methane emissions. This makes it difficult to use the foraminiferal fauna compositions as a single tool for reconstructions of past methane release and its intensity.

SUPPLEMENTARY INFORMATION

Table S1. Direct counts of Rose Bengal stained foraminifera from samples from Siboglinidae filed, bacterial mats and control site

	Siboglinidae filed									**Control site**							**Bacterial mats**	
Core ID	**MUC 8**	**MUC 10A**					**MUC 10C**			**MUC 11A**			**MUC 11B**				**MUC 12 A**	**MUC 12B**
Depth (cm)	0-1	0-1	1-2	2-3	3-4	4-5	0-1	1-2	2-3	0-1	1-2	2-3	0-1	1-2	2-3	3-4	0-1	
C.neoteretis	107	154	2		2		107	34		106	4		136	7	1	1	1	
C.reniforme	103	24	1				40	11		17			9				1	
M.barleeanus	30	25	69	27	3		11	137	139	6	57	56	11	92	41			2
Quinqueloculina sp.	46	12		1			27						6					
C.wuellerstorfi	6	58	13	10	10	4	4	9	3	29	1		19	1			1	
P. bulloides	29	17		3			21	12		27	3		21	7	1			
Oridorsalis sp.	13	3		2	1		3			8	1		2					
A. galloway					3												3	
other		6		1														
Reophax sp.	262	98	20	16	13		209	65	13	39	4	9	123	29	12	2	4	
R. scorpiurus	11		4	5	4		1	9		36	5		27	16	4			
R. guttifera	85	57	4	1			80	31		107	2	2	39	13				
S. ramosa		6	4				10	41		9	2		25	1				
Spiroplectammina sp.		2																
C. crassimargo	74	151	5	1	1		73	21		102	3	5	21	2	2			
A. glomerata	14						22	13		10	7		2					
other		16		1								1						
total	670	629	122	67	38	4	608	384	155	552	89	73	441	168	61	8		
Shannon´s index	1.95	2.05	1.33	1.36	1.42		1.94	1.98	0.38	1.94	1.16	0.63	1.93	1.32	0.75			
Evenness	0.58	0.59	0.54	0.78	0.83		0.58	0.66	0.48	0.67	0.45	0.62	0.62	0.62	0.70			
Cho-1	12	13	7	5	5		12	11	3	12	7	3	11	6	3			

References

Aharon P., and Fu B. 2000. "Microbial sulfate reduction rates and sulfur and oxygen isotope fractionations at oil and gas seeps in deepwater Gulf of Mexico." *Geochimica et Cosmochimica Acta* 64 (2): 233-246.

Aloisi G., Bouloubassi I., Heijs S.K., Pancost R.D., Pierre C., Sinninghe Damsté J.S., Gottschal J.C., Forney L.J., and Rouchy J-M. 2002. "CH_4-consuming microorganisms and the formation of carbonate crusts at cold seeps." *Earth and Planetary Science Letters* 203 (1): 195-203.

Alve E., Sergei K., Schönfeld J., Dijkstra N., Golikova E., Hess S., Husum K., and Panieri G. 2016. "Foram-AMBI: A sensitivity index based on benthic foraminiferal faunas from North-East Atlantic and Arctic fjords, continental shelves and slopes." *Marine Micropaleontology* 122: 1-12. https://www.sciencedirect.com/science/article/pii/S0377839815300128.

Ambrose W.G., Panieri G., Schneider A., Plaza-Faverola A., Carroll M.L., Åström E.K.L., Locke W.L., and Carroll J. 2015. "Bivalve shell horizons in seafloor pockmarks of the last glacial-interglacial transition: a thousand years of methane emissions in the A rctic O cean." *Geochemistry, Geophysics, Geosystems* 16 (12): 4108-4129.

Åström E.K. L., Carroll M.L., Ambrose W.G., and Carroll J. 2016. "Arctic cold seeps in marine methane hydrate environments: impacts on shelf macrobenthic community structure offshore Svalbard." *Marine Ecology Progress Series* 552: 1-18. https://www.int-res.com/abstracts/meps/v552/p1-18/.

Åström E.K. L., Carroll M.L., Ambrose W.G., Sen A. , Silyakova A., Carroll J. 2018. "Methane cold seeps as biological oases in the high-Arctic deep sea." *Limnology and Oceanography* 63 (S1): S209-S231. https://aslopubs.onlinelibrary.wiley.com/doi/abs/10.1002/lno.10732.

Bergquist D.C., Andras J.P., McNelis T., Howlett S., van Horn M.J., and Fisher C.R. 2003. "Succession in Gulf of Mexico Cold Seep Vestimentiferan Aggregations: The Importance of Spatial Variability." *Marine Ecology* 24 (1): 31-44. https://onlinelibrary.wiley.com/doi/abs/10.1046/j.1439-0485.2003.03800.x.

Bernhard J.M., Buck K.R., and Barry J.P. 2001. "Monterey Bay cold-seep biota: Assemblages, abundance, and ultrastructure of living foraminifera." *Deep Sea Research Part I: Oceanographic Research Papers* 48 (10): 2233-2249.https://www.sciencedirect.com/science/article/pii/S0967063701000176.

Bernhard J.M., Martin J.B., Rathburn A.E. 2010. "Combined carbonate carbon isotopic and cellular ultrastructural studies of individual benthic foraminifera: 2. Toward an understanding of apparent disequilibrium in hydrocarbon seeps." *Paleoceanography* 25: PA4206. https://doi.org/10.1029/2010PA001930, 2010.

Bernhard J.M., and Panieri G. 2018. "Keystone Arctic paleoceanographic proxy association with putative methanotrophic bacteria." *Scientific Reports* 8 (1): 10610. https://doi.org/10.1038/s41598-018-28871-3.

Boetius A., Ravenschlag K., Schubert C.J., Rickert D., Widdel F., Gieseke A., Amann R., Jørgensen B.B., Witte U., and Pfannkuche O. 2000. "A marine microbial consortium apparently mediating anaerobic oxidation of methane." *Nature* 407 (6804): 623-626. https://doi.org/10.1038/35036572.

Bünz S., Polyanov S., Vadakkepuliyambatta S., Consolaro C., and Mienert J. 2012. "Active gas venting through hydrate-bearing sediments on the Vestnesa Ridge, offshore W-Svalbard." *Marine Geology* 332-334: 189-197. https://www.sciencedirect.com/science/article/pii/S0025322712002137.

Chapman M.G., and Underwood A.J. 1994. "Dispersal of the intertidal snail, *Nodilittorina pyramidalis*, in response to the topographic complexity of the substratum." *Journal of Experimental Marine Biology and Ecology* 179 (2): 145-169.

Cline J.D. 1969. "Spectrophotometric determination of hydrogen sulfide in waters". *Limnology and Oceanography* 14 (3): 454-458. https://aslopubs.onlinelibrary.wiley.com/doi/abs/10.4319/lo.1969.14.3.0454.

Consolaro C., Rasmussen T.L., Panieri G., Mienert J., Bünz S., and Sztybor K. 2015. "Carbon isotope ($\delta^{13}C$) excursions suggest times of major methane release during the last 14 kyr in Fram Strait, the deep-water gateway to the Arctic." *Clim. Past* 11 (4): 669-685. https://cp.copernicus.org/articles/11/669/2015/.

Consolaro C., Rasmussen T.L., and Panieri G. 2018. "Palaeoceanographic and environmental changes in the eastern Fram Strait during the last 14,000years based on benthic and planktonic foraminifera." *Marine Micropaleontology* 139: 84-101. https://www.sciencedirect.com/science/article/pii/S0377839816301359.

Corliss B.H., Martinson.G., and Keffer T. 1986. "Late Quaternary deep-ocean circulation." *GSA Bulletin* 97 (9): 1106-1121.

Dayton P.K., and Hessler R.R. 1972. "Role of biological disturbance in maintaining diversity in the deep sea." Deep Sea Research and Oceanographic Abstracts.

Dickens G.R., Castillo M.M, and Walker J.C.G. 1997. "A blast of gas in the latest Paleocene: Simulating first-order effects of massive dissociation of oceanic methane hydrate." *Geology* 25 (3): 259-262.

Eiken O., and Hinz K. 1993. "Contourites in the Fram Strait." *Sedimentary Geology* 82 (1): 15-32. https://www.sciencedirect.com/science/article/pii/003707389390110Q.

Etiope G., P., Fattorini D., Regoli F., Vannoli P., Italiano F., Locritani M., and Carmisciano C.. 2014. "A thermogenic hydrocarbon seep in shallow Adriatic Sea (Italy): Gas origin, sediment contamination and benthic foraminifera." *Marine and Petroleum Geology* 57: 283-293.

Gebruk A.V., Krylova E.M., Lein A.Y., Vinogradov G.M., Anderson E., Pimenov N.V., Cherkashev G.A., Kathleen Crane.2003. Methane seep community of the Håkkon Mosby mud volcano (the Norwegian Sea): composition and trophic aspects. Sarsia 88, 394–403.

Gooday A.J., and FJorissen F.J. 2012. "Benthic Foraminiferal Biogeography: Controls on Global Distribution Patterns in Deep-Water Settings." *Annual Review of Marine Science* 4 (1): 237-262. https://www.annualreviews.org/doi/abs/10.1146/annurev-marine-120709-142737.

Hald M., and Steinsund P.I. 1996. "Benthic foraminifera and carbonate dissolution in the surface sediments of the Barents and Kara Seas." *Berichte zur Polarforschung* 212: 285-307.

Hansen J., Mohamed M. E., Åström E.K.L., and Rasmussen T.L. 2020. "New late Pleistocene species of Acharax from Arctic methane seeps off Svalbard." *Journal of Systematic Palaeontology* 18 (2): 197-212.

Hansen J., Hoff U., Sztybor K., and Rasmussen T.L. 2017. "Taxonomy and palaeoecology of two Late Pleistocene species of vesicomyid bivalves from cold methane seeps at Svalbard (79 N)." *Journal of Molluscan Studies* 83 (3): 270-279.

Herguera J.C., Paull C., Perez E.,Ussler III W., and Peltzer E.T. 2014. "Limits to the sensitivity of living benthic foraminifera to pore water carbon isotope anomalies in methane vent environments." *Paleoceanography* 29 (3): 273-289. https://agupubs.onlinelibrary.wiley.com/doi/abs/10.1002/2013PA002457.

Hill T.M., Kennett J.P., and Spero H.J. 2003. "Foraminifera as indicators of methane-rich environments: A study of modern methane seeps in Santa Barbara Channel, California." *Marine Micropaleontology* 49 (1): 123-138. https://www.sciencedirect.com/science/article/pii/S037783980300032X.

Hustoft, S., Bünz S., Mienert J., and Chand S. 2009. "Gas hydrate reservoir and active methane-venting province in sediments on <20 Ma young oceanic crust in the Fram Strait, offshore NW-Svalbard." *Earth and Planetary Science Letters* 284 (1): 12-24. https://www.sciencedirect.com/science/article/pii/S0012821X09002027.

Jakobsson M., Mayer L.A., Bringensparr C., et al. 2020. "The International Bathymetric Chart of the Arctic Ocean Version 4.0. ." *Scientific Data* 7(1):176. https://doi.org/10.1038/s41597-020-0520-9.

Jauffrais, T., LeKieffre C., Koho K.A., Tsuchiya M., Schweizer M.,Bernhard J.M., Meibom A., and Geslin E. 2018. "Ultrastructure and distribution of kleptoplasts in benthic foraminifera from shallow-water (photic) habitats." *Marine Micropaleontology* 138: 46-62.

Jauffrais, T., LeKieffre C., Schweizer M., Jesus B.,Metzger E., and Geslin E. 2019. "Response of a kleptoplastidic foraminifer to heterotrophic starvation: Photosynthesis and lipid droplet biogenesis." *FEMS microbiology ecology* 95 (5): fiz046.

Jerosch K.,Schluter M., Foucher J.P., Allais A.-G., Klages M., Edy C. 2007. Spatial distribution of mud flows, chemoautotrophic communities, and biogeochemical habitats at Håkkon Mosby Mud Volcano. Marine Geology 243 (1–4), 1–17.

Jørgensen B.B.. 1978. "A comparison of methods for the quantification of bacterial sulfate reduction in coastal marine sediments."

Jorissen F.J., de Stigter H.C., and Widmark J.G.V. 1995. "A conceptual model explaining benthic foraminiferal microhabitats." *Marine Micropaleontology* 26 (1): 3-15. https://www.sciencedirect.com/science/article/pii/037783989500047X.

Kallmeyer J., Ferdelman T.G., Weber A., Fossing H., and Jørgensen B.B. 2004. "A cold chromium distillation procedure for radiolabeled sulfide applied to sulfate reduction measurements." *Limnology and Oceanography: Methods* 2 (6): 171-180.

LeKieffre, C., Jauffrais T., Geslin E., Jesus B., Bernhard J.M., Giovani M.-E., and Meibom A. 2018. "Inorganic carbon and nitrogen assimilation in cellular compartments of a benthic kleptoplastic foraminifer." *Scientific reports* 8 (1): 1-12.

LeKieffre C., Spangenberg J.E., Mabilleau G., Escrig S., Meibom A., and Geslin E. 2017. "Surviving anoxia in marine sediments: The metabolic response of ubiquitous benthic foraminifera (Ammonia tepida)." *PloS one* 12 (5): e0177604.

LeKieffre, Charlotte, Howard J. Spero, Jennifer S. Fehrenbacher, Ann D. Russell, Haojia Ren, Emmanuelle Geslin, and Anders Meibom. 2020. "Ammonium is the preferred source of nitrogen for planktonic foraminifer and their dinoflagellate symbionts." *Proceedings of the Royal Society B* 287 (1929): 20200620.

Levin L.A. 2005. Ecology of cold seep sediments: Interactions of fauna with flow, chemistry and microbes. In: Oceanography and Marine Biology: An Annual Review, Gibson RN, Atkinson RJA, Gordon JDM (eds) CRC Press-Taylor & Francis Group, Boca Raton, 1–46. DOI: 10.1201/9781420037449.ch1

Lutze G.F., and Heinz T. 1989. "Epibenthic foraminifera from elevated microhabitats; Cibicidoides wuellerstorfi and Planulina ariminensis." *Journal of Foraminiferal Research* 19 (2): 153-158. https://doi.org/10.2113/gsjfr.19.2.153.

Mackensen A., Sejrup H.P., andJansen E. 1985. "The distribution of living benthic foraminifera on the continental slope and rise off southwest Norway." *Marine Micropaleontology* 9 (4): 275-306. https://www.sciencedirect.com/science/article/pii/0377839885900015.

Martin R.A., Nesbitt E.A., and Campbell K.A. 2010. "The effects of anaerobic methane oxidation on benthic foraminiferal assemblages and stable isotopes on the Hikurangi Margin of eastern New Zealand." *Marine Geology* 272 (1): 270-284. https://doi.org/https://doi.org/10.1016/j.margeo.2009.03.024.

Melaniuk K. 2021. "Effectiveness of Fluorescent Viability Assays in Studies of Arctic Cold Seep Foraminifera." *Frontiers in Marine Science* 8 (198). https://doi.org/10.3389/fmars.2021.587748.

Millo C., Sarnthein M.,Erlenkeuser H.,Grootes P.M., and Andersen N. 2005. "Methane-induced early diagenesis of foraminiferal tests in the southwestern Greenland Sea." Marine Micropaleontology 58 (1): 1-12. https://doi.org/https://doi.org/10.1016/j.marmicro.2005.07.003.

Murray J.W. 2006. Ecology and Applications of Benthic Foraminifera. Cambridge University Press, Cambridge.

Niemann H., Lösekann T., de Beer D.,Elvert M., Nadalig T.,Knittel K.,Amann R., Sauter E.J., Schlüter M., Klages M., Foucher J.P., andBoetius A. 2006. "Novel microbial communities of the Haakon Mosby mud volcano and their role as a methane sink." *Nature* 443 (7113): 854-858.

Dessandier P.-., Borrelli C., Kalenitchenko D.,Panieri G. 2019. "Benthic Foraminifera in Arctic Methane Hydrate Bearing Sediments." *Frontiers in Marine Science* 6: 765.

Pimenov N. V., Savvichev A.S., Rusanov I.I., Lein A.Y., Ivanov M.V., 2000. Microbial processes of the carbon and sulphur cycles at cold methane seeps of the North Atlantic. Microbiology 69, 709–720

Plaza-Faverola A., Bünz S., Johnson J.E., Chand S., Knies J., Mienert J.,Franek P. 2015. "Role of tectonic stress in seepage evolution along the gas hydrate-charged Vestnesa Ridge, Fram Strait." *Geophysical Research Letters* 42 (3): 733-742. https://agupubs.onlinelibrary.wiley.com/doi/abs/10.1002/2014GL062474.

Rasmussen T .L., andThomsen E. 2017. "Ecology of deep-sea benthic foraminifera in the North Atlantic during the last glaciation: Food or temperature control."*Palaeogeography, Palaeoclimatology, Palaeoecology* 472: 15-32. https://www.sciencedirect.com/science/article/pii/S0031018217301578.

Rathburn A.E., Levin L.A., Held Z., and Lohmann K.C. 2000. "Benthic foraminifera associated with cold methane seeps on the northern California margin: Ecology and stable isotopic composition." *Marine Micropaleontology* 38 (3): 247-266. https://www.sciencedirect.com/science/article/pii/S0377839800000050.

Ruppel C., and Kessler J.D. 2017. "The interaction of climate change and methane hydrates." *Reviews of Geophysics* 55 (1): 126-168. https://doi.org/https://doi.org/10.1002/2016RG000534.

Rybakova E., Galkin S., Bergmann M., Soltwedel, T., and Gebruk A. (2013). Density and distribution of megafauna at the Håkon Mosby Mud Volcano (the Barents Sea) based on image analysis. *Biogeosciences* 10, 3359–3374. doi: 10.5194/bg-10-3359-2013

Schneider A. ., Crémière A., Panieri G., Lepland A., and Knies J. 2017. "Diagenetic alteration of benthic foraminifera from a methane seep site on Vestnesa Ridge (NW Svalbard)." *Deep Sea Research Part I: Oceanographic Research Papers* 123: 22-34. https://www.sciencedirect.com/science/article/pii/S0967063716301996.

Sejrup Hans P., Nagy J., and Brigham-Grette J. 1989. "Foraminiferal stratigraphy and amino acid geochronology of Quaternary sediments in the Norwegian Channel, northern North Sea." *Norsk geologisk tidsskrift* 69 (2): 111-124.

Sen Gupta B.K., Smith L.E., and Lobegeier M.K. 2007. "Attachment of Foraminifera to vestimentiferan tubeworms at cold seeps: Refuge from seafloor hypoxia and sulfide toxicity." *Marine Micropaleontology* 62 (1): 1-6. https://www.sciencedirect.com/science/article/pii/S0377839806001101.

Smith L. M., Sachs J.P., Jennings A.E., Anderson D.M., and deVernal A. 2001. "Light δ13C events during deglaciation of the East Greenland Continental Shelf attributed to methane release from gas hydrates." *Geophysical Research Letters* 28 (11): 2217-2220 https://agupubs.onlinelibrary.wiley.com/doi/abs/10.1029/2000GL012627.

Somero G.N., Childress J.J., and Anderson A.E. 1989. "Transport, metabolism, and detoxification of hydrogen sulfide in animals from sulfide-rich marine environments." *Reviews in Aquatic Sciences RAQSEL* 1 (4).

Sommer S., Linke P., Pfannkuche O., Schleicher T., Schneider J. Deimling V., Reitz A., Haeckel M., Flögel S., and Hensen C. 2009. "Seabed methane emissions and the habitat of frenulate tubeworms on the Captain Arutyunov mud volcano (Gulf of Cadiz)." *Marine Ecology Progress Series* 382: 69-86. https://www.int-res.com/abstracts/meps/v382/p69-86/.

Stocker T. F., Qin D., Plattner G.-K., Tignor M., Allen S.K., Boschung J., Nauels A., Xia Y., Bex V. and Midgley P.M. (eds.). IPCC, 2013: Climate Change 2013: The Physical Science Basis. Contribution of Working Group I to the Fifth Assessment Report of the Intergovernmental Panel on Climate Change *Cambridge University Press, Cambridge, United Kingdom and New York, NY, USA,*, 1535 (2013).

Sztybor K., and Rasmussen T.L. 2017. "Diagenetic disturbances of marine sedimentary records from methane-influenced environments in the Fram Strait as indications of variation in seep intensity during the last 35 000 years." *Boreas* 46 (2): 212-228. https://onlinelibrary.wiley.com/doi/abs/10.1111/bor.12202.

Tanner J.E., Hughes T.H., and Connell J.H. 1994. "Species coexistence, keystone species, and succession: a sensitivity analysis." *Ecology* 75 (8): 2204-2219.

Thomas E., Booth L.,Maslin M., and Shackleton N.J. 1995. "Northeastern Atlantic benthic foraminifera during the last 45,000 years: Changes in productivity seen from the bottom up." *Paleoceanography* 10 (3): 545-562. https://agupubs.onlinelibrary.wiley.com/doi/abs/10.1029/94PA03056.

Thomsen E., Rasmussen T.L., Sztybor K., Hanken N.-M., Tendal O.S., Uchman A. 2019. "Cold-seep fossil macrofaunal assemblages from Vestnesa Ridge, eastern Fram Strait,

during the past 45 000 years." *Polar Research* 38 (0). https://polarresearch.net/index.php/polar/article/view/3310.

Torres M.E., Mix A. C., Kinports K., Haley B., Klinkhammer G. P., McManus J., de Angelis, M. A. 2003. "Is methane venting at the seafloor recorded by δ13C of benthic foraminifera shells?" *Paleoceanography* 18 (3). https://agupubs.onlinelibrary.wiley.com/doi/abs/10.1029/2002PA000824.

Treude T, Krause S.,Steinle L., Burwicz E., Hamdan L.J., Niemann H., Feseker T., Liebetrau V., Krastel S., and Berndt C.. 2020. "Biogeochemical Consequences of Nonvertical Methane Transport in Sediment Offshore Northwestern Svalbard." *Journal of Geophysical Research: Biogeosciences* 125 (3): e2019JG005371. https://agupubs.onlinelibrary.wiley.com/doi/abs/10.1029/2019JG005371.

Treude T., Orphan V., Knittel K., Gieseke A., House C.H., and Boetius A. 2007. "Consumption of Methane and CO_2 by Methanotrophic Microbial Mats from Gas Seeps of the Anoxic Black Sea." *Applied and Environmental Microbiology* 73 (7): 2271-2283. https://journals.asm.org/doi/abs/10.1128/AEM.02685-06

Wefer G., Heinze P.-M., and Berger W.H. 1994. "Clues to ancient methane release." *Nature* 369 (6478): 282-282. https://doi.org/10.1038/369282a0.

Wollenburg J.E., and Mackensen A. 2009. "The ecology and distribution of benthic foraminifera at the Håkon Mosby mud volcano (SW Barents Sea slope)." *Deep Sea Research Part I: Oceanographic Research Papers* 56 (8): 1336-1370. https://www.sciencedirect.com/science/article/pii/S0967063709000363.

Wollenburg J.E., and Mackensen A. 1998. "Living benthic foraminifers from the central Arctic Ocean: faunal composition, standing stock and diversity." *Marine Micropaleontology* 34 (3): 153-185. https://www.sciencedirect.com/science/article/pii/S0377839898000073.

Yao H., Hong W.-L, Panieri G., Sauer S., Torres M.E., Lehmann M.F., Gründger F., and Niemann H. 2019. "Fracture-controlled fluid transport supports microbial methane-oxidizing communities at Vestnesa Ridge." *Biogeosciences* 16 (10): 2221-2232. https://bg.copernicus.org/articles/16/2221/2019/.